Anaerobic Fermentation with Ethanol and Lactate as Co-Electron Donors for Medium-Chain Carboxylic Acid Production

Han Wang

Supervisor: Prof. Dr. Ir. Largus T. Angenent

Environmental biotechnology group

Geoscience department

Tuebingen University

2022.03.09

Anaerobic Fermentation with Ethanol and Lactate as Co-Electron Donors for Medium-Chain Carboxylic Acid Production

Dissertation

der Mathematisch-Naturwissenschaftlichen Fakultät

der Eberhard Karls Universität Tübingen

zur Erlangung des Grades eines

Doktors der Naturwissenschaften

(Dr. rer. nat.)

vorgelegt von HAN WANG

aus LU ZHOU/ CHINA

Tübingen

2023

Gedruckt mit Genehmigung der Mathematisch-Naturwissenschaftlichen Fakultät der Eberhard Karls Universität Tübingen.

Tag der mündlichen Qualifikation:	27.06.2023
Dekan:	Prof. Dr. Thilo Stehle
1. Berichterstatter/-in:	Prof. Dr. Ir. Largus Angenent
2. Berichterstatter/-in:	Prof. dr hab. Eng. Piotr Oleśkowicz-Popiel

Anaerobic Fermentation with Ethanol and Lactate as Co-Electron Donors for Medium-Chain Carboxylic Acid Production

HAN WANG, Ph.D

Tuebingen University 2023

Developing alternative technologies for producing chemical compounds, previously based on fossil sources, is the first step into a circular economy. Current environmental pressures and the net-zero carbon emission goal require a more efficient waste management technology. Accordingly, using organic waste to produce high-value chemical compounds (*e.g.,* medium-chain carboxylic acids [MCCAs]) is a promising alternative to re-valorize waste and reduce fossil fuel dependency. MCCAs (ranging from six to twelve carbons) are essential industrial chemicals that could be employed in several applications, including as antimicrobial agents, fodder-annexing agents, rubbers, and precursors of aviation fuels. The most commonly used electron donors for microbial MCCA production were ethanol and lactate, which could be available in many waste-fermentation broths (*e.g.,* syngas, liquor-making wastewater, food waste, or acid whey). With expanding application of real waste into microbial MCCA production, it was found that both ethanol and lactate were present in the fermentation broth of some waste (*e.g.,* maize silage, food waste, or acid whey) due to fermentation way of waste. Few studies have focused on the co-utilization of ethanol and lactate for MCCA production. More research was required to understand using ethanol and lactate as co-electron donors for MCCA production and to lay a foundation for further conversion of more real waste into MCCAs. In this dissertation, I studied anaerobic fermentation with ethanol and lactate as co-electron donors for MCCA production. In the first study, I present the process regulation in MCCA production in open cultures with ethanol and lactate as co-electron donors; in the second study, I explored the microbial ecology of the microbiome for MCCA production in a long-term run bioreactor with ethanol and lactate as co-electron donors; in the third study, I investigated the parameter affecting MCCA production with ethanol and lactate with co-substrates.

Dedication

I dedicate this dissertation to my family: my parents, Nianhua Wang and Yulan Chen and my cousin sisters-Yanxi Chen and Jing Zhou. I greatly appreciate all their support and encouragement over the years.

Acknowledgments

I thank my supervisor, Lars Angenent, for inspiring, encouraging, and supporting me throughout my Ph.D. study. I really appreciate the lab environment he provided. I feel super lucky to study in this lab. I really enjoyed working with all the colleagues from around the world in this lab. I also thank my committee members, Prof. Dr. Andreas Kappler, Prof. Dr. Christiane Zarfl, and Prof. dr hab. Eng. Piotr, Oleśkowicz-Popiel for their support. I would like to thank all the members of this lab, past and present, for their help, support, and understanding. Mainly, I would like to thank Dr. Bastian Molitor for helping me get used to the new environment; I would like to thank Dr. Ir. Joseph G. Usack for helping me order bioreactor stuff; I would like to thank Byoung Seung Jeon for helping me with building the bioreactor, maintaining the GC-MS, and giving positive advice; I would like to thank Nils Rohbohm for helping me with the English writing, computer equipment, and microscope introduction; I would like to thank Caroline Schlaiss, Lucas Muhling, and Gabriela Contreras for their microbiology advice; I would like to thank Patrick Schweizer and Monika Temovska for their help with maintaining the bioreactor and GC; I would like to thank Kurt Gemeinhardt for helping me with isolation of bacteria; I would like to thank Juan Ramires, Rodolfo, and Ulrike for their suggestions on writing; I would like to thank Andres Ortiz Ardila for helping me with sequence and microbial analysis; I would like to thank Jean Nepo Ntihuga for helping me with thermodynamic calculation; I would like to thank Nicolai Kreitli for assisting me with lab safety; I would like to thank Mei Zhou for printing my dissertation. In addition, I would like to thank my friends in this lab for their support and accompany over the past few years. I would like to thank the Geoscience department and Tuebingen University for providing such a confortable environment for study and research. At last, I would like to Chinese Scholar Council for their support.

TABLE OF CONTENTS

CHAPTER 1

Introduction

1.1 General aim

For sustainability and ecosystem health, developing new ways of resource recovery from some organic waste streams (*e.g.,* wastewaters, agricultural residues) for high-value renewable chemical production is necessary. The renewable chemical production from waste by microbes *via* the carboxylate platform recently garnered much attention (Angenent, Richter *et al*. 2016). MCCAs are essential industrial chemicals (Angenent, Richter *et al*. 2016). Chain elongation *via* reverse β-oxidation (rBOX) utilizes ethanol, lactate, or other substrates as electron donors. Short-chain carboxylic acids (SCCAs, *e.g.,* acetate, propionate, and *n*-butyrate) serve as electron acceptors (Spirito, Richter *et al*. 2014). Ethanol and lactate are the most used electron donors. MCCA production with ethanol has resulted in relatively high production yields and rates in both the pure cultures with *Clostridium kluyveri* (*C. kluyveri*; Gildemyn, Molitor *et al*. 2017) and open cultures (Andersen, Candry *et al*. 2015, Kucek, Spirito *et al*. 2016, Spirito, Marzilli *et al*. 2018), implying the feasibility and prospective of this biosynthesis process. Lactate accounts for a large proportion of the intermediates in the anaerobic fermentation of carbohydrates from municipal wastewaters or food processing wastewaters (Gómez, Cuetos *et al*. 2009, Arslan, Steinbusch *et al*. 2013, Kucek, Nguyen *et al*. 2016). Studies from Zhu *et al.* showed that lactate could be converted to a high concentration of *n*-caproate (23.4 g L^{-1}) with a reactor microbiome (Zhu, Tao *et al*. 2015). Kucek *et al.* observed a C6 production rate of 6.9 g COD L^{-1} d^{-1} (this is already as high as methane production rates with anaerobic digesters) in a continuous bioreactor fed with lactate (Kucek, Nguyen *et al*. 2016). Importantly, lactate in the contained fermentation broth can be fermented from other organic wastes without adding other electron donors (*e.g.,* grass fermentation and acid whey waste; Khor, Andersen *et al*. 2017, Xu, Hao *et al*. 2017, Duber, Zagrodnik *et al*. 2020). Therefore, lactate is also considered to be a promising electron donor for MCCA production. The fermentation effluent from some organic waste streams (*e.g.,* acid whey, maize silage, and food waste) may contain both ethanol and lactate due to the storage condition and a natural presence of lactic acid bacteria (Otto 1983, Duber, Jaroszynski *et al*. 2018). However, only several publications studied the interaction of ethanol and lactate when they serve as co-

electron donors, but it was not fully clear whether they would be utilized simultaneously (Wu, Guo *et al*. 2018, Wu, Guo *et al*. 2019). Some studies showed that ethanol and lactate in the fermentation broth were not consumed simultaneously (Lambrecht, Cichocki *et al*. 2019). The above results showed that the co-utilization of ethanol and lactate for chain elongation needed more investigation. My research investigated the process control, microbial ecology, and fermentation characteristics of using ethanol and lactate as electron donors for MCCA production. Specifically, this study intended to address the following issues: **1)** to explore the control strategy for MCCA production in a product-extracted bioreactor with ethanol and lactate as co-substrates; **2)** to enable greater insight into microbial dynamics and interactions using ethanol and lactate as co-electron donors producing MCCAs under different conditions; **3)** to unravel more fermentation characteristics of using ethanol and lactate as co-electron donors for MCCA production. All the results from this study may lay a foundation for optimizing bioreactors for product-based selective fermentation.

1.2 Introduction

This dissertation describes previous work on chain elongation to MCCAs and new work performed to explore the expanding application of microbial MCCA production with more substrates. Chapter 2 is a literature review introducing the mechanism of MCCA production, the operating parameters affecting the MCCA-producing process, the MCCA-producing microorganisms, and the microbial analysis tools. Chapters 3, 4, and 5 describe the three aims of my dissertation work and experiments performed towards those aims. Chapter 3 describes experiments performed with two 6.5-L laboratory-scale bioreactors to explore the substrate utilization and the effect of substrate structure and operating temperature on MCCA production with co-utilization of ethanol and lactate as co-electron donors. Chapter 4 describes experiments investigating the microbial dynamics caused by different environmental factors in a long-term run bioreactor for MCCA production with ethanol and lactate as co-electron donors, based on 16S rRNA gene sequencing. Chapter 5 describes experiments performed in serum bottles to examine the effect of electron donors, electron acceptors, hydrogen partial pressure (pH_2), and acrylic acid on MCCA production. Chapter 6 focuses on the summary of all the experiments. Appendices 1, 2, and 3 contain supplementary material for Chapters 3, 4, and 5, respectively. Appendix 4

includes experiment protocols: a protocol for preparing environmental samples for Illumina 16S rRNA gene sequencing and a protocol for initial analysis of the resulting sequences.

1.3 Summary of experiments

Section 1- Aim: To explore the substrate utilization and the effect of substrate structure and operating temperature on MCCA production with the co-utilization of ethanol and lactate as co-electron donors.

- Two 6.5-L (a maximum wet volume of ~6.0 L) continuously fed up-flow anaerobic bioreactors with in-line extraction systems were fed with ethanol and lactate for two years to shape the microbiome. Then different E_L_ratios and operating temperatures were applied to the bioreactor to control the product spectrum.

During the entire operating period, operating parameters (*e.g.,* ORP, biomass, pH, and temperature), gas production, and MCCA production were measured to evaluate and compare the performance of both reactors.

Section 2- Aim: To investigate the microbial dynamics caused by different environmental factors in a long-term run bioreactor for MCCA production with ethanol and lactate as co-electron donors.

- Time-course of the samples in two long-term run bioreactors for MCCA production with ethanol and lactate as co-electron donors.
- Isolating DNA and preparing the sample for 16S rRNA gene sequencing
- Microbial analysis of the sequence result *via* QIIME2 and R.

Section 3-Aim: To examine the effect of electron donors, electron acceptors, pH_2, and acrylic acid on MCCA production.

- Triplets were performed in serum bottles according to different experimental designs.
- The substrate and product concentrations, the pH, and pH_2 were measured.

CHAPTER 2

Anaerobic Fermentation with Ethanol and Lactate as Co-Electron Donors for Medium-Chain Carboxylic Acid Production

2.1 Introduction

The growing demand and consumption of fossil oil require the discovery of new oil reserves or the generation of renewable energy. Our societies produce much organic waste daily (*e.g.,* industrial and agricultural wastewater and food waste; Agler, Wrenn *et al*. 2011). Biowaste could be reused *via* biorefinery upgrading, which is a way to maximize the value of waste or biomass to generate a spectrum of bio-based products (*e.g.,* food, feed, chemicals, and materials) and bioenergy (*e.g.,* biofuels and heat), while simultaneously recycling carbon and water as resources (Agler, Wrenn *et al*. 2011). Recovering resources from waste is vital for implementing a circular economy to satisfy environmental and economic demands (Angenent, Richter *et al*. 2016, De Groof, Coma *et al*. 2019). The three best-known biorefinery platforms are: **1)** the sugar platform in which five- and six-carbon sugars are produced as intermediate feedstocks by pure enzymes; **2)** the syngas platform in which biomass is converted into syngas such as CO, H_2, and CO_2; **3)** the carboxylate platform in which organic feedstocks from industrial and agricultural wastes are converted to SCCAs as intermediate feedstocks chemicals under anaerobic conditions (Holtzapple and Granda 2009, Agler, Spirito *et al*. 2014). The difference between platforms depends on the method of biomass conversion and its resultant chemicals (*e.g.,* sugar, syngas, or carboxylates). The intermediates in the carboxylate platform are mainly some SCCAs (*e.g.,* acetate, propionate, lactate, or *n*-butyrate), and these organic products are valuable. These SCCAs could also be further fermented to MCCAs (*e.g., n*-caproate, *n*-heptanoate, and *n*-caprylate; Agler, Wrenn *et al*. 2011).

Compared with traditional biorefinery products (*e.g.,* ethanol or methane), MCCAs have a higher energy density, higher product value, and broader applications (Angenent, Richter *et al*. 2016). MCCAs can be utilized as essential precursors to liquid biofuels (*e.g.,* alkanes and alcohols) and commercial chemicals. For example, *n*-caproate could be used in green antimicrobials, animal feed additives, flavorings, and plant growth promoters (Van Immerseel, De Buck *et al*. 2004, Rossi, Pastorelli *et al*. 2010, Huang, Alimova *et al*. 2011). In addition, MCCAs are more

hydrophobic than SCCAs. The solubility of *n*-caproate, *n*-heptanoate, and *n*-caprylate in water in their undissociated forms are as low as 10.82, 2.42, and 0.68 g L^{-1}, respectively, while ethanol, lactate, and SCCAs are entirely miscible (Xu, Hao *et al*. 2017). Such solubility of MCCAs means that they could be separated from the fermentation broth in a more economical and efficient separation way (Agler, Spirito *et al*. 2012, Ge, Usack *et al*. 2015).

Microbial production of MCCAs from SCCAs is the process of carbon-chain elongation for which rBOX is the most well-known pathway (Steinbusch, Hamelers *et al*. 2011, Agler, Spirito *et al*. 2012, Spirito, Richter *et al*. 2014). There are two steps in this process. First, electron donors (*e.g.,* ethanol, lactate, or carbohydrates) are oxidized to provide energy, reducing equivalents, and acetyl-CoA for the next step (reverse ß-oxidation pathway); then, electron acceptors (*e.g.,* acetate or propionate) are elongated with two additional carbons in the way of acetyl-CoA *via* rBOX (Spirito, Richter *et al*. 2014). Ethanol and lactate are most commonly used electron donors (De Groof, Coma *et al*. 2019). Applying ethanol in MCCA production has resulted in relatively high production yields and rates in both the pure cultures with *Clostridium kluyveri* (Gildemyn, Molitor *et al*. 2017) and open cultures (Andersen, Candry *et al*. 2015, Kucek, Spirito *et al*. 2016), implying the feasibility and prospective of this biosynthesis process. Lactate accounts for a large proportion of the intermediates in the anaerobic fermentation of carbohydrates from municipal wastewaters or food processing wastewaters (Gómez, Cuetos *et al*. 2009, Arslan, Steinbusch *et al*. 2013, Kucek, Nguyen *et al*. 2016). Studies by Zhu *et al*. showed that lactate could be converted to a high concentration of *n*-caproate (23.4 g L^{-1}) with a reactor microbiome (Zhu, Tao *et al*. 2015). Kucek *et al*. observed a *n*-caproate production rate of 6.9 g COD L^{-1} d^{-1} (this is already as high as methane production rates with anaerobic digesters) in a continuous bioreactor fed with lactate (Kucek, Nguyen *et al*. 2016). Importantly, lactate in the contained fermentation broth can be fermented from other various wastes without adding other electron donors (*e.g.,* grass and acid whey waste; Khor, Andersen *et al*. 2017, Xu, Hao *et al*. 2017, Duber, Zagrodnik *et al*. 2020). Therefore, lactate is also considered to be a promising electron donor for MCCA production. The fermentation effluent from some organic waste streams (*e.g.,* acid whey, maize silage, and food waste) may contain both ethanol and lactate due to the storage condition and the natural presence of lactic acid bacteria (Otto 1983, Duber, Jaroszynski *et al*. 2018). Ethanol and lactate served as co-

substrates in the liquor-making wastewater for MCCA production, indicating that applying a combination of electron donors (ethanol and lactate) broadly promoted the conversion of substrates from SCCAs into MCCAs (Wu, Guo *et al*. 2018). The coexisting by-products (H_2 and CO_2) from ethanol and lactate also contributed to additional MCCA generation, albiet in an indirect way *via* homoacetogenesis (Wu, Sun *et al*. 2020). The above publications showed the interesting interaction between ethanol- and lactate-based chain MCCA production.

Appying open-culture biotechnology for bioenergy production in carboxylate platforms is vital (Kleerebezem and van Loosdrecht 2007). Open and anaerobic systems require no sterilization and oxygen supply (Angenent, Richter *et al*. 2016), and complex microbial diversity leads to a resilient, robust, and adaptive system, which is capable of utilizing mixed substrates or being run for a continuous process (Cavalcante, Leitão *et al*. 2017). However, the microbial composition and functional microbiomes are more complex than pure cultures. And the bioreactor performance with open cultures has been performed by different groups (Candry and Ganigue 2021). Well-known chain-elongating bacteria, such as *Clostridium kluyveri* (*C. kluyveri*; Waselefsky 1985), *Megasphaera elsdenii (M. elsdenii*; Marounek, Fliegrova *et al.* 1989*)*, or *Ruminococcaceae* bacterium CPB6 (Zhu, Zhou *et al*. 2017), were often abundant (Steinbusch, Hamelers *et al*. 2011, Zhu, Tao *et al*. 2015, Roghair, Liu *et al*. 2018) or were related to the dominant microbiomes for MCCA production in open cultures (Agler, Spirito *et al*. 2012, Agler, Werner *et al*. 2012, Contreras-Davila, Carrion *et al*. 2020, Wu, Feng *et al*. 2020). However, more unexpected microbial communities were found responsible for MCCA production (Kim, Kang *et al*. 2022). *Bacteroides* spp. with *Oscillospira* spp. were also positively correlated to volumetric production rates of MCCA in an ethanol-based bioreactor (Kucek, Spirito *et al*. 2016, Kucek, Jiajie Xu *et al*. 2016). Many studies displayed that *Lactobacillus* spp. were highly abundant in the microbiome when producing MCCAs in a lactate-based bioreactor (Xu, Hao *et al*. 2017, Zhu, Zhou *et al*. 2017, Carvajal-Arroyo, Candry *et al*. 2019, Duber, Zagrodnik *et al*. 2020). The microbiology and microbial interactions of open cultures are complex, especially with natural wastes as feedstocks. Understanding the microbial interactions is key to optimizing and engineering the bioreactor performance.

pH, temperature, hydraulic, and sludge retention times were essential for controlling one

bioreactor (Cavalcante, Leitão *et al*. 2017). The temperature influences the thermodynamics and kinetic rates of metabolic processes (Kleerebezem and Van Loosdrecht 2010, González-Cabaleiro, Lema *et al*. 2013), as well as microbial structure and dynamics (Hollister, Forrest *et al*. 2010). Most microbial MCCA production has taken place at mesophilic temperatures (between 30˚C and 40˚C; Duber, Jaroszynski *et al*. 2018, Spirito, Marzilli *et al*. 2018, De Groof, Coma *et al*. 2019). Promising microbial MCCA production rates could not be achieved at 55°C with ethnaol as he electron donor (Agler, Spirito *et al*. 2014).

This review will provide a comprehensive introduction to the chain elongation mechanism, functional microbes, available feedstock types, and operating conditions to enhance the performance of MCCA production. In addition, this review will focus more on comparing the difference between ethanol- and lactate- based chain elongation. This work is expected to provide a thorough understanding of chain-elongation technology.

2.2 Chain elongation mechanism and relative competitive reactions

The rBOX is the best-known pathway in the chain elongation process (Seedorf, Fricke *et al*. 2008, Spirito, Richter *et al*. 2014, Tao, Zhu *et al*. 2017). Recently, some research displayed that the fatty acid biosynthesis pathway (FAB) also played an important role in MCCA production (Han, He *et al*. 2018, Wu, Sun *et al*. 2020, Zhu, Feng *et al*. 2021). FAB is a cyclic pathway similar to rBOX but with malonyl-CoA as a 2-C donor (**Figure 2.1**). It is unclear whether FAB plays an important role because all bacterial will use FAB to produce their cell membrane.

The FAB pathway is less efficient than rBOX because acetyl-CoA should be first converted to malonyl-CoA and then transferred to malonyl-ACP before entering the FAB pathway cycle. Additionally, the net consumption of 1 ATP per molecule is required to synthesize malonyl-ACP (Cronan and Thomas 2009, Han, He *et al*. 2018). The reductive tricarboxylic acid cycle was involved in producing *n*-caproate when *M. elsdenii* utilized glucose as substrate (Lee, Lee *et al*. 2020). Here, we only focused on chain elongation *via* rBOX. Open cultures for MCCA production make the bioreactor system robust and flexible, leading to diverse microbial functions. Some thermodynamically feasible metabolic pathways compete with chian elongation and could consume substrates or intermediates, resulting in a lower substrate utilization ratio and MCCA yield (Cavalcante, Leitão *et al*. 2017, Wu, Sun *et al*. 2020). The competition for biological organic

substrates reduces the process efficiency and must be avoided. Here, we will also discuss the main ethanol or lactate competing pathways (*e.g.,* excessive oxidation of ethanol or lactate reduction to propionate).

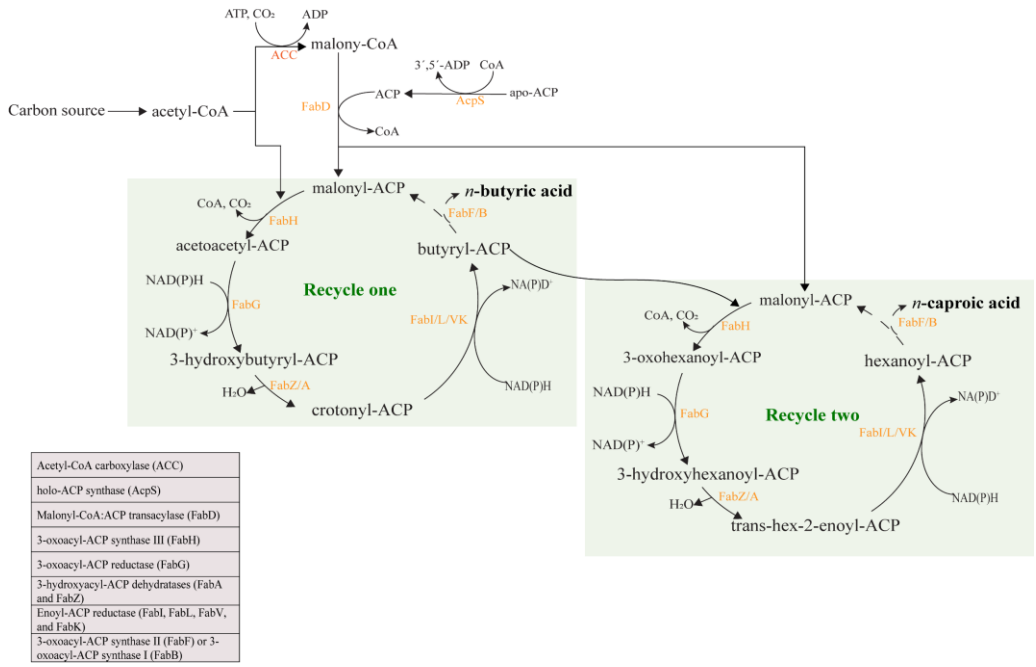

Figure 2.1 The fatty acid biosynthesis pathway (FAB) for MCCA production, adapted from (Han, He *et al*. 2018). The key enzymes in the metabolic pathway are noted in the frame at the bottom left.

2.2.1 Chain elongation mechanism

Chain elongation involves electron donor oxidation and the following cyclic rBOX (Seedorf, Fricke *et al*. 2008, Spirito, Richter *et al*. 2014). The process is separated into three steps (**Figure 2.2**). In the first step, ethanol or lactate is converted to acetyl-CoA, coupling NADH and ATP production. For ethanol, it is oxidized to acetaldehyde by ethanol dehydrogenase and then to acetyl-CoA catalyzed by acetaldehyde dehydrogenase, compared with NADH production. For every 5/6 molecules of acetyl-CoA from ethanol (every 1/5 or 1/6 depends on the substrate concentration; Angenent, Richter *et al*. 2016), one molecule of acetyl-CoA is converted to acetate by substrate-level phosphorylation along with ATP generation. Similarly, the oxidation of lactate to acetyl-CoA starts with pyruvate production by lactate dehydrogenase (Munoz-Tamayo, Laroche *et al*. 2011, Prabhu, Altman *et al*. 2012, González-Cabaleiro, Lema *et al*. 2013). Then the pyruvate is catalyzed to acetyl-CoA by pyruvate dehydrogenase, releasing an equimolar CO_2 and harvesting energy (ATP). Part of the acetyl-CoA from lactate is also converted into acetate by

substrate-level phosphorylation and produces ATP. In each cycle, acetyl-CoA is a 2-C donor, adding two carbon atoms to the initial acyl-CoA or acetate.

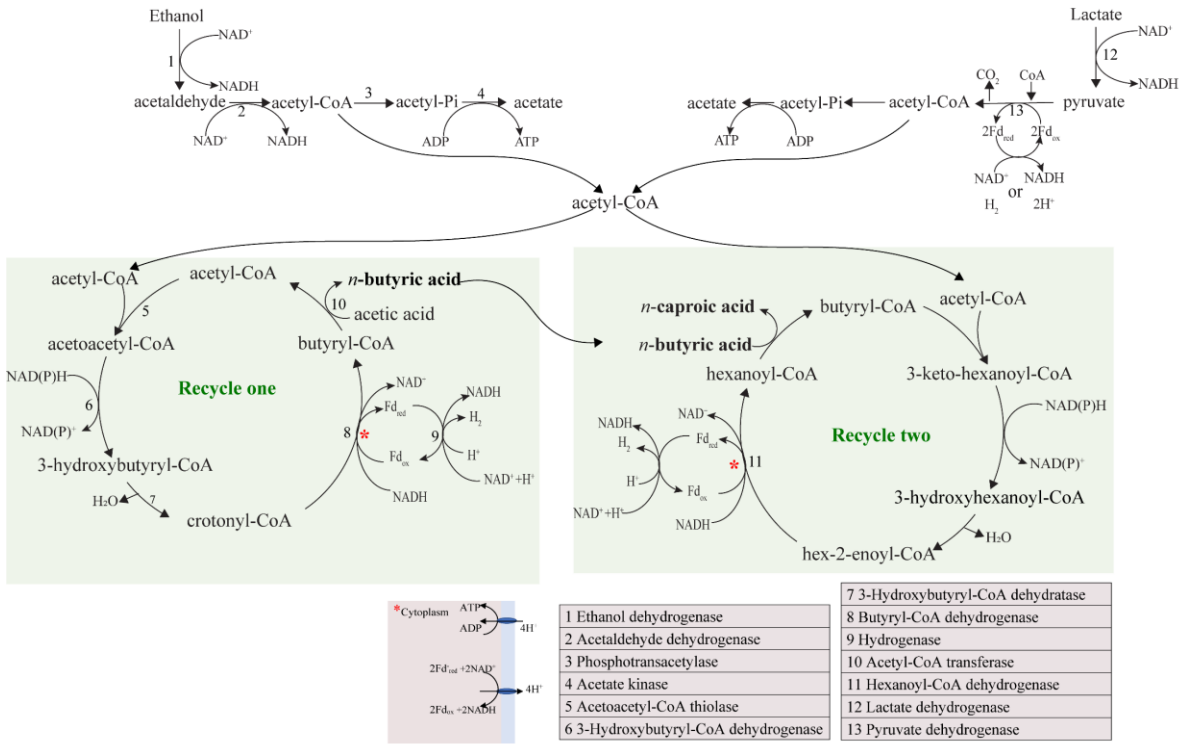

Figure 2.2. Chain elongation with ethanol and lactate as electron donors. Adapted from previous studies (Seedorf, Fricke *et al*. 2008, Prabhu, Altman *et al*. 2012, Spirito, Richter *et al*. 2014). The key enzymes in the metabolic pathway are labeled with numbers of 1-13 that are explained at the lower left figure.

The second step is rBOX. The rBOX pathway is a cyclic process that elongates the original carboxylate chain length with two carbon atoms (C2) in the form of the acetyl-CoA molecule. For example, acetate elongates to *n*-butyrate and *n*-caproate (**Figure 2.2**). One acetyl-CoA coupled to another acetyl-CoA is catalyzed by acetoacetyl-CoA thiolase to generate acetoacetyl-CoA. Then acetoacetyl-CoA is gradually converted into different intermediates (**Figure 2.2**) *via* a series of enzymatic reactions (involving the enzymes NAD- and NADP-dependent 3-hydroxybutyryl-CoA dehydrogenase, 3-hydroxybutyryl-CoA dehydratase, and NAD-dependent butyryl-CoA dehydrogenase). Finally, acetate-CoA transferase catalyzes the transfer of CoA between butyryl-CoA and acetate, along with butyrate generation and acetyl-CoA release.

The released acetyl-CoA is recycled with other acetyl-CoA from ethanol or lactate oxidation to begin a new acetate-based elongation. The critical intermediates butyryl-CoA from the last

cycle with one new acetyl-CoA could also start the second *n*-butyrate-based elongation cycle to *n*-caproate with 3-ketohexanoyl-CoA, 3-hydroxyhexanoyl-CoA, hex-2-enoyl-CoA, and hexanoyl-CoA as intermediates. MCCA products host both even-carbon chains and odd-carbon chains, which are determined by the substrate. If the substrate is propionate (odd-chain electron acceptor), the product will be odd-chain products (*e.g., n*-valerate or *n*-heptanoate, **Figure 2.3).**

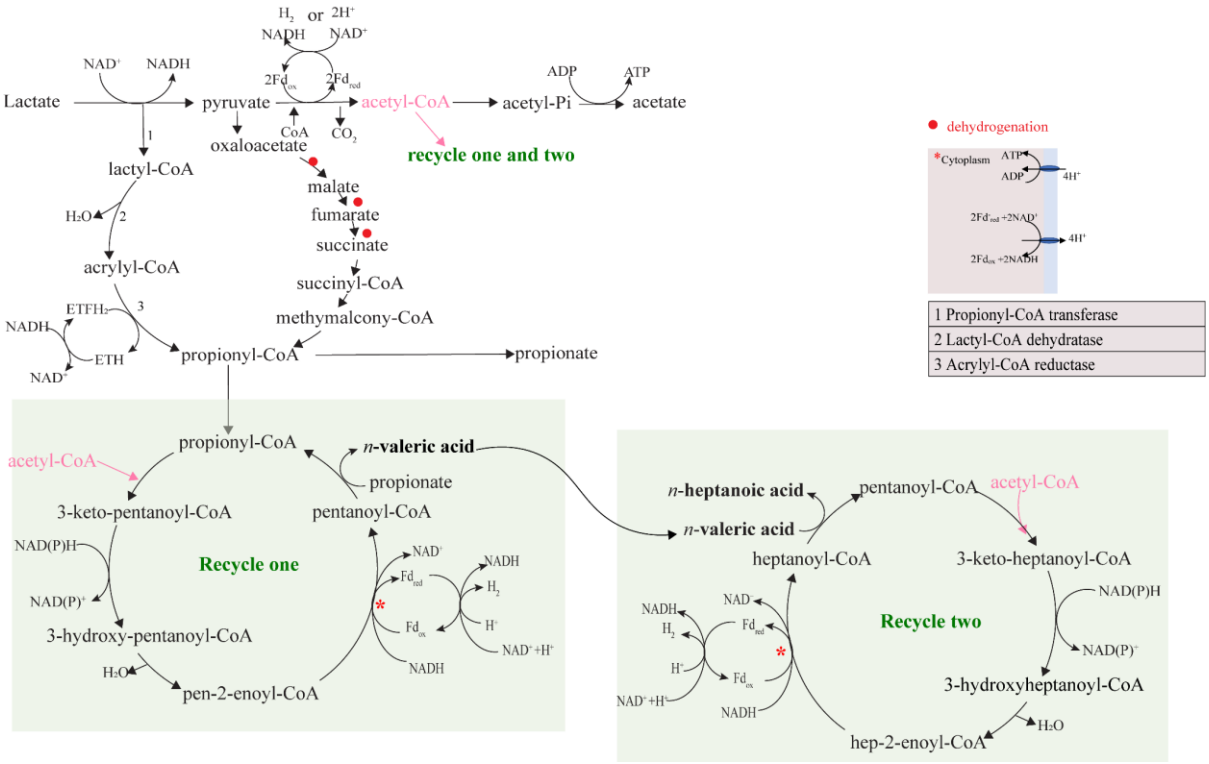

Figure 2.3. Propionate production from lactate and further chain elongtion to odd-chain MCCAs. Adapted from previous studies (Seedorf, Fricke *et al.* 2008, Prabhu, Altman *et al*. 2012, Spirito, Richter *et al*. 2014). The key enzymes in the metabolic pathway are labeled with numbers of 1-3 that are explained in the upper-right frame.

During rBOX, energy (ATP) harvest occurs in the energetically favorable process of crotonyl-CoA reduction to butyryl-CoA (E0′ = -10mV) with NADH (E0′ = -320 mV) and hex-2-enoyl-CoA reduction to hexanoyl-CoA (E0′ = -10mV) with NADH (E0′ = -320 mV) *via* proton translocation from the oxidation of reduced ferredoxin (Fd_{red}). Two enzymes in this energy metabolism process are ferredoxin:NAD oxidoreductase (RnfA-E) and ATP-synthase (AtpA-I), which are associated with the cell membrane (Seedorf, Fricke *et al*. 2008, González-Cabaleiro, Lema *et al*. 2013, Spirito, Richter *et al*. 2014, Angenent, Richter *et al*. 2016). The biochemical reactions and thermodynamic information of some pathways are shown in **Table 2.1.**

Table 2.1 Chain elongation reactions *via* ethanol and lactate			
Equation	Chain Elongation Stoichiometry	ΔG_r° (kJ mol^{-1})	Reference
Ethanol-based overall chain elongation			
2.1	Ethanol oxidation		
	$(CH_3CH_2OH + H_2O \rightarrow CH_3COO^- + H^+ + 2H_2)$ ×1	10.50	(Spirito, Richter *et al*. 2014)
2.2	5× Reverse β-oxidation to C4		
	$(CH_3CH_2OH + CH_3COO^- \rightarrow CH_3(CH_2)_2COO^- + H_2O)$ × 5	-193.00[a]	(Spirito, Richter *et al*. 2014)
$6CH_3CH_2OH + 4CH_3COO^- \rightarrow 5CH_3(CH_2)_2COO^- + H^+ + 2H_2 + 4H_2O$		-182.50 [a]	(Spirito, Richter *et al*. 2014)
2.3	Ethanol oxidation		
	$(CH_3CH_2OH + H_2O \rightarrow CH_3COO^- + H^+ + 2H_2)$ × 1	10.50	(Spirito, Richter *et al*. 2014)
2.4	Reverse β-oxidation to C6		
	$(CH_3CH_2OH + CH_3(CH_2)_2COO^- \rightarrow CH_3(CH_2)_4COO^- + H_2O)$ × 5	-194.00 [a]	(Spirito, Richter *et al*. 2014)
$6CH_3CH_2OH + 5CH_3(CH_2)_2COO^- \rightarrow CH_3COO^- + 5CH_3(CH_2)_4COO^- + H^+ + 2H_2 + 4\ H_2O$		-183.50 [a]	(Spirito, Richter *et al*. 2014)
Lactate-based overall chain elongation			
2.5	Lacate to acetate for ATP generation		
	$CH_3CH(OH)COO^- + H_2O \rightarrow CH_3COO^- + 2H_2 + CO_2$	-8.79	(Cavalcante, Leitão *et al*. 2017)
2.6	Overall chain elongation to C4		
	$CH_3CH(OH)COO^- + CH_3COO^- + H^+ \rightarrow CH_3(CH2)_2COO^- + H_2O + CO_2$	-57.52	(Cavalcante, Leitão *et al*. 2017)
2.7	Overall chain elongation to C6		
	$CH_3CH(OH)COO^- + CH_3(CH_2)_2COO^- + H^+ \rightarrow CH_3(CH_2)_4COO^- + H_2O + CO_2$	-57.56	(Cavalcante, Leitão *et al*. 2017)
*Thermodynamic information with concentrations and pressures of all components at 1 M or 1 bar, pH=7 at 25°C. [a] the unit is kJ/5 mol of product .			

2.2.2 Stoichiometric model

A stoichiometric model was first built for chain elongation to *n*-caproate *via* rBOX (Angenent, Richter *et al*. 2016), which was later developed to predict the thermodynamic favorability of *n*-caprylate formation at different ethanol-to-acetate substrate ratios (Spirito, Marzilli *et al*. 2018) (**Figure 2.4**). In the research of Spirito *et al*., the result showed that for the most part, the model described what they observed experimentally.

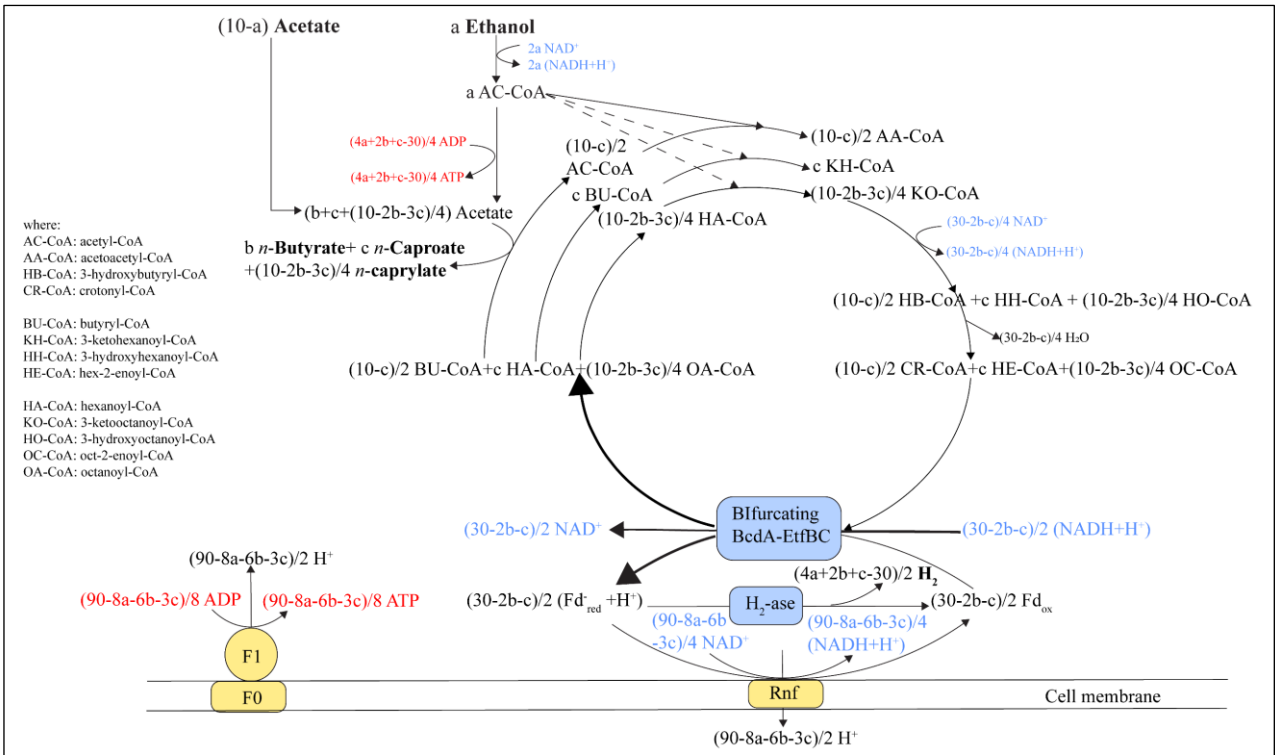

Figure 2.4 Visualization of the stoichiometric model for the fermentation of ethanol and acetate to *n*-butyrate, *n*-caproate, *n*-caprylate, and molecular hydrogen by C. *kluyveri*. This model is the extended version of the model developed by Angenent *et al*. (Angenent, Richter *et al*. 2016), and was developed for relatively high substrate and product concentrations with relatively low partial pressures of hydrogen gas. The variable "a" represents moles of ethanol, "b" represents moles of *n*-butyrate, and "c" represents moles of *n*-caproate. Boundaries for "a" are mentioned in the text. Redox factors are highlighted in blue; energy conservation in red font; and recently described mechanisms of energy conservation by transport-coupled phosphorylation in yellow. F_0F_1 is H^+ /Na^+-pumping ATP synthase complex and Rnf is the ferrodoxin-NAD reductase complex.

In the research of Spirito *et al*., the model uses stoichiometric relationships to evaluate the moles of *n*-caprylate, *n*-caproate, *n*-butyrate, hydrogen gas, and ATP that would be produced based on the moles of ethanol and acetate provided to the bacteria. The maximum boundary for the metabolic flux is set to 10 mol of ethanol and acetate combined (by setting moles of ethanol to "a" and moles of acetate to "10 - a", **eq 1.8**) and with a total of 20 mol of carbon for the substrate and the products. "b" and "c" represent the mole of *n*-butyrate, and *n*-caproate. The stoichiometry of all other metabolites (*e.g*., *n*-caprylate, molecular hydrogen, water, intermediary metabolites, redox mediators, and ATP) depended on the variables "a", "b", and "c". Similarly, the

stoichiometry for reoxidation of reduced ferredoxin *via* H_2-ase or Rnf and ATP synthase varied depending on the variables "a", "b", and "c", which determined the molecular hydrogen production and ATP production, respectively (**Figure 2.4**). The net consumption of one mole of water during acetate production from acetyl-CoA *via* substrate level phosphorylation (due to ATP hydrolysis) was considered when balancing the overall equation. Spirito *et al*., tested three scenarios by varying the values of "b" and "c" (*e.g.,* moles of *n*-butyrate and *n*-caproate in the stoichiometric equation), for which the most part of the model described what was observed experimentally. The model predicted that higher ethanol-to-acetate ratios which was experienced by the bacteria led to more favorable thermodynamic conditions for chain elongation to *n*-caprylate. In addition, the model predicted that higher ethanol-to-acetate ratios lead to higher ATP yields.

Eq 2.8: ethanol to C8:

$$a\ C_2H_6O + (10 - a)\ C_2H_3O_2^- \longrightarrow b\ C_4H_7O_2^- + c\ C_6H_{11}O_2^- + (10 - 2b - 3c)/4\ C_8H_{15}O_2^- + (30 - 2a - 2b - c)/2\ H_2O + (4a + 2b + c - 30)/2\ H_2 + (4a + 2b + c - 30)/4\ H^+ + (30 - 2b - c)/8\ ATP$$

I compared the ΔG^0 produced when *n*-butyrate, *n*-caproate, or *n*-caprylate was dominant product based on **eq 2.8**. The standard Gibbs free energy of formation values except *n*-caprylate were from Kleerebezem and van Loosdrecht (Kleerebezem and Van Loosdrecht 2010) and the standard Gibbs free energy of formation for *n*-caprylate was calculated to be -323.8 kJ mol^{-1} with the group contribution method (Mavrovouniotis 1990). The Gibbs free energy of formation for all the compounds under other conditions were calculated with the method from previous research (Alberty 1998, Alberty 2001).

For the ethanol-based chain elongation, we tested three different ratios of ethanol to acetate with **eq 2.8**. When a longer-chain MCCA (*e.g., n*-caprylate) was the main product, there will be more energy released either with different ratios of ethanol to acetate or different temperatures (**Table 2.2** and **Figure 2.5**). When *n*-butyrate was the dominant product in **eq 2.8**, with increasing temperature, the reaction became more and more unlikely to occur (**Figure 2.5 A**). Only under standard conditions (25°C; pH=7.0) with the ratio of ethanol to acetate at 8:2, the Gibbs energy value was negative, which means that only under this condition the reaction with *n*-butyrate as a dominant product in **eq 2.8** was spontaneous. When *n*-caproate was the dominant product in **eq 2.8**, with the increasing temperature, more energy was released (**Figure 2.5 B**). When the ratio of ethanol and acetate was at 10:0, producing *n*-caproate as the main product in **eq 2.8** only happens

at standard conditions. When *n*-caprylate was the dominant product in **eq 2.8**, all reactions under different conditions were thermodynamically feasible.

Table 2.2 ΔG^0 from the reaction in **eq 2.8** with different dominant products under different ratios of ethanol to acetate (kJ mol^{-1})

Dominant products	Ratios of ethanol to acetate	Temp (°C) - pH				
		25-7	25-5.5	30-5.5	37-5.5	42-5.5
n-butyrate	10:0	53.00	368.70	366.20	360.25	351.85
n-caproate		-100.46	102.75	101.10	97.19	91.67
n-caprylate		-176.60	-20.75	-22.20	-25.63	-30.45
n-butyrate	9:1	3.60	256.36	254.36	249.62	243.30
n-caproate		-149.86	-9.60	-10.74	-13.44	-16.89
n-caprylate		-226.00	-133.09	-134.04	-136.26	-139.00
n-butyrate	8:2	-45.80	144.02	142.52	138.99	134.75
n-caproate		-199.26	-121.94	-122.58	-124.07	-125.44
n-caprylate		-275.40	-245.43	-245.88	-246.89	-247.55

The ratio of ethanol to acetate was changed until the stoichiometry of any compounds in **eq 2.8** was negative.

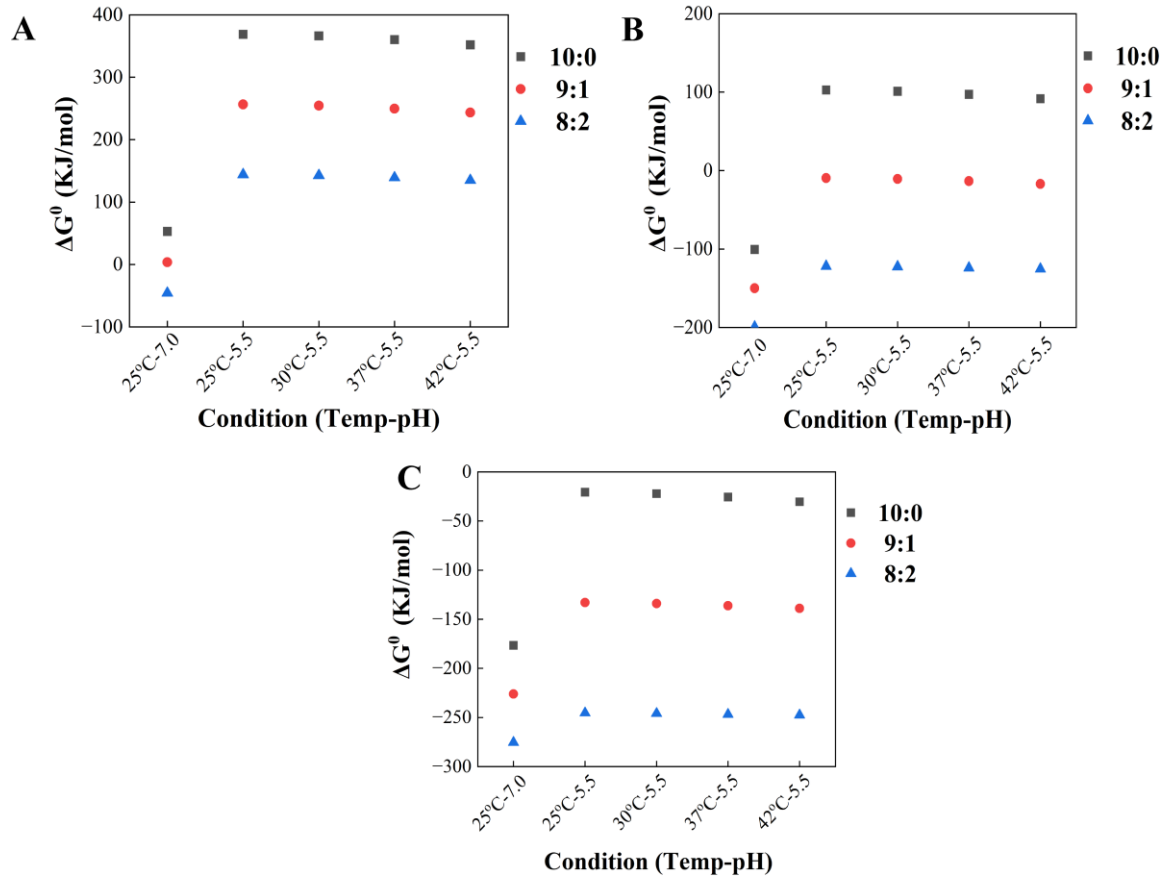

Figure 2.5 Gibbs free energy of the reaction in **eq 2.8** with *n*-butyrate (A), *n*-caproate (B), or *n*-caprylate (C) as dominant products under different ratios of etahnol to acetate and different conditions (temp-pH).

When increasing the ratio of ethanol to acetate, less energy was released (**Figure 2.5 C**), while more energy was produced when increasing the temperature. The above results implied that

a longer MCCA was more favorable to be produced and a higher ratio of ethanol to acetate was suitable for the reaction to *n*-butyrate, *n*-caproate, or *n*-caprylate happen.

2.2.3 competitive pathways

2.2.3.1 Excessive oxidation of ethanol

Excessive ethanol oxidation (**Table 2.3, eq 2.10**) is performed by ethanol-oxidizing microorganisms rather than the chain elongating bacterium, especially with a large amount of ethanol as substrate (Grootscholten, Strik *et al*. 2014, Ge, Usack *et al*. 2015, Roghair, Hoogstad *et al*. 2018). Excessive ethanol oxidation led to the reduction of ethanol into acetyl-CoA and a consequent decrease in MCCA production. The chain elongating bacterium can oxidize ethanol at a higher pH_2 than other ethanol-oxidizing microorganisms (Li, Hinderberger *et al*. 2008). So, making excessive ethanol oxidation thermodynamically unfavorable *via* adjusting the pH_2 ($0.03 < pH_2 < 0.1$ atm) can benefit the conversion of ethanol into acetyl-CoA for MCCA production (Li, Hinderberger *et al*. 2008, Grootscholten, Strik *et al*. 2014, Angenent, Richter *et al*. 2016). Controlling the H_2 flow for the chain-elongation process is the direct way to adjust the pH_2. Some studies also showed that CO_2 content in the system could affect the pH_2 because of hydrogenotrophic methanogenesis. When the CO_2 content is low enough, hydrogenotrophic methanogen is limited (Ge *et al*., 2015), resulting in high pH_2. Conversely, hydrogenotrophic methanogenesis consumes more H_2 with enough CO_2, which leads to low pH_2, and thus facilitates excessive ethanol oxidation.

2.2.3.2 Lactate oxidation into propionate

Lactate can be converted into propionate in open cultures *via* the acrylate pathway (Prabhu, Altman *et al*. 2012). Kucek *et al*. first discussed that the acrylate pathway (**Figure 2.3**) can compete with chain elongation in open cultures (Kucek, Nguyen *et al*. 2016). The author found that some *n*-valerate, which is a chain elongation product from propionate, was produced, especially during periods when residual lactate concentrations were non-zero. Later, Nzeteu *et al*. also found propionate accumulation *via* the acrylate pathway (Nzeteu, Trego *et al*. 2018). Under lactate-rich conditions, lactyl-CoA forms as an intermediate and is converted to acryl-CoA and propionyl-CoA. Consequently, available lactate would be continually directed towards propionate production (Prabhu, Altman *et al*. 2012). This pathway is mediated by propionyl-CoA transferase, lactyl-CoA dehydratase, and acrylyl-CoA reductase (Tholozan, Touzel et al. 1992, Hetzel, Brock et al. 2003). In addition to the acrylate pathway, the succinate pathway was also found to convert lactate into propionate with *Selenomonas ruminantium* subsp. *lactilytica* strains 63 and 73, *Veillonella parvula* strain 803, and *Propionibacterium acnes* strain 81 (Counotte 1981).

Competing pathways could disappear or be outcompeted based on some unique environmental selection process: **1)** a low residual concentration of lactate would be necessary to prevent the production of propionate *via* the acrylate pathway (Prabhu, Altman *et al*. 2012, Kucek, Nguyen *et al*. 2016); **2)** a lower pH ($5 < pH < 6$) stimulate lactate-based chain-elongating bacteria through kinetic effects and improve MCCA production (Kucek, Nguyen *et al*. 2016, Candry, Radic *et al*. 2020).

2.2.3.3 Methanogens

Methanogens include acetoclastic methanogens and hydrogenotrophic methanogens, which consume acetate and H_2 and CO_2. Methanogens are not a competitor for ethanol or lactate. However, acetate could come from excessive ethanol oxidation, and acetate consumption for methane production facilitates more excessive ethanol oxidation (EEO) due to acetate removal. Moreover, the high activity of hydrogenotrophic methanogens consumes more H_2, which may reduce the pH_2 and lead to more EEO (Agler, Spirito *et al*. 2012, Roghair, Hoogstad *et al*. 2018). Therefore, we consider methanogens as a competitive pathway for ethanol- and lactate-based chain elongation, albeit inderectly, and discuss it in this chapter.

Grootscholten *et al*. reported that shortening the hydraulic retention time (HRT) to 4 h to suspend methanogens forming a biofilm at pH=6.5-7 could achieve the highest MCCA production rate (57.4 g L^{-1} d^{-1}). However, this method might only be applicable in an up-flow reactor (Grootscholten, Steinbusch *et al*. 2013). Then, the main methods are to inhibit methanogen: **1)** adding methanogen inhibitors, such as 2-bromoethanesulfonic acid (2-BES; Zinder, Anguish et al. 1984, Siriwongrungson, Zeng et al. 2007) and $CHCl_3$ (Arslan, Steinbusch *et al*. 2013); **2)** decreasing pH to weakly acidic value. Steinbusch *et al*. achieved sustainable *n*-caproate (8.17 g L^{-1}) and *n*-caprylate (0.32 g L^{-1}) production at pH=7 for 115 d by adding 10 g L^{-1} 2-BES to suppress methanogenesis. However, the high cost of chemical addition could considerably increase the MCCA production cost. Controlling an appropriate weakly acidic pH could be a more general method. Part of the MCCAs exists in the undissociated forms under weakly acidic pH conditions (Agler, Spirito *et al*. 2012). The methanogens are susceptible to the toxicity of undissociated MCCAs (Cavalcante, Leitão et al. 2017), but chain-elongating bacteria resist the toxic effects of undissociated MCCAs within a specific concentration range (Ge, Usack *et al*. 2015, Roghair, Liu *et al*. 2018). The chain-elongating bacteria became inhibited at undissociated *n*-caproic acid concentrations of 6.9 mM (Weimer, Nerdahl *et al*. 2015), 7.5 mM (Ge, Usack *et al*. 2015), and 17.2 mM (Duber, Jaroszynski *et al*. 2018), respectively.

Table 2.3 Biochemical reactions that compete with chain elongation[a]

Equation	Process	Stoichiometries	$\Delta G_r°$ (kJ mol^{-1})	Reference
2.10	Ethanol oxidation: as determined for *C. formicoaceticum*	$2CH_3CH_2OH + 2CO_2 \rightarrow 3CH_3COO^- + 3H^+$	-76.90[b]	(Arslan, Steinbusch *et al*. 2016)
2.11	Lactate reduction to propionate: as found in *Selenomonas ruminantium*	$CH_3CH(OH)COO^- + H_2O \rightarrow CH_3COO^- + CO_2 + 2H_2 \times 1$	28.5[c]	(Agler, Wrenn *et al*. 2011)
		$CH_3CH(OH)COO^- + H_2 \rightarrow CH_3CH_2COO^- + H_2O \times 2$	-86.63[c]	
			Total = -58.12	
2.12	Lactate reduction to propionate: as determined for *C. propionicum*	$CH_3CH(OH)COO^- + H_2 \rightarrow CH_3CH_2COO^- + H_2O$	-83.80[b]	(Arslan, Steinbusch *et al*. 2016)
2.13	Hydrogenotrophic methanogenesis	$4H_2 + CO_2 \rightarrow CH_4 + 2H_2O$	-130.74[b]	(Agler, Wrenn *et al*. 2011)
2.14	Acetoclastic methanogenesis	$CH_3COO^- + H^+ \rightarrow CH_4 + CO_2$	-39.06[c]	(Agler, Wrenn *et al*. 2011)

[a]Thermodynamic information with concentrations and pressures of all components at 1 M or 1 bar: [b] 25 °C, pH=7; [c] 37 °C, pH=6.82.

2.3 Reactor operating conditions

Reactor conditions, such as operating pH, temperature, and different gas partial pressures, become essential selective pressure tools that could determine the substrate utilization and the product spectrum. This work summarized the research on the effect of operating parameters on the MCCA-producing process.

2.3.1 Gas partial pressure

The pH_2 is vital in MCCA production *via* chain elongation (Angenent, Richter *et al*. 2016, De Groof, Coma *et al*. 2019). First, adequate pH_2 avoids the oxidation of carboxylates or excessive oxidation of ethanol. Ge *et al.* have calculated at certain experimental conditions that the pH_2 limits for oxidation of acetate was 1.45×10^{-4} atm, for *n*-butyrate was 6.65×10^{-6} atm, and for *n*-caproate was 2.52×10^{-6} atm (Ge, Usack *et al*. 2015). When controlling the pH_2 at 0.007% at standard conditions, the excessive oxidation of ethanol would be inhibited (Roghair, Hoogstad *et al*. 2018). On the other hand, H_2 is a byproduct of ethanol- or lactate- oxidation at the first step of chain elongation (Spirito, Richter *et al*. 2014), so high pH_2 (above ~0.1 bar) could reduce the thermodynamic favorability of the chain elongation process (Rodriguez, Kleerebezem *et al*. 2006, Angenent, Richter *et al*. 2016). In addition, carboxylates are reduced to their corresponding alcohol when pH_2 exceeds ~1.5 bar (Steinbusch, Hamelers *et al*. 2008), even though this is a relative slow process.

The CO_2 partial pressure (pCO_2) is also an important parameter for microbial MCCA production *via* chain elongation (De Groof, Coma *et al*. 2019). The growth of *C. kluyveri*, which is the most well-known chain elongating bacterium, needs nutritional CO_2 (Tomlinson and Barker 1954). In addition, pCO_2 influences dissolved carbonate, and thus the alkalinity. Experimental studies have also shown that CO_2 addition in the headspace improved chain elongation (Grootscholten, Steinbusch et al. 2013, Roghair, Hoogstad et al. 2018) and a combination of CO_2 and H_2 in the reactor headspace reduced SCCAs (*e.g.,* propionate) formation (Arslan, Steinbusch et al. 2012, Wu, Guo et al. 2019). The ratio of H_2 to CO_2 could also affect the process of chain elongation. Weimer *et al*. suggested that a ratio of H_2 to CO_2 at about 1 to 0.3 bar was the optimal thermodynamic condition for chain elongation (Weimer and Kohn 2016).

2.3.2 Temperature

The temperature has a considerable influence on the energy released and the kinetic rates of metabolic reactions (Kleerebezem and Van Loosdrecht 2010). For a given pure culture, the optimal temperature range was from 28ºC to 55ºC (mostly at 37ºC, 38ºC, and 39ºC) (**Figure 2.6**). The optimal temperature range for microbial MCCA production with open cultures was wider and

changed from 30ºC to 37ºC (**Figure 2.6**). 30ºC was the most used operating temperature for ethanol-based and lactate-based chain elongation. A study by Agler *et al*. showed that promising MCCA production rates with ethanol could not be achieved at 55ºC (Agler, Spirito *et al*. 2014). However, recently, a study from Zhang *et al*. displayed that a lactate-based semi-continuous bioreactor produced *n*-caproate with a maximum concentration of 10.23 g COD L^{-1} at 55ºC (Zhang, Pan et al. 2022). In the research of Zhang *et al.*, the specificity for *n*-caproate was the highest at 40.19 ± 3.95%, and the soluble COD conversion rate of *n*-caproate reached up to 22.50 ± 1.09% at the end of batch fermentation. Strain MDTJ8 is a thermophilic and sugar-utilized chain-elongating bacterium. It was isolated from a thermophilic acidogenic anaerobic digestor producing *n*-caproate from human waste, growing optimally at 50-55°C and pH=6.5 (Tinh Van Nguyen 2023). It is possible that some newly thermophilic and lactate-utilized chain-elongating bacteria could be isolated from the bioreactor of zhang *et al.*

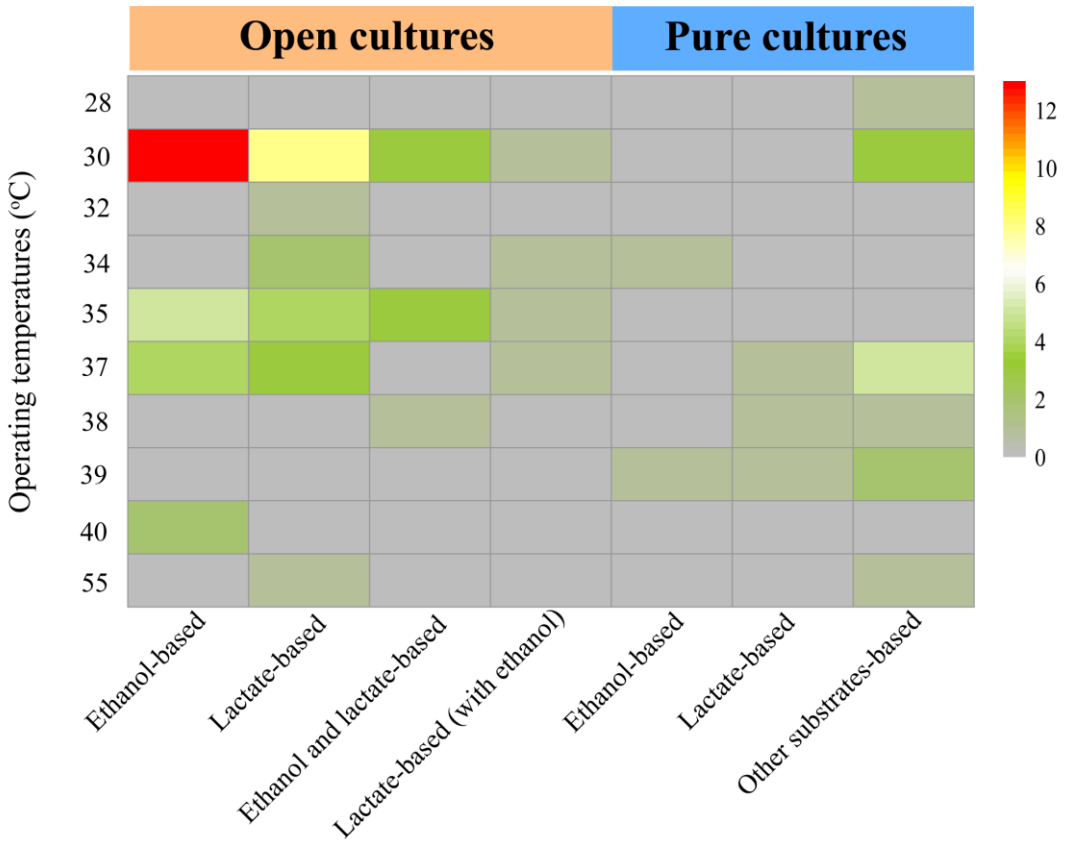

Figure 2.6 The heatmap of the operating temperature of different MCCA-producing process in pure or open cultures with different electron donors. Ethanol-/ lactate-/ ethanol and lactate-/ lactate- (with ethanol)/ other substrates- based mean MCCA production with ethanol, lactate, both ethanol and lactate, lactate (with ethanol), or other compounds that serve as electron donors. The data was from **Tables 2.4** and **2.5.**

When using some real waste for MCCA production, it may require pre-fermentation for which heat is one of the methods (Xu, Hao *et al*. 2017, Zhang, Wang *et al*. 2022). A two-stage system

was used for *n*-caproate production from acid whey (Xu, Hao *et al*. 2017). In that research, the temperature of 50ºC was set in the first stage for lactate production. While, the operating tempearature of 37ºC was set in the second stage for *n*-caproate production. In addition, the temperature has a specific effect on the extraction efficiency in the MCCA-producing system with in-line MCCA extraction set. In the research of Yesil *et al*., the increase in temperature enhanced the coextraction of water with amine-acid complexes, which led to decreased *n*-valerate and *n*-caproate permeance with elevated temperature (Yesil, Taner *et al*. 2018).

2.3.3 pH

The pH is one of the most important operating factors in chain elongation process, which could affect the thermodynamics of metabolic pathways, hydrolysis, and product spectrum (Angenent, Richter *et al*. 2016, Tang, Wang *et al*. 2017, Sträuber, Bühligen *et al*. 2018, De Groof, Coma *et al*. 2019, Candry, Radic *et al*. 2020).

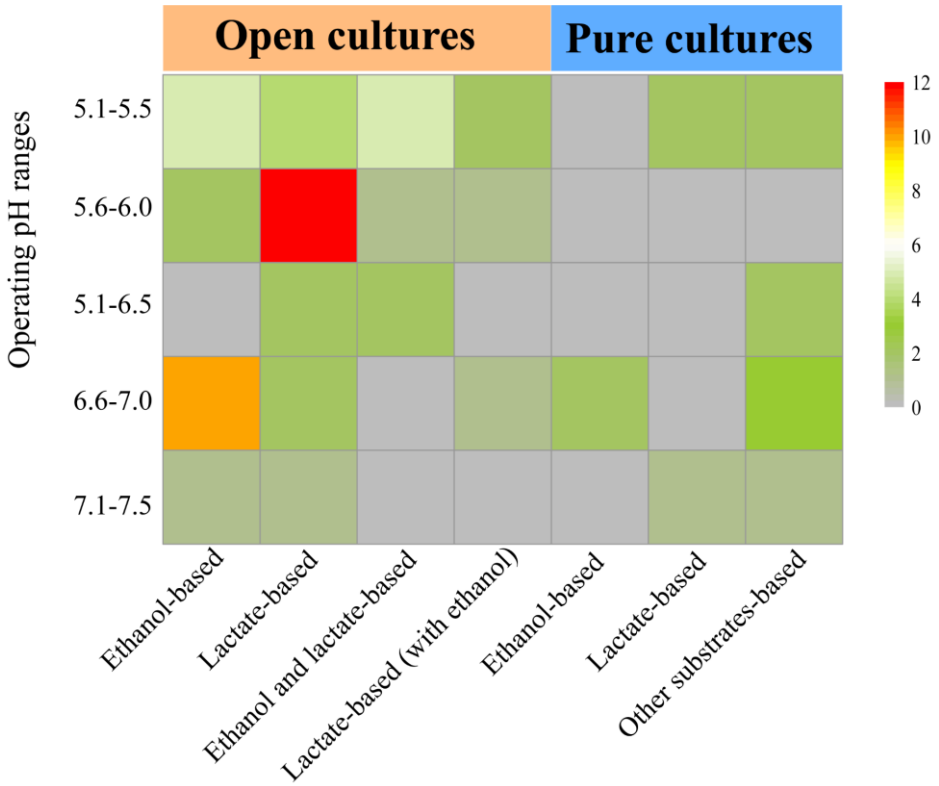

Figure 2.7 The heatmap of the operating pH of different MCCA-producing process in pure or open cultures with different electron donors. Ethanol-/ lactate-/ ethanol and lactate-/ lactate-(with ethanol)/ other substrates-based mean MCCA production with ethanol, lactate, ethanol and lactate, lactate (with ethanol), or other compounds serve as electron donors. The data was from **Tables 2.4** and **2.5.**

Compared with pure cultures, microbial MCCA production in open cultures was more challenging to control because open cultures contain various communities (Han, He *et al*. 2019). For ethanol-based MCCA production systems with open cultures, a pH range of 6.6-7.0 was most applied

among all research (**Figure 2.7**). In contrast, lactate-based chain elongating bacterium can produce MCCA in an either acidic or neutral environment (5.1-5.5 and 7.1-7.5). Interestingly, when open cultures with lactate as substrate were used for MCCA production, the pH range of 5.6-6.0 was most used. When ethanol and lactate served as co-electron donors, most studies with open cultures were performed at a pH of 5.1-5.5. One reason could be that these well-known pure cultures were not the functional microbiomes for MCCA production in the bioreactor (Candry and Ganigue 2021), which also reminded us the possibility that there were more unknown chain-elongating bacteria or mechanisms.

The operating pH was an influential control factor determing the substrate utilization and product spectrum. When ethanol and lactate served as co-electron donors, lactate was more favorable to be utilized at a pH 5.5, with the highest *n*-caproate production. In contrast, ethanol was favorable to be utilized at pH=6.25, with the highest *n*-caprylate production (Lambrecht, Cichocki *et al*. 2019). A lower pH (below 6) inhibited the production of propionate, thus, increasing *n*-caproate production (Kucek, Nguyen *et al*. 2016, Candry, Radic *et al*. 2020). The acidic pH could also suppress methanogenesis (Agler, Spirito *et al*. 2014). Studies displayed that a concentration of undissociated carboxylates higher than 5.0 mM could inhibit methanogenesis (Grootscholten, Kinsky dal Borgo *et al*. 2013). De smit *et al*. found a decreasing relative abundance of methane-producing archaea of the family Thermoplasmatales, from 5.8 to 5.5 (de Smit, de Leeuw *et al*. 2019). The inhibition of methanogenesis led to more carbon flow to chain elongation, rather than methanogenesis (Kleerebezem and van Loosdrecht 2007).

In addition, the pH could affect the dissolution equilibrium of organic acids. The status of H_2CO_3 affected the pCO_2, which was essential to MCCA production (Roghair, Hoogstad *et al*. 2018). *n*-Caproate (pKa at 4.85) and *n*-caprylate (pKa at 4.89) are known to be about 50% of the total carboxylate in the acidic form at a pH equal to their pKa (De Groof, Coma *et al*. 2019). Different inhibitory concentrations in open cultures for chain elongation have been reported. According to Weimer *et al*., the undissociated *n*-caproic acid was toxic in concentrations higher than ~6.9 mM at pH=5.7 (Weimer, Nerdahl *et al*. 2015). Likewise, Ge *et al*. found that the undissociated *n*-caproic acid was toxic in concentrations higher than ~7.5 mM at a pH =5.5 (Ge, Usack *et al*. 2015). Therefore, methods avoiding the toxic effect of MCCAs, such as extraction, seemed necessary for such anaerobic systems.

2.3.4 extraction

As mentioned above, the accumulation of undissociated MCCAs can inhibit chain-elongating microbiomes. Therefore, the sustainable technology of microbial MCCA production requires

preventing product inhibition. Selective extraction of MCCAs concurrently with their generation was a potential solution for this issue, which also laid the foundation for the industrial application (Agler, Spirito *et al*. 2012, Xu, Guzman *et al*. 2015, Cavalcante, Leitão *et al*. 2017). In addition, the extraction and separation of MCCAs from the fermentation broth are also necessary for further application in the industry (Xu, Bian *et al*. 2021). Here, we summarized the extraction methods for MCCAs used in previous studies.

1) Off-line extraction. Biphasic extraction of *n*-caproate has been reported for batch assays with pure cultures (Choi, Jeon *et al*. 2013). Biphasic extraction transferred MCCAs from the aqueous phase to an extraction medium, and the extraction medium contained extractors and solvents (Tarasov, Borzenkov *et al*. 2011). Wang *et al*. used trialkylphosphine oxide dissolved in kerosene to extract *n*-caproate (Yundong Wang 2001). The tri-n-butyl phosphate (TBP) with benzene and toluene was also effective for *n*-caproate extraction (Shende 2010). Recently, an electrodialysis system was tested for recovering carboxylates from a model solution, mimicking the effluent of a microbial electrochemical system producing SCCAs and MCCAs. Under batch extraction conditions, the electrodialysis scheme enabled the recovery of 60% (mol mol^{-1}) of the total carboxylic acids present in the model fermentation broth. The particular arrangement of conventional monopolar ion exchange membranes and hydraulic recirculation loops allowed the progressive acidification of the extraction solution, enabling phase separation of *n*-caproate as an immiscible oil with 76% purity (Hernandez, Zhou et al. 2021).

2) In-line extraction. **I)** Biphasic extraction. Choi *et al*., operated an *in-situ* biphasic extraction system with alamine 336 in oleyl alcohol to achieve simultaneous MCCA production and extraction, and about a four times increase in *n*-caproate production was presented with this *in-situ* biphasic extractive fermentation system (Choi, Jeon *et al*. 2013); **II)** Membrane-based liquid-liquid extraction (*e.g.,* pertraction). Pertraction for in-line extraction of MCCAs has been well studied due to its low energy cost (mainly requiring electric power to pump the fermentation broth, hydrophobic solvent, and pertraction solution) and selective extraction of the longest possible carbon chain of carboxylate (Agler, Spirito *et al*. 2012, Angenent, Usack *et al*. 2018). This system contained forward and backward membranes (hydrophobic hollow-fiber membrane), with trioctylphosphine oxide (TOPO) dissolved in mineral oil as the solvent. The driving force for this system was a pH gradient (~5.0-9.4). In the forward membrane, the low solubility of MCCAs in fermentation broth (~ 5-5.5) facilitated its transfer into the oil side. Then in the second membrane, the MCCAs were re-extracted into an alkaline solution (pH=9.4). This extraction technology avoided direct contact between the extraction solvent and the microbiome. Additionally, the

extraction rates could be increased by expanding the membrane contact area between the biotic and extraction media (Agler, Spirito *et al*. 2012). This in-line extraction system improved the volumetric *n*-caproate production rate (Kucek, Nguyen *et al*. 2016).

Recently, a novel pertraction system with submerged hollow-fiber membranes in the fermentation bioreactor was applied and achieved the highest average surface-corrected MCCA extraction rate of 655.2 ± 86.4 mmol C m^{-2} d^{-1}, which was higher than any other previous reports (Xu, Bian *et al*. 2021). This submerged extraction system could continuously extract MCCAs with a high extraction rate for more than eight months. The average extraction rate of MCCAs by internal membrane was 3.0- to 4.7- fold higher than the external pertraction (traditional pertraction) in the same bioreactor.

III) The combination of the membrane electrolysis cell with the pertraction extraction unit. Xu *et al*. connected the bioreactor, membrane liquid-liquid extraction (pertraction) system, and membrane electrolysis cell to to separate undissociated MCCAs continuously. An oil solution with over 90% *n*-caproate and *n*-caprylate formed in this system, which made the direct *n*-caproate extraction from the biotic medium possible (Xu, Guzman *et al*. 2015). A subsequent study compared solvent extraction based on pertraction followed by electrochemical phase separation of the acids through a 2-compartment membrane electrolysis (ME) cell and direct electrochemical extraction from the fermentation broth using a 3-compartment ME cell. The 3-compartment ME cell was able to phase-separate oil extracted directly from the fermentation broth. Still, it was not selective for longer-chain carboxylates due to the co-extraction of SCCAs and inorganic anions. The selectivity of longer-chain carboxylates and capacity to up-concentrate MCCAs in an alkaline-pH extract with the first extraction method enabled more efficient use of the electricity for ME (Carvajal-Arroyo, Andersen *et al*. 2021).

IV) Membrane-based reactive extraction (Sitter, Garcia-Gonzalez *et al*. 2018; Xu, Bian *et al*. 2021). Membrane-based reactive extraction was evaluated for the recovery of carboxylic acids from the system, converting thin stillage to MCCAs (Sitter, Garcia-Gonzalez *et al*. 2018). Both off-line and in-line experiments were performed. The off-line experiments were promising, reaching extraction efficiencies of *n*-caproate to almost 100%. Longer-chain carboxylates could be selectively and nearly completely extracted with in-line experiments. However, the overall on-line extraction rates were lower than in off-line tests, and the total carboxylate production rate was also decreasing. The author suggested that repeating contact between the organic phase and fermentation broth *via* the membrane interface probably limited the efficiency of in-line extraction.

2.4 MCCA-producing microorganisms

With the development of microbial MCCA production *via* chain elongation, more chain-elongating bacteria have been discovered (Candry and Ganigue 2021). Also, various natural waste has been applied for MCCA production with open cultures. The complex microbial interactions in open cultures benefited the utilization of a broader range of substrates for MCCA production (Chwialkowska, Duber *et al*. 2019, Chen, Huang *et al*. 2020). The functional microbiomes for MCCA production in open cultures were more diverse, which were not only related to those well-known chain-elongating bacteria but some other microorganisms as well. Here, I summarized the chain-elongating bacteria and functional microbiomes in MCCA-producing open cultures to better understand the microbial ecology for MCCA production.

2.4.1 Pure cultures

The first chain-elongating bacteria—*C. kluyveri*, is a rod-shaped and spore-forming anaerobic bacteria (Barker and Taha 1942), which utilized ethanol and acetate to produce *n*-butyrate, *n*-caproate, and molecular hydrogen (Barker. By H. A. 1945). Gradually, other chain-elongating bacteria have been isolated and characterized (**Table 2.4**). ***C. kluyveri*** was isolated from canal mud (Barker and Taha 1942) and bovine rumen (Weimer and Stevenson 2012). Several alcohols and organic acids could be used by *C. kluyveri* to produce different MCCAs. For example, when C. *kluyveri* was fed with propanol and acetate, the products were propionate, *n*-butyrate, *n*-valerate, *n*-caproate, and a trace of *n*-heptanoate. Acetate, *n*-butyrate, and *n*-caproate were the main products when it utilized ethanol and succinate (Waselefsky 1985). Till now, ethanol and acetate are still the optimal substrates for C. *kluyveri* to produce *n*-caproate (Seedorf, Fricke *et al*. 2008). ***M. elsdenii*** was isolated from sheep rumen samples (Elsden 1956). *M. elsdenii* can utilize different carbon sources, including lactate, glucose, fructose, and sucrose, with the fermentation of SCCAs and *n*-caproate, H_2, and CO_2 (Marounek, Katerina Fliegrova *et al*. 1989, Weimer and Moen 2013). ***Ruminococcaceae bacterium* CPB6** was isolated by Zhu *et al*. from a microbiome and affiliated with Clostridium IV. It was found responsible for *n*-caproate production from lactate (Tao, Zhu *et al*. 2017, Zhu, Zhou *et al*. 2017). ***Caproiciproducens galactitolivirans*** (*C. galactitolivirans*) was isolated from anaerobic digester sludge from a Korean wastewater treatment plant, which represents a novel genus within Clostridium IV (Jeon, Kim *et al*. 2010). This bacterium efficiently produces *n*-caproate from D-galactitol. It can also utilize glucose to produce *n*-caproate but is less efficient than galactitol (Jeon, Kim *et al*. 2010). ***Eubacterium limosum*** (*E. limosum*) was isolated from the rumen of a sheep (Weimer and Stevenson 2012). *E. limosum* formed acetate, *n*-butyrate, and *n*-caproate from methanol and acetate. However, *n*-

butyrate was the main product, with *n*-caproate as a by-product (Genthner, Davis *et al*. 1981). Later, it was reported that when *E. limosum* was cultured with methanol, *n*-butyrate, and CO_2 as feedstocks, *n*-caproate could become the main product (Lindley 1987, Tarasov, Borzenkov *et al*. 2011). In addition, glucose fermentation resulted in some *n*-caproate production (Genthner, Davis *et al*. 1981). For its low *n*-caproate selectivity, *E. limosum* is now more often studied for *n*-butyrate production from syngas fermentation (Park, Yasin *et al*. 2017, Song, Shin *et al*. 2017).

Seven bacteria, *C. kluyveri*, *M. elsdeni*, *Ruminococcaceae bacterium* CPB6, Strain BL-4/Strain BL-6, *C. galactitolivirans*, *Caproiciproducens* 7D4C2, have been confirmed to utilize rBOX pathway for MCCA production. Most known chain-elongating bacteria belong to Firmicutes except *R. rubrum. R. rubrum* came from the phylum Proteobacteria, class Alpha-proteobacteria, and family Rhodospirillaceae. The seven pure cultures, which are capable of rBOX, came from Clostridia (Clostridiaceae and Oscillospiraceae) or Negativicutes (Veillonellaceae). Recently, *Candidatus Pseudoramibacter fermentans,* which was from Eubacteriacaeae*,* was identified as a likely chain elongator *via* a metagenomic analysis (Scarborough, Myers *et al*. 2020). In the same research project, *Candidatus Weimeria bifida* from Lachnospiraceae has been also identified *via* metagenomic analysis as a chain-elongating organism (Scarborough, Myers *et al*. 2020).

Table 2.4 Characteristics and performances of main chain-elongating bacteria

	Phylum /Class/Family	Origin	Optimum temperature (°C)	Optimum pH	Optimum electron donor	Main MCCAs	Reference
Ethanol-based chain-elongating bacteria							
Clostridium kluyveri	Firmicutes/ Clostridia/Clostridiaceae	canal mud	34	6.8	ethanol	*n*-caproate	(Barker and Taha 1942)
Clostridium kluyveri	Firmicutes/ Clostridia/ Clostridiaceae	silage	39	6.8	ethanol and propanol	*n*-caproate	(Weimer and Stevenson 2012)
Lactate-based chain-elongating bacteria							
Megasphaera elsdeni	Firmicutes/ Negativicutes/ Veilonellaceae	sheep rumen	38	7.4	DL-lactate and sugars	*n*-caproate	(Elsden 1956)
Ruminococcaceae bacterium CPB6	Firmicutes/ Clostridia/ Oscillospiraceae	CE reactor microbiome	30–40	5.0–6.5	lactate	*n*-caproate	(Zhu, Zhou *et al*. 2017)
Strain BL-4/ Strain BL-6	Firmicutes/ Clostridia/ Oscillospiraceae Firmicutes/ Clostridia/ Oscillospiraceae	CE reactor microbiome	37	5.5	lactate	*n*-caproate	(Liu, Popp *et al*. 2020)
Other substrates-based chain-elongating bacteria							
Caproiciproducens galactitolivirans	Firmicutes/ Clostridia/ Oscillospiraceae	anaerobic digester sludge	37	6.8	D-galactitol	*n*-caproate	(Jeon, Kim *et al*. 2010)
Caproiciproducens 7D4C2	Firmicutes/ Clostridia/Oscillospiraceae	CE reactor microbiome	30	5.2	fructose	*n*-caproate	(Esquivel-Elizondo, Bagci *et al*. 2020)
Caproiciproducens fermentans	Firmicutes/ Clostridia/Oscillospiraceae	Biogas reactor microbiome	30/37	5-9	fructose	*n*-caproate	(Flaiz, Baur *et al*. 2020)

Eubacterium limosum	Firmicutes /Clostridia/ Eubacteriaceae	sheep rumen	39	7.4	methanol	*n*-caproate	(Lindley 1987)
Eubacterium pyruvativorans	Firmicutes /Clostridia/ Eubacteriaceae	sheep rumen	39	7	amino acids, peptides, and pyruvate	*n*-caproate	(Wallace, McKain *et al*. 2003, Wallace, Chaudhary *et al*. 2004)
Pseudoramibacter alactolyticus	Firmicutes/ Clostridia/ Eubacteriaceae	/	30	5.0-5.6	glucose	*n*-caproate	(WILLEMS 1996)
Megasphaera indica	Firmicutes/ Negativicutes/ Veilonellaceae	feces	37	/	glucose	*n*-caproate	(Lanjekar, Marathe *et al*. 2014)
Megasphaera hexanoica	Firmicutes/ Negativicutes/Veilonellaceae	cow rumen	30–40	5.5–7.5	fructose	*n*-caproate	(Jeon, Choi *et al*. 2016)
Megasphaere cerevisiae	Firmicutes/ Negativicutes/Veilonellaceae	/	28	7.0	glucose, fructose, or lactate	*n*-caproate	(Engelmann and Weiss 1985)
Clostridium luticellarii	Firmicutes/ Clostridia/ Clostridiaceae	liquors-producing mud cellar	37	6.5	Palatinose, l-fucose, β-hydroxybutyric acid, l-rhamnose, α-ketobutyric acid	*n*-butyrate	(Wang, Wang *et al*. 2015)
Clostridium carboxidivorans	Firmicutes/ Clostridia/ Clostridiaceae	agricultural settling lagoon	38	6.2	H_2/ CO_2 or CO	*n*-butyrate and small amount of *n*-caproate	(Liou, Balkwill *et al*. 2005, Phillips, Atiyeh *et al*. 2015)
Rhodospirillum rubrum	Proteobacteria/ Alpha-proteobacteria/ Rhodospirillaceae	dead mouse or tap water	37	/	pyruvate	*n*-caproate (dark fermentation)	(Gest 1995)
strain MDTJ8	Firmicutes/ Clostridia/Oscillospiraceae	a thermophilic acidogenic anaerobic digestor	50–55	6.5	starch and hemicellulose	*n*-caproate	(Tinh Van Nguyen 2023)

2.4.2 Open cultures

The microbial ecosystem is more complex when open cultures are applied for microbial MCCA production (Candry and Ganigue 2021). So far, the well-known chain-elongating bacteria are from Firmicutes. However, other microbiomes in open cultures, which were relatively high and correlated with MCCA production, were classified as Proteobacteria (*e.g.,* unclassified Rhodocyclaceae, unclassified Acetobacteraceae, *Acinetobacter* spp.) and Bacteroidetes. In addition, the functional microbiomes changed with various substrates or operating conditions (Agler, Werner *et al*. 2012). When the ethanol and acetate from syngas effluent served as substrates, the microbial composition was predominantly made of *Acinetobacter* spp. and *Rhodocyclaceae* K82 spp. (Kucek, Spirito *et al*. 2016). When wine lees, which consisted of settled yeast cells and ethanol, was used as a feedstock, *Bacteroides* spp. became the dominant species (Kucek, Xu *et al*. 2016). When the lactate-rich effluent from acid whey were used as feedstock, *Bacteroidales* spp. (21.7%) and *Clostridiales* spp. (12.6%) were most abundant in the microbiomes (Xu, Hao *et al*. 2017). After changing the feedstock to lactate and *n*-butyrate, the main species became *Rhodocyclaceae* K82 spp. (63.3%) after 30 days, and then *Acinetobacter* spp. (62.9%) after 140 days, respectively (Kucek, Nguyen *et al*. 2016).

In some research, the necessarily abundant microbial communities in the consortium was related to the well-known chain elongation functional bacteria (Han, He *et al*. 2019). For example, *C. kluyveri* made up 55.3% of the bacterial group when supplied with acetate and ethanol as substrates (Steinbusch, Hamelers *et al*. 2011). *Ruminococcaceae* bacterium CPB6 and *Clostridium* sp. MT1 played a crucial role in *n*-caproate production from lactate-rich food waste (Nzeteu, Trego *et al*. 2018). However, in other studies, the microbial community, which was significantly correlative to MCCA production, was irrelative to those well-known bacteria. In the experiment of Steinbusch *et al*., C. *kluyveri* and *A. oryzae* were positively related to *n*-caprylate production. However, *A. oryzae* (also known as *Dechlorosoma oryzae*) is a nitrogen-fixing ß-proteobacterium that could reduce chlorate or selenite (Steinbusch, Hamelers *et al*. 2011).

2.4.3 Comparison of the dominant microbiomes in MCCA-producing open cultures

Among the studies in chain elongation with reactor microbiomes, ethanol- and lactate- based MCCA production account for a large proportion of the research. Here, I summarized the research with ethanol or lactate as electron donors (**Table 2.5**).

Ethanol-based CE: The readily biodegradable biowaste, which contained a high concentration of ethanol, such as ethanol-rich yeast fermentation beer (Agler, Spirito *et al*. 2012, Ge, Usack *et al*. 2015), corn beer (Urban, Xu *et al*. 2017), wine fermentation residue (Kucek, Xu *et al*. 2016),

and thin stillage (Andersen, Candry *et al*. 2015), could be directly utilized as substrates for the chain elongation process.

Figure 2.8 The sunset graph of the dominant microbiomes in ethanol-based MCCA-producing open cultures. The microbiomes were devided into five levels: Domain, Phylum, Class, Order, and Family. Data was from **Table 2.5**.

Moreover, for some complex waste-derived substrates, chemical, physical, or biological pretreatment could be applied to improve the accessibility to the chain-elongating strains, thus, enhancing the yield and production rate. For example, pre-acidification of food waste significantly enhanced MCCA production (Roghair, Liu *et al*. 2018). Interestingly, syngas could also serve as the indirect substrate for MCCA production becaame its fermentation effluent, containing ethanol and acetate, can be converted to MCCAs (Vasudevan, Richter *et al*. 2014, Kucek, Spirito *et al*. 2016). I summarized the dominant microbial community in ethanol-based MCCA-producing open cultures from previous publications **(Figure 2.8)**. The summary showed that Archaea (phylum Methanobacteria) accounted for only 5% of microbiomes, and Bacteria were dominant in the microbial community. Most of the microbiomes came from the phylum Firmicutes, and a small part of the members was from other phyla (Bacteroidota, Proteobacteria, and Thermodesulfobacteriota). At the class level, most microbial communities came from

Clostridia (mainly from families Oscillospiraceae and Clostridiaceae).

Lactate-based CE: Lactate is an important intermediate in the anaerobic breakdown of carbohydrates (Kleerebezem and van Loosdrecht 2007). Carbohydrates comprise ~18% of the COD in municipal wastewaters (Raunkjær 1994) and up to ~70% of the COD in some food processing wastewaters (Gómez, Cuetos *et al*. 2009, Arslan, Steinbusch *et al*. 2013). Kucek *et al*., performed the first continuous lactate-based chain elongation for MCCAs production in open cultures with a synthetic medium (Kucek, Nguyen *et al*. 2016).

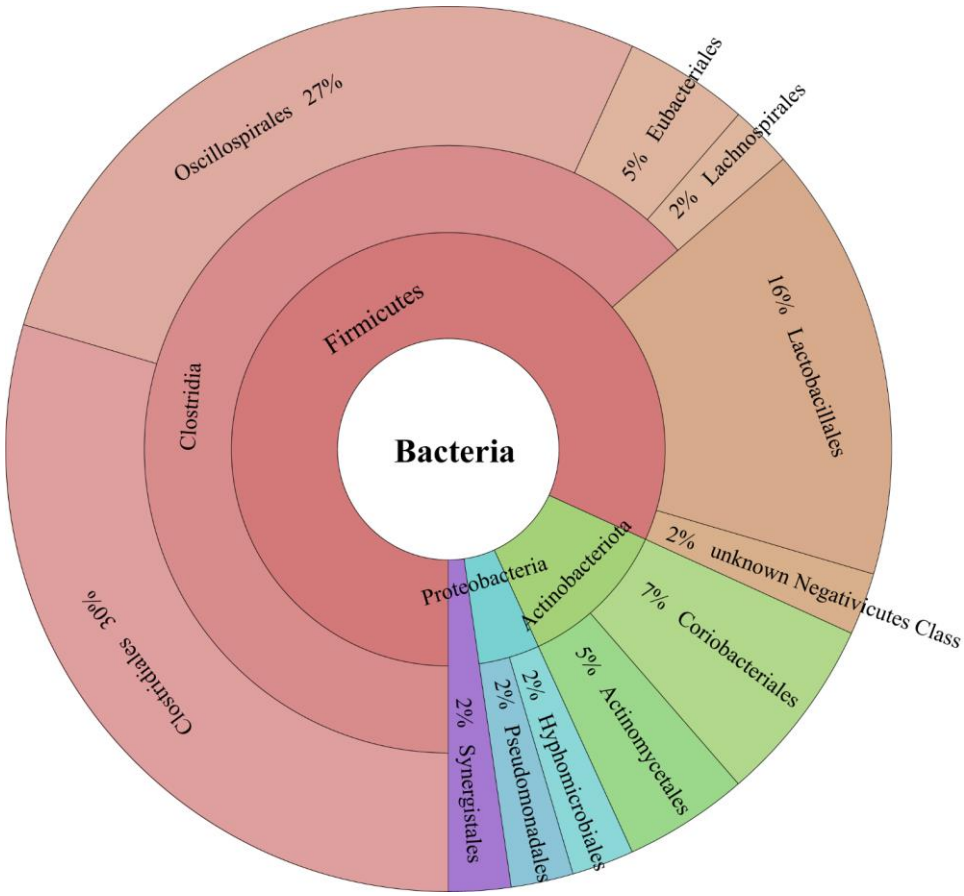

Figure 2.9 The sunset graph of the dominant microbiomes in some lactate-based MCCA-producing open cultures. The microbiomes were devided into five levels: Domain, Phylum, Class, Order, and Family. Data was from **Table 2.5.**

Then, other studies applied lactate-rich waste for microbial MCCA production, such as maize silage (Sträuber, Lucas *et al*. 2016), pre-fermented grass (Khor, Andersen *et al*. 2017), waste from liquor-making factory (Zhu, Feng *et al*. 2021), and the effluent from thermophilic acid whey fermentation (Xu, Hao *et al*. 2017). Food waste was most used for MCCA prodcution (Yu, Huang *et al*. 2019, Contreras-Davila, Carrion *et al*. 2020, Zhang, Pan *et al*. 2022). I collected and analyzed all the dominant microbiomes for MCCA production with lactate as co-electron donors from most publications (**Figure 2.9**). I found that most of the dominant microbiomes in lactate-

based MCCA-producing open cultures came from the phylum Firmicutes. Other involved phyla were Proteobacteria, Actinobacteriota, and Synergistota. Members from the class Clostridia (mianly from families Oscillospiraceae and Clostridiaceae) were most assigned. Compared with the microbiomes abundant in ethanol-rich substrates, Ruminococcaceae was more enriched here, which was probably because most of the lactate-based chain-elongating bacteria were from Ruminococcaceae. Lactobacillaceae, which was correlated with lactate production (Wang, Wu et al. 2021), was also enriched in the microbiomes.

Both ethanol and lactate were in the substrate: The fermentation effluents from actual waste, such as acid whey, maize silage, and food waste, may contain both ethanol and lactate due to the storage conditions and the natural presence of lactic acid bacteria (LAB; Otto 1983, Marshall, LaBelle et al. 2013, Duber, Zagrodnik et al. 2020).

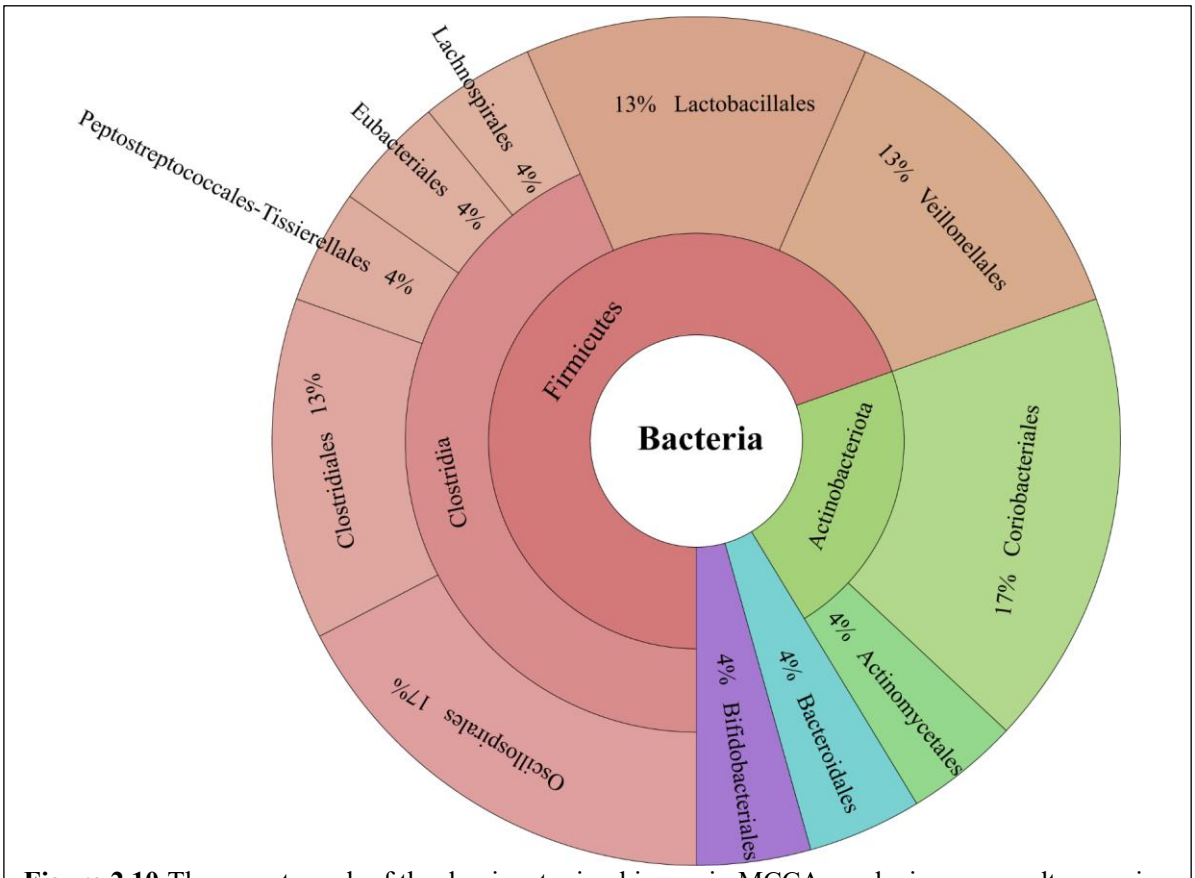

Figure 2.10 The sunset graph of the dominant microbiomes in MCCA-producing open cultures using ethanol and lactate as co-electron donors. The microbiomes were devided into five levels: Domain, Phylum, Class, Order, and Family. Data was from **Table 2.5**.

In general, LAB may spontaneously ferment carbohydrates in two major routes: **1)** through homofermentation to lactate; **2)** through heterofermentation to lactate, CO_2, and ethanol or acetate (Otto 1983). Some research show ethanol and lactate as the co-substrates (Wu, Guo *et al*. 2018, Lambrecht, Cichocki *et al*. 2019). It was found that the co-electron donors of ethanol and lactate

stimulated the transformation of dispersive lactate-carbon flux from the competing acrylate pathway into *n*-heptanoate. The coexisting by-products (H_2 and CO_2) from ethanol and lactate also contributed to the more MCCA generation (Wu, Guo *et al*. 2018). However, there was a different conclusion in the research using the fermentation of acid whey as feedstock for MCCA production. When both ethanol and lactate were in the substrate (ethanol concentration was higher than lactate), there was more SCCA generation. More MCCAs were produced when changing the feedstock composition to a higher lactate to ethanol ratio (Duber, Zagrodnik *et al*. 2020). I collected and analyzed all the dominant microbiomes for MCCA production with ethanol and lactate as co-electron donors from all the available research **(Table 2.5)**. Phyla of Firmicutes, Actinobacteriota, Actinomycetota, and Bacteroidota were involved. Most members came from the class Clostridia (families Oscillospiraceae and Clostridiaceae). Interestingly, Class Coriobacteriia was more enriched here compared with other groups. The family Lactobacillaceae also took a large portion because lactate was used as electron donors (**Figure 2.10**).

2.4.4 Microbial community analysis

For a stable and effective MCCA production system with open cultures, microbial tools are required to help researchers understand the complex ecosystem and identify the critical functional microbiomes. Researchers have widely utilized microbial analysis approaches based on high-throughput 16S rRNA gene sequencing to deepen the knowledge about the process, and the correlations of the process data and the microbial composition revealed the key players involved in the process (Langille, Zaneveld *et al*. 2013, Quince, Walker *et al*. 2017, Kennedy, Prost *et al*. 2020).

From the results of 16S rRNA gene sequencing, we can obtain the alpha diversity (within the group) and beta diversity (between groups) analyses of the microbial community in samples from a specific environment (Bolyen, Rideout *et al*. 2019). Quantitative Insights Into Microbial Ecology (QIIME2) is one open-source software pipeline designed to analyze high-throughput sequencing data (J Gregory Caporaso 2010 , Bolyen, Rideout et al. 2019). The alpha diversity showed the richness (*e.g.,* number of species), evenness (*e.g.,* the relative abundance of species), the Shannon diversity index (Shannon 1948), observed species (*e.g.,* richness), and Gini coefficient metrics (Wittebolle, Marzorati *et al*. 2009) in a sample. The bray-Curtis, unweighted and weighted UniFrac distance metrics were used to analyze beta diversity (Lozupone 2005, Lozupone, Lladser *et al*. 2011). To visually display beta diversity data, researchers can carry out unconstrained ordination (*e.g.,* principal coordinates analysis [PCoA]). Through constrained ordination (*e.g.,* distance-based redundancy analysis [db-RDA]), metadata can be used to find a

link between changes in microbial composition and function. PCoA was used to visualize the differences in community between the samples *via* the vegan package (version 2.4-3) in R. Heat maps were created to represent OTUs (Operational Taxonomic Units) relative abundance *via* the plots package in R. The Pearson correlation coefficient, principal coordinates analysis, and constrained redundancy analysis were calculated with the Vegan community ecology package in R (Oksanen 2022). ANOVA analysis in R determines whether each constraint added a significant amount of information to the constrained model (if $p < 0.05$) or if it could be left out (if $p > 0.05$). In addition to ANOVA, the variance inflation factor (VIF) could be used to determine whether constraints describe the same β diversity (*e.g.,* constraints are redundant in the model when VIF is large). The calculating correlation function in R 4.1.3 and Cytoscape v3.9.1could be used to build a microbial network.

Table 2.5 A summary of the MCCA production with different subsrates.

Feedstock	Reactor	Extraction	pH	Temp (°C)	Dominated microbiomes	Main products	Reference
Ethanol-Rich substrates							
Synthetic medium(ethanol, acetate and hydrogen)	feed-batch	no	7	30	*Clostridium kluyveri*	C6 /C8	(Steinbusch, Hamelers *et al*. 2011)
Diluted yeast fermentation beer	continuous	LLE[a]	5.5	30	*Clostridium* spp.	C6	(Agler, Spirito *et al*. 2012)
Synthetic medium (ethanol and acetate)	continuous	no	6.5-7.2	30	NA	MCCAs	(Grootscholten, Steinbusch *et al*. 2013)
Synthetic medium (ethanol and propionate)	continuous	no	6.5-7.0	30	NA	C7	(Grootscholten, Steinbusch *et al*. 2013)
Municipal solid waste and ethanol	continuous	no	6.5-7.0	35[b]/30	NA	C6	(Grootscholten, Kinsky dal Borgo *et al*. 2013)
Syngas fermentation effluent, with nutrients	continuous	no	5.44	30	NA	C6	(Vasudevan, Richter *et al*. 2014)
Diluted yeast fermentation beer	continuous	LLE[a]	5.5	30	NA	C6	(Ge, Usack *et al*. 2015)
Cellulosic biomass	batch	no	/	39	*Clostridium kluyveri*	C5 and C6	(Weimer, Nerdahl *et al*. 2015)
Diluted wine fermentation residue	continuous	LLE[a]	5.2	37	*Bacteroides* spp., *Oscillospira* spp., and *Clostridium* spp.	C6 /C8	(Kucek, Xu *et al*. 2016)
Syngas fermentation effluent	continuous	LLE[a]	5.4	30	*Acinetobacter* spp. and *Rhodocyclaceae* K82 spp.	C8	(Kucek, Spirito *et al*. 2016)
Yeast fermentation beer and thin stillage	continuous	no	5.5	35	*Clostridium* group IV *Lactobacillus* spp. and *Acetobacterium* sp.	MCFAs	(Andersen, De Groof *et al*. 2017)
Yeast fermentation beer	continuous	LLE and Kolbe electrolysis	6.5	30	NA	C6	(Urban, Xu *et al*. 2017)
Synthetic medium (ethanol and acetate)	batch	no	7.5	37	*Clostridium kluyveri*	C6	(Yin, Zhang *et al*. 2017)

Synthetic medium	batch	no	7.0	37	*Proteiniphilum, Desulfovibrio, Brassicibacter, Macellibacteroides, and Peptoclostridium*	C6	(Yang, Leng *et al*. 2018)
Food waste and ethanol	continuous	no	5.5[b]/6.8	35[b]/30	*Clostridium kluyveri*	C6	(Roghair, Liu *et al*. 2018)
Synthetic medium (methanol and propionate)	continuous	no	5.5-5.8	36	*Clostridium luticellarii* and *Candidatus Methanogranum*	C5	(de Smit, de Leeuw *et al*. 2019)
Food and vegetable waste	batch	no	6.5[b]/7.5	35[b]/30	*Clostridium kluyveri*	C6	(Yu, Liao *et al*. 2019)
Synthetic medium (with acetate, propionate, and *n*-butyrate)	batch	no	6.5-7.0	35	*Clostridium_sensu_ stricto_12, Sporanaerobacter, Proteiniphilum, Lachnospiraceae_NK3A20_ group, and Syntrophobacter*	C6	(Bao, Wang *et al*. 2019)
Synthetic medium (with propionate)	batch	no	/	37	*Clostridium kluyveri*	C5, C6, and C7	(Candry, Ulcar *et al*. 2020)
Synthetic medium (with CO_2)	batch	no	/	30	*Clostridium_sensu_ stricto*_12, Oscillibacter, g__norank_f__Ruminococcaceae, and Acetobacterium	C6	(Jiang, Chu *et al*. 2020)
Synthetic medium (with methanol)	continuous	no	6.6	35	*Eubacterium, Clostridium sensu stricto 12, and Methanobrevibacter*	i-C4and i-C6	(Chen, Huang *et al*. 2020)
Liquor-making wastewater	continuous	no	5.4	40	*Bacilli*, *Clostridia*, and *Bacteroidia*	C6 and C8	(Wu, Feng *et al*. 2020)
Synthetic wastewater	Batch[b] and continuous	no	6.0[b]/5.4	37[b]/40	*Clostridium sensu stricto* and *Clostridium IV*	C6, C7, and C8	(Wu, Feng *et al*. 2020)
Synthetic medium	continuous and batch	no	6.5/7	35	/	i-C6, C6, and i-C7[f]	(de Leeuw, Ahrens *et al*. 2021)

Synthetic medium	batch	no	7.5	30	*Clostridium kluyveri , and Oscillibacter*	C4, C6, and C8	(Joshi, Robles *et al*. 2021)
Synthetic medium	batch	no	6.5	35	C*lostridium_sensu_ stricto*	C6	(Cheng, Liu *et al*. 2022)
Lactate-Rich substrates							
Diluted yellow water	batch-feed	no	6.0	30	*Clostridium* cluster IV	C6	(Zhu, Tao *et al*. 2015)
Synthetic medium (L-lactate and *n*-butyrate)	continuous	LLE[a]	5.0	34	*Acinetobacter* spp.	C6	(Kucek, Nguyen *et al*. 2016)
Diluted cheese whey powder	continuous	no	6.0	37	*Lactobacillus* , *Olsenella* , and *Actinomyces*	VFAs	(Domingos, Martinez *et al*. 2016)
Maize silage	semi-continuous	no	4.2-5.7[b] /7.6	37	*Lactobacillus* [b]*/Clostridium, Ruminococcus* , and *Synergistaceae*	MCFAs	(Sträuber, Lucas *et al*. 2016)
Acid whey	continuous	LLE[a]	5.0	50[b]/30	*Lactobacillus* , *Bulgaricus*, and *Ruminococcus*	C6	(Xu, Hao *et al*. 2017)
Grass fermentation	semi-continuous	electrochemical extraction	4.8-5.8[b]/ 5.5-6.3	32	*Clostridium IV* and *Lactobacillus*	C6	(Khor, Andersen *et al*. 2017)
Synthetic medium	batch	no	7.0	35	*Clostridium spp.*	C6	(Wu, Guo *et al*. 2019)
Synthetic medium	batch	no	7.0	35	*Clostridium spp.*	C6, C7, and C8	(Wu, Guo *et al*. 2019)
Food waste	batch	no	6.0	35	*Lactobacillus* and *Caproiciproducens*	C6	(Contreras-Davila, Carrion *et al*. 2020)
Synthetic medium	continuous	no	<6 or >6	34	*Veillonella and Aminobacterium*(for pH above 6); *Caproiciproducens* (for pH below 6)	C3 (or pH above 6); C6 (or pH below 6)	(Candry, Radic *et al*. 2020)
Synthetic medium and real wastewater	continuous	no	6.0	30	*Ruminococcaceae*	C6	(Zhu, Feng *et al*. 2021)
Synthetic medium	batch	no	5.5	30	/	C6	(Xie, Ma *et al*. 2021)

Synthetic medium	continuous	extraction with sunflower oil	5.0	30	*Caproiciproducens, Clostridium tyrobutyricum, Clostridium luticellarii, and Lactobacillus* spp.	C6 and C8	(Contreras-Davila, Zuidema *et al*. 2021)
Food waste	semi-continuous	no	6.0	37±2	*Actinomyces, Atopobium, Olsenella , and Pseudoramibacter*	C6	(Crognale, Braguglia *et al*. 2021)
Food waste	batch	no	6.0	35	*Clostridium IV*	C6	(Wei, Ren *et al*. 2021)
Synthetic medium	batch	no	5.5	30	*Clostridium luticellarii, Caproiciproducens, and Ruminococcaceae related species were associated with n*-valerate and *n*-caproate production; *n*-butyrate *with Clostridium tyrobutyricum, Lachnospiraceae, Oscillibacter,* and *Sedimentibacter*	C4, C5, and C6	(Contreras-Davila, Esveld *et al*. 2021)
Synthetic medium	continuous	no	6.0	30	*Rummeliibacillus* with *n*-butyrate; *Caproiciproducens*, unclassified *Peptostreptococcales*, and *Methanobrevibacter*	C4 and C6 (a little C8)	(Baleeiro, Ardila *et al*. 2021)
Food waste	batch and semi-continuous	no	6.0	55	*Caproiciproducens, Rummeliibacillus, Clostridium_sensu_stricto_12, Clostridium_sensu_stricto_7*	C4 and C6	(Zhang, Pan *et al*. 2022)
Swine manure and corn stalk silage	continuous	no	5.0/6.0	55[b]/30	*Pseudoramibacter and Caproiciproducens*	C6	(Zhang, Wang *et al*. 2022)
Containing both Ethanol and Lactate in the broth							
Ethanol and Lactate as co-electron donors							

Thin stillage fermentation (ethanol and lactate)	continuous	membrane electrolysis	5.4-5.7	35	*Megasphaera* sp. and *Lactobacillus* spp.	C4	(Andersen, Candry *et al*. 2015)
Liquor-making waste water	batch	no	6.5	35	*Negativicutes* class and *Ruminococcaceae* family	C6	(Wu, Guo *et al*. 2018)
Switch grass hydrolysate	continuous	no	5.5	35	Firmicutes phylum (*Lactobacillus, Roseburia*, and *Pseudoramibacter*) and Actinobacteria phylum (*Olsenella* and *Atopobium).*	C4-C8	(Scarborough, Lynch *et al*. 2018)
Maize silage	continuous	no	5.5/6.5	38	*Bifidobacterium* and *Olsenella*	C6/C8	(Lambrecht, Cichocki *et al*. 2019)
Acid whey	batch	no	5.5	30	NA	C6	(Chwialkowska, Duber *et al*. 2019)
Acid whey (ethanol or lactate is the main fermentation product)	continuous	no	5.5	30	*Coriobacteriaceae* family and *Clostridia* class (*Veillonellaceae, Ruminococcaceae, Caproiciproducens* ssp.)	C4/C6	(Duber, Zagrodnik *et al*. 2020)
Synthetic medium (ethanol and lactate [c])	batch	no	7.5	30	*Sporanaerobacter, Paraclostridium, Haloimpatiens, Clostridium, and Bacillus*	C6	(Zagrodnik, Duber *et al*. 2020)
Ethanol and Lactate occur in the substrate but only ethanol or lactate could be used							
Acid whey (ethanol and lactate [d])	continuous	No	5.5	30	Families *Coriobacteriaceae*, *Ruminococcaceae*, and *Prevotellaceae*	C6	(Duber, Jaroszynski *et al*. 2018)
Food waste (ethanol and lactate [d])	semi-continuous	No	7	37	*Clostridium* sp.	C6	(Nzeteu, Trego *et al*. 2018)
Thin stillage (add ethanol or lactate [d] separately)	continuous	no	5.5	34	*Ruminococcaceae*	C6	(Carvajal-Arroyo, Candry *et al*. 2019)
Food waste (ethanol and lactate[d])	batch	no	6.0	35	*Lactobacillus spp. and Caproiciproducens* spp.	C6	(Contreras-Davila, Carrion *et al*. 2020)
*a:liquid-liquid extraction, b: for pre-fermentation, c: only used under certain conditions, d: the real substrate, C4-C6 represent *n*-butyrate, *n*-valerate, *n*-caproate, *n*-heptanoate, or *n*-caprylate.							

CHAPTER 3

The Process Regulation in MCCA Production in Open Cultures with Ethanol and Lactate as Co-Electron Donors

Abstract

Most studies focused on MCCA production *via* chain elongation with ethanol or lactate as an electron donor. However, some real waste contains both ethanol and lactate. Exploring the co-utilization of ethanol and lactate as co-electron donors for MCCA production expanded the substrate range for microbial MCCA production. This study examined the possibility of co-utilization of ethanol and lactate and the strategy to control the bioreactor for specific MCCA production with ethanol and lactate as co-electron donors. The results showed that ethanol and lactate could be used as co-electron donors at the same time with an in-line extraction system. In addition, different ratios of ethanol to lactate or operating temperatures steer the bioreactor for specific MCCA production. The results displayed that increasing the ethanol - to - lactate ratio (E_L_ratio) from 1 to 3 resulted in more even-chain product production. *n*-Caproate was the main (47.04 mmol C L^{-1} d^{-1}) product with an E_L_ratio of 1, and *n*-caprylate was dominant in the product (76.59 mmol C L^{-1} d^{-1}) with an E_L_ratio of 3. Afterwards, I changed the operating temperature in the bioreactor from 25ºC to 42ºC with an E_L_ratio of 1. The results showed that the relatively high temperatures of 37ºC-42ºC inhibited odd-chain product production. With relatively low temperatures of 25ºC-30ºC, *n*-caprylate was the main product, with a maximum production rate of 58.68 mmol C L^{-1} d^{-1} at 25ºC. With relatively high temperatures of 37ºC-42ºC, *n*-caproate was dominant in the bioreactor, with a maximum production rate of 48.74 mmol C $L^{-1}d^{-1}$ at 42ºC.

3.1 Introduction

Developing alternative technologies for producing chemical compounds, previously based on fossil sources, is the first step into a circular economy (Di Maio, Rem *et al*. 2017, de Leeuw, Buisman *et al*. 2019). Current environmental pressures and the net-zero carbon emission goal require a more efficient waste management

technology (Candry and Ganigue 2021, Kim, Kang *et al*. 2022). Accordingly, the use of organic waste to produce high-value chemical compounds (*e.g*., MCCAs) is a promising alternative to re-valorize waste and reduce fossil fuel dependency (Angenent, Richter *et al*. 2016). MCCAs (ranging from six to twelve carbons) are essential industrial chemicals (Angenent *et al*., 2016), which could be employed in several applications, including as antimicrobial agents (Huang *et al*., 2011), fodder-annexing agents (Van Immerseel *et al*., 2004), rubbers (Angenent *et al*., 2016), and precursors of a*via*tion fuels (Bergthorson & Thomson, 2015; Cavalcante *et al*., 2017).

Previously, organic liquid waste (*e.g.,* cellulosic hydrolysates, acid whey, food waste, and liquor-making wastewater) and syngas-fermentation effluent streams have been applied for the bioproduction of MCCAs (Zhu, Tao *et al*. 2015, Xu, Hao *et al*. 2018, Carvajal-Arroyo, Candry *et al*. 2019). The microbial MCCA production process generally involves two phases: **1)** electron donor oxidation; **2)** chain elongation of the electron acceptor *via* rBOX (Angenent *et al*., 2016). Usually, ethanol, lactate, or other energy-rich reduced substrates serve as electron donors, while SCCAs (*e.g.,* acetate, propionate, and *n*-butyrate) function as electron acceptors. For chain elongation, acetyl-CoA, which is a two-carbon molecule, is derived from electron donors and then added to carboxylates (electron acceptors) to elongate the carbon chain length of the electron acceptors. The process yields metabolic energy (ATP) and reducing equivalents (NADH) for microbiomes (Spirito *et al*., 2014).

It is known that mostly even-chain MCCAs, such as *n*-butyrate, *n*-caproate, and *n*-caprylate, are produced when only even-chain electron acceptors are available in the bioreactor (Grootscholten, Steinbusch *et al*. 2013). The odd-chain MCCAs (*e.g*., *n*-valerate, *n*-heptanoate) could be produced *via* chain elongation when odd-chain SCCAs serve as electron acceptors (Candry, Ulcar *et al*. 2020). When lactate was used as an electron donor, which could be oxidized to acetate and reduced to propionate, both even-chain and odd-chain MCCAs could be produced (Kucek, Nguyen *et al*. 2016, Candry, Radic *et al*. 2020).

Ethanol and lactate are the most commonly reported electron donors for chain

elongation (Marounek, Fliegrova *et al*. 1989, Seedorf, Fricke *et al*. 2008, Spirito, Richter *et al*. 2014, Zhu, Zhou *et al*. 2017). Ethanol in yeast-fermentation beer, wine-fermentation residue, and syngas-fermentation effluent is employed for microbial MCCA production as an electron donor (Agler, Spirito *et al*. 2012, Vasudevan, Richter *et al*. 2014, Diender, Parera Olm *et al*. 2019). Also, lactate from the fermentation broth of acid whey, food waste, and yellow water from liquor-making factories has been tested for MCCA production (Zhu, Tao *et al*. 2015, Xu, Hao *et al*. 2018, Contreras-Davila, Carrion *et al*. 2020). Ethanol and lactate are present in many fermentation effluents from organic waste (*e.g.,* acid whey, maize silage, and food waste). Lambrecht *et al.* shifted the carbon flux to specific MCCAs *via* changing the ratio of ethanol to lactate in a acid whey-feeding bioreactor (Lambrecht, Cichocki *et al*. 2019). The microbial MCCA production with liquor-making wastewater showed that using ethanol and lactate as co-electron donors could enhance MCCA production (Wu, Guo *et al*. 2018). More research about the co-utilization of ethanol and lactate as electron donors was required to lay the foundation for applying these real waste for microbial MCCA production.

The operating condition (pH, temperature, or hydraulic retention time) were essential for controlling the MCCA production in the bioreactor (Cavalcante, Leitão *et al*. 2017). The temperature affects the thermodynamics and kinetics of the metabolic processes (Kleerebezem and Van Loosdrecht 2010, González-Cabaleiro, Lema *et al*. 2013). For MCCA production, microbes commonly require mesophilic temperatures (Agler, Spirito *et al*. 2014, De Groof, Coma *et al*. 2019). However, few studies showed how the operating temperature affects the MCCA production process. More details of the effect of the operating temperature on microbial MCCA production are required.

This research investigated the process regulation of MCCA production with ethanol and lactate as co-electron donors in a long-term continuous bioreactor. I explored the effect of the ratio of ethanol to lactate and the operating temperature on MCCA production in the bioreactor. This study provided the possibilities of controlling bioreactor performance for specific and designed MCCA production.

3.2 Materials and Method

3.2.1 Inoculum and growth medium, bioreactor setup, and bioreactor operating conditions

The inoculum was from a long-term chain-elongating bioreactor that used ethanol as substrate (Agler, Spirito *et al*. 2012, Ge, Usack *et al*. 2015). The selected inoculum was pretreated to deplete all the organic matter and substrates remnants before inoculation (Xu *et al*., 2017). Micronutrients were supplemented as basal medium formulation based on previous reports (Vasudevan *et al*., 2014; Weimer and Moen 2013; Kucek, Nguyen, *et al*., 2016; Spirito *et al*., 2018), and details were shown in **Tables S3.1-3.3**.

A glass-jacketed and up-flow 6.5-L anaerobic reactor with a working volume of ~ 6.00 L was used. The bioreactor was with constant broth recirculation through an in-line, membrane-based liquid-liquid extraction system (**Figure 3.1**). I set up two bioreactors (reactor one: R1; reactor two: R2), R1 is for test one, and R2 is for control. The temperature was controlled using a heating bath (Huber KISS E, -30-200^{o}C, Germany) through all the experimental conditions. The pH was measured by a probe (SL 80-425pH, Xylem Analytics, Germany) that was mounted on the lid of the bioreactor. The pH was maintained at 5.5 with an automatic controller (Eutech Instruments alpha-pH560, Vernon Hills, IL, USA) and pumps system (Masterflex® L/S® Economy Fixed-Speed Drives, OU-07540-01, Cole-Parmer Instrument Company, USA) with hydrochloric acid (*e.g.,* 4 M HCl) and sodium hydroxide (*e.g.,* 5 M NaOH).

Fresh media containing ethanol and lactate was continuously fed from a refrigerated reservoir (4^{o}C) using a peristaltic pump (Masterflex L/S® Variable-Speed Digital Drive, OU-07528-10, Cole-Parmer Instrument Company, USA) with a flow rate from 0.65 mL min^{-1}. The effluent was continuously recycled *via* an overflow line that was connected to the pertraction system, using a peristaltic feed pump (Masterflex L/S® Variable-Speed Digital Drive, OU-07528-10, Cole-Parmer Instrument Company, USA), at average rates of 0.94 L d^{-1}. The produced biogas was used to mix the broth by continuously recycling it bottom-to-top in the bioreactor. The biogas volumetric

production was measured with a flow meter (BPC® μFlow, BPC Instruments, Sweden) that was connected to the biogas outlet. The biogas collection system consisted of: **1)** a gas-sample septum; **2)** a glass airlock; and **3)** a two-bottle system with water as an equalization system to prevent air intrusion during sampling. Finally, a lateral sampling port on the bioreactor was placed to take biomass samples periodically. The pertraction system was composed of two membrane contactors (BET area:1.4 m^2 each, Membrana Liqui-Cel 2.5-8, X50 membrane, Charlotte, NC, USA) that was used as the forward and backward extraction units of the MCCA recovery unit (**Figure 3.1**). The MCCA recovery unit consisted of a liquid-liquid extraction system using mineral oil and 30 g L^{-1} tri-n-octyl phosphine oxide (TOPO) as a solvent mix (Sigma Aldrich, St. Louis, MO, USA). The extraction solution was initially buffered with 0.3 M sodium borate and then maintained at a pH=9.4 with 5 M NaOH using an automatic pump controller (Eutech Instruments alpha-pH800, the Bluelab pH Controller Connect M, Bluelab, USA). The regeneration of the extraction system was performed every eight months; membrane contactors were washed using 2% NaOH, 1% HCl, and distilled water. The extraction solution was entirelly replaced to prevent losses in the extraction by solvent saturation.

Both bioreactors were fed with ethanol and lactate (total carbon was 695 mM C) during the long-term adaptation period (May 2019 - June 2020). The pH was 5.5, the organic loading rate (OLR) was 110 mM C^{-1} d^{-1}, the hydraulic retention time (HRT) was 6.4 days, and the ratio of ethanol to lactate (E_L_ratio) was 1:1. After a long-term start-up and acclimation period, both bioreactors had the same performance. Then, I changed the E_L_ratio and operating temperature in R1 (**Table 3.1**). Stage I (*e.g.,* periods I-IV), the E_L_ratio was modified progressively, and the temperature was maintained at 30°C. Stage II (*e.g.,* periods V-VI) corresponded to a collapse in the extraction system. Finally, during stage III (*e.g.*, periods VII-XI), the operating temperature was modified from 25°C-42°C, with an E_L_ratio of 1. Each experimental period corresponded to an active bioreactor time of three HRTs (19 days). The operating period of R2 was divided into six periods (**Table 3.1**): **1)** period **a** corresponded to the operation as control of the R1 during periods I-IV; **2)** period **b**, a collapse in the

extraction system; **3)** period **c**, recovery from period **b**; **4)** period **d**, regular operation as control of the R1 bioreactor during periods VII - XI; 5) period **e**, a failure in the pH probe, with a pH was lower than 5.5 (about 5.0); **6)** period **f**, recovery from period **e**.

Table 3.1 The operating conditions for different periods in R1and R2

	E_L_ratio	Temperature	pH	HRT (d)	OLR (mmol C L^{-1} d^{-1})	Time (d)	Steady stage (d)
				R1			
Period I	1:1	30ºC	5.5	6.4	110	1-25	1-25
Period II	2:1	30ºC	5.5	6.4	110	26-107	65-107
Period III	3:1	30ºC	5.5	6.4	110	108-171	151-171
Period IV	1:1	30ºC	5.5	6.4	110	172-187	172-187
Period V (collapse)	3:1	30ºC	5.5	6.4	110	188-239	
Period VI (recovery)	1:1	30ºC	5.5	6.4	110	240-259	240-259
Period VII	1:1	25ºC	5.5	6.4	110	260-299	260-299
Period VIII	1:1	30ºC	5.5	6.4	110	300-318	300-318
Period IX	1:1	37ºC	5.5	6.4	110	319-363	334-363
Period X	1:1	42ºC	5.5	6.4	110	364-395	381-395
Period XI	1:1	30ºC	5.5	6.4	110	396-468	418-468
				R2			
Period a (Control)	1:1	30ºC	5.5	6.4	110	0-50	0-50
Period b (collapse)	1:1	30ºC	5.5	6.4	110	51-119	
Period c (recovery)	3:1	30ºC	5.5	6.4	110	120-149	
	1:1	30ºC	5.5	6.4	110	150-197	
Period d (Control)	1:1	30ºC	5.5	6.4	110	198-339	198-339
Period e (collapse)	1:1	30ºC	5.5	6.4	110	340-371	
Period f (recovery)	1:1	30ºC	5.5	6.4	110	372-471	372-471

*E: ethanol; and L: L-lactate.

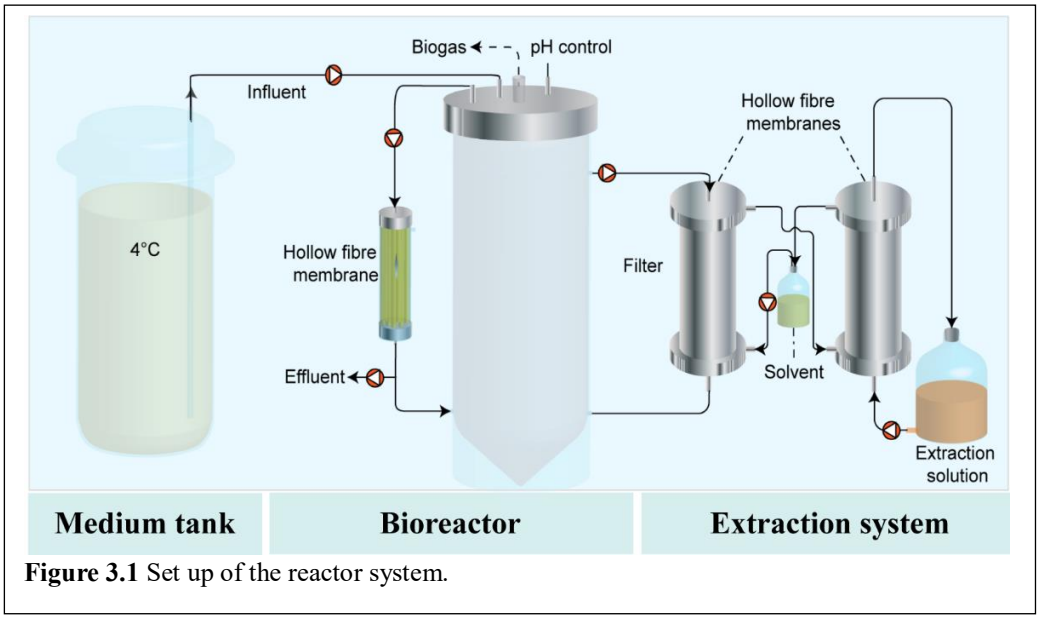

Figure 3.1 Set up of the reactor system.

3.2.2 Liquid Sampling and analytical procedures

All methods were based on the previous research from my lab (Usack and Angenent 2015; Xu *et al*., 2018). Bioreactor-mixed liquid samples (1.5 mL) were collected every other day (sometimes every day) from a sampling tube located in the middle of the bioreactor height. Extraction solution samples were also collected directly from the well-mixed reservoir at the same time. All carboxylates were determined by gas chromatography (GC, 7890B GC System, Agilent, USA), which was equipped with a thermal conductivity detector (TCD), using a capillary column Nukol Capillary Column (15m X 0.25 mm I.D. X 0.25um). The method was modified according to the previous research from my lab (Usack and Angenent 2015), which was with a temperature of injection at 200°C and the detector to 250°C, ramp temperature program (initial temperature 80°C for 0.5 min, temperature ramp 20°C per 1 min to 180°C, and final temperature 180°C for 2 min), and a hydrogen flow of 21.4 mL min^{-1} as a carrier gas. Ethanol and lactate concentrations were measured using high-performance liquid chromatography (HPLC) system (Shimadzu LC 20AD), which was coupled with a refractive index and UV detector (Shimadzu, Kyoto, Japan). Separation conditions were 60ºC with 5 mM sulfuric acid as the mobile phase at a flow rate of 0.6 mL min^{-1} in an Aminex HPX-87H column (Bio-Rad, Hercules, CA, USA). Prior to the analysis, samples were filtered through a sterile Acrodisc 0.22-mm pore size, polyvinylidene fluoride membrane syringe filter (Pall Life Sciences, Port Washington, NY, USA) to remove possible biological and particulate contaminants. Finally, production rates for

MCCAs (mmol C L^{-1} d^{-1}) were calculated using the MCCA concentrations in the pertraction system and the effluent of the bioreactor (**Table 3.2**), according to Xu *et al*. (Xu *et al*., 2018). Biogas samples were taken from the headspace of the reactor daily and were measure with GC (SRI gas GCs, SRI Instruments, USA). H_2 and CO_2 contents were assessed using thermal conductivity detector-gas chromatography (GC-TCD) and CH_4 content was assessed with flame ionization detector-gas chromatography (GC-FID).

3.2.3 Calculations

3.2.3.1 The production rate

Table 3.2 The equation of volumetric production rate on day n (mM C L^{-1} d^{-1})

Equation	$\left[\frac{C_{e,n}V}{HRT} + \frac{(C_{b,n} - C_{b,n-1})V_b}{T_n - T_{n-1}} \right] \frac{1}{1000V}$
$C_{e,n}$	concentration of carboxylates in effluent on the day n, mM
V	volume of reactor, L
HRT	hydraulic retention time on the day n, d
$C_{b,n}$, - $C_{b,n-1}$	concentrations of carboxylates in the stripping solution on the day n and n-1, mM
V_b	volume of the stripping solution on the day n, L
T_n	the day n, d

3.2.3.2 Thermodynamics of biochemical reactions

The thermodynamic calculation of biochemical reactions was based on the research of Alberty *et al*. (Alberty 1998, Alberty 2001).

The transformed Gibbs free energy ($\Delta rG'_T$):

$$\Delta rG'_T = \Delta rG'^0_T + RT\ln Q \qquad \textbf{Eq. 3.1}$$

where $\Delta rG'^0_T$ is the standard transformed Gibbs free energy of a reaction at a temperature (T). Q is a factor related to the activities of reactants and products defined as:

$$Q = \frac{(\alpha_A)^a(\alpha_B)^b\ldots(\alpha_C)^c}{(\alpha_X)^x(\alpha_Y)^y\ldots(\alpha_Z)^z} \qquad \textbf{Eq. 3.2}$$

where the numerator represents the activity of products A, B, C, *etc*. and the denominator represents the activity of reactants X, Y, Z, *etc*. The powers are the stoichiometric coefficients of the products and reactants in each reaction.

To obtain $\Delta rG'^0_T$, the standard Gibbs free energy of formation ($\Delta_f G^0$) and standard enthalpy of formation ($\Delta_f H^0$) for each reactant and product at T = 298.15 K and ionic

strength (I) = 0 M were looked up in references (Kleerebezem and Van Loosdrecht 2010). For those chemicals, whose values of standard Gibbs free energy of formation (Δ_fG^0) and standard enthalpy of formation (Δ_fH^0) were not available, we calculated those values based on the methods from Mavrovouniotis (Mavrovouniotis 1991) and Hanselmann (Hanselmann 1991).

For a given condition of 303 K, the Gibbs free energy of formation at T = 303 K, $\Delta_fG^0_{i,303}$ is adjusted with **Eq. 3.3:**

$$\Delta_fG^0_{i,303k} = \left(\frac{303k}{298.15k}\right) \times \Delta_fG^0_{i,298.15k} + \left(1 - \frac{303k}{298.15k}\right) \times \Delta_fH^0_{i,298.15} \qquad \textbf{Eq. 3.3}$$

Subsequently, the standard transformed Gibbs free energies of formation at different pH and ionic strength, $\Delta_fG^0_{i,310k}(pH, I)$ are calculated as follows:

$$\Delta_fG'^0_{I,303k}(pH, I) = \Delta_fG^0_{i,303k} - N_{H,i}RT\ln 10^{-pH} - RT\alpha(Z_i^2 - N_{H,i})I^{1/2}/(1+BI^{1/2}) \qquad \textbf{Eq. 3.4}$$

where $RT\alpha = 9.20483 \times 10^{-3}\ T - 1.28467 \times 10^{-5}T^2 + 4.95199 \times 10^{-8}T^3$, $B = 1.6\ kg^{1/2}mol^{-1/2}$, $N_{H,i}$ is the number of hydrogen atoms in a substance, and Z_i is the charge number. Finally, with the standard transformed Gibbs free energies of formation of each reactant and product, the standard transformed Gibbs free energy of each biochemical reaction is calculated using **Eq. 3.5**,

$$\Delta_rG'^0_T = \sum Vprod\,\Delta_fG'^0_T - \sum VReac\,\Delta_fG'^0_T \qquad \textbf{Eq. 3.5}$$

In this study, we had two conditions for thermodynamic analysis, one was on standard condition and another one was with a pH at 5.5 and temperature at 30°C.

3. 3 Result and discussion

3.3.1 The effect of E_L_ratio on bioreactor performance

3.3.1.1 A higher E_L_ratio benefited even-chain product production, especially *n*-caprylate

Different E_L_ratios were applied to R1 to explore the effect of E_L_ratio on MCCA production. A constant E_L_ratio of 1 was set in R2 as control (period **a**, **Figure 3.3**). The results showed that a higher E_L_ratio improved even-chain product production, especially *n*-caprylate production (periods I-III, **Figure 3.2** and **Table S3.4**). During periods I-III, odd-chain products (propionate, *n*-valerate, *n*-heptanoate, and *n*-nonanoate) were produced in the bioreactor but at a low production rate (**Figure 3.2 A**). With increasing E_L_ratio from 1 to 3, the ratio of even-chain (acetate, *n*-butyrate, *n*-caproate, *n*-caprylate) to odd-chain products increased (**Figure 3.2 C**), implying more

even-chain products were produced with a higher E_L_ratio. With an E_L_ratio of 1 (period I), *n*-caproate (47.04 mmol C L^{-1} d^{-1}) was dominant in the bioreactor. When more ethanol was added to the bioreactor during period II (an E_L_ratio of 2), *n*-caprylate production increased gradually while *n*-caproate production decreased. During the steady state of period II, the production rate of *n*-caproate was lower than that of *n*-caprylate (28.74 *vs.* 36.63 mmol C L^{-1} d^{-1}). The E_L_ratio was increased to 3 during period III, and *n*-caprylate was the main product in the bioreactor (76.59 mmol C L^{-1} d^{-1}). The increase of E_L_ratio from 1 to 3 during periods I-III led to a correlated growth of the ratio of *n*-caprylate to *n*-caproate (**Figure 3.2 B**). With a fixed E_L_ratio of 1 during period a in R2, the product spectrum was stable with *n*-caproate (43.48 mmol C L^{-1} d^{-1}) as the main product (**Figure 3.3 A** and **Table S3.4**).

Propionate, which was the electron acceptor for odd-chain MCCAs (Grootscholten, Steinbusch *et al*. 2013), could be produced from lactate *via* the Wood-Werkman cycle or acrylate pathway (Kucek, Nguyen *et al*. 2016, Candry, Radic *et al*. 2020). Therefore, when lactate was present for biological MCCA production, odd-chain MCCAs were produced. The lactate concentration decreased when a higher E_L_ratio was applied to the bioreactor. And low residual lactate in the bioreactor reduced the lactate conversion towards propionate, resulting in fewer odd-chain products produced (Kucek, Nguyen *et al*. 2016). So, a higher E_L_ratio in the substrates led to more even-chain MCCA production. In addition, microbiomes tend to produce longer-chain MCCAs (*e.g.*, *n*-caprylate) when enough electron donors are available (Spirito, Marzilli *et al*. 2018). Thus, the higher concentration of ethanol in the substrate is beneficial for *n*-caprylate production.

3.3.1.2 A higher E_L_ratio inhibited hydrogenotrophic methanogens

During periods I-III in R1, the biogas consisted of methane, carbon dioxide, hydrogen, and nitrogen (**Figure 3.4** and **Table S3.6**). The majority of nitrogen gas likely came from the dissolved air in the medium. The carbon dioxide mainly came from the oxidation of lactate to acetate or acetyl-CoA (Cavalcante, Leitão *et al*. 2017). The hydrogen was from the chain elongation process (Spirito, Richter *et al*. 2014, Angenent, Richter *et al*. 2016). Methanogenesis can be suppressed with a pH of 5.5 in the bioreactor (Ge, Usack *et al*. 2015, Kleerebezem, Joosse *et al*. 2015). However, acidic pH can inhibited acetoclastic methanogenesis completely, but hydrogenotrophic methanogens only partly (Koomen 1988, Karri, Sierra-Alvarez *et al*. 2006, Siggins,

Enright *et al*. 2011). Thus, the bioreactor still produced methane from hydrogen and carbon dioxide. Researchers found that the low level of methane production in bioreactors did not affect achieving high chain elongation rates (Agler, Spirito *et al*. 2012, Ge, Usack *et al*. 2015). With E_L_ratio increasing from 1 to 2, and to 3, hydrogen content showed no significant change ($p>0.05$). The percentage of methane in biogas decreased obviously at two timings during periods I-III: **1)** from an unsteady state to a steady state during period II; **2)** from an unsteady state to a steady state during period III (**Figure 3.4 A** and **Table S3.6**). The carbon dioxide content reduced at four timings during periods I-III: **1)** when E_L_ratio increased from 1 to 2 at the beginning of period II (32.03% to 26.28%); **2)** when E_L_ratio increased from 2 to 3 at the beginning of period III (18.64% to 15.11%); **3)** from an unsteady state to a steady state during period II; **4)** from an unsteady state to a steady state during period III (**Figure 3.4 A** and **Table S3.6**). The increased E_L_ratio initiated the decrease of lactate concentration in the bioreactor, which reduced carbon dioxide production. Therefore, the carbon dioxide content decreased at the beginning of periods II and III. From an unsteady to a steady state during periods II and III, the carbon dioxide content decreased again. From an unsteady state to a steady state during periods II and III, more *n*-caprylate was produced (**Figure 3.2 A**). I inferred that hydrogenotrophic methanogens were inhibited in the bioreactor. Carbon dioxide and hydrogen were used for acetate production *via* homoacetogenesis (Agler, Wrenn *et al*. 2011). Thus, methane content dropped from an unsteady state to a steady state during periods II and III. Moreover, one mole of methane requires one mole of carbon dioxide. However, two moles of carbon dioxide are needed to produce one molecular acetate (**Table S3.9**, **eq.9**). The more molecular carbon dioxide required for producing acetate than methane led to carbon dioxide decrease again. Increasing E_L_ratio from 1 to 3 resulted in a higher *n*-caprylate production, which inhibited methane production.

3.3.2 The effect of operating temperature on bioreactor performance

3.3.2.1 Higher temperature favored higher *n*-caproate production, but lower temperature benefited high *n*-caprylate production.

I applied different operating temperatures from 25ºC, to 30ºC, to 37ºC, and to 42ºC from periods VII to XI in R1, with a fixed E_L_ratio of 1 (**Figure 3.1** and **Table S3.4**). The relatively low operating temperatures of 25ºC-30ºC, *n*-caprylate was the dominant product in the bioreactor (periods VII and VIII, **Figure 3.2**). In addition, *n*-caprylate production rate was slightly higher at 25ºC than 30ºC (46.43 mmol C L^{-1} d^{-1} *vs.* 58.68

mmol C L^{-1} d^{-1}). With the operating temperature rising from 30°C to 37°C during period IX, the *n*-caproate production rate increased from 18.81 to 46.44 mmol C L^{-1} d^{-1} and was dominant in the bioreactor (**Figure 3.2 A** and **Table S3.3**). When the operating temperature rose to 42°C during period X, the *n*-caproate production rate increased slightly to 48.74 mmol C L^{-1} d^{-1}. However, *n*-caprylate production was zero during period X. With the temperature rising from 25°C to 42°C during periods VII to XI, the ratio of *n*-caprylate to *n*-caproate decreased (**Figure 3.2 B**). In the control bioreactor (period **d** in R2), the operating temperature was kept constantly at 30°C, resulting in a stable MCCA production and product spectrum (**Figure 3.3 A** and **Table S3.4**).

Little was known about the effect of the operating temperature on MCCA production from previous studies (Angenent, Richter *et al*. 2016). My research showed that the lower operating temperature improved *n*-caprylate production, while *n*-caproate production was favored at higher temperatures. In general, the longer the MCCAs are produced, the more reduced the chemical is, and the more ATP is released (**Table S3.8, eq. 6-15**), which is advantageous for chain-elongating bacteria (Angenent, Richter *et al*. 2016). No research reported that *n*-capricate (C10) was produced with chain elongation, and thus *n*-caprylate was the most reductive product for MCCA production. The temperature significantly influences the energy released from reactions and affects the kinetic rates of metabolic reactions (Kleerebezem and Van Loosdrecht 2010). The enzyme activity of the functional reactor microbiomes for *n*-caprylate production was probably suppressed at 37°C and 42°C in this study. Another possibility is that the all membrane was compromised at a higher temperature due to *n*-caprylate. The apparent SCCA accumulation in the bioreactor during periods IX and X, especially acetate and *n*-butyrate, also helped to explain this (**Figure 3.2 A and Table S3.4**). Acetate and *n*-butyrate were the intermediate substrates for MCCA production and would have accumulated if they were not used for further chain elongation (Spirito, Richter *et al*. 2014).

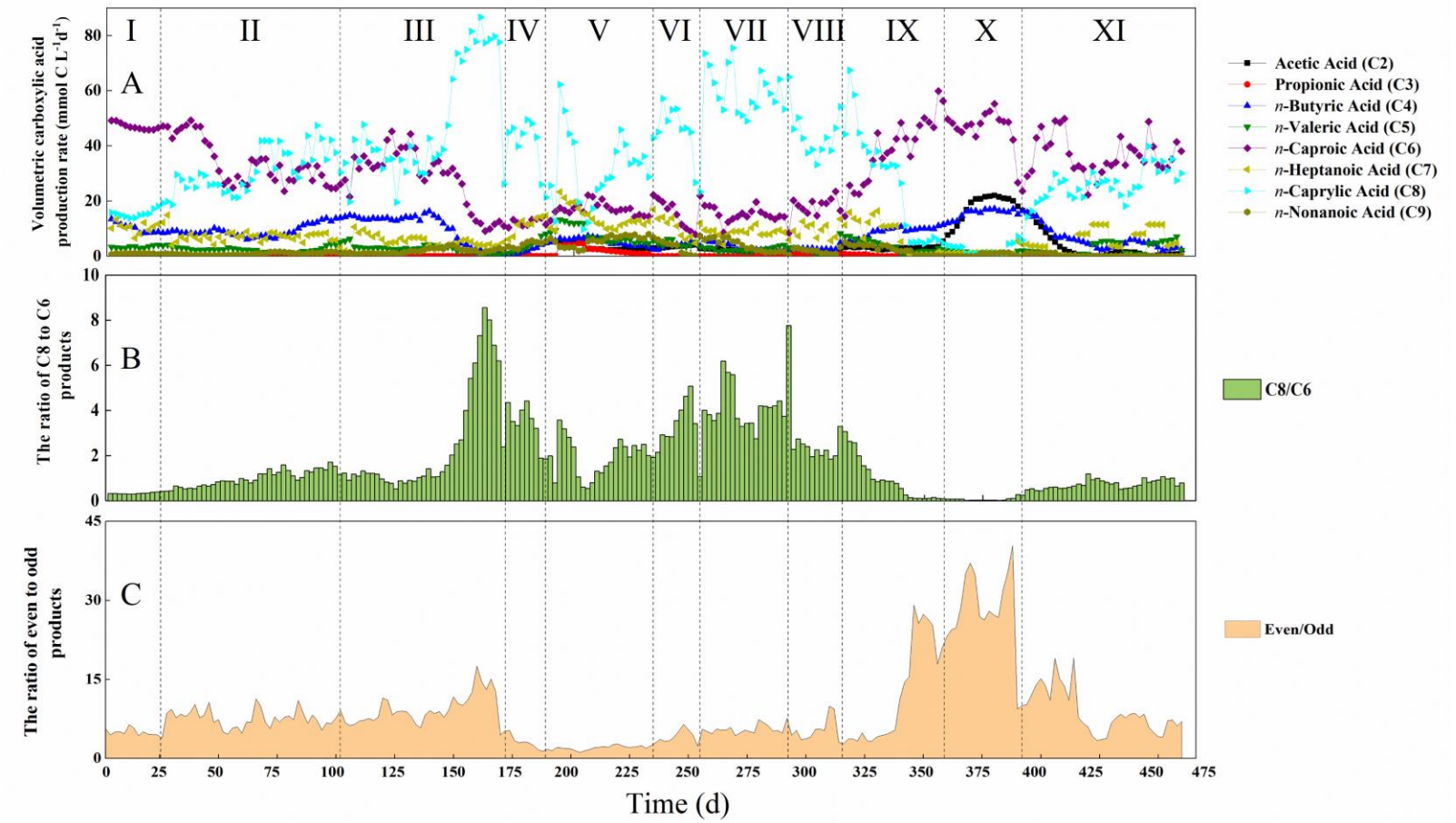

Figure 3.2. Performance for test reactor (R1) during Periods I-XI. Line-area chart for the production rates of carboxylic acids (A); column chart for ratio of C8 to C6 (B); stacked chart for ratio of even to odd (C). The data represent a 6-day moving average.

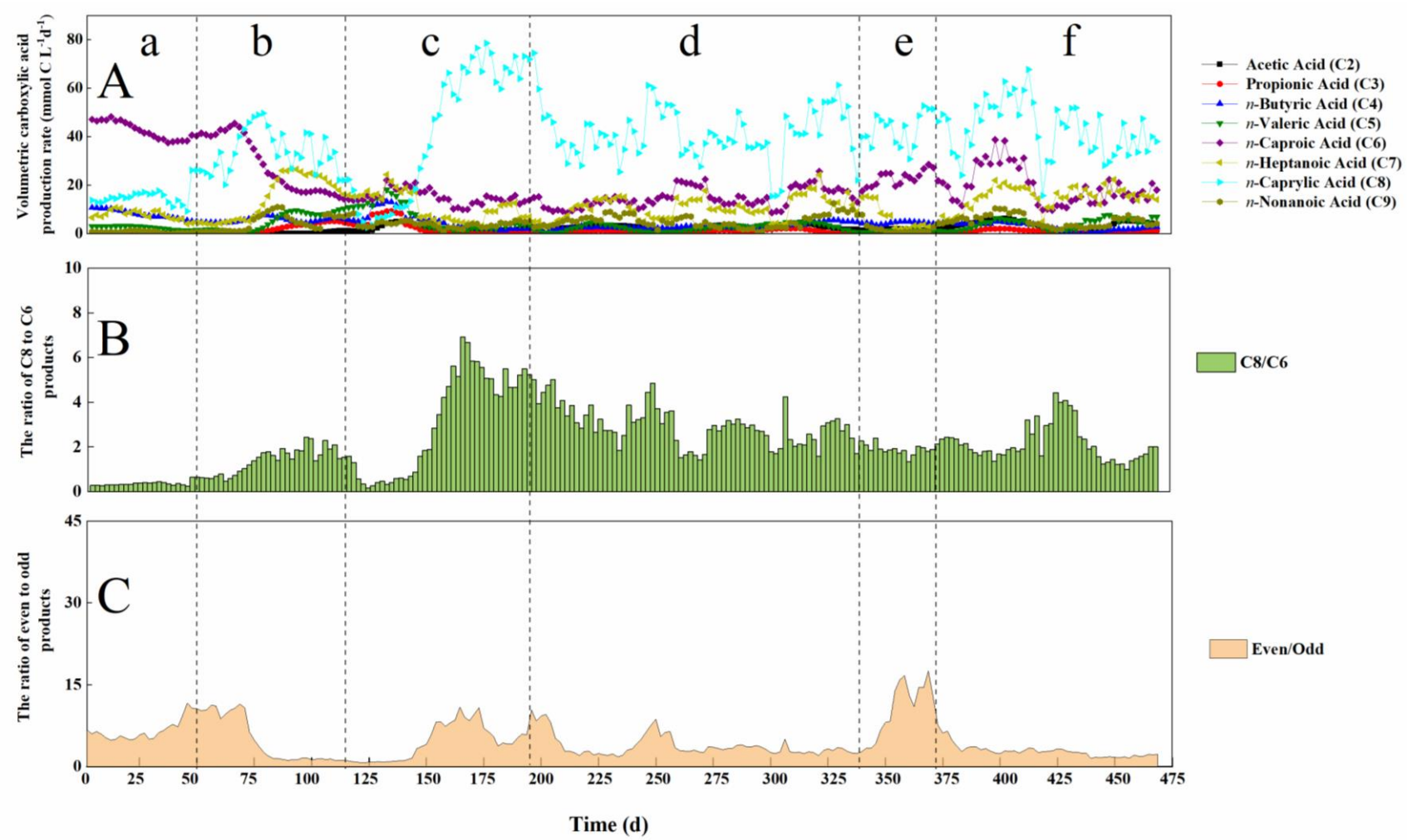

Figure 3.3. Performance for control reactor (R2) during periods a-f. Line-area chart for the production rates of carboxylic acids (A); column chart for ratio of C8 to C6 (B); stacked chart for ratio of even to odd (C). The data represent a 6-day moving average.

3.3.2.2 Higher operating temperature inhibited odd-chain product production

The ratio of even- to odd-chain products increased with the operating temperature rising from 25ºC to 42ºC during periods VII-X, displaying that the production of odd-chain products was suppressed with higher operating temperatures (**Figure 3.2 C).** In addition, the production of all odd-chain products (propionate, *n*-valerate, *n*-heptanoate, and *n*-nonanoate) was almost absent in the bioreactor at 42ºC (**Figure 3.2** and **Table S3.4**). As discussed, the odd-chain MCCAs were present in my bioreactor because of the conversion of lactate to propionate. The decrease in total odd-chain MCCAs could be because of the inhibition of high operating temperatures on propionate production. I found that the free energy changes (ΔG°'at pH=5.5) for propionate production became less negative with rising operating temperatures (**Table S3.9, eq.7**), which means that lower temperatures favored lactate reduced to propionate. The inhibition of odd-numbered products resulted in only even-chain MCCAs produced in the bioreactor at 42ºC. The selective effect of operating temperature on MCCA production gave us a control tool to steer the bioreactor to the target product.

3.3.2.3 The methanogens helped to maintain a appropriate pH_2 in a temperature-changed bioreactor

The biogas consisted of methane, carbon dioxide, hydrogen, and nitrogen (**Figure 3.4** and **Table S3.6**). More *n*-butyrate and *n*-caproate were produced by increasing the operating temperature from 25ºC to 42ºC during periods VIII-IX (**Figure 3.2 A**). From the model of Spirito *et al.,* the more *n*-butyrate and *n*-caproate produced, the more hydrogen is produced (Spirito, Marzilli *et al*. 2018). However, I noticed that hydrogen content in the biogas was of no obvious change with increasing the operating temperature from 25ºC to 42ºC during periods VIII-IX. The odd-chain product production decreased with increasing operating temperatures in the bioreactor (**Figure 3.2 A**), implying more lactate into acetyl-CoA or acetate, not propionate. The carbon dioxide was produced with lactate oxidization into acetyl-CoA or acetate. Thus, more carbon dioxide was produced with increased operating from 25ºC to 42ºC during periods VIII-IX. The carbon dioxide and hydrogen were converted to methane *via* hydrogenotrophic methanogenesis (Roghair, Hoogstad *et al*. 2018), resulting in higher methane production during periods VIII-IX (**Figure 3.4 A**). Therefore, I inferred that the hydrogen was consumed with carbon dioxide into methane during periods VIII-IX, leaving pH_2 constant during the process. During period X, the methane content (61.28%) was significantly higher ($p<0.05$) than during periods VI-IX (**Figure 3.4 A** and **Table**

S3.6). It was because there was higher production of acetate, *n*-butyrate, and *n*-caproate during period X than during other periods, with much more hydrogen produced from the chain elongation process according to the previous model (Angenent, Richter *et al*. 2016, Spirito, Marzilli *et al*. 2018). The hydrogen reacted with carbon dioxide into methane, resulting in a noticeable increase in methane content. The carbon dioxide content decreased during period X also confirmed this. Thus, the hydrogenotrophic methanogenesis helped to stabilize the pH_2 in the bioreactor (**Figure 3.4** and **Table S3.6**).

Maintaining an appropriate pH_2 is crucial in an MCCA-producing bioreactor (Angenent, Richter et al. 2016). A certain minimum pH_2 is needed to prevent the oxidation of MCCAs and SCCAs *via* fatty acid degradation. On the other hand, hydrogen is a product of ethanol- and lactate-based chain elongation (Spirito, Richter *et al*. 2014). A high pH_2 (above ~0.1 bar) could reduce the thermodynamic favorability of the chain elongation process (Rodriguez, Kleerebezem *et al*. 2006, Angenent, Richter *et al*. 2016). In addition, carboxylates are reduced to their corresponding alcohol when pH_2 is above ~1.5 bar (Grootscholten, Strik *et al*. 2014). Therefore, a stable and appropriate pH_2 was crucial to an effective chain elongation process.

3.3.3 Lower pH in the bioreator inhibited the production of odd products

I discussed above that less residual lactate in the bioreactor led to decreased odd-chain MCCAs. I found that lower pH also reduced the production of odd-chain products. During period **e** in R2, the pH was about 5.0, which was caused by a pH probe problem. The ratio of even- to odd-chain products decreased during period **e** (**Figure 3.3 C**), which implied fewer odd products were produced during period **e**. An acidic pH drove the carbon flux from odd-chain MCCAs to even-chain MCCAs (Kucek, Nguyen *et al*. 2016, Candry, Radic *et al*. 2020), which is another control to steer MCCA production.

3.3.4 An efficient in-line extraction system was crucial to the stable and promising MCCA production with ethanol and lactate as co-substrates

The in-line extraction system helped to co-utilize ethanol and lactate for MCCA production. When increased E_L_ratio from 1 to 2 (at the beginning of period II) and from 2 to 3 (at the beginning of period III), I found some ethanol was left in the effluent (**Figure S3.1 A**). After keeping the bioreactor for several HRTs without any changes, all ethanol was consumed. At the beginning of period b in R2, during which the extraction system collapsed, some ethanol and lactate were left in the effluent (**Figure**

S3.1 B). However, all the ethanol and lactate in the bioreactor was removed again by recovering the extraction system. Thus, during period **c** in R2 during which the extraction system worked well, the left ethanol was removed without changing any operating parameters. The above results showed that the in-line extraction system benefited substrate utilization.

The in-line extraction system was also crucial to a promising MCCA production, especially for *n*-caprylate. During period **b** in R2, the extraction system was not working well and I found a higher concentration of total carboxylates in the bioreactor, especially *n*-butyrate, *n*-caproate, and *n*-caprylate (**Figure S3.2 B**). I tried to improve the extraction efficiency by increasing the pump rate for the forward membrane in the extraction system. The increased pump rate for the forward membrane raised the production of *n*-caprylate in the bioreactor (**Figure 3.3 A**). Still, this operation did not help to reduce the total carboxylate concentration in the bioreactor (**Figure S3.2 B**). Then, the production of *n*-caprylate and *n*-caproate decreased sharply, and the total MCCA production was at a low level at the end of period b (**Figure 3.3 A**). The extraction system was recovered during period c. At the beginning of period c, the total MCCA production recovered at a low rate, especially *n*-caprylate. According to the experiment during period III in R1, we applied an E_L_ratio of 3 in R2 to recover the *n*-caprylate production, which increased the *n*-caprylate production rate to 76.59 mmol C L^{-1} d^{-1} at the end of period **c**.

The collapse of the extraction system led to the accumulation of undissociated carboxylates in the bioreactor, which was toxic to microbiomes and led to worse reactor performance. The two bioreactors in this study were set at a pH of 5.5 (Kucek, Spirito *et al*. 2016). The pH value was close to the pKa of SCCAs and MCCAs (*e.g.*,4.88 and 4.89 for *n*-caproate and *n*-caprylate, respectively), which led to the undissociated form of carboxylic acids in the bioreactor. The undissociated carboxylic acids in the reactor were toxic to the chain elongation process (Spirito, Marzilli *et al*. 2018). Previous studies have shown that concentrations of undissociated *n*-caproic acid higher than ~6.9 mM at a pH of 5.7 or higher than ~7.5 mM at a pH of 5.5 inhibited chain elongation (Ge, Usack *et al*. 2015, Weimer, Nerdahl *et al*. 2015). The concentration of undissociated *n*-butyric acid, *n*-caproic acid, and *n*-caprylic acid in the bioreactor during period **b** was ~1.35 mM, ~1.76 mM, and ~0.23 mM, respectively (calculated with **Table S3.5**). The concentration of undissociated *n*-caproic acid of ~1.76 mM was much lower

than 7.5 mM. However, a strong correlation exists between the length of the carbon chain of undissociated carboxylic acids and their toxicity (Huang, Alimova *et al*. 2011). Therefore, I inferred that the undissociated *n*-caprylic acid was more toxic than undissociated *n*-caproic acid in period **b**, which played the main role in toxic effect.

3.3.5 A higher E_L_ratio and higher operating temperature reduced the acid consumption for controling pH in the bioreactor

The pH in the bioreactor in this study was kept at 5.5. I used both ethanol and lactate as co-substrates in the bioreactor. One proton (H^+) will be produced from ethanol-based chain elongation (6 ethanol + 5 *n*-butyrate$^-$ ⟶ acetate + 5 *n*-caproate$^-$ + H^+ + $2H_2$ + $4H_2O$; (Spirito, Richter et al. 2014). However, there were more requirements for H^+ in the bioreactor in this study: **1)** H^+ would be consumed with lactate-based chain elongation (Lactate$^-$ + *n*-butyrate$^-$ + H^+ ⟶ *n*-caproate$^-$ + CO_2 + H_2O); **2)** the extraction system partly extracted the H^+. So, HCl was needed to keep the pH in the bioreactor at 5.5. With a stable bioreactor performance (periods a and d in R2), the average consumed HCl concentration was constant (**Figure S3.4** and **Table S3.7**). However, the acid consumption in the bioreactor in R1 was variable according to the different operating conditions applied (**Figure 3.5** and **Table S3.7**).

Interestingly, I found that no HCl was needed to maintain the pH during the unsteady state of period III and the whole period X. I found that there was that more SCCAs (*e.g.*, acetate and *n*-butyrate) were produced during these two periods (**Figure 3.2**). The in-line extraction system that I used in this study was considerably more efficient with longer carboxylates (higher extraction efficiency for MCCAs *vs.* SCCAs; (Ge, Usack et al. 2015). The carboxylates that left in the bioreactor, which were not extracted, consisted mainly of acetate, propionate, or *n*-butyrate. During the unsteady state of period III and the whole period X, the higher production of acetate and *n*-butyrate, which were not easy for this extraction system to extract (**Figure S3.2**), avoided the loss of H^+ in the bioreactor. So the balance between H^+ production and consumption resulted in zero acid addition to maintain the pH. The pH control of the fermentation broth with chemical input could be entirely avoided by changing the product spectrum by changing the E_L_ratio or operating temperature. One previous study controlled the pH using membrane electrolysis (Andersen, Candry *et al*. 2015). However, the authors mentioned that the membrane electrolysis route had a cost associated with power input. Compared with that, changing the E_L_ratio or operating

temperature to change the product spectrum to balance the H^+ was more cost-effective. This method of pH control may be further optimized, but it demonstrated possibilities to improve the environmental sustainability of this biotechnology for further industry application (Chen, Strik *et al*. 2017).

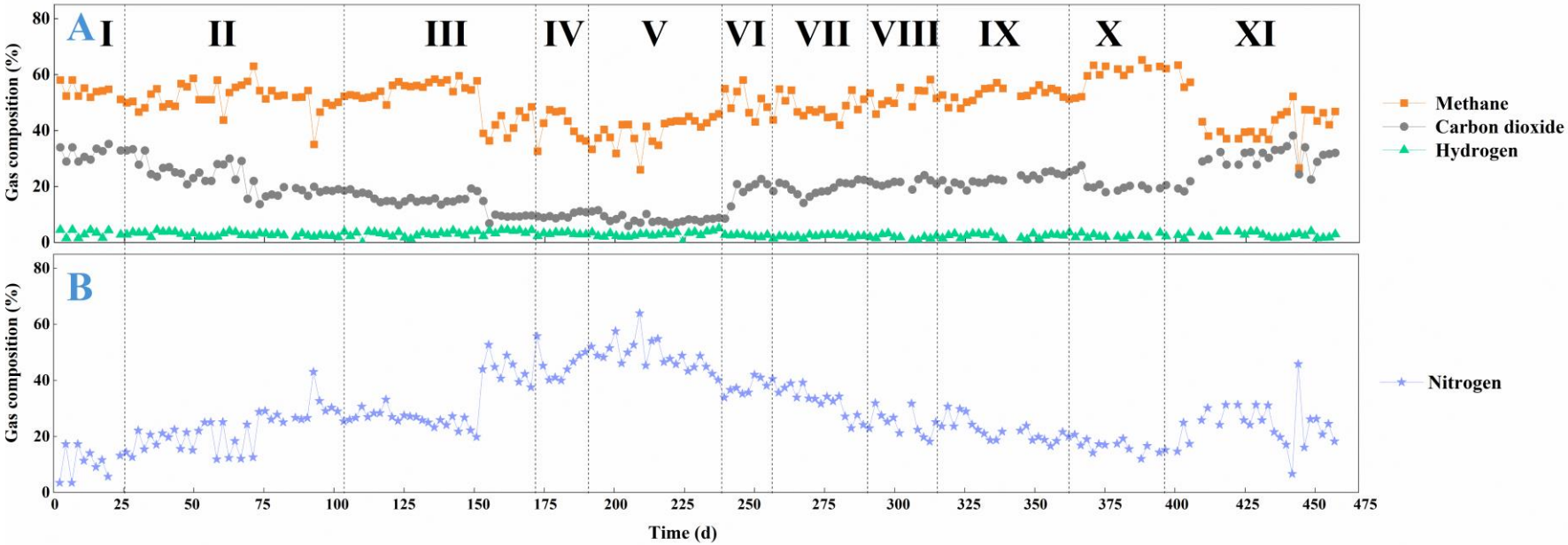

Figure 3.4. Biogas data over the operating periods in test reactor (R1): methane, carbon dioxide, and hydrogen percentages in the biogas (A); nitrogen percentages in the biogas (B).

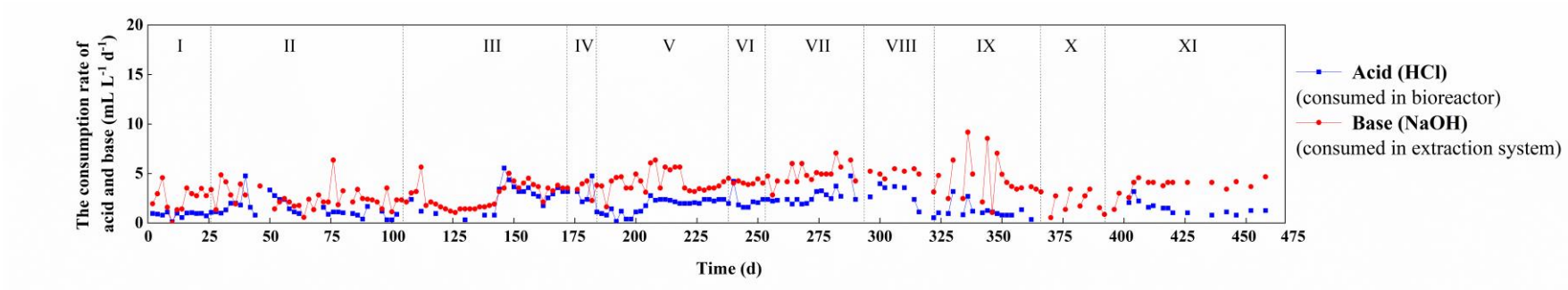

Figure 3.5 The acid consumed in bioreactor and base consumed in extraction system during the operating periods I-XI in test reactor (R1).

3.4. Conclusion

I acclimated the microbiomes of two bioreactors to producing MCCAs with ethanol and lactate as co-electron donors. This study showed that in-line extraction helped to miantain a stable and effective MCCA-producing bioreactor. To explore the strategy for controlling the bioreactor for specific MCCA production with ethanol and lactate as co-electron donors, I applied two environmental factors (E_L_ratio and operating temperature) in the bioreactor. The results showed that the product spectrum could be changed with these two parameters, and the bioreactor could be controlled for target products (*e.g.,* even-/odd-chain products, *n*-caproate/*n*-caprylate). A higher E_L_ratio or higher operating temperatures steer the microbiomes to produce more even-chain products. The E_L_ratio of 1 or higher operating temperatures of 37ºC-42ºC resulted in *n*-caproate being the main product for the bioreactor. High *n*-caprylate production was achieved under an E_L_ratio of 3 or operating temperatures of 25ºC-30ºC. The flexibility and adaptedness of microbial MCCA production with microbiomes were found to be controlled. However, managing competing reactions and driving carbon sources into the chain elongation process, especially to target MCCAs, was crucial to developing a functional and stable process. Here, we have effectively controlled those competitive pathways in our system. For example, methane, carbon dioxide, and hydrogen were the byproducts of the bioreactor. When the E_L_ratio increased, a high concentration of ethanol stimulated homoacetogenesis, contributing more acetate for MCCA production. In addition, hydrogenotrophic methanogenesis in the bioreactor helped to maintain an appropriate pH_2 when much more hydrogen was produced. Finally, co-feeding ethanol and lactate gave us several conditions that no pH control for the bioreactor was necessary.

CHAPTER 4

Steering Microbiomes for Specific MCCA Production with Ethanol and Lactate as Co-Electron Donors

Abstract

Detailed knowledge about microbial dynamics and their correlation to process conditions is crucial for effective process control. This study revealed microbial community dynamics in the MCCA-producing bioreactor. The bioreactor was installed with an in-line extraction system and was fed with both ethanol and lactate as co-electron donors. An E_L_ratio of 1 or a relatively high operating temperature at 37^{o}C or 42^{o}C shifted the microbiomes towards higher *n*-caproate production. Clostridia, Negatives, and Methanobacteria were enriched in the microbiome for higher *n*-caproate production. *Clostridium_sensu_stricto_12* spp., *[Eubacterium]_nodatum_group* spp., *Incertae_Sedis* spp., and other two genera from the order Oscillospirales were found positively correlated with *n*-caproate production. Three microbial networks for high *n*-caproate production under three different conditions were built *via* co-occurrence analysis of species based on 16S rRNA gene amplicon sequences. Under a relative high E_L_ratio of 3 or a relative low operating temperature at 25^{o}C or 30 ^{o}C, *n*-caprylate was dominant in the bioreactor. The microbiomes for high *n*-caprylate production were more assigned to Clostridia, Coriobacteriia, and Bacteroidia. *Dialister* spp., *Colidextribacter* spp., *Rikenellaceae_RC9_gut_group* spp., and *Bacteroides* spp. were found positively correlated with *n*-caprylate production. One typical microbial network for high *n*-caprylate production was conducted based on the relative microbial community. I also found that *Propionibacterium* spp. played an essential role in odd-chain carboxylate production. This research also provided more details about the characteristics of the microbial community for specific MCCA production and the strategy to engineer a bioreactor toward to target product.

4.1 Introduction

Anaerobic fermentation with open cultures is an appealing option for producing MCCAs (Spirito, Richter *et al*. 2014, Angenent, Richter *et al*. 2016). To be useful for

microbial MCCA production, the microbial community must have a stable metabolic function over time, despite unavoidable perturbations and disturbances (Werner, Knights *et al*. 2011). However, the complex microbial interactions and involved metabolic processes within microbiomes made it difficult to control the bioprocess (Scarborough MJ 2018). It is crucial to understand the response of to microbial networks to disturbances and develop more robust fermentation processes (Lawson, Harcombe *et al*. 2019). On the other hand, the complexity of the ecosystem in open cultures gives the process more potential to be shaped for target products and possibly to be controlled for us to steer the product spectrum (Agler, Werner *et al*. 2012, Lambrecht, Cichocki *et al*. 2019). Several operating conditions, such as pH, operating temperature, and substrate ratio, could all be effective tools to control the bioprocess (Agler, Spirito *et al*. 2014, Candry, Radic *et al*. 2020, Wu, Ren *et al*. 2022). Steering microbiomes to specific processes *via* effective strategies (operating conditions) was a crucial step in the process of bioenergy production (Suzanne Read 2011, Koch, Muller et al. 2014). Exploring the correlation between the operating conditions and the microbial dynamics and function could help us better steer the microbiome to the target process (Liu, Kleinsteuber *et al*. 2020, Cheng, Liu *et al*. 2022). In addition, more robust relationships were found between community structure and its function rather than its environment, which further expanded the method for engineering communities (Werner, Knights *et al*. 2011).

The microbial MCCA production with reactor microbiomes resulted from the cooperation of different microbial communities, and the functional communities were diverse (Candry and Ganigue 2021). *Clostridium* spp., *Bacteroides* spp., and *Oscillospira* spp. were positively correlated to volumetric production rates of MCCA in ethanol-based open cultures (Kucek, Spirito *et al*. 2016, Leo A. Kucek, Jiajie Xu *et al*. 2016). In the lactate-based open cultures for MCCA production, a higher odd-chain carboxylate production occurred with the high abundance of *Megasphaera* and *Prevotella* (Scarborough, Lynch *et al*. 2018). Many studies displayed that *Lactobacillus* spp., *Caproiciproducens* spp., and the member from *Ruminococaceae* were highly

involved in MCCA production, especially *n*-caproate production (Xu, Hao *et al*. 2017, Zhu, Zhou *et al*. 2017, Carvajal-Arroyo, Candry *et al*. 2019, Duber, Zagrodnik *et al*. 2020). In the experiment of Steinbusch *et al*., *C. kluyveri* species and *A. oryzae* were positively related to *n*-caprylate productivity. However, *A. oryzae* (also known as *Dechlorosoma oryzae*) is a nitrogen-fixing ß-proteobacterium that could reduce chlorate or selenate (Steinbusch, Hamelers *et al*. 2011). Understanding and exploring these diverse microbiomes shaped by different environmental factors is key to optimizing bioprocess performance.

I conducted two continuously-feed bioreactors for MCCA production with ethanol and lactate as co-electron donors in this research to investigate interactions among operating conditions, reactor performance, and microbial dynamics. For the study, two different environmental fators (E_L_ratio and operating temperature) were used as the selective pressure. The goal was: **1)** to study the resilience of the reactor microbiomes to disturbance; **2)** to explore the dynamics of communities with different environmental factors (operating conditions); **3)** to explore the key functional communities for specific MCCA production; **4)** to build the microbial network for specific MCCA production.

4.2 Materials and Method

4.2.1 Biomass Sampling and Sequencing

The microbial analysis here was based on the technology of high-throughput sequencing of bacterial 16S rRNA gene amplicons. Biomass samples were taken from the bioreactor broth at 56 time points throughout the experimental period of ~1.3 years from the two reactors (in total, 112 samples). Each sample was collected in a 2 mL Eppendorf tube to further centrifugation at 16873 g for 4 min, and the supernatants were discarded. The pelleted biomass samples were stored at -80 ± 1ºC until further processing. Genomic DNA was extracted using the FastDNA™ SPIN Kit for Soil (MO BIO Laboratories Inc., Carlsbad, CA). The DNA amplification protocol was described previously (Regueiro *et al*., 2015; Xu *et al*., 2018) with slight modifications (**appendix 4. protocol**). Amplicon library preparation was performed using barcoded indexes Nextera XT Index kit V2 (Illumina inc.) following the manufacturer's instructions for

dual indexing (**appendix 4. protocol**). Sequencing with the Illumina MiSeq platform was performed at the Max Planck Institute for Developmental Biology (Tübingen, Germany) using the MiSeq Reagent Kit v2 (500 cycles). Obtained sequences were processed using the QIIME2 (J Gregory Caporaso 2010 , Bolyen, Rideout et al. 2019). Demultiplexing was performed using the QIIME2 default pipeline, quality filtering sequence joining, chimera removal, and general denoising were performed using the Divisive Amplicon Denoising Algorithm (DADA2) (Callahan, McMurdie *et al*. 2016). After adapter trimming and joining paired reads, a total of 12,058,446 sequences were obtained for the 112 investigated samples (12404-626827 reads per sample). This process resulted in 3001 OTUs with at least two reads. Taxonomic classification was performed through machine learning Scikit-learn naive-Bayes classifier (Wang, Garrity et al. 2007, Fabian Pedregosa 2011) using Silva 138_99 database (Prabhu, Altman et al. 2012, Quast, Pruesse et al. 2013) and setting an 80% acceptance as a cut-off match identity with the obtained OTUs.

4.2.2 Statistical Analyses

Alpha diversity, for example the Shannon diversity index, observed species (*e.g.,* richness), and Chao1 were achieved with QIIME2 and analyzed with R (version 4.1.3). The bray-Curtis (Beals 1984, Ricotta and Podani 2017), and unweighted and weighted UniFrac distance metrics (Lozupone 2005) also resulted from QIIME2. They were used to evaluate and visualize the beta diversity with R. All plots were generated with the ggplot2 package in R (Wickham 2016) if not specified otherwise.

For this research, community dissimilarities were compared with permutational multivariate analysis of variance (PERMANOVA) *via* the vegan package (Oksanen 2022). ANOVA, Kruskal–Wallis test, and pairwise Wilcoxon rank sum test was used for other comparations to identify the significant differences. The assumption of normality was tested by using the Shapiro–Wilk test on the residuals. P-values were adjusted using the Benjamini–Hochberg correction method. All the analyses were carried out in R. Violin chart of alpha diversity comparisons were conducted to reveal dynamics of reactor microbiomes with different environmental factors as visualized by

sampling points and experimental stages. Non-metric multidimensional scaling (NMDS) analysis (Zorz, Sharp *et al*. 2019) and Principal coordinate (PCoA) analysis (Krause, Wassan *et al*. 2021) were used to visualize the differences in community among the samples with bray-Curtis or Unifrac distance *via* the vegan package (Oksanen 2022). Distance-based Redundancy Analysis (db-RDA) (Legendre 1999) was carried out with weighted Unifrac distance to study the relationship among the microbial structure, the reactor performance, and the environmental factors *via* the vegan package (Oksanen 2022). I used the variance inflation factor (VIF) to determine whether constraints describe the same β diversity (*e.g.,* constraints are redundant in the model when VIF is large). Spearman's rank correlation coefficient was performed to ascertain whether the microbiomes were significantly correlated or not to MCCA production *via* the psych package (Revelle 2022). Heat maps were created to visualize the abundance of OTU in different sample points and experimental stages *via* pheatmap package (Kolde 2019). Ternary plots were used to display the proportion of each genus in different groups *via* ggtern package (Hamilton 2022). To explore microbial interactions and network diversity of reactor microbiomes under different conditions, co-occurrence networks were built and visualized *via* igraph package (Csardi 2005, Amestoy 2022) and Cytoscape 3.9.1 (Shannon, Markiel *et al*. 2003). The Spearman coefficient was calculated based on the relative abundances of each OTU. Only OTUs with >0.1% relative abundance in more than three samples were included in the analysis. Spearman's rank correlations between selected OTUs were calculated. Pairs with Spearman's correlation coefficient $0.75 \leq \rho \leq 1$ and FDR-corrected p-value ≤ 0.05 were used for co-occurrence network construction. Network parameters (*e.g.,* clustering coefficient, number of edges [correlations] and nodes [OTUs], degree of nodes) were achieved *via* the igraph package.

4.3 Results

4.3.1 The taxonomic level of the reactor microbiomes throughout the operating period

The reactor microbiomes from all samples were classified into 2 domains, 9 phyla, 18 classes, 42 orders, 76 families, 130 genera, and 173 species. 97.6% of the

microbiomes were from Bacteria, with 2.31% from Archaea (**Figure 4.1**). Firmicutes, Spirochaetota, Bacteroidota, and Actinobacteriota (47.71%, 35.23%, 8.73%, and 5.56%, respectively) were the main bacterial phyla. The reactor microbiomes at the class level were represented mainly by Clostridia, Spirochaetia, Bacteroidia, Actinobacteria, Negativicutes, Bacilli, and Methanobacteria (37.52%, 35.23%, 8.73%, 4.33%, 4.21%, 4.00%, and 2.31%, respectively).

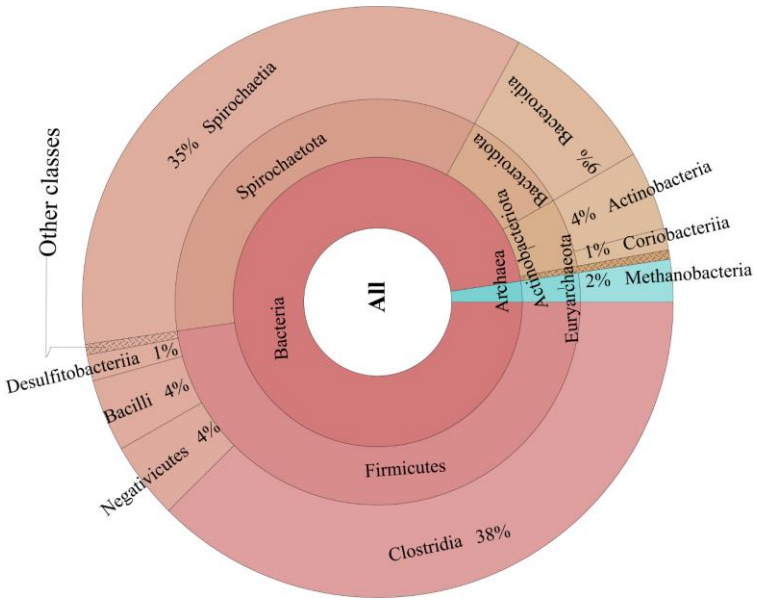

Figure 4.1. Sunburst chart analysis showing the taxonomic level of the reactor microbiomes.

4.3.2 The reactor microbiomes were shaped by different E_L_ratios

The E_L_ratio from 1 to 3 were applied to R1 to explore the effect of the E_L_ratio on reactor performance (**Figure 3.2**). The E_L_ratio of 1 was set as control in R2 (**Figure 3.3**). I investigated the microbial dynamics of the reactor microbiomes caused by the changed E_L_ratio in R1 (**Figure 4.2**). With increasing E_L_ratio from 1 to 3, the Shannon index of the microbiomes decreased (**Figure 4.2 A**). Other alpha diversity indexes also showed that the dissimilarity of the microbiomes arose from changeable E_L_ratio (**Table S4.1**). PCoA analysis showed that the microbial composition under different E_L_ratios formed significantly separated clusters (PERMANOVA: adonis, $p<0.001$; **Figure 4.2 B**).

At the class level, Spirochaetia (20.28%-36.99%) and Clostridia (25.27%-54.05%) dominated the reactor microbiomes in all groups (**Figure 4.3** and **Table S4.3**). Other

functional groups related to Actinobacteria, Bacteroidia, Bacilli, Negativicutes, Methanobacteria, Desulfitobacteriia, and Coriobacteriia showed a noticeable proportion difference among groups. Members from Clostridia was most enriched with a E_L_ratio of 2. Members from Bacteroidia, Desulfitobacteriia, and Coriobacteriia were more enriched with E_L_ratio of 3.

At the genus level, *Sphaerochaeta* spp. (26.62%-36.81%) dominated the reactor microbiomes in all groups (**Figure 4.4** and **Table S4.6**). The lactate concentration in the bioreactor decreased with an increase of E_L_ratio from 1 to 3, and I found *Lactobacillus* spp. was less enriched during this process (from 5.01% to 0.24%). With an E_L_ratio of 1, *Clostridia_UCG-014* spp., *Clostridium_sensu_stricto_12* spp., *Pseudoramibacter* spp., and *[Eubacterium]_nodatum_group* spp. were more enriched. The relative abundance of *Oscillibacter* and one genus from the family Oscillospiraceae was much higher with an E_L_ratio of 2. *Colidextribacter* spp., *Bacteroides* spp., *Lactococcus* spp., and one genus from the family Coriobacteriales were predominately enriched in the microbiomes with an E_L_ratio of 3. With the E_L_ratio increasing from 1 to 3, *n*-caproate production decreased, while *n*-caprylate production increased (**Figure 3.2A**). Thus, we used the Spearman method to correlate the change in the relative abundance of these genera and identified some bacteria that were significantly correlated with specific MCCA production (**Figure S4.3**). The production of *n*-caproate was positively correlated with *Clostridium_sensu_stricto_12* spp., *Lactococcus* spp., *RF39* spp. (from Bacilli Class), *Dialister* spp., and one genus from the family Coriobacteriales were found positively correlated with *n*-caprylate production. Genera of *UCG*-009 spp. and *Proteus* spp. were indentified a strong positive correlation with *n*-caprylate production, but they were of a very low portion in the reactor microbiomes (**Figure S4.7**). The production of odd-chain products was found positively correlated with one genus from the order Veillonellales-Selenomonadales. *Tannerellaceae* spp. and one genus form the family Izemoplasmatales were indentified to have a strong positive correlation with odd-chain product production, but they were of a very low abundance in the reactor microbiomes (**Figure S4.7**).

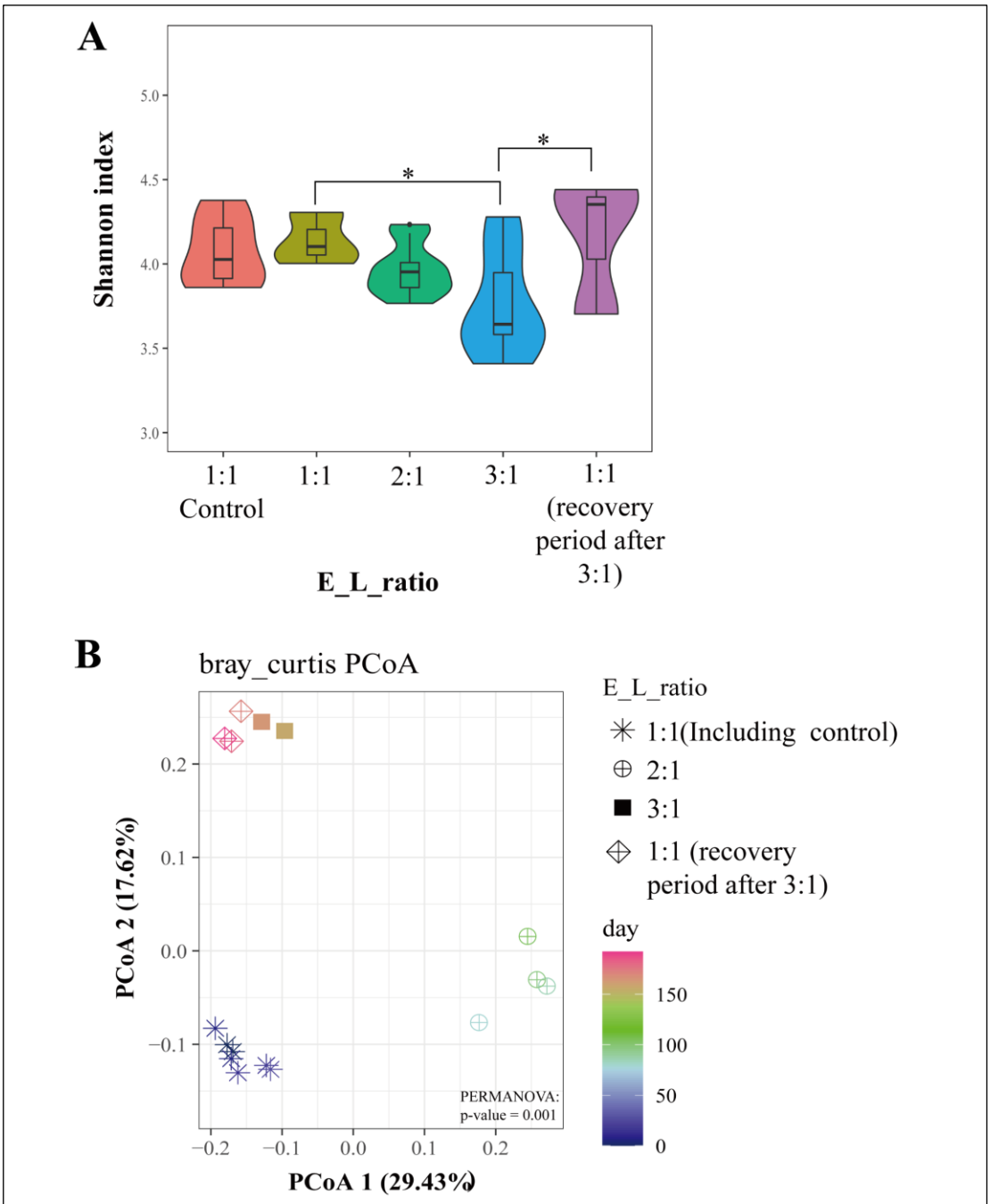

Figure 4.2. The microbial dynamics shaped by different E_L_ratios. The Shannon index of the microbiomes (A); PCoA analysis of the microbiomes at steady state with Bray-Curtis distance matrix among groups (B). The PCoA analysis of all samples during periods I-IV was shown in **Figure S4.1.**

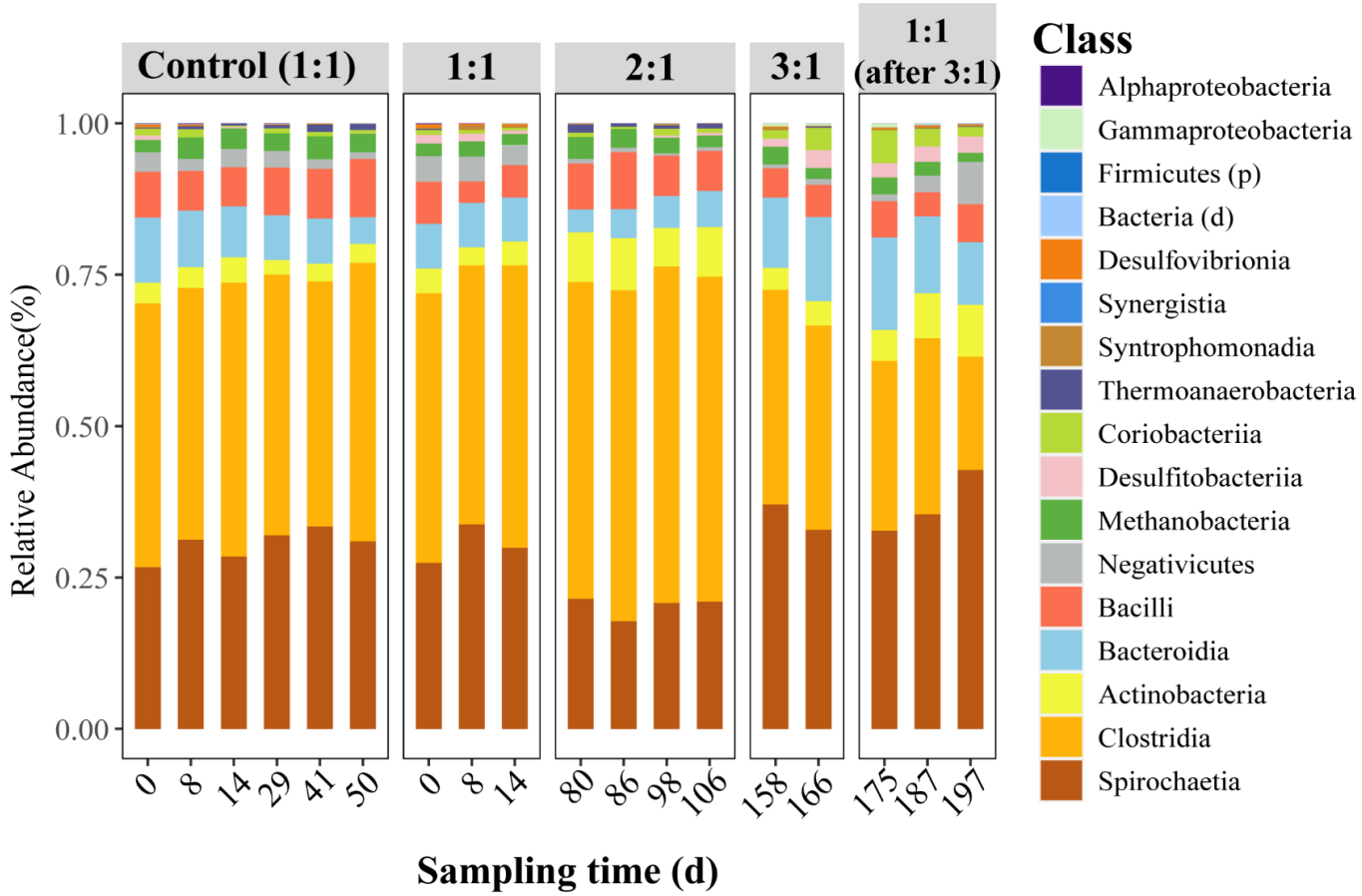

Figure 4.3. Bar graphs showing the relative abundance of reactor microbiomes with different E_L_ratios in R1. OTU taxonomy is given at the class level unless taxonomy assignment was not that specific (k: kingdom, p: phyla).

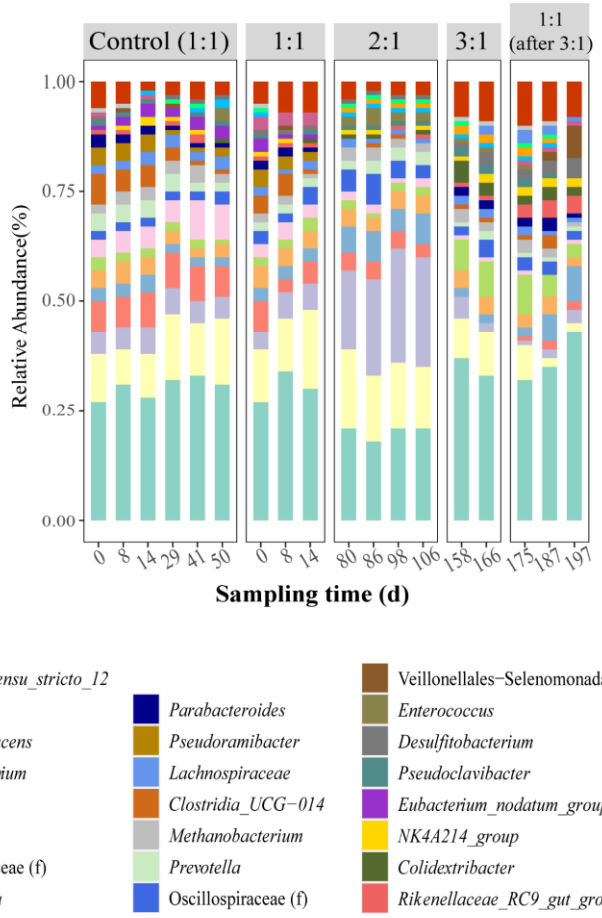

Figure 4.4. Bar graphs showing the relative abundance of top 30 most abundant genera in the reactor microbiome with different E_L_ratios. OTU taxonomy is given at the genus level unless taxonomy assignment was not that specific (k: kingdom, p: phyla, c: class, o: order, f: family).

4.3.3 The reactor microbiomes were shaped by different operating temperatures

The various operating temperatures (25ºC, 30ºC, 37ºC, and 42ºC) applied in the bioreactor also shaped the microbial community (**Figure 4.5**). The Shannon index of the microbiomes under different operating temperatures was different (**Figure 4.5A**). More parameters for evaluating the alpha diversity also displayed the difference among groups (**Table S4.1**). And, groups of reactor microbiomes with different temperatures separated significantly within the PCoA analysis (PERMANOVA: adonis, $p<0.001$) (**Figure 4.5B**).

More details in the microbial composition difference among groups were displayed *via* the analysis of the relative abundance of the class and genus (**Figures 4.6 and 4.7**).

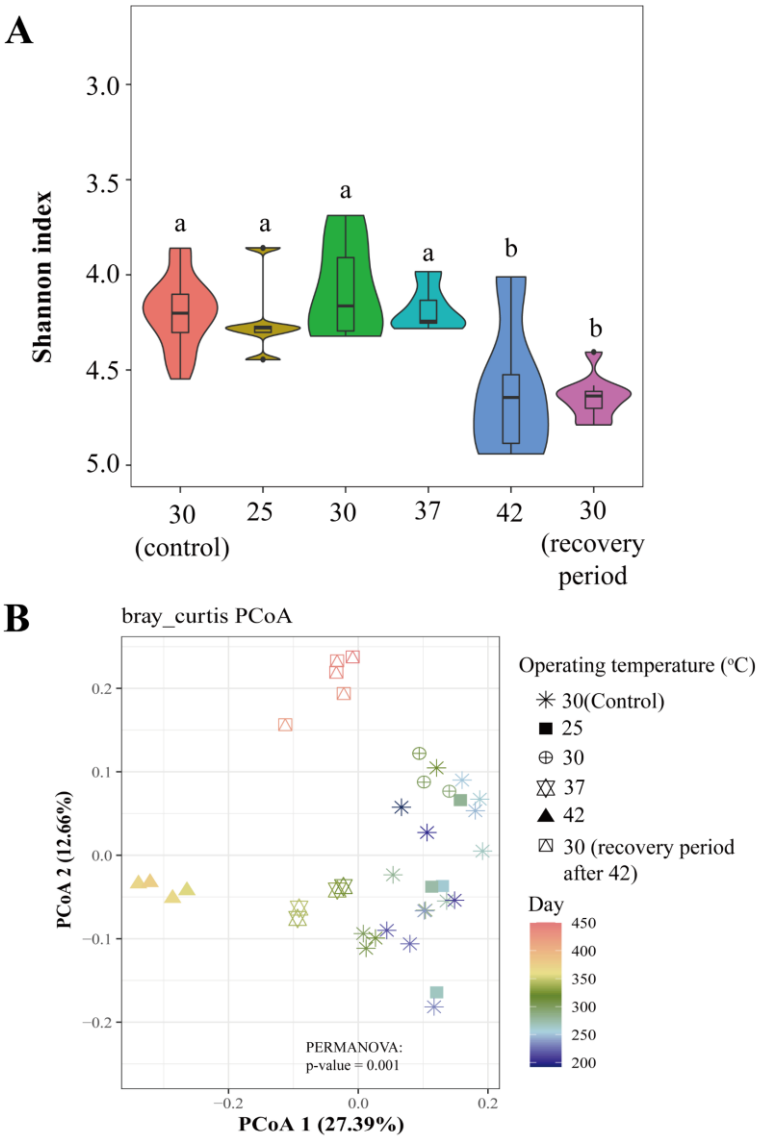

Figure 4.5. The microbial dynamics shaped by different operating temperatures. The Shannon index of the microbiomes (A); Principal coordinate analysis (PCoA) of the microbiomes at steady state with Bray-Curtis distance matrix (B). The PCoA analysis of all samples during periods I-IV was shown in **Figure S4.2.**

At the class level, Spirochaetia (37.22%-42.65%) and Clostridia (31.58%-40.54%) dominated the reactor microbiomes in all groups (**Figure 4.6 and Table S4.3**). I found that with the operating temperature increasing from 25°C to 42°C, the relative abundance of Clostridia, Actinobacteria, Bacteroidia, Bacilli, and Coriobacteriia decreased. On the contrary, the relative abundance of Negativicutes, Methanobacteria, and Desulfitobacteriia increased when the operating temperature increased from 25°C

to 42ºC. At the genus level, *Sphaerochaeta* spp. (37.14%-42.65%) and one genus from the family Ruminococcaceae (8.46%-6.56%) were dominated in the microbiomes (**Figure 4.7 and Table S4.6**). *Clostridia_UCG-014* spp. and *Oscillibacter* spp. were more enriched in the microbiomes with a relatively low operating temperature at 25ºC or 30ºC. *Rikenellaceae_RC9_gut_group* spp., *Propionibacterium* spp., *Bacteroides* spp., and one genus from the order Veillonellales-Selenomonadales were primarily present at 25ºC, but almost disappeared in the microbiomes at 42ºC (0.49%, 0.37%, 0.43%, and 0.47% respectively). *Methanobacterium* spp., *Desulfitobacterium* spp., and one genus from the class Negativicutes had higher relative abundance in the microbiomes with a relatively high temperature at 37ºC or 42ºC. *Clostridium_sensu_stricto_12* spp. and one genus from the family Oscillospiraceae were more enriched when the temperature went back to 30ºC after 42ºC. The microbial composition of the control (at class and genus level) showed no obvious change without changing the operating temperature (**Figures S4.5 and S4.6**).

I connected the microbial change with the reactor performance *via* Spearman's rank correlation and identified several bacteria significantly correlated with specific MCCA production (**Figure S4.4**). The production of *n*-caproate was positively correlated with *Methanobacterium* spp., *Incertae_Sedis* spp., *[Eubacterium]_nodatum_group* spp., one genus from the order Oscillospirales, one genus from the family Ruminococcaceae, and one genus from the class Negativicutes. *Sutterella* spp. and one genus from the family Sporomusaceae were found to be positively correlated with *n*-caproate production, but they were of a very low portion in the reactor microbiomes (**Figure S4.7**). Genera of *Rikenellaceae_RC9_gut_group* spp., *Propionibacterium* spp., *Bacteroides* spp., Anaerofilum spp., and Colidextribacter spp. were indentified own a strong positive correlation with *n*-caprylate production. The production of odd-chain products was found positively correlated with *Propionibacterium* spp.

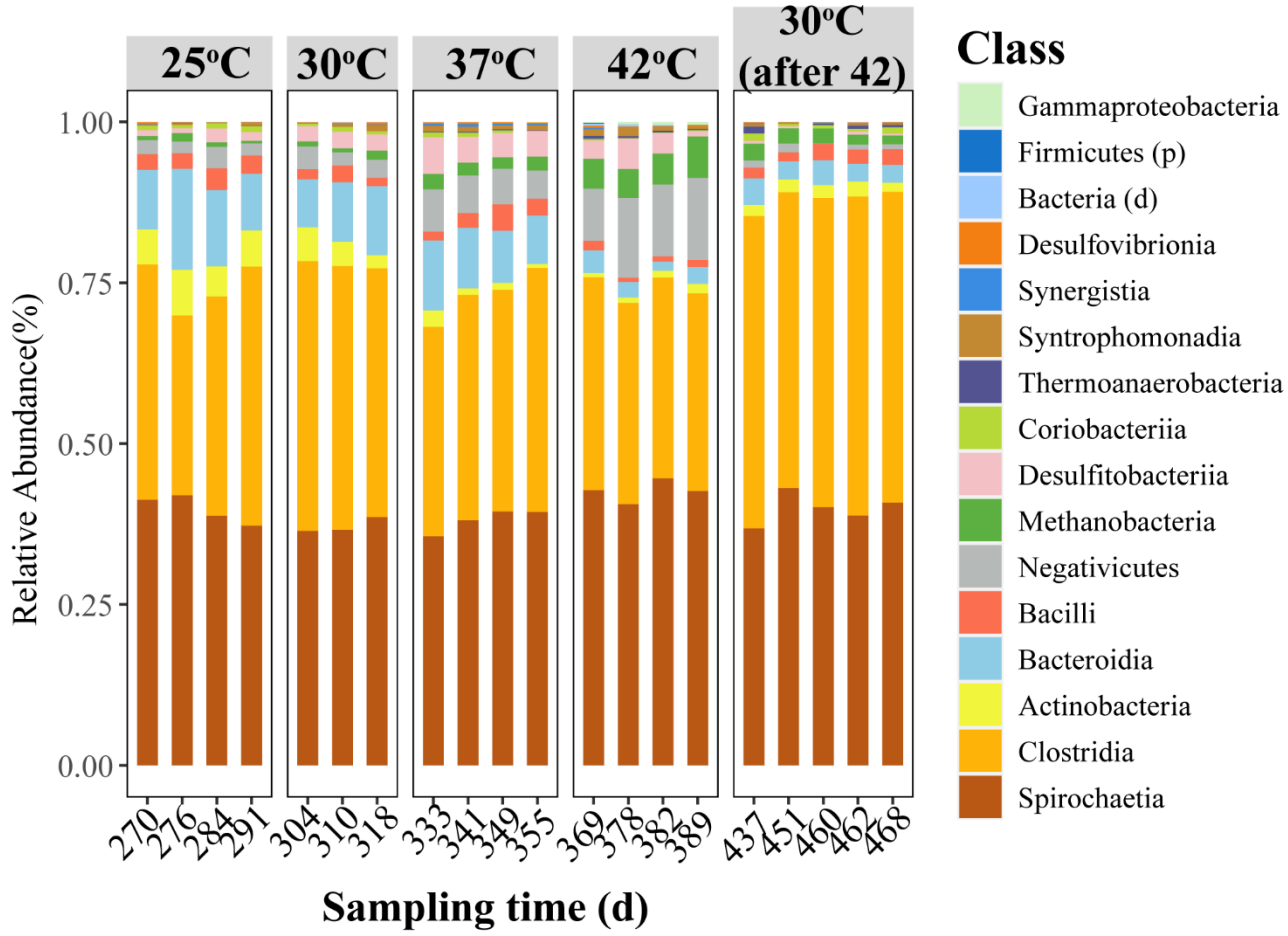

Figure 4.6. Bar graphs showing the relative abundance of reactor microbiomes with different operating temperatures in R1. OTU taxonomy is given at the class level unless taxonomy assignment was not that specific (k: kingdom, p: phyla).

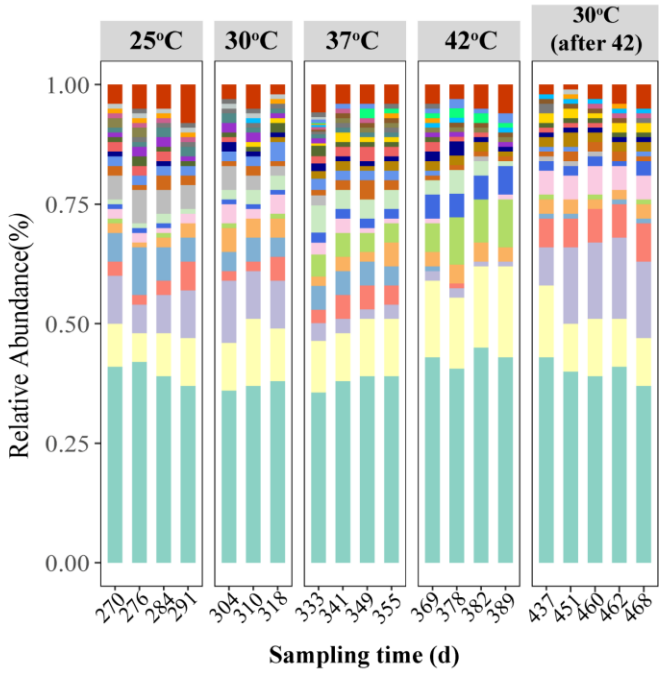

Figure 4.3. Bar graphs showing the relative abundance of top 30 genera in the reactor microbiome with operating temperatures. OTU taxonomy was given at the genus level unless taxonomy assignment was not that specific (k: kingdom, p: phyla, c: class, o: order, f: family).

4.3.4 Environmental factors associated with microbial dynamics

I performed a Weighted_Unifrac distance-based redundancy analysis for five explanatory variables (two environmental factors and three reactor performance) to identify factors modulating microbial community structure in the bioreactor (**Figure 4.8**). These factors contributed to 22.25% of the explanation in the taxonomic structure, with 86.48% represented in the first two axes of the db-RDA. The microbial structure was shaped with the effect of environmental factors (E_L_ratio and operating temperature) and the impact of reactor performance (the production rate of *n*-caproate, *n*-caprylate, and odd products) (**Figure 4.8 B**). The applied environmental factors affected the microbial dynamics more (14.42% *vs.* 6.63%). These results implied that the ecological and reactor performance shaped the microbial reactor community, creating to a unique composition in each experimental group.

To better display the dissimilarity of the two microbial communities shaped by different E_L_ratios or operating temperatures, the taxonomic differences (at class and genus level) in the microbial composition between the two microbial communities in the two stages were explored here (**Figure 4.9**). The dominant class in both microbial communities was Actinobacteria, Bacilli, Bacteroidia, Clostridia, Coriobacteriia, Desulfitobacteriia, Methanobacteria, Negativicutes, and Spirochaetia (**Figure 4.9 A**). Actinobacteria, Bacilli, Clostridia, and Coriobacteriia were more related to the microbiomes shaped with E_L_ratio, with 19 genera significantly enriched (**Figure 4.9 B**). However, Desulfitobacteriia, Negativicutes, and Spirochaetia were more enriched in the microbiomes shaped with operating temperature, with five genera significantly enriched (**Figure 4.9 B**).

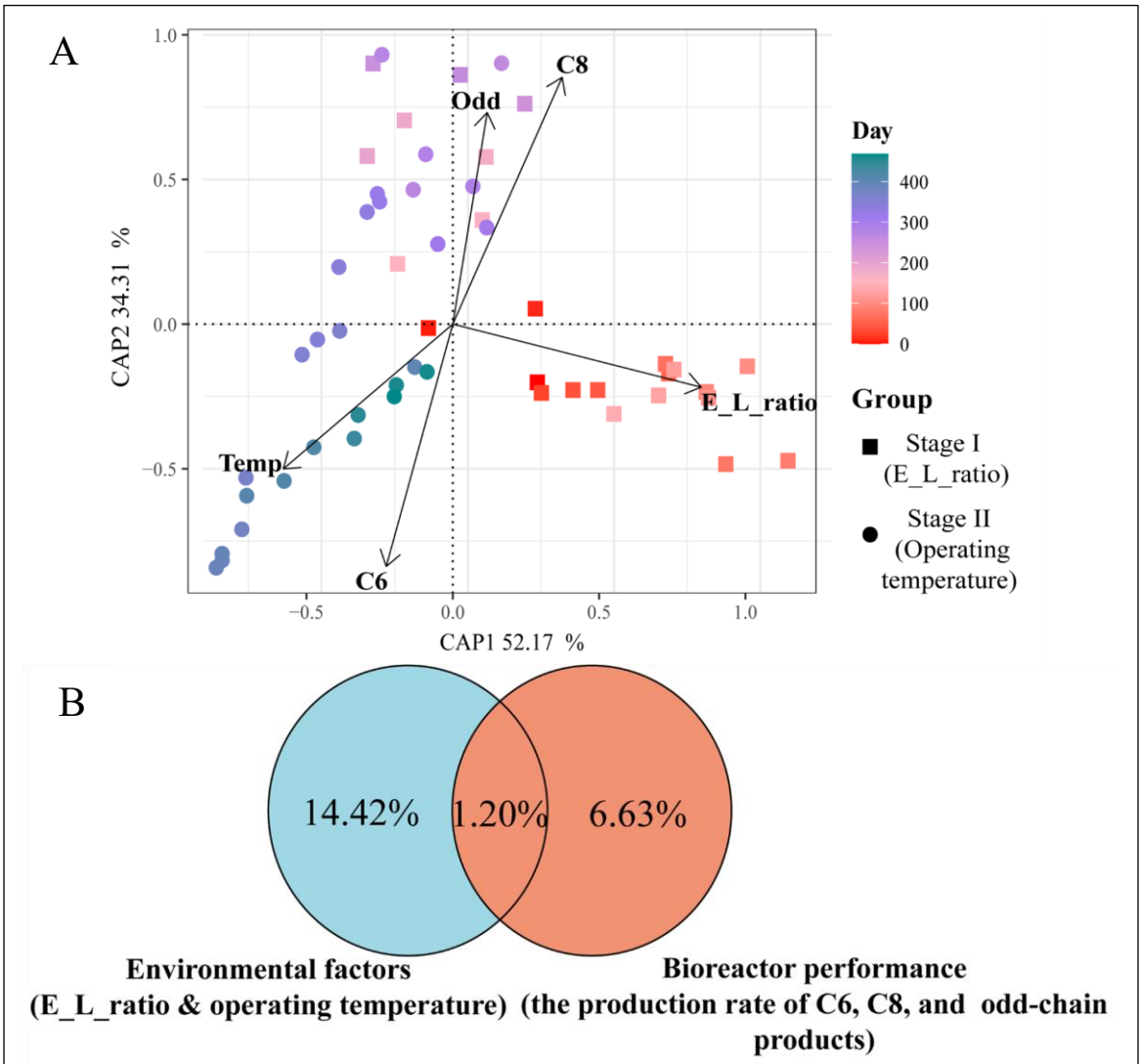

Figure 4.8. Redundancy analysis based on weight_Unifrac (tb-RDA) of the reactor microbiome from the two stages in R1. The microbial community structure constrained by the selected factors (A); Variation partitioning analysis (VPA) separating the variation of community structure explained by the CCA model (B). The constrained factors were selected by a stepwise forward selection method in R. The whole model was statistically significant ($P<0.001$), and the adjusted explained variation was 22.25%. (Temp: the operating temperature; C6: the production rate of *n*-caproate; C8: the production of *n*-caprylate; odd: the production rate of odd-chain products).

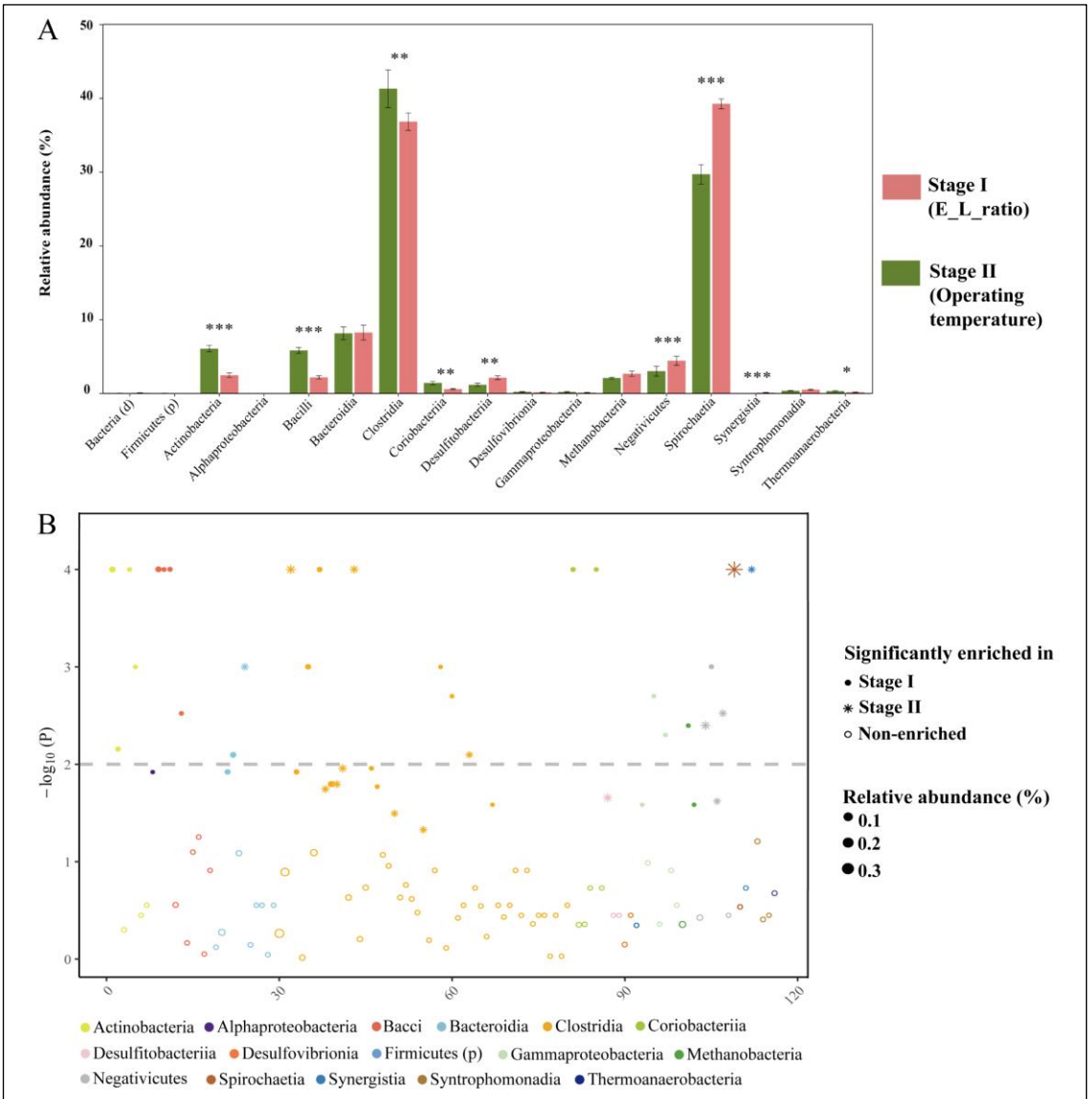

Figure 4.9 The microbial composition of the reactor microbiomes in E_L_ratio experiment (stage I) and operating temperature experiment (stage II) from R1. Bar graphs of mean relative abundance of the microbiomes (class level) contributing to the microbial group in stage I and stage II. Error bars denote the standard error of the mean. (*, $p < 0.05$; **, $p < 0.01$; ***, $p < 0.001$, Wilcox.test, R package ggpubr) (A); Manhattan plot showing OTUs (at genus level) enriched in stage I or stage II. Each OTU was colored according to the Class. The size of the shape was weighted by the relative abundance. The OTUs enriched in stage I (asterisk); The OTUs enriched in stage II (dot); the OTUs not enriched in any stage (circle). The y axis represents -log (two-sided p-values), which was evelueated by a p-value < 0.05, false discovery rate (FDR) adjusted with "BH" method, Wilcox test (B).

4.3.5 The effect of the in-line extraction collapse on the microbial community for MCCA production

The defective in-line extraction system affected the reactor performance (**Figures 3.2 and 3.3**) and also changed the microbial community in the bioreactor (**Figures 4.10**). I divided the process of repairing the in-line extraction system into three parts (before collapse, collapse, and recovery) and compared the microbial change. The PCoA

analysis showed the cluster of the microbiomes of each process separated (**Figure 4.10**), which displayed the fact that the microbial composition was significantly changed during the process with the collapse of the extraction system (PERMANOVA: adonis, p-value<0.001).

The collapse process in R2 lasted longer than in R1 and could provide more details. The process of the collapse in the in-line extraction system in R2 could be divided into six parts - before the collapse (period **a**), period I of the collapse (the beginning of period **b**), period II of the collapse (the end of period **b**), recovery with an E_L_ratio of 1(the beginning of period **c**), recovery with an E_L_ratio of 3 (the end of period **c**), and recovery with an E_L_ratio of 1 (the beginning of period **d**). During period I of the collapse, I improved the pump rate of the forward membrane in the extraction system to improve the extraction efficiency. However, improving the pump rate could not remove the accumulation of the products in the bioreactor. The accumulated carboxylates increased the total concentration of undissociated carboxylates in the bioreactor, which was toxic to the microbiomes, leading to the complete collapse of reactor performance during period II of the collapse (**Figure 3.3**). The production of *n*-caprylate increased during period I of the collapse (**Table S4.2**). *Oscillibacter* spp., *Pseudoramibacter* spp., *Prevotella* spp., *Clostridium_sensu_stricto_12* spp., *Methanobacterium* spp., and some genera from families Ruminococcaceae, Oscillospiraceae or Lachnospiraceae were found less abundant during period II of the collapse (**Figure 4.12 and Table S4.7**). Still, I found *Bacteroides* spp. and one genus from the order Veillonellales-Selenomonadales was more enriched during period II of the collapse. The extraction system was recovered during the recovery period with an E_L_ratio of 1, but the MCCA production did not increase, especially the production of *n*-caprylate (**Table S4.2**). Thus, I increased the E_L_ratio from 1 to 3, which increased the MCCA production in the bioreactor, especially *n*-caprylate production. The microbial community was varied with different E_L_ratios in the bioreactor (**Figure 4.10 B**). *Caproiciproducens* spp. and one genus form the family Ruminococcaceae were more enriched during recovery with an E_L_ratio of 3 (**Figure 4.12 and Table S4.7**).

Similarly, I found an increase in the relative abundance of the members from the order Veillonellales-Selenomonadales when the extraction system collapsed in R1 (**Figure S4.9 and Table S4.6**).

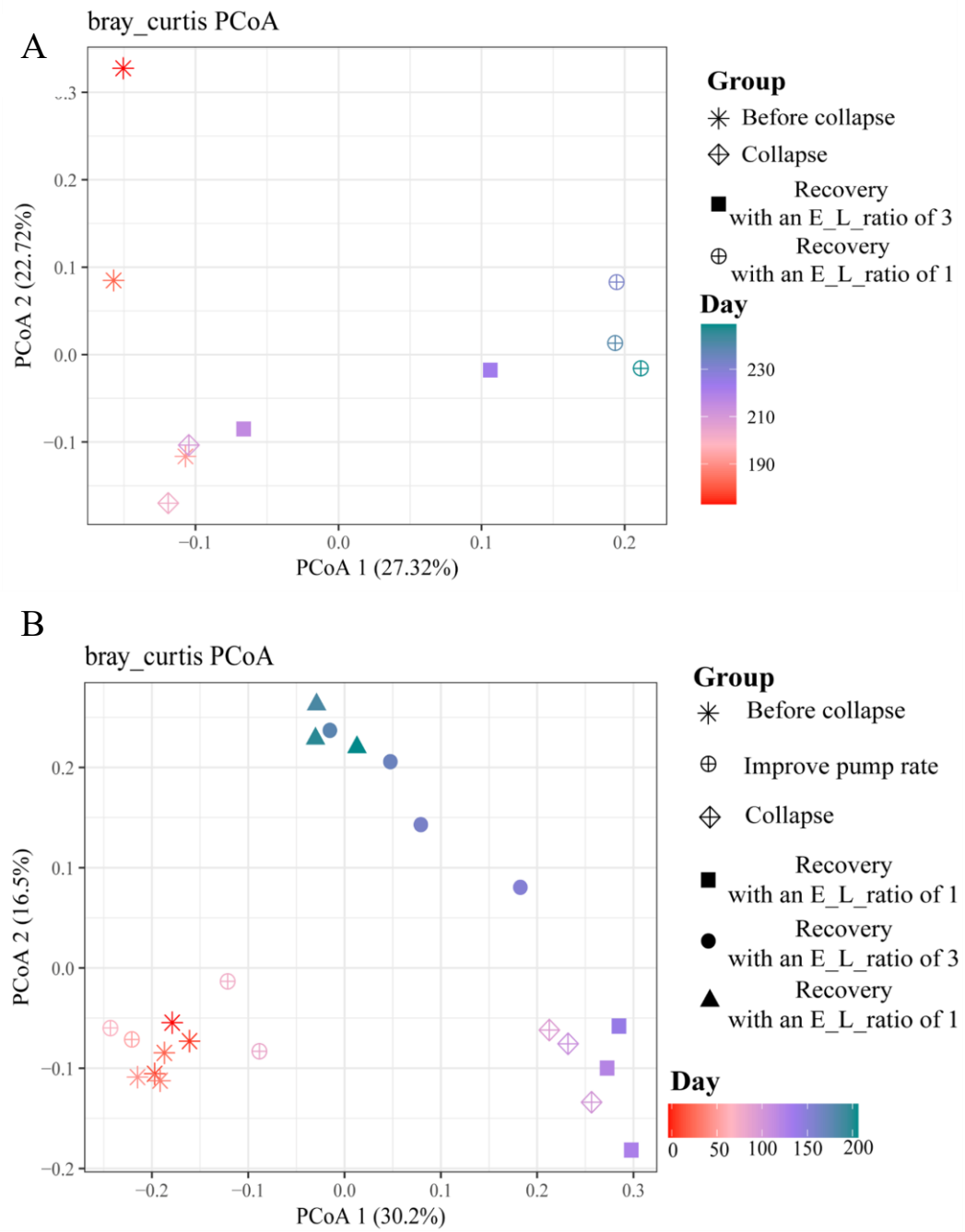

Figure 4.10. Principal coordinate analysis (PCoA) of the microbiomes with Bray-Curtis distance matrix. The microbiomes during the periods before the collapse/ with collapse/ recovery in R1 (A); The microbiomes during the periods before the collapse/ with collapse/ recovery in R2 (B).

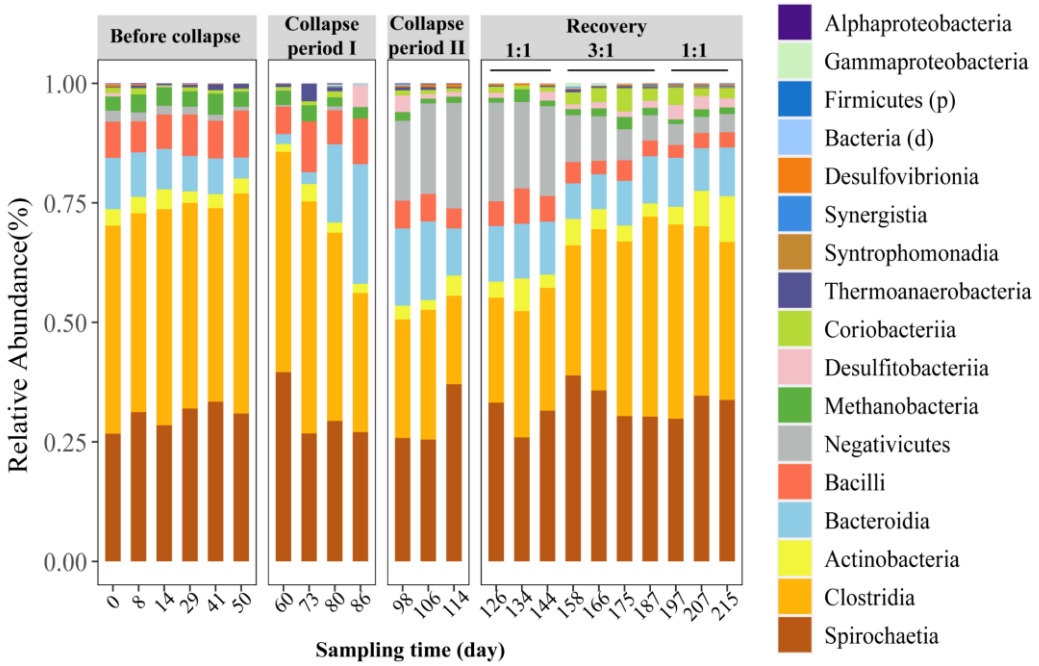

Figure 4.11. Bar graphs showing the relative abundance of reactor microbiomes during the periods before the collapse/ with collapse/ after collapse in R2 at class level. OTU taxonomy was given at the class level unless taxonomy assignment was not that specific (k: Kingdom, p: Phyla).

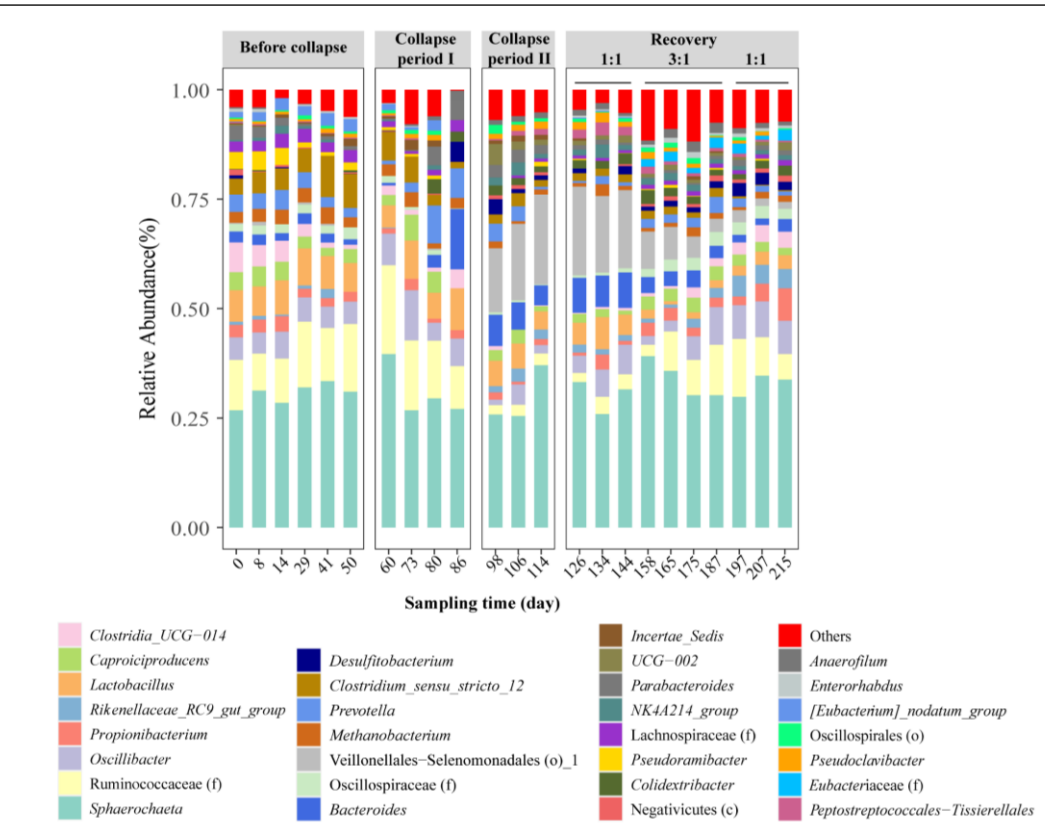

Figure 4.12. Bar graphs showing the relative abundance of the top 30 most abundant genera of reactor microbiomes in different groups (during the periods before the collapse/ with collapse/ after collapse). OTU taxonomy was given at the class/genus level unless taxonomy assignment was not that specific (k: Kingdom, p: Phyla, c: Class, o: Order, f: Family).

4.3.6 The microbial ecology of the reactor microbiomes when *n*-caproate was dominant in the product

An E_L_ratio of 1 during stage I or operating temperatures of 37ºC-42ºC during stage II drove more substrate-carbon into *n*-caproate production and made *n*-caproate dominant in the product (**Table S4.8**). I characterized the microbial communities shaped by different environmental factors for high *n*-caproate production. The PCoA analysis showed that the microbial community steered by various environmental factors was significantly separated (PERMANOVA: adonis, p-value < 0.001; **Figure S4.10 and Table S4.9**).

At the class level, Spirochaetia and Clostridia were dominated in the microbial communities across all the clusters (**Figure 4.13**). Clostridia was more enriched in the first cluster (steered by an E_L_ratio of 1) than in the second cluster (steered by an operating temperature of 37ºC) or the third cluster (steered by an operating temperature of 42ºC) with a propotion in each cluster of 43.75%, 35%, 32.58%, repectively. Actinobacteria and Bacilli showed a higher relative abundance in the first cluster. However, Desulfitobacteriia accounted for an higher total abundance in the second and third clusters. In addition, Bacteroidia were less abundant in the third cluster, while the relative abundance of Negativicutes or Methanobacteria increased much in the third cluster.

To explore more details about the ecological interactions within the microbial community, three networks based on the three clusters were conducted (Spearman's r ≥ 0.75, p-value < 0.05; **Figure 4.14**). The three microbial networks showed different characteristics (**Table S4.10**). The first microbial network based on the first cluster consisted of three subgroups (**Figure 4.14 A**). Subgroup (a) was formed with three key genera: *Clostridium_sensu_stricto_12* spp., *Pseudoclavibacter* spp., and *[Eubacterium]_nodatum_group* spp. And, *Clostridium_sensu_stricto_12* spp. and *[Eubacterium]_nodatum_group* spp. were identified to be positively correlated with *n*-caproate production (**Figures S4.3** and **S4.4**). Subgroup (b) was independent of the other two subgroups. Positive correlations of *Oscillibacter* spp. with *Caproiciproducens* spp., *Clostridia_UCG-014* spp., and *Pseudoramibacter* spp. characterized subgroup (c). In addition, I found that the co-occurrence of subgroups (a) and (b) was mainly linked by connecting to *Lactobacillus* spp. and *Prevotella* spp. The second microbial network was based on the second cluster, which owned more significantly negative connections than the first one (**Figure 4.14 B**). I also identified

three subgroups within this network. *Incertae_Sedis* and one genus from the order Oscillospirales, which were determined to be positively correlated with *n*-caproate production, were enriched in this microbial network (**Figure 4.14 B**). In subgroup (a), *[Eubacterium]_nodatum_group* spp. was found negatively connected with one genus from the order Veillone-Selenomonadales, which was found to be positively correlated with the production of odd-chain products **(Figures S4.3 and S4.4)**. Subgroup (b) reacted as the bridge for subgroups (a) and (c). Subgroup (c) was characterized by the co-occurrence of *Sphaerochaeta* spp., *Desulfitobacterium* spp., *Clostridia_UCG-014* spp., and one genus from the order Oscillospirales. The third microbial network was based on the third cluster and consisted of three subgroups (**Figure 4.14 C**). The genera enriched in this cluster (**Figure S4.11**) were mainly involved in the subgroup (a). The subgroup (a) was characterized by the co-occurrence of *Peptostreptococcales-Tissierellales* spp., *Sphaerochaeta* spp., *Methanobacterium* spp., *Incertae_Sedis* spp., *[Eubacterium]_nodatum_group* spp., one genus from the family Ruminococcaceae, one genus from the class Negativicutes, and one genus from the order Oscillospirales. Also, *Methanobacterium* spp., *Incertae_Sedis* spp., *[Eubacterium]_nodatum_group* spp., the genus from the family Ruminococcaceae, the genus from the class Negativicutes, and the genus from the order Oscillospirales were identified positively correlated with *n*-caproate production. In subgroup (b), we found that *Rikenellaceae_RC9_gut_group* spp. was positively associated with *n*-caprylate production **(Figure S4.3 and S4.4)** and showed some negative connections with others.

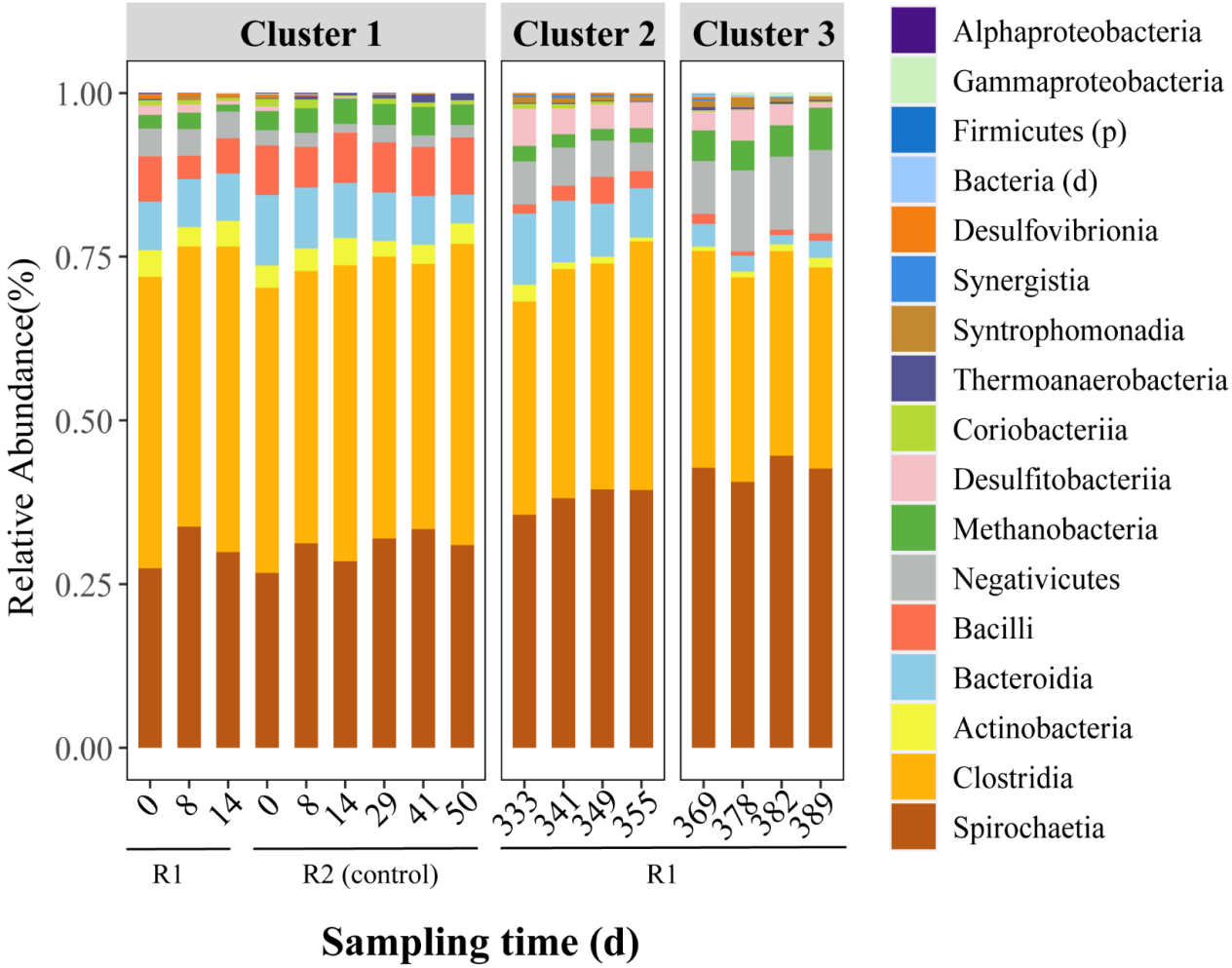

Figure 4.13. Bar graphs showing the relative abundance of reactor microbiomes from the three clusters shaped by different conditions for high *n*-caproate production. OTU taxonomy is given at the class level unless taxonomy assignment was not that specific (k: Kingdom, p: Phyla).

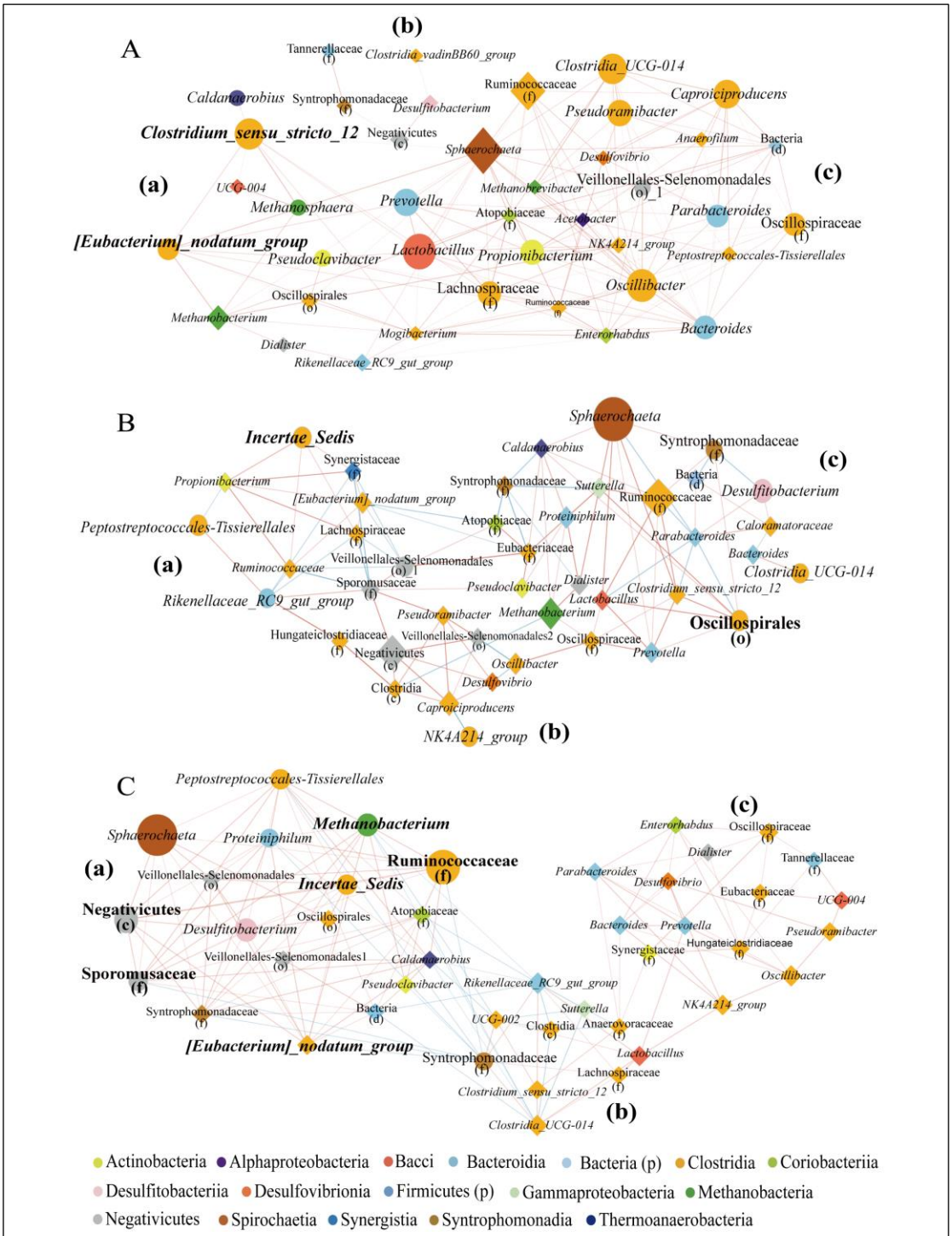

Figure 4.14. Co-occurrence network based on correlation analysis of the microbial community from the three clusters (p-value < 0.05, r >= 0.75). A: based on the first cluster; B: based on the second cluster; C: based on the third cluster. OTU taxonomy was given at the genus level unless taxonomy assignment was not that specific (k: Kingdom, p: Phyla, c: Class, o: order, f: family). The nodes were colored according to the Class to which the OTUs belonged, and were shaped based on if the OTUs were enriched in the cluster community (diomond:non-enriched; ellipse:enriched) (**Figure S4.11**). Nodes were also weighted by the relatibve abundance of the OTUs. The edges were colored by the correlation (red: positive; blue: negative), and were also weighted by the strength of the correlation. Bold labels mean that the OTUs were significantly positively correlated with the production of *n*-caproate (**Figures S4.3 and S4.4**).

4.3.7 The microbial ecology of the reactor microbiomes when *n*-caprylate was dominant in the bioreactor

n-Caprylate was dominated product in the bioreactor with an E_L_ratio of 3 during stage I or with the operating temperatures of 25ºC-30ºC during stage II (**Table S4.11**). I explored the microbial ecology of the microbial communities with a high *n*-caprylate production rate shaped by different environmental conditions. The NMDS analysis showed no significant difference among the three groups (PERMANOVA: anosim, $p > 0.05$), which implied that the microbial communities that were steered for high *n*-caprylate production by E_L_ratio or operating temperature were similar (**Figure 4.15 and Table S4.12**). I found that the in the *n*-caprylate production relative microbial community, Spirochaetia and Clostridia were the most abundant taxonomic classes, with an average abundance of 35.62% and 34%, respectively (**Figure 4.16**). The other seven main classes were Bacteroidia (11.37%), Actinobacteria (5.5%), Bacilli (3.12%), Negativicutes (3.66%), Desulfitobacteriia(1.84%), and Coriobacteriia (1.71%), Methanobacteria (1.45%).

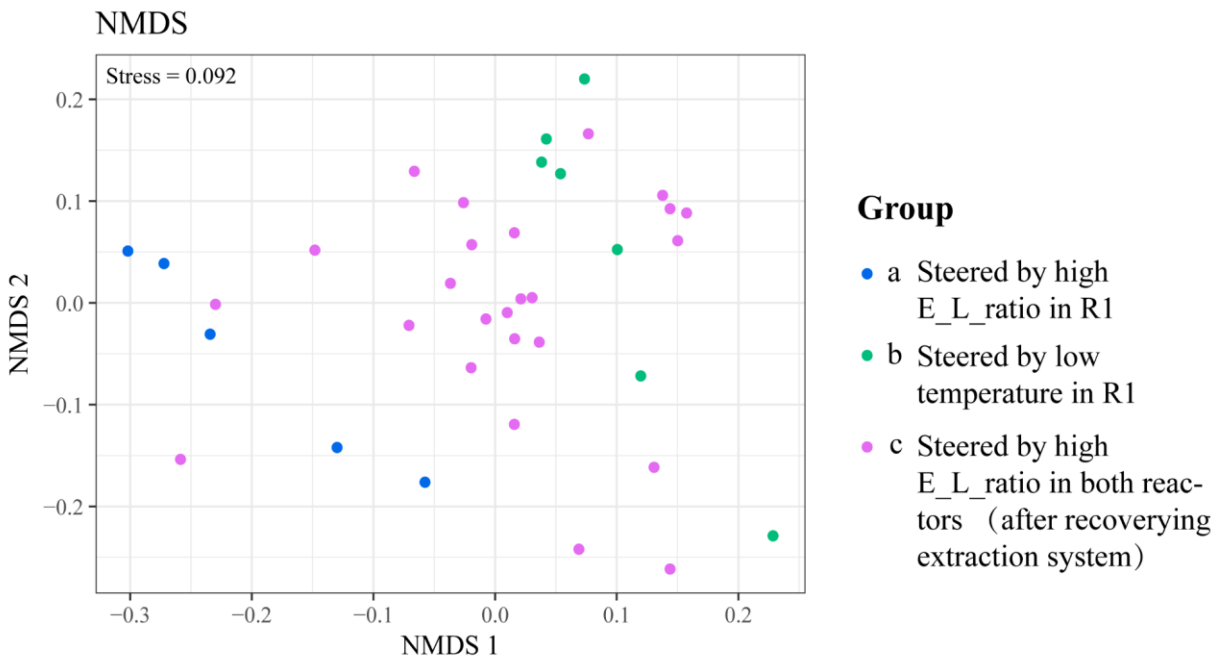

Figure 4.15. Non-metric multidimensional scaling (NMDS) of the bacterial communities at the genus level based on Bray-Curtis distance. Group a, b, and c represented microbiomes with high *n*-caprylate production steered by different environmental factors.

Network analysis of the microbial communities relative to high *n*-caprylate production was conducted here to explore the potential interactions between microbial taxa to decipher the structure of complex microbial communities and to gain a more integrated understanding of the

microbial community structure (**Figure 4.17**). The network (nodes: 43, links: 100, and more properties were shown in **Table S4.10**) showed a higher number of total positive correlations among bacteria in comparison with the negative ones (Spearman's $\rho \geq 0.6$, p-value < 0.05). The members owned high degree (the size of each node is proportional to the number of connections) were *Colidextribacter* spp., *Bacteroides* spp., *Dialister* spp., *Enterorhabdus* spp., *Anaerofilum* spp., and two genera from the families Mogibacterium and Coriobacteriales.

In the microbial network, three subgroups were identified (**Figure 4.17**). In subgroup (a), *Lactococcus* spp. was identified as positively correlated with *n*-caprylate production (**Figures S4.3 and S4.4**). *Lactococcus* spp. was co-occurrenced with *Oscillibacter* spp., *Clostridia_UCG-014* spp., and one genus from the family Ruminococcaceae. Subgroup (b) was separated from the other two subgroups, and within this subgroup, *Rikenellaceae_RC9_gut_group* spp. was indentified as positively correlated with *n*-caprylate production. In subgroup (c), *Colidextribacter* spp., *Bacteroides* spp., *Dialister* spp., *Anaerofilum* spp., and one genus from the family Coriobacteriales were the key genera. These four bacteria were all identified as positively correlated with *n*-caprylate production.

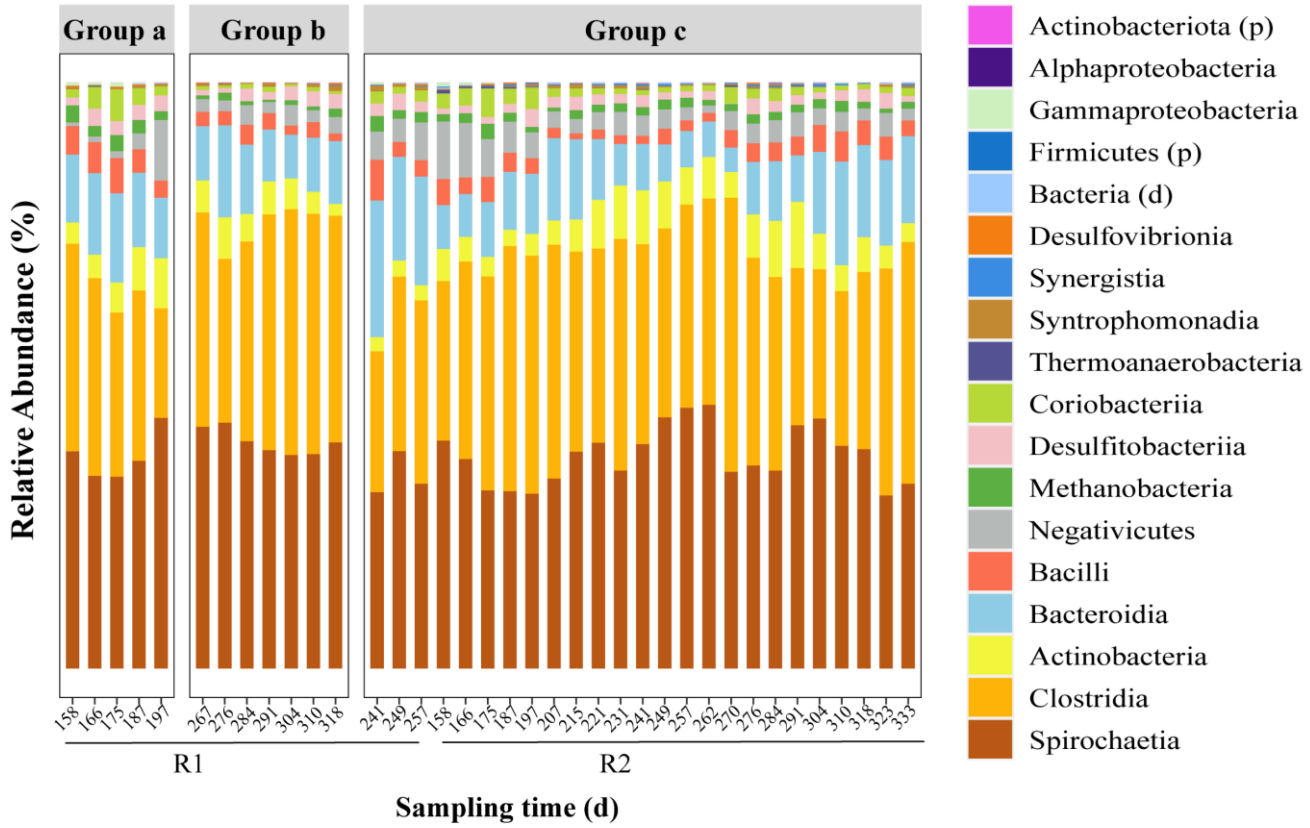

Figure 4.16. Bar graphs showing the relative abundance of reactor microbiomes. Groups a, b, and c represented the microbiomes with high *n*-caprylate production steered by different environmental factors. OTU taxonomy is given at the class level unless taxonomy assignment was not that specific (k: kingdom, p: phyla).

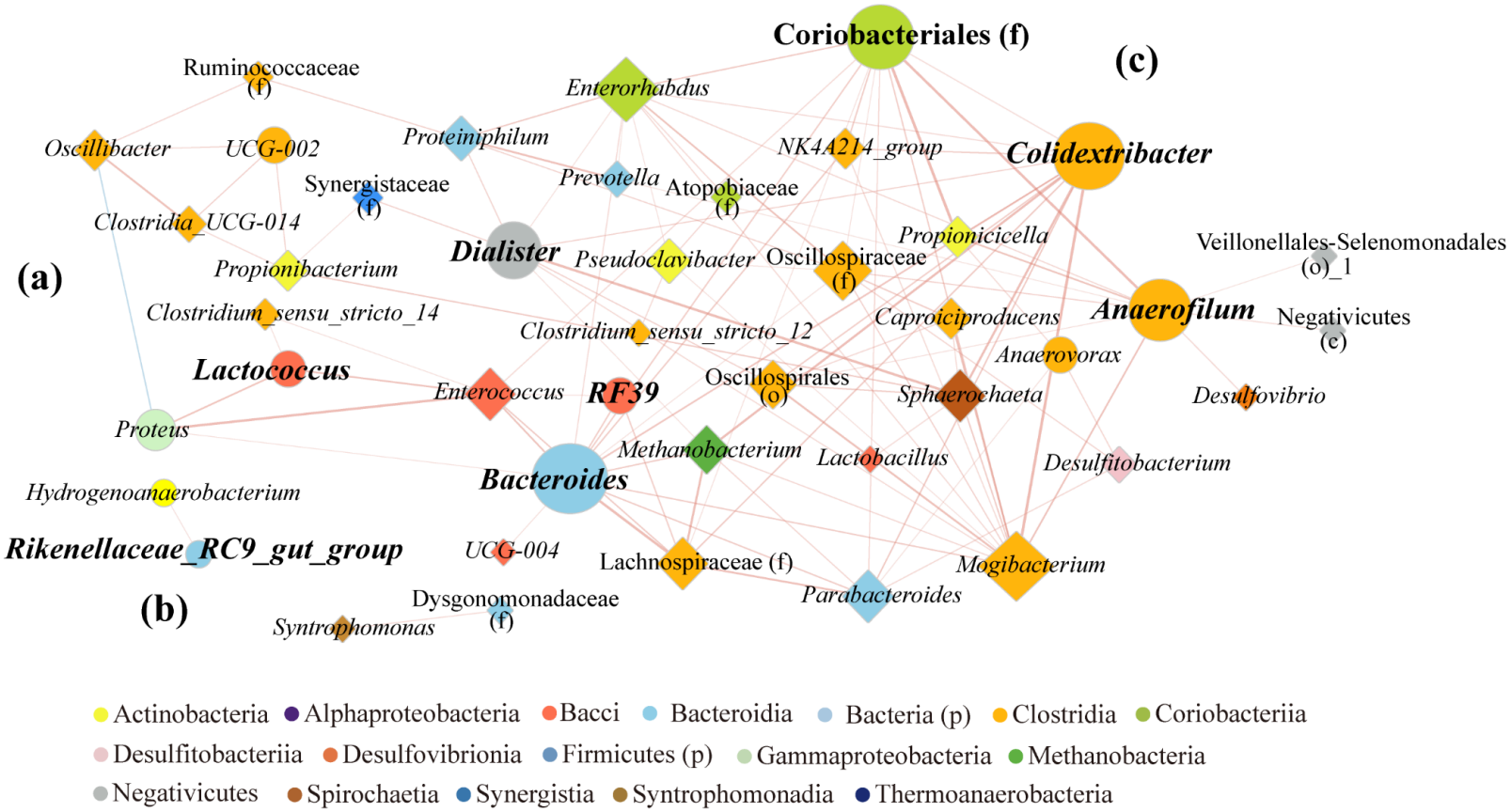

Figure 4.17. Co-occurrence network based on correlation analysis of the microbial community from the three groups with high production of *n*-caprylate (p-value < 0.05, r >= 0.75). The nodes were colored according to the Class to which the OTUs belonged, and were shaped if the OTUs were significantly positively correlated with the production of *n*-caprylate **(Figures S4.3 and S4.4)** (diomond:non-correlated; ellipse:correlated). Nodes were weighted by its proportional to the number of connections (its degree). The edges were colored by the correlation (red: positive; blue: negative), and were also weighted by the strength of the correlation. OTU taxonomy is given at the genus level unless taxonomy assignment was not that specific (k: Kingdom, p: Phyla, c: Class, o: order, f: family). Bold size of the lable means the genus is positively correlated with *n*-caprylate production.

4.3.8 The comparison of the microbial community for specific MCCA production

The different environmental factors (applied operating conditions) shaped the product spectrum in the bioreactor (**Table S4.13**). *n*-Caproate was dominant in the bioreactor with an E_L_ratio of 1 during stage I or the operating temperatures of 37°C -42°C during stage II. In comparison, An E_L_ratio of 3 during stage I or the operating temperatures of 25°C-30°C derived the bioreactor producing more *n*-caprylate than *n*-caproate. Also, under some conditions, *n*-caproate had a similar production rate with *n*-caprylate (**Table S4.13**). I investigated and compared the microbial diversity over the microbiomes with different MCCAs as the dominant product. For a better description, I defined the microbiomes into three groups here. Group 1: with higher *n*-caproate production than *n*-caprylate; Group 2: with similar *n*-caproate production with *n*-caprylate; Group 3: with higher *n*-caprylate production than *n*-caproate. The PCoA analysis showed the dissimilarity in community composition among the groups (PERMANOVA: adonis, p-value < 0.001, **Figure 4.18**).

A ternary plot was used to assess the distribution of each genus in the three groups (**Figure 4.19 A**). The ternary plot showed that most of the genera came from Clostridia. Comparing the relative abundance of each class in each group, we found that Clostridia was most abundant in group 2 (**Figure 4.19 B**). Spirochaetia was the second abundant class for all groups, showing no significant difference among groups (**Figure 4.19 B**). The relative abundance of Bacilli did not show significant differences among groups either. Negativicutes and Methanobacteria were found to be more enriched in group 1. Bacteroidia and Coriobacteriia were significantly abundant in group 3. Actinobacteria were mainly associated with group 2 and group 3. Groups 1 and 3 harbored a higher portion of Synergistia, Desulfitobacteriia, and Desulfovibrionia.

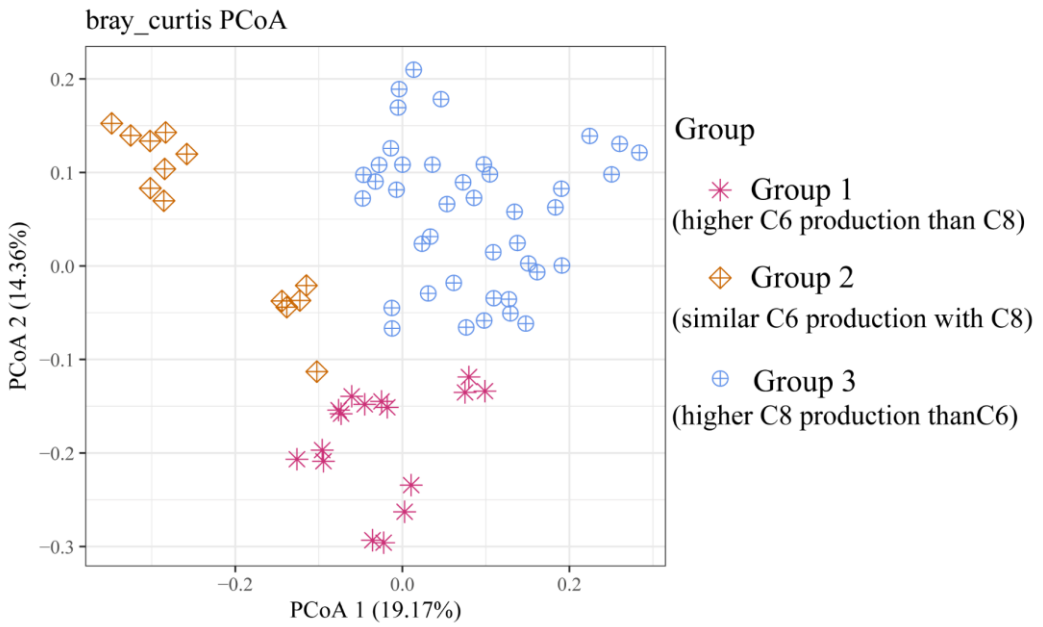

Figure 4.18. Non-metric multidimensional scaling (NMDS) analysis of the bacterial communities at the genus level based on Bray-Curtis distance. (Group 1: microbiomes with high production of *n*-caproate; Group 2: microbiomes with similar production of *n*-caproate to *n*-caprylate; Group 3: microbiomes with high production of *n*-caprylate).

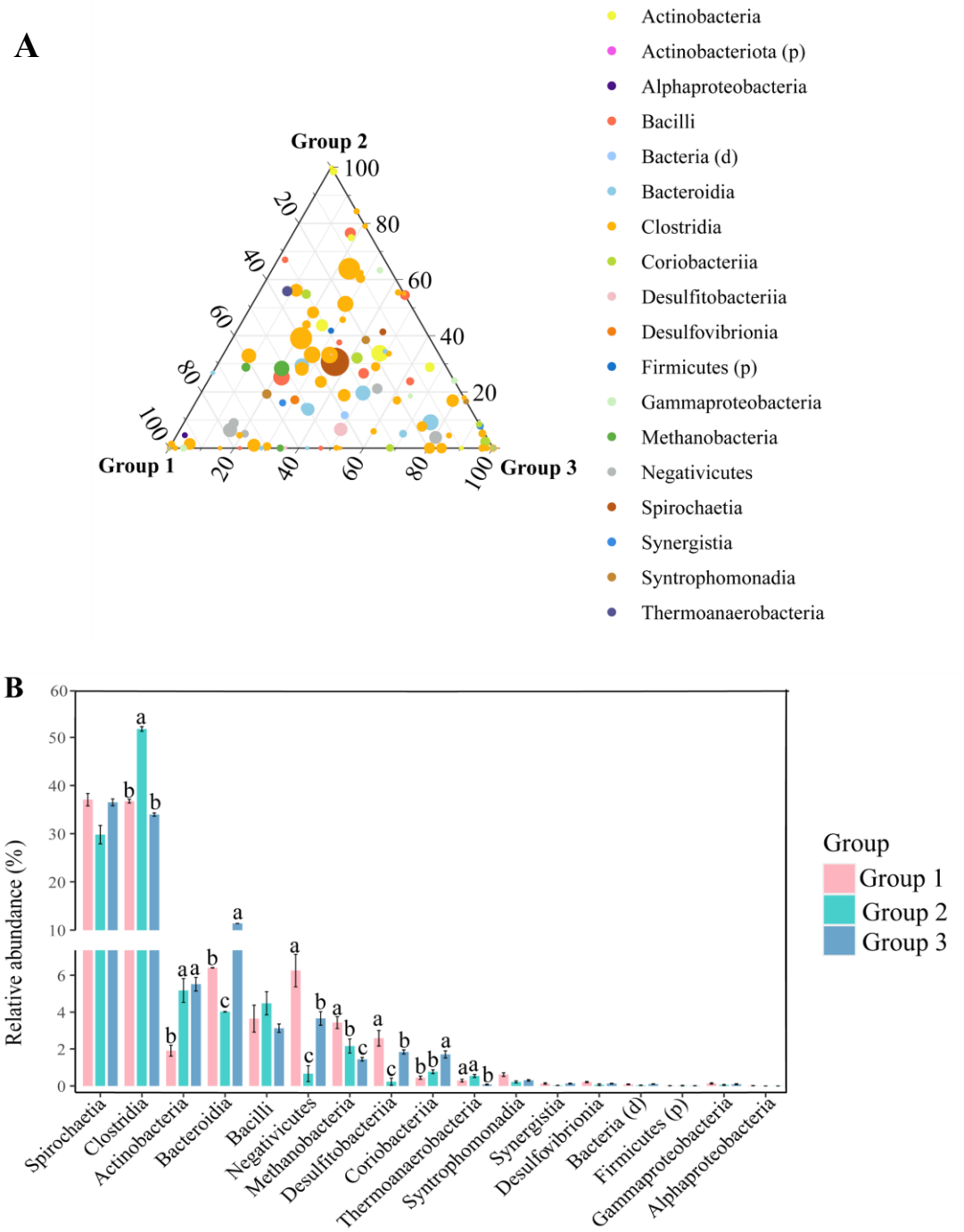

Figure 4.19. Characteristics of the microbial community. (Group 1: microbiomes with high production of *n*-caproate; Group 2: microbiomes with high production of *n*-caprylate; Group 3: microbiomes with similar production of *n*-caproate to *n*-caprylate). Ternary plot of OTUs showing the distribution of OTUs in different groups (A). Each corner of the triangle represented a sort of group. The size of the circles was proportional to the mean abundance in the community. Position was determined by the contribution of three fertilisation treatments to the total relative abundance. Colours of circles were correspond to different Class; The relative abundance of reactor microbiomes in each group at class level (B). Error bars denote the standard error of the mean. (a, b, and c showing the singinificant difference among groups, Kruskal-Wallis test + Dunn test, R package).

4. 3.9 Lower pH or higher operating temperature inhibited the microbiomes for the production of odd products

The production of odd-chain products in the bioreactor was low (**Figures 3.2 and 3.3**). I chose the microbiomes with the highest or lowest odd-chain product production in both bioreactors to explore the microbial dissimilarity among groups and find the key microbiomes for the production of odd-chain products. The highest production of the odd-chain products was about nine times the lowest one in R1, and the highest production of odd-chain products was about three times the lowest one in R2 (**Table S4.14**). The microbial communities with higher odd-chain product production were clustered close with no significant difference (p-value > 0.05, **Figure 4.20 and Table S4.15**). However, microbiomes with high or low production of odd-chain products were significantly separated (**Figure 4.20 and Table S4.15**). The heatmap of the microbiomes displayed more microbial differences (**Figure 4.21**). *Propionibacterium* spp. and one genus from the order Veillonellales-Selenomonadales were more enriched in the microbiomes with high odd-chain product production. *Propionibacterium* spp. and one genus from the order Veillonellales-Selenomonadales were positively correlated with odd-chain product production in this research (**Figures S4.3 and 4.4**). I found that *Lactobacillus* spp. was also enriched in the microbiomes with high

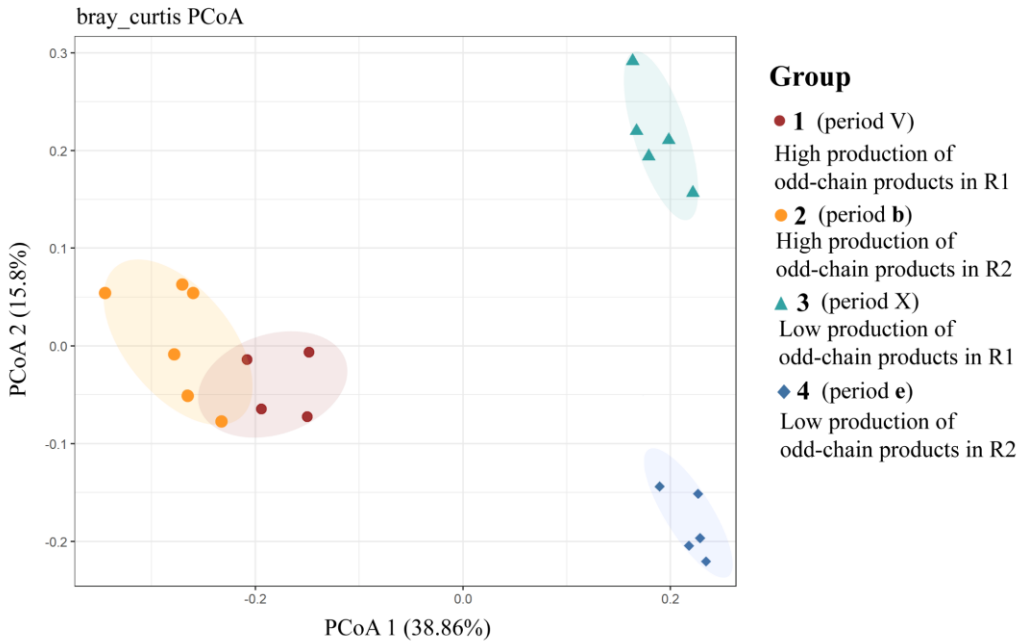

Figure S4. 20. Principal coordinate analysis (PCoA) of microbiomes with high or low production of odd-chain products with Bray-Curtis distance matrix. (Groups 1 and 2: high production of odd-chain products; Group 3: low production of odd-chian products shaped by a higher operating temperature; Group 4: low production of odd-chain products shaped by a lower pH).

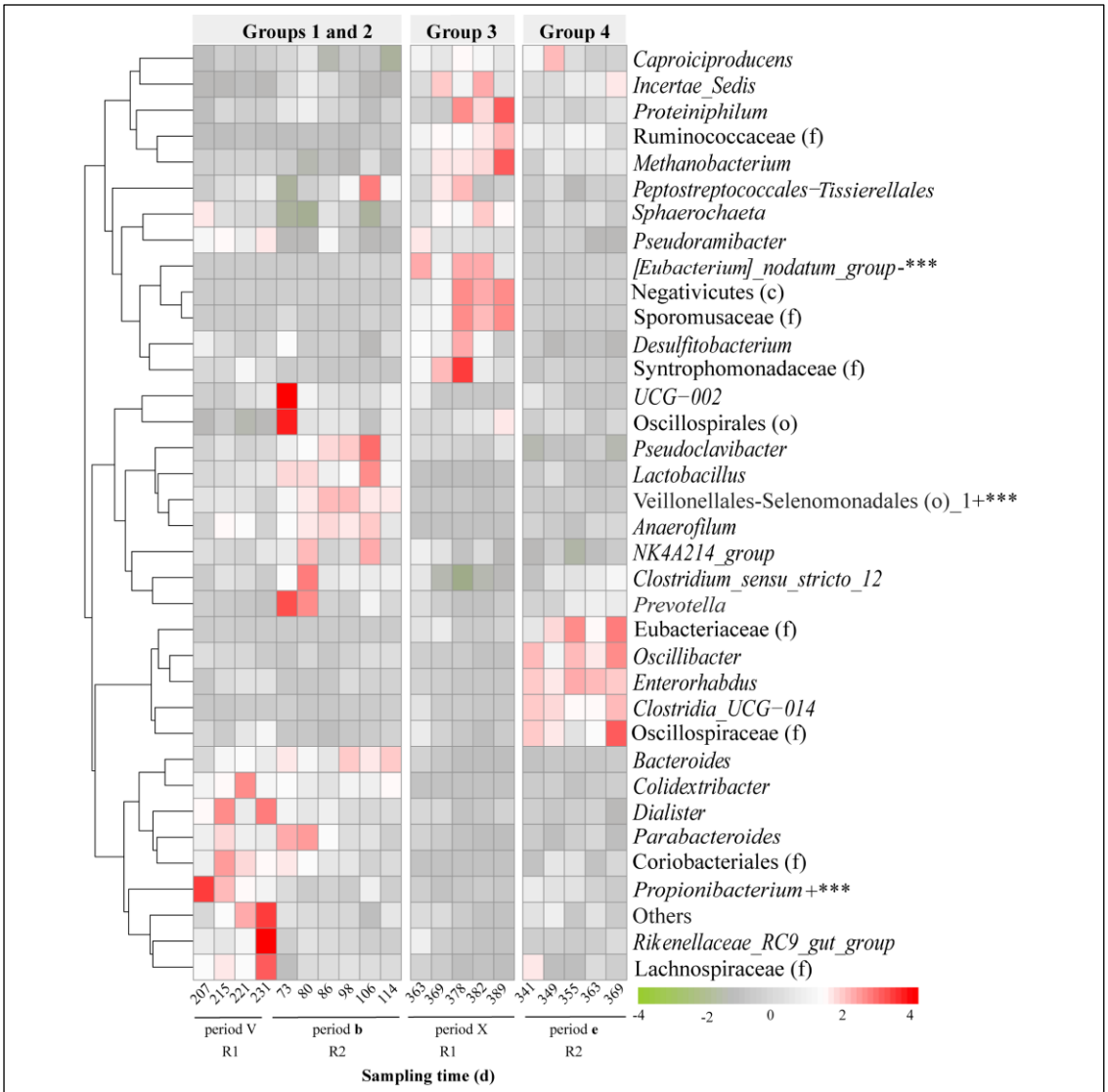

Figure 4.21. Heatmaps of reactor microbiomes. (Groups 1 and 2: high production of odd-chain products; Group 3: low production of odd-chain products shaped by a higher operating temperature; Group 4: low production of odd-chain procuts shaped by a lower pH). Relative abundance (%) is represented by the color gradient shown. OTUs that reached higher than 1% relative abundance in any one sample are represented. Log-transformed relative abundance (%) is represented by the color gradient shown. The odd product production significantly correlated genus (**Figure S4.3** and **4.4**) was marked with + or – symbols, representing whether the genera were found to be significantly positively (+) or negatively (−) correlated with odd product production. (** indicates FDR-adjusted p-value < 0.01; *** indicates FDR-adjusted p-value <0.001). OTU taxonomy is given at the genus level unless taxonomy assignment was not that specific (k: kingdom, p: phyla, c: class; f: family).

4.4 Discussion

4.4.1 The interactions between environmental factors, reactor performance, and microbial community

Operating conditions (Agler, Spirito et al. 2014), substrate composition (Duber, Zagrodnik *et al*. 2022), or bioreactor history (Agler, Werner *et al*. 2012) were vital tools for shaping the reactor microbiomes. Two environmental factors (E_L_ratio and operating temperature) were applied in the bioreactor. The changed environmental factors affected the microbial dynamics in the bioreactor (**Figures 4.2 and 4.5**), which led to a different product spectrum in the bioreactor (**Figure 3.2**). In addition, the microbial function (reactor performance) also played an important role in engineering microbial communities in the bioreactor (**Figure 4.8**). The strong relationships between community structure and its function have been shown in a previous study (Werner, Knights et al. 2011). This study provided us with more details about the relationships among environmental factors, reactor performance, and microbial community.

4.4.2 The microbial community relative to specific MCCA production

Spirochaetia and Clostridia were the dominant class in the microbiomes throughout all the time points (**Tables S4.3 and S4.4**). Clostridia contained most of the discovered chain-elongtors and played an important role in many MCCA-producing open cultures (Angenent, Richter *et al*. 2016, Candry and Ganigue 2021). *Sphaerochaeta* spp. was reported for *n*-caproate production with lignocellulosic ethanol (Yang, Leng *et al*. 2018) or with CO_2 and ethanol *via* microbial electrochemical bioconversion (Jiang, Chu *et al*. 2020). *Sphaerochaeta* spp. was also involved in biomethanation production (Saha, Basak *et al*. 2020). Even though it accounted for a large portion of the microbiomes of my research, *Sphaerochaeta* spp. was not identified to be significantly correlated with any carboxylates produced in the bioreactor (**Figures S4.3 and S4.4**). *Sphaerochaeta* spp. is an anaerobic bacteria and was isolated from natural cultures (*e,g.,* subseafloor sediment or production water of heavy oil reservoirs; (Miyazaki, Sakai et al. 2014, Bidzhieva, Sokolova et al. 2018). *Sphaerochaeta* spp. is involved in biofilm formation (Bidzhieva, Sokolova *et al*. 2020) and can utilize sugars, yeast extract, or lactate to

produce acetate, CO_2, and H_2 (Ritalahti, Justicia-Leon *et al*. 2012, Bidzhieva, Sokolova *et al*. 2020).

During the whole process of experiments in the bioreactor, *n*-caproate and *n*-caprylate were the two main products. Lower E_L_ratio or higher operating temperature led to a higher *n*-caproate production rate than *n*-caprylate, while higher E_L_ratio or lower operating temperature resulted in a higher *n*-caprylate production rate than *n*-caproate. Under certain conditions, for example, with an E_L_ratio of 2 or decreasing operating temperature from 42ºC to 30ºC, *n*-caproate had similar production rate with *n*-caprylate. I found that when *n*-caproate had similar production rate with *n*-caprylate, Clostridia was more enriched in the microbiomes (**Figure 4.19**), with *Oscillibacter* spp. and one genus from the family Oscillospiraceae being more enriched (**Figures 4.4 and 4.7**). *Oscillibacter* spp. was the dominant genera using ethanol and lactate as co-electron donors (Wu, Ren *et al*. 2022). *Oscillibacter* spp. has been reported in chain-elongating bioreactors converting acetate and ethanol to *n*-butyrate, *n*-caproate, and *n*-caprylate at acidic pH (Kucek, Spirito *et al*. 2016, Spirito, Marzilli *et al*. 2018). And the family Oscillospiraceae contained *Ruminococcaceae* CPB6 (Zhu, Zhou *et al*. 2017) and Strain BL-4 (Liu, Popp *et al*. 2020), which could utilize lactate for *n*-caproate production. When *n*-caproate or *n*-caprylate was dominated in the product, some specific microbiomes were involved. More details are displayed below. The production of odd products was low during the process, but I still figured out some key bacteria that positively correlated with its production.

4.4.2.1 Members from Clostridia, Negativicutes, and Methanobacteria were more enriched in the core microbiome for high *n*-caproate production

When *n*-caproate was dominant in the product, members from Clostridia, Negativicutes, and Methanobacteria were found to be more enriched in the microbiomes (**Figure 4.13**). The microbial community was shaped for high *n*-caproate production by an E_L_ratio of 1 during stage I or the operating temperature of 37ºC-42ºC during stage II. When steered the microbiomes with an E_L_ratio of 1, more bacteria from Clostridia were found to be enriched (*Clostridia_UCG-014* spp.,

Pseudoramibacter spp., *Clostridium_sensu_stricto_12* spp., and *[Eubacterium]_nodatum_group* spp.; **Figures 4.4 and 4.7**). *[Eubacterium]_nodatum_group* spp. was reported to be correlated with *n*-butyrate production in an MCCA-producing bioreactor with xylan and lactate as sole carbon sources (Liu, Kleinsteuber *et al*. 2020). And in this research, it was found to be positively correlated with *n*-caproate production (**Figure S4.4**). Chain elongation with ethanol or lactate could produce *n*-butyrate and *n*-caproate, and *n*-butyrate was the electron acceptor for *n*-caproate production. Thus, I theorized that *[Eubacterium]_nodatum_group* spp. was, to a certain extent, involved in microbial MCCA production in open cultures. *Clostridium_sensu_stricto_12* spp., which was also found positively correlated with *n*-caproate in this research, is a common participant in *n*-caproate production. A high relative abundance of *Clostridium_sensu_stricto_12* spp. was found in the microbiome for *n*-caproate production with ethanol and acetate as substrates (Bao, Wang *et al*. 2019, Candry, Huang *et al*. 2020). *Clostridium_sensu_stricto_12* spp. was also found as the key genus related to *n*-caproate production with lactate as substrates (Zhang, Pan *et al*. 2022). My finding confirmed that *Clostridium_sensu_stricto_12* spp. played an essential role in MCCA production. *Pseudoramibacter* spp. is also involved in many MCCA-producing processes with open cultures (Scarborough, Lynch et al. 2018, Crognale, Braguglia et al. 2021, Wei, Ren et al. 2021). However, for the condition with higher operating temperature, I observed that besides members from Clostridia (genera from the order Oscillospirales), bacteria that belonged to Negativicutes and Methanobacteria also had higher relative abundance in the microbiomes (**Figure 4.13**). With increasing operating temperature, methane production increased (**Figure 3.4**). I found *Methanobacterium* spp. was more abundant in the microbiomes with higher operating temperature (**Figure 4.7**). Some genera from the order Oscillospirales (which contains the family Ruminococcaceae) or the class Negativicutes were positively correlated with *n*-caproate production (**Figure S4.4**). For the order Oscillospirales, it contained several well-known chain-elongating bacteria (*e.g., Ruminococcaceae bacterium* CPB6 (Zhu,

2017 #76), *C. galactitolivirans* (Jeon, Kim *et al*. 2010), and *Caproiciproducens* 7D4C2 (Esquivel-Elizondo, Bagci *et al*. 2020)). And these bacteria were also reported to be important in MCCA-producing bioreactors (Contreras-Davila, Zuidema *et al*. 2021, Zhu, Feng *et al*. 2021). Similarly, Negativicutes includes some *n*-caproate producers (Candry and Ganigue 2021). *M. elsdeni* (Elsden 1956) and *M. hexanoica* (Jeon, Choi *et al*. 2016), which were assigned to class Negativicutes, could utilize lactate or sugars for *n*-caproate production. Some genera, which were identified to be positively correlated with *n*-caproate production in our research, could be only classified into class, order, or family, implying that we can isolate new chain-elongating bacteria.

4.4.2.2 Members of Clostridia, Bacteroidia, and Coriobacteriia were more enriched in the core microbiomes for high *n*-caprylate production

A higher E_L_ratio or lower operating temperatures was beneficial for converting substrate to more *n*-caprylate production (**Figure 3.2**). The microbiomes shaped by a higher E_L_ratio or lower operating temperatures were similar (**Figure 4.15**). Members of Clostridia, Bacteroidia, and Coriobacteriia were more enriched in the microbiomes (**Figure 4.19**). Five genera - *Colidextribacter* spp., *Anaerofilum* spp., *Rikenellaceae_RC9_gut_group* spp., *Bacteroides* spp., and one genus from the family Coriobacteriaceae were found more eneriched in the microbiome for high *n*-caprylate production (**Figures 4.4 and 4.7**). And these genera were positively correlated with *n*-caprylate production (**Figures S4.3 and 4.4**). *Colidextribacter* spp. and *Anaerofilum* spp. were from the family Oscillospiraceae, which contained many well-known chain-elongating bacteria (Candry and Ganigue 2021). *Anaerofilum* spp. could ferment sugars into lactate, ethanol, and acetate (Gerhard Zellner 1996), which were the substrates for *n*-caprylate production. *Rikenellaceae_RC9_gut_group* spp. and *Bacteroides* spp. were from Bacteroidia. In the previous study, it was found that members from Bacteroidia were abundant in the reactor microbiome for *n*-caproate production (Kucek, Spirito *et al*. 2016, Leo A. Kucek, Jiajie Xu *et al*. 2016). *Bacteroides* spp. is among the most abundant microorganism inhabiting the human intestine, which is saccharolytic bacteria and could ferment amino acids and sugars into succinic acid, acetate, lactate, and

propionate (Smith 1998, Rios-Co*via*n, Arboleya *et al*. 2013). Then, these SCCAs could be useful intermediates for MCCA production (Coma, Vilchez-Vargas *et al*. 2016). Moreover, *Bacteroides* spp. can also utilize exopolysaccharides (EPSs), which are complex carbohydrates (Rios-Co*via*n, Sanchez *et al*. 2015). *Sphaerochaeta* spp. was the dominant bacteria in my bioreactor, and it was reportedly involved in biofilm formation (Bidzhieva, Sokolova *et al*. 2020). It is probable that *Sphaerochaeta* spp. provided the substrates for *Bacteroides* spp., then the SCCAs that are produced from *Bacteroides* spp. could be utilized by MCCA producers. One genus from the family Coriobacteriaceae also showed a strong correlation with *n*-caprylate production, which was also present in some MCCA-producing bioreactors with lactate (Khor, Andersen *et al*. 2017, Duber, Jaroszynski *et al*. 2018, Duber, Zagrodnik *et al*. 2020) or ethanol (Scarborough, Lynch *et al*. 2018) or CO (He, Han *et al*. 2018) as substrates. The family Coriobacteriaceae has been mostly reported to be saccharolytic (Clavel, Lepage *et al*. 2014). This was another saccharolytic genus we found in our reactor that was correlated with *n*-caprylate production. However, no saccharolytic bacteria was shown to be significantly associated with *n*-caproate production (**Figure S4.13**). I would need more investigations to explore the role of the saccharolytic genus in *n*-caprylate production. On the other hand, the genus from the family Coriobacteriaceae (*Olsenella* spp.) is able to convert glucose into lactate as a main product (Dewhirst, Paster *et al*. 2001), which could be utilized as an electron donor for *n*-caprylate production. And *Olsenella* spp. was correlated with *n*-caprylate production in a previous study (Lambrecht, Cichocki *et al*. 2019).

In addition, two genera from Bacilli (*Lactococcus* spp. and *RF39* spp.) and one genus from Negativicutes (*Dialister* spp.) were also found positively correlated with the production of *n*-caprylate (**Figures S4.3 and S4.4**). *Dialister* spp. and the members from Bacilli were often found in MCCA-producing microbiomes with lactate as substrates (Sträuber, Lucas et al. 2016, Duber, Zagrodnik et al. 2020, Zagrodnik, Duber et al. 2020). They were probably correlated with the production of SCCAs (Jumas-Bilak, Jean-Pierre *et al*. 2005, Li, Ren *et al*. 2020), which could be further utilized for MCCA

production. In a previous study, Kucek *et al.* found that members from the family Rhodocyclaceae were correlated relatively to *n*-caprylate production (Kucek, Spirito et al. 2016), which were absent in this research. This also implied that many *n*-caprylate relative microbiomes need to be explored.

4.4.2.3 Propionate-producing bacteria played an important role in producing odd-chain products

Propionibacterium spp. and one genus from the order Veillonellales-Selenomonadales were positively correlated with odd-chain product production in this research (**Figures S4.3 and 4.4**). *Propionibacterium* spp. is a propionate-producing bacterium (Piwowarek, Lipinska *et al*. 2018), and propionate was the primary electron acceptor for odd-chain MCCA production (Grootscholten, Steinbusch *et al*. 2013). Veillonellales-Selenomonadales was found in the MCCA-producing bioreactor with lactate (Kucek, Nguyen *et al*. 2016). *M. elsdenii,* which was assigned into the order Veillonellales-Selenomonadales, could ferment lactate to MCCAs and propionate (Counotte 1981). This also explained why the members from the order Veillonellales-Selenomonadales became enriched in the microbiomes with high odd-chain product production.

Lactobacillus spp. was also found to be abundant in the microbiomes with high odd-chain product production (**Figure 4.21).** *Lactobacillus* spp. is typical lactic acid bacteria (Marshall, LaBelle et al.) and it could produce lactate from sugars (Abedi and Hashemi 2020, Wang, Wu *et al*. 2021). The produced lactate would then be utilized by microbiomes to produce propionate or MCCAs. In addition, I found that members from the family Lachnospiraceae were also enriched in the microbiomes with high production of odd-chain product (**Figure 4.21**). The member from the family Lachnospiraceae was reported to be related with the formation of propionate and *n*-butyrate (Contreras-Davila, Zuidema *et al*. 2021). Moreover, all the necessary chain elongation genes were detected in the family Lachnospiraceae (Scarborough MJ 2018, Zhu, Feng *et al*. 2021). Whether this family can produce MCCA still requires further clarification, recent research implied that the family Lachnospiraceae is closely

associated with MCCA production.

4.4.2.4 *Caproiciproducens* spp. and order Veillonellales-Selenomonadales showed high resistance to the toxic effect of undissocaited *n*-carboxylic acids

The members from the order Veillonellales-Selenomonadales were enriched during the extraction collapse (**Figures 4.12 and S4.9**). I also found that the extraction collapse did not affect the relative abundance of *Caproiciproducens* spp. The extraction system collapse led to the accumulation of undissociated carboxylic acids, which decreased MCCA production (**Figures 3.2 and 3.3**). Studies have displayed that the undissociated *n*-caproic acid was toxic in concentrations higher than ~6.9 mM (Weimer, Nerdahl *et al*. 2015) or ~7.5 mM at a pH of 5.5 (Ge, Usack *et al*. 2015). So, under different conditions, the undissociated carboxylic acids showed a different toxic effect on the MCCA-relative microbiomes. Here, we showed the different resistance of microbiomes to undissociated carboxylic acids, which led to a more selective MCCA production process. Here, the higher abundance of the members of order Veillonellales-Selenomonadales during extraction collapse resulted in slightly higher odd product production (**Figure 4.2**). *Caproiciproducens* spp., which is a well-known MCCA producer (Esquivel-Elizondo, Bagci *et al*. 2020, Contreras-Davila, Zuidema *et al*. 2021, Zhang, Pan *et al*. 2022), showed high resistance, which implied its high potential for MCCA production under complex conditions.

4.4.3 The microbial network relative to high production of *n*-caproate or *n*-caprylate

Functional microorganisms were not alone in microbial MCCA production with open cultures (Contreras-Davila, Zuidema *et al*. 2021, Zhu, Feng *et al*. 2021). Collaboration between different microbial groups resulted in the target product (Liu, Kleinsteuber *et al*. 2020). The microbial interactions have affected the flow of carbon toward products, which needs to be considered in the bioprocess design (Agler, Werner *et al*. 2012). Applying co-occurrence analyses to microbial systems based on 16S rRNA gene amplicon sequences can provide valuable information on ecological interactions of microbes at the community scale (Barberan, Bates *et al*. 2012). This research used

ethanol and lactate as co-electron donors for MCCA production with open cultures with an in-line extraction system. I steered the microbiomes for specific MCCA production with different E_L_ratios or operating temperatures. With an E_L_ratio of 1 or operating temperatures of 37ºC-42ºC, *n*-caproate was dominant in the product, with a higher production rate than *n*-caprylate. The three different conditions shaped three unique microbiomes for high *n*-caproate production. Otherwise, *n*-caprylate was the main product in the bioreactor under an E_L_ratio of 3 or oprating temperatures of 25ºC-30ºC. The microbiomes shaped by different conditions for high *n*-caprylate production were highly similar. The co-occurrence analysis could help us gain more details about the interactions within these unique microbiomes. My goals were to investigate how environmental manipulations affect ecosystem functioning and to elucidate the ecological interactions among different functional groups. By building the microbial network, we intended to reveal potential functions and ecological interactions within the microbial community in MCCA-producing bioreactor.

4.4.3.1 The microbial network for high *n*-caproate production

I identified three significantly different microbial communities for high *n*-caproate production (**Figure S4.10**) and built three unique microbial networks (**Figure 4.14**). The first microbial network (**Figure 4.14 A**) was based on the microbiomes shaped by an E_L_ratio of 1; the second microbial network (**Figure 4.14 B**) was based on the microbiomes shaped by a operating temperature of 37ºC; and the third microbial network (**Figure 4.14 C**) was based on the microbiomes shaped by a operating temperature of 42ºC. I found bacteria that were positively correlated with *n*-caproate production **(Figures S4.3 and 4.4)**, and they were all shared by the three unique microbial communities (**Figure S4.14**). The difference is that these related bacteria were enriched in the different microbial communities, implying their importance in the diverse microbial communities. In the first network, *Clostridium_sensu_stricto_12* spp. and *[Eubacterium]_nodatum_group* spp. were more enriched. Then, *Incertae_Sedis* spp. and one genus from the order Oscillospirales had higher relative abundance in the second network. Last, in the third netwrok, *Methanobacterium* spp., *Incertae_Sedis*

spp., *[Eubacterium]_nodatum_group* spp., and some genera from the family Ruminococcaceae or the order Negativicutes were more abundant. A more significant proportion of the genera from the class Clostridia occurred in the first network. The genera enriched in each microbial network showed strong relationships with the corresponding reactor performance. With higher operating temperatures, odd-chain product production was deficient, and we also found that *Propionibacterium* spp. and *Lactobacillus* spp. only co-occurred in the first network. And, *n*-caprylate was produced more under the condition with lower E_L_ratio than under higher operating temperature so that *Rikenellaceae_RC9_gut_group* spp. and *Bacteroides* spp. showed more positive connections with other members in the first network. *Desulfitobacterium* spp. co-occurred with one genus from the family Syntrophomonadaceae and was more enriched in both second and third networks. *Desulfitobacterium* spp. was also identified to be responsible for MCCA production from CO (He, Han *et al*. 2018). And, it occurred in our previous study and was reported to be able to oxidize ethanol (Agler, Spirito *et al*. 2012). Syntrophomonadaceae was reported to be correlated with acetate production in an MCCA-producing bioreactor (Liu, Kleinsteuber *et al*. 2020). I did find that more acetate was produced at higher temperatures in the bioreactor, which could have been oxidized from ethanol. Besides, I also found that *Incertae_Sedis* spp. co-occurred with *Methanobacterium* spp. and was enriched in the third network. *Incertae_Sedis* spp. was from the family Ethanoligenens, which could generate ethanol, acetate, H_2, and CO_2 (Li, Lou *et al*. 2020). It explained the accumulation of acetate, butyrate, and CH_4 at a temperature of 42°C. The microbial network for *n*-caproate production was diverse according to substrate utilization or operating conditions. Recently, in a lactate and xylose-based MCCA-producing bioreactor, the authors identified a whole microbial network that involved various functions, including hydrolysis of xylan, primary fermentation of xylose to acids (*e.g.,* to acetate by *Syntrophococcus* spp., to *n*-butyrate by Lachnospiraceae, and to lactate by *Lactobacillus* spp.) and chain-elongation with lactate (by *Ruminiclostridium* 5 spp. and *Pseudoramibacter* spp.). In a lactate-based bioreactor, the family Ruminococcaceae (with functional strain CPB6) was marked as

a key bacterial in the core microbiome related to long-term and effective *n*-caproate production (Zhu, Feng *et al*. 2021). Here, I showed three unique microbial co-occurrences for high *n*-caproate production that were shaped by different conditions in one bioreactor throughout time. The three networks were characterized by the co-occurrence of various key microorganisms. To be useful for bioenergy production, a microbial community must have a stable metabolic function over time, despite unavoidable perturbations and disturbances (Werner, Knights *et al*. 2011). A functionally diverse microbial community provides a suite of parallel pathways for each trophic step that play important roles in maintaining a stable and robust community function (Hashsham, Fernandez *et al*. 2000).

4.4.3.2 The microbial network for high *n*-caprylate production

The microbial composition of the microbiomes that were shaped by different conditions for high *n*-caprylate production showed no significant difference (**Figure 4.15**). I built one typical microbial network based on the microbiomes *via* co-occurrence analysis (**Figure 4.17**). The genera from classes Clostridia, Bacteroidia, Coriobacteriia, and Actinobacteria represented this network (**Figure 4.17**). *Oscillibacter* spp., which could produce *n*-butyrate (Lee, Rhee *et al*. 2013) and *n*-valerate (Iino, Mori *et al*. 2007), was shown in this network. *Sphaerochaeta* spp. was also co-occurred in this network. It was reportedly involved in biofilm formation (Bidzhieva, Sokolova *et al*. 2020). *Enterococcus* spp., *Lactococcus* spp., and *RF39* spp. were from the class Bacilli. The members for the class Bacilli was characterized as having high hydrolytic capacities (Mazzucotelli, Ponce *et al*. 2013, Sikora, Baszczyk *et al*. 2013, Li, Ren *et al*. 2020). *Parabacteroides* spp. and *Bacteroides* spp. from the class Bacteroidia. The strain from the class Bacteroidia was able to utilize EPS (Gorvitovskaia, Holmes *et al*. 2016, Ezeji, Sarikonda *et al*. 2021).The members from classes Bacilli and Bacteroidia were probably responsible for hydrolysis, hydrolyzing the biofilm produced from *Sphaerochaeta* spp. Thus, the hydrolysate of biofilm could be further used for *n*-caprylate or other MCCA production. In addition, some genera from Clostridia were shown in this network: **1)** *Mogibacterium* spp. was known to be a saccharolytic bacteria (Futoshi Nakazawa 2000);

2) *Clostridium_sensu_stricto_12* spp. and *Caproiciproducens* spp., which were well-known MCCA producers. And some genera from the order Oscillospirales that contained some chain-elongating bacteria co-occurenced with the family Lachnospiraceae, which could convert xylose to *n*-caproate and other MCCAs (Scarborough MJ 2018). The members from the family Coriobacteriaceae also palyed an important role in this network, which was reported to be positively correlated with *n*-caproate and *n*-caprylate production in a lactate-based MCCA-producing bioreactor (Liu, Kleinsteuber *et al*. 2020). This co-occurrence of *Propionibacterium* spp. in this network implied the close relationship between odd-chain product and *n*-caproate production (**Figure 3.3**). The close relationship between the odd-chain product and *n*-caprylate production was because both odd-chain products and *n*-caprylate production were preferred to be produced at a relatively low temperature (25ºC-30ºC), while they were strongly inhibited at a relatively high temperature (37ºC-42ºC).

In conclusion, it was the first time we conducted a microbial network for high *n*-caprylate production with ethanol and lactate as co-electron donors and with an in-line extraction system. The microorganisms relative to SCCA and MCCA production were involved. Also, I found some bacteria with high hydrolytic capacities that co-occurred, which implied more potential pathways that took part in microbial MCCA production, especially for *n*-caprylate.

4.5 Conclusion

I operated a continuously feed bioreactor with an in-line extraction system to produce MCCAs with ethanol and lactate as substrates. My goal was to shape the reactor microbiomes for specific MCCA production. The results showed that the changeable substrate structure or operating temperature could enrich communities facilitated the selection of reactor microbiomes with desired ecological functions (*e.g.,* high *n*-caproate or *n*-caprylate procdution rate). The microbial dynamics in the bioreactor was not only caused by environmental factors but also by the microbial function (reactor performance). Clostridia played an important role in the MCCA-producing bioreactor, collaborating with the members from Negativicutes,

Methanobacteria, Bacteroidia, and Coriobacteriia. I identified three unique microbial networks for high-caproate production steered by an E_L_ratio of 1 or operating temperatures of 37ºC-42ºC. An E_L_ratio of 3 or operating temperatures of 25ºC-30 ºC shifted the microbial communities producing more *n*-carprylate. I made one typical microbial network for high *n*-caprylate production based on the microbiomes shaped by different conditions. The production of odd-chain products was strongly correlated with propionate-producing strains. Some potential pathways involved in MCCA production were also shown in this research. To sum up, we could control our bioreactor for target products. And the high resilience, resistance, and redundancy of the bioreactor gave the microbial community a stable metabolic function, which was important to our biotechnology production platform.

CHAPTER 5

Being in Control of MCCA Production with Ethanol and Lactate as Co-Electron Donors

Abstract

Ethanol and lactate are the most commonly used electron donors for microbial MCCA production. In this study, I explored the factors that affected the product spectrum with ethanol and lactate as co-substrates. The results displayed that ethanol was a better electron donor than lactate for *n*-caprylate production. Adding *n*-butyrate into the medium improved *n*-caprylate production, and *n*-valerate addition favored *n*-heptanoate production. This study also showed that an appropriate initial partial hydrogen pressure was crucial to MCCA production. Lastly, I found the inhibition effect of acrylic acid on MCCA production. This study supplied more details for MCCA production with ethanol and lactate as co-electron donors.

5.1 Introduction

The electron donor provides the carbon source, energy source, and intermediate acetyl-CoA for microbial MCCA production (Spirito, Richter *et al*. 2014). Several energy-rich reduced substances, including sugars (*e.g.,* glucose and fructose; Jeon, Kim et al. 2017, Esquivel-Elizondo, Bagci et al. 2020), methanol (Chen, Huang *et al*. 2020), D-galactitol (Jeon, Kim *et al*. 2010), ethanol (Steinbusch, Hamelers *et al*. 2011, Agler, Spirito *et al*. 2012), and lactate (Kucek, Nguyen *et al*. 2016, Zhu, Zhou *et al*. 2017), have been used as electron donors. Among them, ethanol and lactate were the most suitable and commonly used electron donors (Cavalcante, Leitão *et al*. 2017, De Groof, Coma *et al*. 2019). Ethanol is an electron donor providing energy for coupling acetyl-CoA formation and elongating acyl-CoA units (Henning Seedorf, Birgit Veith *et al*. 2008). Besides ethanol, lactate was also a suitable electron donor for microbial MCCA production (Zhu *et al*., 2015; Kucek *et al*., 2016; Khor *et al*., 2017). Ethanol- or lactate-based microbial MCCA production differentiates in their products. Ethanol could only be upgraded into even-chain MCCAs (*e.g., n*-caproate or *n*-caprylate) without additional electron acceptors (Grootscholten, Steinbusch et al. 2013, Roghair, Hoogstad

et al. 2018, Spirito, Marzilli et al. 2018). For lactate-based MCCA production, propionate could be converted from lactate as an electron acceptor, which results in both even- and odd-chain products (*e.g.,n*-caproate and *n*-heptanoate; Kucek, Nguyen et al. 2016, Candry, Radic et al. 2020). Recently, combining ethanol and lactate as co-electron donors was found to achieve a higher substrate utilization rate and MCCA production and selectivity than the single electron donor of ethanol or lactate (Wu, Guo *et al*. 2018). However, ethanol was also reported to inhibit the conversion rate of lactate to MCCA in the presence of lactose (Duber, Zagrodnik *et al*. 2022). Even though the interaction of ethanol- and lactate-based chain elongation was more complex than expected when both were used as electron donors, there was some real waste containing both ethanol and lactate in the fermentation broth (Carvajal-Arroyo, Candry *et al*. 2019, Lambrecht, Cichocki *et al*. 2019). Exploring more details about the co-utilization of ethanol lactate was important to lay the foundation for expanding microbial MCCA with more real organic waste.

Microbial MCCA production is a process of elongating the carbon chain of the electron acceptor (Spirito, Richter *et al*. 2014). The ratio of electron donor to acceptor was shown to be important to the selectivity of a targeted product for both ethanol- and lactate-based chain elongation (Spirito, Marzilli *et al*. 2018, Wang, Li *et al*. 2018). Therefore, the studies comparing the chain elongation performance of different electron acceptors and optimizing their dosing ratio and concentration are significant for enhancing MCCA production and product specificity.

Appropriate gas composition is also essential for efficient MCCA production, especially H_2 and CO_2 (Angenent, Richter *et al*. 2016, De Groof, Coma *et al*. 2019). First, adequate pH_2 avoids the oxidation of carboxylates or excessive ethanol oxidation. Ge *et al.* have calculated at certain experimental conditions that the hydrogen pressure limits for oxidation of acetate were 1.45×10^{-4} atm, *n*-butyrate was 6.65×10^{-6} atm, and *n*-caproate was 2.52×10^{-6} atm (Ge, Usack *et al*. 2015). When controlling the pH_2 at 0.007% at standard conditions, the excessive oxidation of ethanol would be inhibited (Roghair, Hoogstad *et al*. 2018). On the other hand, H_2 is a product of ethanol- and

lactate-oxidation occurring during the first step of chain elongation (Spirito, Richter *et al*. 2014), so high pH_2 (above ~0.1 bar) could reduce the thermodynamic favorability of the chain elongation process (Rodriguez, Kleerebezem *et al*. 2006, Angenent, Richter *et al*. 2016). In addition, carboxylates are reduced to their corresponding alcohol when pH_2 is above ~1.5 bar (Steinbusch, Hamelers *et al*. 2008). In thermodynamic fermentation models, it is assumed that dissolved H_2 affects the $NADH/NAD^+$ ratio directly, and hence the thermodynamic feasibility of specific pathways (Rodriguez, Kleerebezem *et al*. 2006). A high pH_2 causes the accumulation of *n*-butyrate and/or propionate, affecting the ratio of even to odd products (Pohland 1986, Cavalcante, Leitão *et al*. 2017). The CO_2 partial pressure (pCO_2) also plays an important role in microbial MCCA production *via* chain elongation. The growth of *C. kluyveri*, which is the most well-known chain elongating bacterial, needs nutritional CO_2 (Tomlinson and Barker 1954). As mentioned, H_2 is produced by ethanol or lactate oxidation to Acetyl-CoA for chain elongation. In addition, lactate oxidation could produce CO_2 (Prabhu, Altman *et al*. 2012). Weimer *et al*. calculated the H_2 to CO_2 ratio that showed the optimal thermodynamics for chain elongation and suggested about 1 bar pH_2 with 0.3 bar pCO_2 (Weimer and Kohn 2016). Excess H_2 was found to react with CO_2 to generate acetate and ethanol by homoacetogenesis and subsequent acetate reduction to ethanol when ethanol and lactate served as co-electron donors (Wu, Bao *et al*. 2019, Wu, Guo *et al*. 2019). Therefore, keeping an appropriate ratio of H_2 to CO_2 is crucial for MCCA production when ethanol and lactate serve as co-electron donors.

MCCAs in the undissociated form were toxic to microbiomes (Wilbanks and Trinh 2017). According to Weimer *et al*., at a pH of 5.7, the undissociated *n*-caproate was toxic in concentrations higher than ~6.9 mM (Weimer, Nerdahl *et al*. 2015). Likewise, Ge *et al*. found that the undissociated *n*-caproate was toxic in concentrations higher than ~7.5 mM at a pH of 5.5 (Ge, Usack *et al*. 2015). Lactate could be converted into propionate *via* the acrylate pathway (Kucek, Nguyen *et al*. 2016). Acrylic acid was the intermediate product of some propionate-producing bacteria (Straathof, Sie *et al*. 2005). Here, we wondered about the effect of acrylic acid on MCCA production.

To this end, I compared the product composition with ethanol or lactate or ethanol and lactate as electron donors. Also, the influence of additional electron acceptors on the substrate utilization rate, product distribution, and MCCA selectivity was investigated. Furthermore, the carbon-flow distribution under different initial pH_2 was quantified. Finally, the effect of acrylic acid on MCCA production was explored. This study aims to reveal more fermentation characteristics of the microbiomes with ethanol and lactate as co-electron donors to provide a reference for future MCCA production with real waste, which contains both ethanol and lactate.

5.2 Materials and Methods

5.2.1 The inoculum and medium

The inoculum for this project was from the bioreactor. The experiment was conducted with a synthetic medium, and electron donor sand electron acceptors were added additionally based on specific experimental objectives. The composition of synthetic medium (**Tables S3.1-3.3**) referred to previous reports (Vasudevan, Richter *et al*. 2014). These tests were conducted in triplicates with the 100 mL serum bottle. Each of them was filled with 50 mL medium, and the headspace volume was about 50 mL. The medium was purged with nitrogen. The initial pH was 5.5, and the bottles were incubated at 30°C.

5.2.2 the experiment design

5.2.2.1 The comparation of the MCCA production with ethanol or lactate or ethanol and lactate as electron donors

Table 5.1 Experimental designs

	Group 1	Group 2	Group 3
Electron donor	100 mM Ethanol	100 mM Lactate	100 mL Ethanol and 100 mL Lactate
The incubation time was 7 days.			

5.2.2.2 The effect of the addition of electron acceptors on MCCA production

Five groups were tested here: **1)** control: 100 mM ethanol and 100 mM lactate as electron donors without additional electron acceptor; **2)** group 2: 100 mM ethanol and 100 mM lactate + 10 mM sodium butyrate; **3)** group 3: 100 mM ethanol and 100 mM

lactate + 10 mM sodium valerate; **4)** group 4: 100 mM ethanol and 100 mM lactate + 10 mM sodium caproate; 5) group 5: 100 mM ethanol and 100 mM lactate + 10 mM sodium heptanoate. The incubation time was seven days.

Table 5.2 The experiment design for the effect of additional electron acceptors on MCCA production

	Control	Group 2	Group 3	Group 4	Group 5
Electron acceptors	No	+ 10 mM sodium butyrate	+ 10 mM sodium valerate	+ 10 mM sodium caproate	+ 10 mM sodium heptanoate
Electron donors	100 mM ethanol and 100 mM lactate				

5.2.2.3 The effect of initial pH_2 on MCCA production.

Fourteen different initial pH_2 from 0.1 to 3.0 bar were applied in this experiment. Control was purged with nitrogen gas (99.9%) for 5 min to ensure anaerobic conditions. Other tests were purged with high purity H_2 for 5 min and then kept a final pH_2 according to the design in the headspace. The base medium containing 100 mM ethanol and 100 mM lactate was used in this experiment. The incubation time was seven days.

5.2.2.4 The effect of acrylic acid on MCCA production

The method of the effect of acrylic acid on MCCA production was based in a previous study (Alvarez, Rainer Kalscheuer *et al*. 1997). The base medium containing 100 mM ethanol and 100 mM lactate with (experimental group) or without (control) 1 mg ml^{-1} of acrylic acid was used for the test.

5.2.3 Analytical methods

All the carboxylates were determined by gas chromatography (GC, 7890B GC System, Agilent, USA)equipped with a thermal conductivity detector (TCD) using a capillary column Nukol Capillary Column (15m X 0.25 mm I.D. X 0.25um). The method was modified according to the previous research from our lab (Usack and Angenent 2015), which is with the temperature of injection was 200°C and the detector to 250°C, ramp temperature program (initial temperature 80°C for 0.5 min, temperature ramp 20°C per 1 min to 180 °C, and final temperature 180°C for 2 min), and a hydrogen flow of 21.4 mL min^{-1} as a carrier gas. Ethanol and lactate concentrations were measured using high-performance liquid chromatography (HPLC) system (Shimadzu

LC 20AD) coupled with a refractive index and UV detector (Shimadzu, Kyoto, Japan). Separation conditions were 60°C with 5mM sulfuric acid as the mobile phase at a flow rate of 0.6 mL min^{-1} in an Aminex HPX-87H (Bio-Rad, Hercules, CA, USA) column. Before the analysis, samples were filtered through a sterile Acrodisc 0.22-mm pore size polyvinylidene fluoride membrane syringe filter (Pall Life Sciences, Port Washington, NY, USA) to remove possible biological and particulate contaminants. H_2 and CO_2 contents were assessed using thermal conductivity detector-gas chromatography (GC-TCD). A flame ionization detector-gas chromatography (GC-FID) was used for CH_4 measure (SRI gas GCs, SRI Instruments, USA).

5.3 Result and discussion

5.3.1 Ethanol was a better electron donor than lactate for *n*-caprylate production

I explored the performance difference in carboxylate production with ethanol (E group), lactate (L group), or ethanol and lactate (EL group) as electron donors (**Figure 5.1**). When only ethanol served as an electron donor, there were only even products produced, with *n*-butyrate most abundant in product (**Figure 5.1 A**). When only lactate was used as an electron donor, there were both even- and odd-chain products, and more odd- than even-chain products were produced (**Figure 5.1 B**). When both ethanol and lactate were used as electron donors, both even and odd products were produced, with more even- than odd-chain products produced (**Figure 5.1 B**). Ethanol and lactate were well-studied electron donors for MCCA production. In the process of chain elongation, electron donors are first oxidized into two-carbon unit-acetyl-CoA. Then the acetyl-CoA is connected to the electron acceptor, thus, elongating the carbon chain of the electron acceptor by two carbons in one cycle (Spirito, Richter *et al*. 2014). For ethanol, only even products could be produced (*e.g.,* acetate, *n*-butyrate, *n*-caproate, and *n*-caprylate) without adding odd-numbered electron acceptors (Waselefsky 1985, Grootscholten, Steinbusch *et al*. 2013). Lactate could be oxidized into acetate and propionate by microbiomes (Prabhu, Altman *et al*. 2012). Therefore, both even- and odd-chain products occurred when lactate was present (Kucek, Nguyen *et al*. 2016).

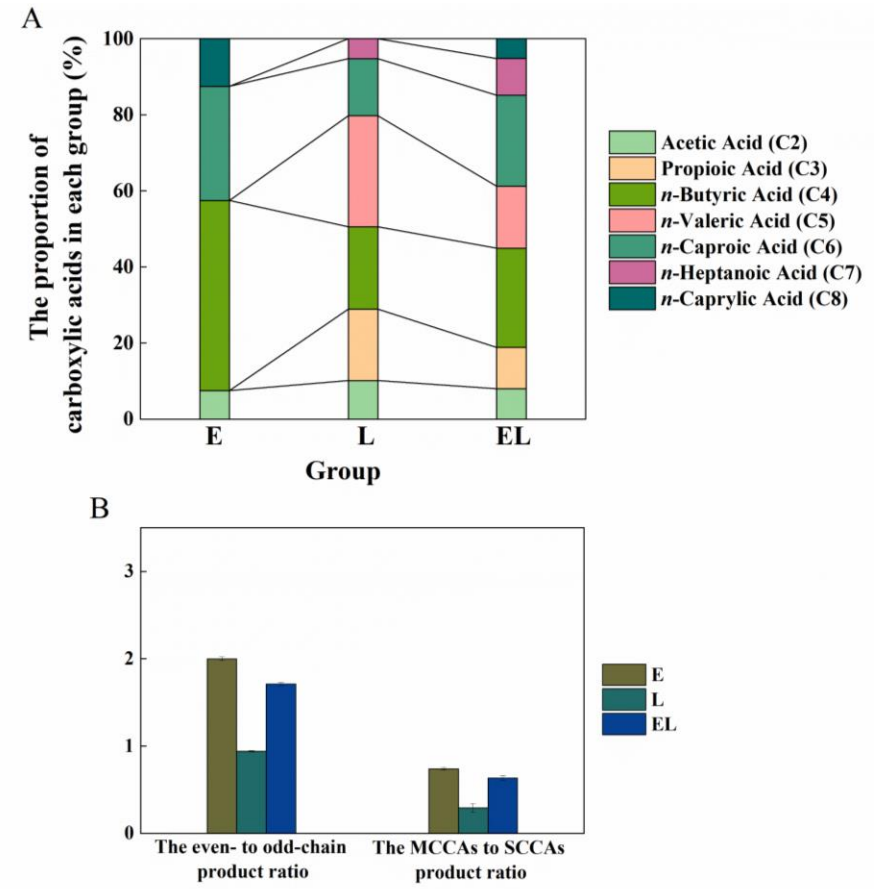

Figure 5.1 The carboxylate production with different substrates. The proportion of different carboxylates produced in each group (A); the even- to odd-chain product ratio/ the MCCAs to SCCAs ratio (B). E: with ethanol as an electron donor; L: with L-lactate as an electron donor; and EL: with ethanol and lactate as co-clectron donors.

Wu et al. found that co-utilization of ethanol and lactate favored longer-chain MCCA production (*e.g., n*-caprylate; (Wu, Guo et al. 2018). However, in this study, the proportion of *n*-caprylate in the product was smaller in the EL group compared within E group (**Figure 5.1 A**). The co-utilization of ethanol and lactate was not beneficial for *n*-caprylate production. When propionate, which was formed from lactate, was present in the broth, the chain-elongating bacteria used propionate as electron donors for the production of *n*-valerate and *n*-heptanoate. The production of odd-chain MCCAs consumed the acetyl-CoA for a longer reduced product (*e.g., n*-caprylate). Also, the thermodynamic calculations showed that when the substrates had a high enough concentration, the production of *n*-valerate and *n*-heptanoate was more feasible than the production of *n*-butyrate and *n*-caproate (**Figure S5.1 and Table S5.1**). *n*-Butyrate and

n-caproate are the electron donors for *n*-caprylate production. The decrease in *n*-butyrate and *n*-caproate production affected *n*-caprylate production. Thus, the decrease in the amount of acetyl-CoA and electron donors (*e.g., n*-butyrate and *n*-caproate) led to less *n*-caprylate production when using both ethanol and lactate as co-electron donors.

The result showed that no *n*-caprylate was produced in the L group and a higher ratio of the odd-chain product (**Figure 5.1**). Firstly, when only lactate was the electron donor, the production of propionate from lactate decreased the ratio of lactate to acetyl-CoA, which was an intermediate product for chain elongation to MCCAs. On the other hand, lactate to odd-chain products was more exergonic than to even-chain products (**Figure S5.1 and Tables S5.2**). I tested if *n*-caprylate could be produced from lactate when enough carbon source (lactate) was present (**Figure S5.2**). The results showed *n*-caprylate could be produced from lactate when enough lactate was present, and the that propionate present in the substrate affected *n*-caprylate production negatively. Even though lactate to odd-chain products (*e.g., n*-valerate or *n*-heptanoate) is more thermodynamically feasible (**Figure S5.1**), producing 5 moles of *n*-valerate or *n*-heptanoate requires more mole of lactate than producing *n*-butyrate, *n*-caproate, or *n*-caprylate (**Tables S5.1 and S5.2**). Thus, keeping lactate at an appropriate concentration in the substate was an excellent choice to avoid producing odd-chain products when lactate was used as an electron donor (Kucek, Nguyen *et al*. 2016).

5.3.2 The effect of additional electron acceptors on the production of carboxylates with ethanol and lactate as co-celectron donors

To explore the difference in product spectrum, different electron acceptors were added to the substrate with ethanol and lactate as co-electron donors (**Figure 5.2**). Adding *n*-butyrate in the medium improved the production of *n*-caproate and *n*-caprylate compared with the control (**Figure 5.2 A**). The addition of *n*-valerate in the medium improved the production of *n*-heptanoate (**Figure 5.2 A**). Thus, the addition of *n*-butyrate and *n*-valerate resulted in a higher ratio MCCAs to SCCAs in the product (**Figure 5.2 B**). The *n*-butyrate has been reported to improve the production of *n*-caproate (Wang, Li *et al*. 2018, Bao, Wang *et al*. 2019) and *n*-caprylate (Wu, Guo *et al*.

2018) as an additional electron acceptor.

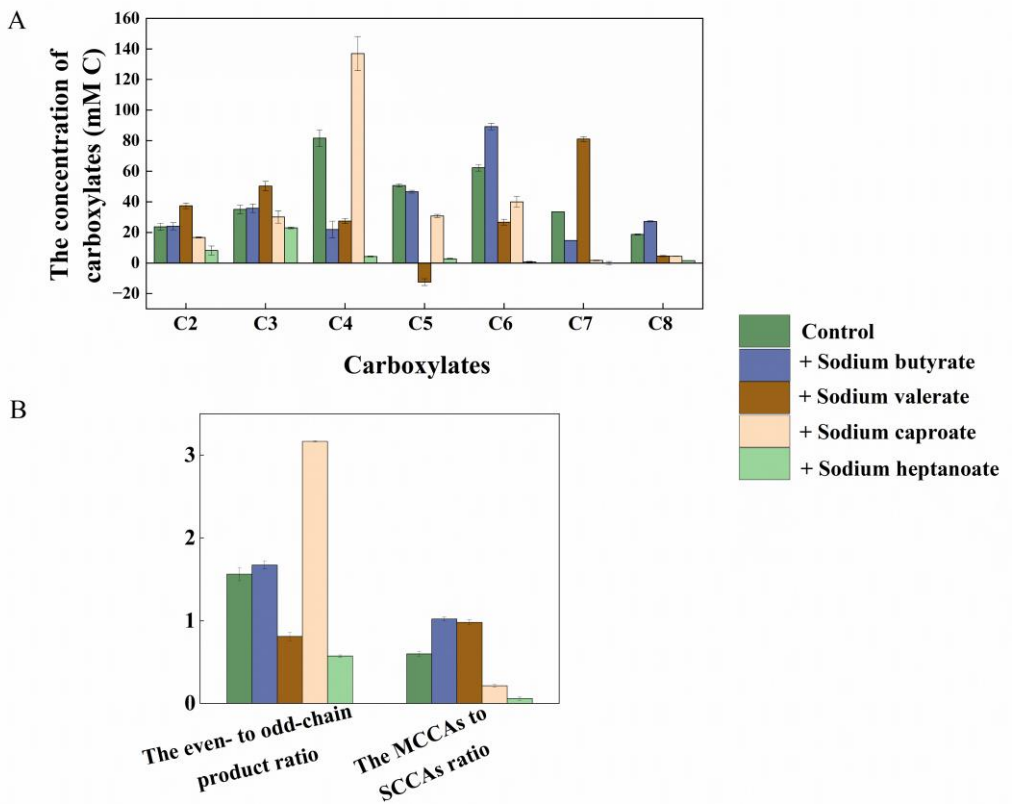

Figure 5.2 Comparisons of carboxylate production with different additional electron donors. The production of carboxylates in each group (A); the even- to odd-chain product ratio/ the MCCAs to SCCAs ratio (B). Control: only 100 mM ethanol and 100 mM lactate as electron donors. + sodium butyrate/ sodium valerate/ sodium caproate/ sodium heptanoate: adding different electron acceptors. The results here were from minusing the original concentration with the final one; the concentration of *n*-valerate was negative meant that the consumption of *n*-valerate was more than the production. (C2: acetate; C3: propionate; C4: *n*-butyrate; C5: *n*-valerate; C6: *n*-caproate; C7: *n*-heptaonate; C8: *n*-caprylate)

n-Valerate was the direct electron donor for *n*-heptanoate production. Thus, the addition of *n*-valerate benefited *n*-heptanoate production. Adding *n*-caproate in the medium led to the accumulation of *n*-butyrate in this study (**Figure 5.2 A**), which was opposite to the previous finding that the addition of *n*-caproate favored *n*-caprylate production (Jeon, Choi *et al*. 2016). The addition of *n*-heptanoate showed a toxic effect on the microbiomes because the consumption rate of ethanol and lactate in this group was slower than in other groups (**Table. S3.4**). I speculated that the additional *n*-caproate and *n*-heptanoate in the medium were toxic to the microbiomes, which

inhibited their function for MCCA production. In this study, at a pH=5.5, the undissociated concentration of *n*-caproic acid or *n*-heptanoic acid was 0.71 mM or 0.67 mM, respectively. The toxic concentration of undissociated *n*-caproic acid to chain-elongating microbiomes was ~7 mM (Ge, Usack *et al*. 2015, Weimer, Nerdahl *et al*. 2015). Even though the concentration of undissociated *n*-caproic acid of 0.71 was lower than the toxic one, the microbial function was still inhibited in this study. One possibility was that the microbiomes in this study were more sensitive to the undissociated carboxylic acids because the biomass used in this study was from the MCCA-producing bioreactor with an in-line extraction. The in-line extraction provided an environment with a very low concentration of undissociated carboxylic acids, especially undissociated MCCAs, reducing the tolerance of the microbiomes to the toxic effect of undissociated carboxylic acids.

5.3.3 The effect of initial pH_2 on MCCA production with ethanol and lactate as co-electron donor

Fourteen different initial pH_2 were applied to test the effect of different initial pH_2 on MCCA production with ethanol and lactate as co-electron donors (**Figures 5.3 and 5.4**). The results showed the highest ratio of MCCAs to SCCAs (0.52) was achieved in the control (**Figure 5.4**). The increased initial pH_2 reduced the ratio of MCCAs to SCCAs in the product (**Figure 5.4**). The initial pH_2 also affected the conversion efficiency of substrates to carboxylates. The highest conversion efficiency of substrates to carboxylates (58.12%) was shown in the control (**Figure 5.3**).

H_2 is a byproduct of ethanol- and lactate- oxidation occurring during the first step of chain elongation (Spirito, Richter *et al*. 2014). A high pH_2 (above ~0.1 bar) in the space could reduce the thermodynamic favorability of chain elongation process (Rodriguez, Kleerebezem *et al*. 2006, Angenent, Richter *et al*. 2016). Thus, these test groups with initial pH_2 >= 0.1 bar showed a lower ratio of MCCAs to SCCAs than in the control. Moreover, we found that with an initial pH_2 >= 0.5 bar, no *n*-caprylate was produced; with an initial pH_2 >= 2.0 bar, *n*-heptanoate was not present anymore (**Figure 5.3 and Figure S5.3**). The possible reason could be that the enzyme for longer MCCA (e.g., *n*-

heptanoate and *n*-caprylate) production was more sensitive to a higher pH_2.

An increasein initial pH_2 led to a decreased conversion efficiency of substrates to carboxylates, especially with an initial pH_2 >=1.5 bar (**Figure 5.3**). And, some substrates were not consumed in the group with an initial pH_2 >=1.5 bar (**Table S5.5**). These results implied that a higher initial pH_2 inhibited the substrate utilization, resulting in a reduced conversion efficiency of substrates to carboxylates. In addition, a pH_2=1.5 bar could reduce carboxylates into corresponding alcohol (Steinbusch, Hamelers *et al*. 2008). So, it was possible that some substrate in the group with an initial pH_2>=1.5 bar were converted into alcohol, which decreased the conversion efficiency of substrates to carboxylates.

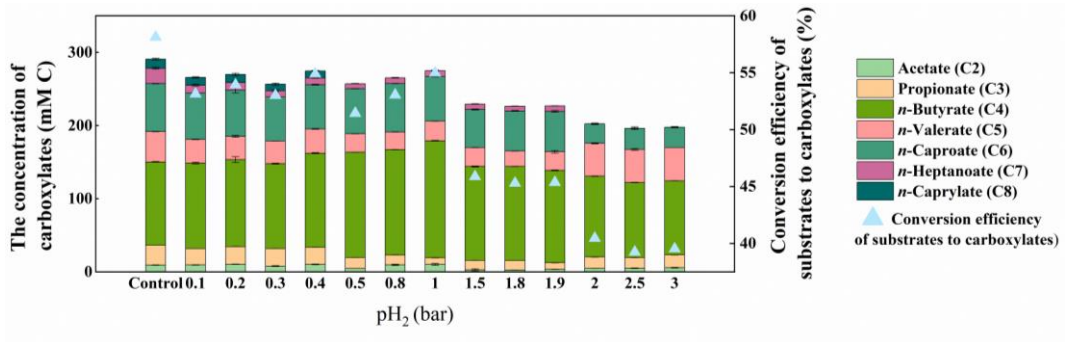

Firgure 5.3. The concentration of produced carboxylates and the conversion efficiency of substrates to total carboxylates under different initial pH_2.

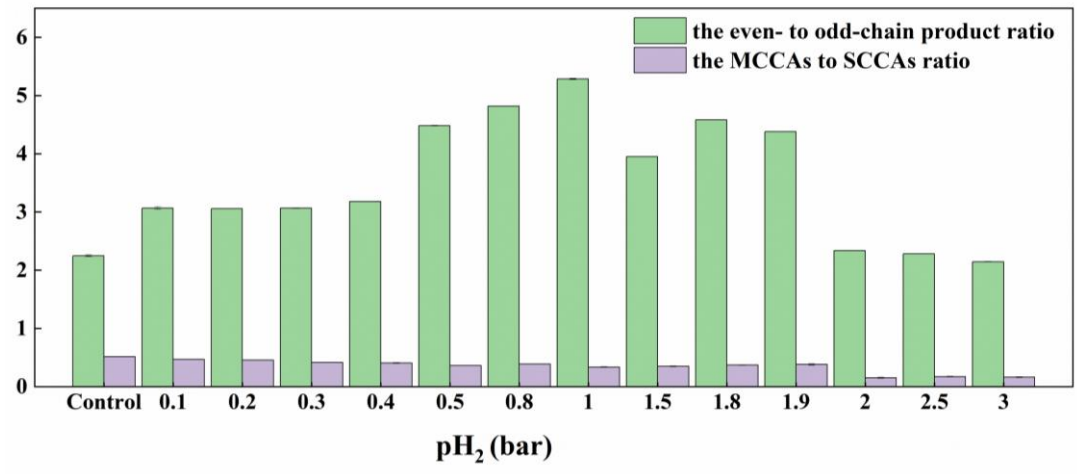

Firgure 5.4. The even- to odd-chain product ratio/ the MCCAs to SCCAs ratio under different initial pH_2.

In addition, I found that the ratio of even- to odd-chain products changed with different initial pH_2 (**Figure 5.4**). It was reported that a high pH_2 caused the accumulation of *n*-butyrate and/or propionate, affecting the ratio of even- to odd-chain products (Pohland 1986, Cavalcante, Leitão *et al*. 2017). In this study, with an initial pH_2 ranging from 0.1 to 1.9 bar, the ratio of even- to odd-chain products was increased compared with in the control. Otherwise, with an initial pH_2 ranging from 2.0 to 3.0 bar, the ratio of even- to odd-chain products was reduced compared with in the control (**Figure 5.4**). These results implied that the initial pH_2 was also a potential tool for steering the product during the process of microbial MCCA production.

5.3.4 The inhibition of acrylic acid on ethanol-based MCCA production

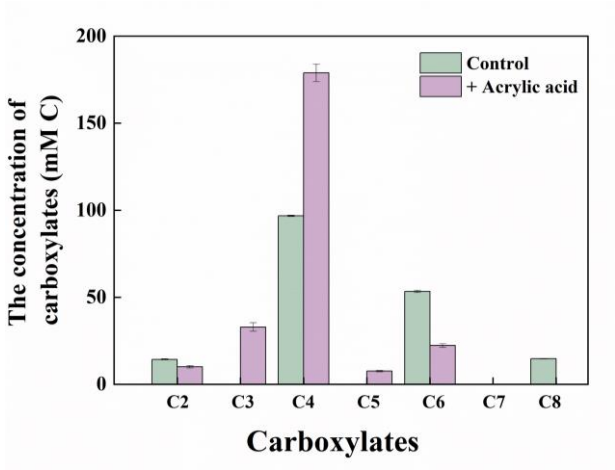

Figure 5.5 The concentration of carboxylates produced without or with acrylic acid. (C2: acetate; C3: propionate; C4: *n*-butyrate; C5: *n*-valerate; C6: *n*-caproate; C7: *n*-heptaonate; C8: *n*-caprylate)

In the ethanol-based chain elongation, only even-chain products (*e.g.,* acetate, *n*-butyrate, *n*-caproate, and *n*-caprylate) could be produced without additional electron acceptors. I found that adding acrylic acid into the medium led to the production of odd-chain products (*e.g.,* propionate and *n*-valerate, **Figure 5.5**). Lactate could be converted to propionate *via* the acrylate pathway (Prabhu, Altman *et al*. 2012, Kucek, Nguyen *et al*. 2016). Microbiomes may use the added acrylic acid to produce propionate. The propionate could serve as the electron donor for *n*-valerate production. So, there were propionate and *n*-valerate produced in the broth. In addition, the addition of acrylic acid decreased the production of *n*-caproate and *n*-caprylate (**Figure 5.5**). As discussed, the

chain elongation from propionate to *n*-valerate consumed acetyl-CoA, which was intermediate for MCCA production. So, the production of MCCAs *via* chain elongation was inhibited without enough intermediate. Also, I hypothesized that the enzyme for longer-chain MCCAs (*e.g., n*-caproate, *n*-heptanoate, or *n*-caprylate) was inhibited by acrylic aicd.

5.4 Conclusion

In this research, I explored the factors affecting the product spectrum with ethanol and lactate as co-electron donors. The results showed ethanol was a better electron donor than lactate for *n*-caprylate production. The propionate production from lactate affected *n*-caprylate production negatively when using ethanol and lactate as co-electron donors. The addition of *n*-butyrate in the medium promoted *n*-caproate and *n*-caprylate production. The results showed that *n*-valerate was an excellent electron acceptor for *n*-heptanoate production. The initial pH_2 >= 0.1 bar lowered the ratio of MCCAs to SCCAs. In addition, an initial pH_2>= 1.5 inhibited the conversion efficiency of substrates to carboxylates and the production of *n*-caprylate. At last, acrylic acid was toxic to microbial MCCA production.

CHAPTER 6

Summary and Recommendations for Future Work

6.1 Summary

In recent years, the possibility of merging technologies for waste recovery has been studied in an attempt to integrate the concept of circular economy in the industry. MCCAs, which could be converted into many kinds of useful products, are a promising alternative biochemical to some fossil fuel-based products. The outstanding features of high energy density, strong hydrophobicity, and versatility of MCCAs made microbial MCCA production economically and environmentally attractive in recycling biotechnology. The most commonly used electron donors for microbial MCCA production are ethanol and lactate, which could be available in many waste-fermentation broths (*e.g.,* syngas, liquor-making wastewater, food waste, or acid whey). Moreover, both ethanol and lactate are available in the fermentation broth of some waste (*e.g.,* maize silage, food waste, or acid whey). In some studies, ethanol and lactate could be utilized as co-electron donors, improving the MCCA productivity. However, in other research, only lactate was used as a substrate for MCCA production, while ethanol remained untouched.

Here, my goal was to explore the possibility of using ethanol and lactate as co-electron donors for MCCA production. Also, I tried to investigate the strategies for controlling the bioreactor for the target product. Last, I studied the microbial dynamics and interactions between microbial communities to better to understand the relationship between environmental factors and microbiomes. In chapter 3, I operated two continuously fed bioreactors with continuous bioreactor-mixed liquor recycling through an in-line pertraction system for product extraction. Reactor one was used as a test reactor, and reactor two was used as a control. The ethanol and lactate were used as co-electron donors. The result showed that ethanol and lactate could be co-utilized as electron donors with an in-line extraction system. The collapse of the in-line extraction system affected the co-utilization of substrates (ethanol was utilized lower than lactate) and caused the accumulation of undissociated carboxylic acids, which were toxic to the

reactor performance. Then, I applied different operating parameters to control the product spectrum. The main MCCAs produced in this bioreactor were even-chain products (*n*-caproate and *n*-caprylate). I found that a relatively low E_L_ratio of 1 or the relatively high operating temperatures of 37ºC-42ºC shaped the bioreactor for high *n*-caproate production, while a relatively high E_L_ratio of 3 or the relativey low operating temperatures of 25ºC-30ºC shaped the bioreactor for high *n*-caprylate production. The total production of odd-chain products decreased with an increase in the E_L_ratio or operating temperature. Also, a pH of around 5.0 was not beneficial for odd-chain product production either. In chapter 4, I elaborated on the interactions between environmental factors, microbial dynamics, and reactor performance. The change in environmental factors (E_L_ratio or operating temperature) shifted the microbial communities. And tb-RDA analysis showed that the various reactor performance led by different conditions also contributed to the microbial dynamics. A relatively low ratio of E_L_ratio of 1 or the relatively high operating temperatures of 37ºC-42 ºC shifted the microbiomes towards predominant *n*-caproate production. The members from Clostridia, Negatives, and Methanobacteria were enriched in the microbiomes with high *n*-caproate production. *Clostridium_sensu_stricto_12* spp., *[Eubacterium]_nodatum_group* spp., *Incertae_Sedis* spp., and other two genera from the order Oscillospirales were found positively correlated with *n*-caproate production. Three microbial networks for high *n*-caproate production under different conditions were built *via* co-occurrence analysis of species based on 16S rRNA gene amplicon sequences. Under a relatively high E_L_ratio of 3 or the relatively low operating temperatures of 37ºC-42 ºC, *n*-caprylate was dominant in the bioreactor. Clostridia, Coriobacteriia, and Bacteroidia were of higher relative abundance in the microbiomes with high *n*-caprylate production. *Diaster* spp., *Colidextribacter* spp., *Rikenellaceae_RC9_gut_group* spp., and *Bacteroides* spp. were found to be positively correlated with *n*-caprylate production. One typical microbial network for high *n*-caprylate production was conducted in this research. I also found that *Propionibacterium* spp. played an important role in odd-chain product production. The

bioreactor was of high resilience (in which a population rebounds following a disturbance) and redundancy (in which a disturbed population is replaced by a new population whose function is redundant with the original) in this study, which made it response more efficiently to disturbances and environmental changes. In chapter 5, I explored some more characteristics of microbial MCCA production using ethanol and lactate as co-electron donors. I compared the product spectrum with ethanol or lactate or ethanol and lactate as substrates. The results showed ethanol was a better electron donor than lactate for *n*-caprylate production. The co-utilization of ethanol and lactate improved the ratio of lactate-carbon to MCCA. I also investigated the effect of electron donors on MCCA production. I found that *n*-butyrate was a better electron acceptor than *n*-caproate for *n*-carprylate production, and the addition of *n*-valerate favored *n*-heptanoate production. I also found that a higher initial partial hydrogen pressure in the headspace inhibited *n*-heptanoate and *n*-caprylate production. Last, acrylic acid was shown to be toxic to MCCA production.

6.2 Recommendations for future work

H_2 is the byproduct of chain elongation to MCCAs, and CO_2 was produced along with the oxidation of lactate. And we also tested the effect of initial hydrogen partial pressure on the MCCA production with ethanol and lactate. Thus, the impact of the ratio of H_2 to CO_2 on MCCA production in a continuously-run bioreactor with ethanol and lactate as co-substrates needs further study. In chapter 4, we explored the microbial communities. I could only speculate on the potential function of the microorganisms that played a crucial role in producing specific MCCAs. Metagenomics, metaproteomics, and metatranscriptomics could help us get a deeper understanding of the microbial function and the relationship between environmental and microbial dynamics. In addition, we found some uncultured bacteria, which were identified to be positively correlated with *n*-caproate or *n*-caprylate production, assigned to well-known families or orders that contained famous chainelongtors. It implied that we had the chance to isolate more pure strains that could produce MCCAs. Here, we found that Spirochaetia take up a great proportion in the reactor microbiomes throughout the

experimental stages. According to a previous study (Bidzhieva, Sokolova et al. 2020), members from Spirochaetia could form biofilms in liquid broth. Further, I found some bacteria that own high hydrolytic ability, which were identified to be positively correlated with *n*-caprylate production, were abundant in the bioreactor. Thus, I hypothesize that the hydrolysis of the EPS may be involved in MCCA production, especially for *n*-caprylate. And this hypothesis needs more experiments.

In summary, my work showed that I could control the microbiomes by changing the operating parameters. For example, to stimulate *n*-caprylate production, I needed to use a relatively high E_L_ratio of 3 or relatively low operating temperatures of 25ºC-30ºC. From an operational perspective, I found an advantage of pH control in an MCCA-producing bioreactor with ethanol and lactate as co-electron donors. Applying a higher E_L-ratio or operating temperature, I did not need to add HCl to my bioreactor to maintain the pH due to the neutralizing effect of H^+ production and consumption from the chain elongation with ethanol and lactate, respectively.

Supplementary Information for Chapter 3

Table S3.1 The components of the basal medium[a].	
Components	L^{-1}
MQ water	772 mL
Mineral stock solution (ml, 10x)	100 ml
KH_2PO_4	0.23 g
Yeast extract	1.25 g
Na_2CO_3	3 g
L-cystein HCL (ml,100x)	10 mL
Vitamin solution (ml, 100x)	5 mL
[a] The ethanol and lactate were added differently according to the experiment design.	

Table S3.2 The components of mineral stock solution (10x)	
Components	g L^{-1}
NaCl	11.7
NH_4Cl	2.37
$CaCl_2 \cdot 2H_2O$	0.65
$MgCl_2 \cdot 6H_2O$	0.25
$MnCl_2 \cdot 4H_2O$	0.31
$ZnCl_2 \cdot H_2O$	0.12
$CoCl_2 \cdot 6H_2O$	0.048

Table S3.3 The compounds of vitamin solution (100x)	
Components	mg L^{-1}
Pyridoxine	20
Thiamine	10
Riboflavin	10
Calcium pantothenate	10
Thioctic acid	10
Para aminobenzoic acid	10
Nicotinic acid	10
Vitamin B_{12}	10
d-Biotin	4
Folic acid	4
2-mercaptoethanesulfonic acid	4

Table S3.4 The average MCCA production during different periods in both reactors

(mmol C L^{-1} d^{-1})	Acetate	Propionate	*n*-Butyrate	*n*-Valerate	*n*-Caproate	*n*-Heptanoate	*n*-Caprylate	*n*-Nonanoate
				R1 (test reactor)				
Period I	0.00	0.00	9.90±0.01	3.38±0.26	47.04±0.65	10.85±0.32	15.96±0.09	0.92±0.02
Period II	0.00	0.00	10.66±0.13	2.56±0.76	28.74±0.34	6.28±0.54	36.63±0.01	0.89±0.19
Period III	0.00	0.00	3.49±0.98	1.29±0.17	17.12±0.55	4.52±0.92	76.59±0.03	1.22±0.22
Period IV	2.92±0.02	2.28±0.34	5.63±0.23	10.56±0.01	15.52±0.04	16.52±0.89	33.93±0.43	1.86±0.04
Period V	2.82±0.15	1.99±0.01	5.23±0.13	7.75±0.56	16.60±0.16	13.78±0.03	30.90±0.01	2.26±0.38
Period VI	3.45±0.16	0.00	3.86±0.07	4.64±0.78	15.18±0.48	10.65±0.45	46.43±0.12	4.01±0.56
Period VII	1.83±0.38	0.15±0.1	3.23±0.32	2.50±0.06	15.03±0.81	8.64±0.15	58.68±0.02	5.50±0.89
Period VIII	1.38±0.45	0.39±0.03	2.59±0.17	1.36±0.04	18.81±0.34	9.10±0.09	41.44±0.05	3.26±0.07
Period IX	3.00±0.09	0.00	9.99±0.13	1.75±0.02	46.44±0.67	2.21±0.34	10.76±0.14	3.86±0.35
Period X	17.02±0.08	0.00	15.26±9.04	1.36±0.16	48.74±0.01	1.05±0.87	2.27±0.72	1.72±0.02
Period XI	3.62±0.12	0.00	6.45±0.04	2.62±0.31	36.01±0.34	5.37±0.05	25.03±0.21	2.47±0.56
				R2 (control reactor)				
Period **a**	0.00	0.09±0.01	8.62±0.92	2.73±0.06	43.48±0.76	8.33±0.58	14.92±0.91	0.73±0.56
Period **b**	0.82±0.01	3.07±0.16	6.59±0.06	6.89±0.78	26.15±0.92	14.60±0.39	25.81±010	4.19±0.15
Period **c**	2.12±0.05	0.54±0.90	3.72±0.43	2.77±0.98	14.50±0.4	7.41±0.22	70.48±0.01	1.27±0.81
Period **d**	2.62±0.34	0.66±0.03	2.84±0.3	2.64±0.57	0.04±0.07	10.46±0.00	44.06±0.21	4.93±0.10
Period **e**	1.65±0.03	0.00	4.49±0.97	1.16±0.98	21.65±0.01	7.50±0.14	42.33±0.57	2.91±0.86
Period **f**	3.48±0.03	0.70±0.05	2.78±0.65	4.10±0.76	20.38±0.33	16.01±0.51	40.73±0.67	5.19±0.03

The data here showed the average production of each MCCAs at a steady state from different periods

Table S3.5 The average concentration of carboxylates in the bioreactor with or without extraction system collapse in both reactors

(mmol L^{-1})	Acetate	Propioate	*n*-Butyrate	*n*-Valerate	*n*-Caproate	*n*-Heptanoate	*n*-Caprylate	*n*-Nonanoate
With a good extraction system								
R1	8.81±0.12	0.90±0.22	10.60±0.51	1.5±0.15	12.51±0.44	0.07±0.01	1.95±0.15	0.00
R2	3.94±0.06	1.01±0.04	6.60±0.20	1.4±0.01	8.30±0.33	0.20±0.02	1.34±0.16	0.00
With extraction system collapse								
R1 (Period V)	3.11±0.33	4.14±0.17	20.85±0.48	0.12±0.02	20.00±0.27	0.13±0.03	4.39±0.11	0.00
R2 (Period b)	0.00	0.78±0.14	21.20±0.98	0.80±0.13	20.41±0.54	0.21±0.08	4.10±0.05	0.00

Table S3.6 The average biogas content (%) in different periods					
Periods		Methane (CH_4)	Carbon dioxide (CO_2)	Hydrogen (H_2)	Nitrogrn (N_2)
R1 (test reactor)					
Period I		54.18±2.42	32.03±2.32	3.16±1.29	10.63±5.13
Period II	before steady state	51.81±4.02	26.28±3.86	3.11±0.85	18.8±4.45
	staedy state	51.99±5.38	18.64±3.12	2.7±0.54	26.67±6.51
Period III	before steady state	55.03±2.65	15.11±1.18	2.83±1.11	27.03±2.41
	staedy state	45.67±7.92	11.52±3.81	3.59±0.78	39.21±11.03
Period IV		39.87±7.95	9.94±7.43	3.09±0.84	47.1±11.44
Period V		41.5±6.12	8.16±1.51	2.95±1.01	47.38±7.01
Period VI		50.48±5	20.23±1.46	2.22±0.48	27.08±5.38
Period VII		48.41±3.58	19.84±2.33	2.32±0.53	29.44±5.05
Period VIII		51.74±3.27	21.04±1.87	1.86±0.79	25.37±4.71
Period IX		54.42±3.09	23.29±2.09	2.46±0.84	19.83±2.54
Period X		61.38±2.84	19.56±1.14	2.32±0.69	16.74±3.33
Period XI		41.69±5.58	30.69±3.5	2.69±0.92	24.92±7.76
R2 (control reactor)					
Period a		51.36±3.11	32.36±4.36	3.18±1.11	13.09±2.57
Period b	before steady state	45.87±6.2	24.55±14.76	3.01±1.1	26.59±15.03
	staedy state	24.56±7.47	8.24±1.23	2.52±1.02	64.68±7.81
Period c	before steady state	27.1±5.94	7.58±0.91	3.03±0.89	62.29±6
	staedy state	47.29±5.88	9.78±2.77	2.97±0.61	40.09±5.87
Period d		42.18±5.25	12.58±2.42	2.76±1.06	42.47±6.68
Period e		44.43±9.87	15.31±3.19	3.12±1.02	37.13±12.06
Period f		39.87±5.68	12.2±1.33	3.14±0.7	44.79±5.95

Table S3.7 The average HCl consumption rate in bioreactor and NaOH consumption rate in extraction system during different periods in both reactors (mL d^{-1} L^{-1})			
Periods		HCl	NaOH
R1 (test reactor)			
Period I		0.86±1.59	2.51±7.26
Period II	before steady state	1.71±6.96	2.1±8.73
	staedy state	0.68±3.37	2.53±6.96
Period III	before steady state	0	1.91±6.43
	staedy state	3.33±5.52	3.72±4.21
Period IV		2.85±6.8	3.53±3.79
Period V		1.69±4.47	4.18±6.94
Period VI		2.25±4.5	4.1±1.46
Period VII		2.66±4.39	4.97±6.06
Period VIII		3.49±2.99	5.06±2.35
Period IX	before steady state	1.26±4.73	4.59±6.08
	staedy state	1.2±5.01	4.64±15.11
Period X	before steady state	0	2.63±7.24
	staedy state	0	2.56±5.42
Period XI		1.24±4.98	3.57±6.38
R2 (control reactor)			
Period a		1.01±5.15	2.45±3.64
Period b		2.15±9.35	4.45±13.12
Period c		2.47±3.09	3.79±6.11
Period d		2.53±6.72	5.63±14.15
Period e		2.09±5.81	4.86±15.54
Period f		2.17±11.01	4.48±8.42

Table S3.8 Thermodynamic calculations of the reactions presumably involved in MCCA production in open cultures[a] (KJ mol^{-1})

	Bioprocess	Reaction	25°C		30°C		37°C		42°C	
			ΔG° (pH 7.0)	$\Delta G^{\circ\prime}$ (pH 5.5)	ΔG° (pH 7.0)	$\Delta G^{\circ\prime}$ (pH 5.5)	ΔG° (pH 7.0)	$\Delta G^{\circ\prime}$ (pH 5.5)	ΔG° (pH 7.0)	$\Delta G^{\circ\prime}$ (pH 5.5)
Methane production										
1	Hydrogenotrophic methanogenesis	$4H_2 + CO_2 \rightarrow CH_4 + 2H_2O$	-130.73	-130.35	-128.69	-128.71	-123.82	-123.75	-116.88	-116.78
2	Acetoclastic methanogenesis	$CH_3COO^- + H^+ \rightarrow CH_4 + CO_2$	-35.69	-138.4	-36.61	-140.1	-38.17	-144.24	-40.37	-150.06
Acetate production										
3	Ethanol oxidation	$CH_3CH_2OH + H_2O \rightarrow CH_3CHOO^- + H^+ + 2H_2$	9.89	112.14	8.33	111.84	4.62	110.64	-0.65	108.95
4	Homoacetogenesis in *C. thermoaceticum*	$4H_2 + 2CO_2 \rightarrow CH_3COO^- + H^+ + 2H_2O$	-94.77	8.05	-92.08	11.39	-85.65	20.49	-76.51	33.28
5	Lactate oxidation	$CH_3CH(OH)COO^- + H_2O \rightarrow CH_3COO^- + 2H_2 + CO_2$	-9.47	52.7	-12.09	51.7	-18.35	47.91	-27.24	42.55
Propionate production										
6	Lactate reduction to propionate: as found in *Selenomonas ruminantium*	$CH_3CH(OH)COO^- + H_2O \rightarrow CH_3COO^- + CO_2 + 2H_2$ $CH_3CH(OH)COO^- + H_2 \rightarrow CH_3CH_2COO^- + H_2O$ ×2	-171.87	15.46	-175.47	17.84	-184.13	14.77	-196.38	13.19
7	Lactate reduction to propionate: as determined for *C. propionicum*	$CH_3CH(OH)COO^- + H_2 \rightarrow CH_3CH_2COO^- + H_2O$	-81.2	-18.62	-81.69	-16.93	-82.89	-16.57	-84.57	-14.68
8	propionate formation in *Pelobacter propionicus*	$3CH_3CH_2OH + 2CO_2 \rightarrow 2CH_3CH_2COO^- + CH_3COO^- + H_2O + 3H^+$	-113.84	193.54	-114.24	197.27	-115.14	202.88	-115.86	181.15
Chain elongation to even-chain products with ethanol										
9	Ethanol to *n*-butyrate	$CH_3CH_2OH + CH_3COO^- \rightarrow CH_3(CH_2)_2COO^- + H_2O$	-38.6	-38.8	-38.59	-38.6	-38.6	-38.59	-38.58	-38.58
10	Ethanol to *n*-caproate	$CH_3CH_2OH + CH_3(CH_2)_2COO^- \rightarrow CH_3(CH_2)_4COO^- + H_2O)$	-38.8	-38.2	-38.8	-38.8	-38.81	-38.8	-38.8	-38.8
11	Ethanol to *n*-caprylate	$CH_3CH_2OH + CH_3(CH_2)_4COO^- \rightarrow CH_3(CH_2)_6COO^- + H_2O$	-43	-43.24	-43.37	-43.32	-43.51	-43.8	-43.4	-43.03
Chain elongation odd-chain products with ethanol										
12	Ethanol to *n*-valerate	$CH_3CH_2OH + CH_3CH_2COO^- \rightarrow CH_3(CH_2)_3COO^- + H_2O$	-38.60	-38.43	-38.60	-39.59	-38.60	-38.59	-38.58	-38.58
13	Ethanol to *n*-heptanoate	$CH_3CH_2OH + CH_3(CH_2)_2COO^- \rightarrow CH_3(CH_2)_5COO^- + H_2O$	-42.05	-41.85	-42.15	-42.11	-42.25	-42.24	-42.42	-42.23
Chain elongation to even-chain products with lactate										
14	Lactate to *n*-butyrate	$CH_3CH(OH)COO^- + CH_3COO^- + H^+ \rightarrow CH_3(CH_2)_2COO^- + H_2O + CO_2$	-57.96	-98.24	-59.01	-98.74	-61.57	-101.32	-65.17	-104.98
15	Lactate to *n*-caproate	$CH_3CH(OH)COO^- + CH_3(CH_2)_2COO^- + H^+ \rightarrow CH_3(CH_2)_4COO^- + H_2O + CO_2$	-58.16	-97.64	-59.22	-98.94	-61.78	-101.53	-65.39	-105.2

16	Lactate to *n*-caprylate	$CH_3CH(OH)COO^- + CH_3(CH_2)_4COO^- + H^+ \rightarrow CH_3(CH_2)_6COO^- + H_2O + CO_2$	-62.60	-102.3	-63.79	-105.3	-66.47	-106.23	-70.34	-110.09
Chain elongation to odd-chain products with lactate										
17	Lactate to *n*-valerate	$CH_3CH(OH)COO^- + CH_3CH_2COO^- \rightarrow CH_3(CH_2)_3COO^- + H_2O$	-57.96	-97.87	-59.02	-99.73	-61.57	-101.32	-65.17	-104.98
18	Lactate to *n*-heptanoate	$CH_3CH(OH)COO^- + CH_3(CH_2)_2COO^- \rightarrow CH_3(CH_2)_5COO^- + H_2O$	-61.41	-101.29	-62.57	-102.25	-65.22	-104.97	-68.01	-108.83
ß-oxidation of fatty acids										
19	*n*-caprylate to *n*-caproate	$CH_3(CH_2)_6COO^- + 2H_2O \rightarrow CH_3(CH_2)_4COO^- + CH_3COO^- + 2H_2 + H^+$	53.13	155.58	51.55	155.04	47.56	154.18	43.00	152.78
20	*n*-caproate to *n*-butyrate	$CH_3(CH_2)_4COO^- + 2H_2O \rightarrow CH_3(CH_2)_2COO^- + CH_3COO^- + 2H_2 + H^+$	48.69	151.14	47.03	150.52	42.87	149.49	38.05	147.83
21	*n*-butyrate to acetate	$CH_3(CH_2)_2COO^- + 2H_2O \rightarrow 2CH_3COO^- + 2H_2 + H^+$	48.49	150.94	46.83	150.32	42.66	149.28	37.83	147.61

[a] Adapted from (Cavalcante, Leitão *et al*. 2017). ΔG°: Gibbs free energy at different temperatures with 1M of substrates and products, a water activity of 1, gas partial pressure of 105 KPa, and pH=7. $\Delta G^{\circ\prime}$: Gibbs free energy at different temperatures with ion concentration of 0, 1M of substrates and products, a water activity of 1, gas partial pressure of 105 KPa, and pH=5.5.

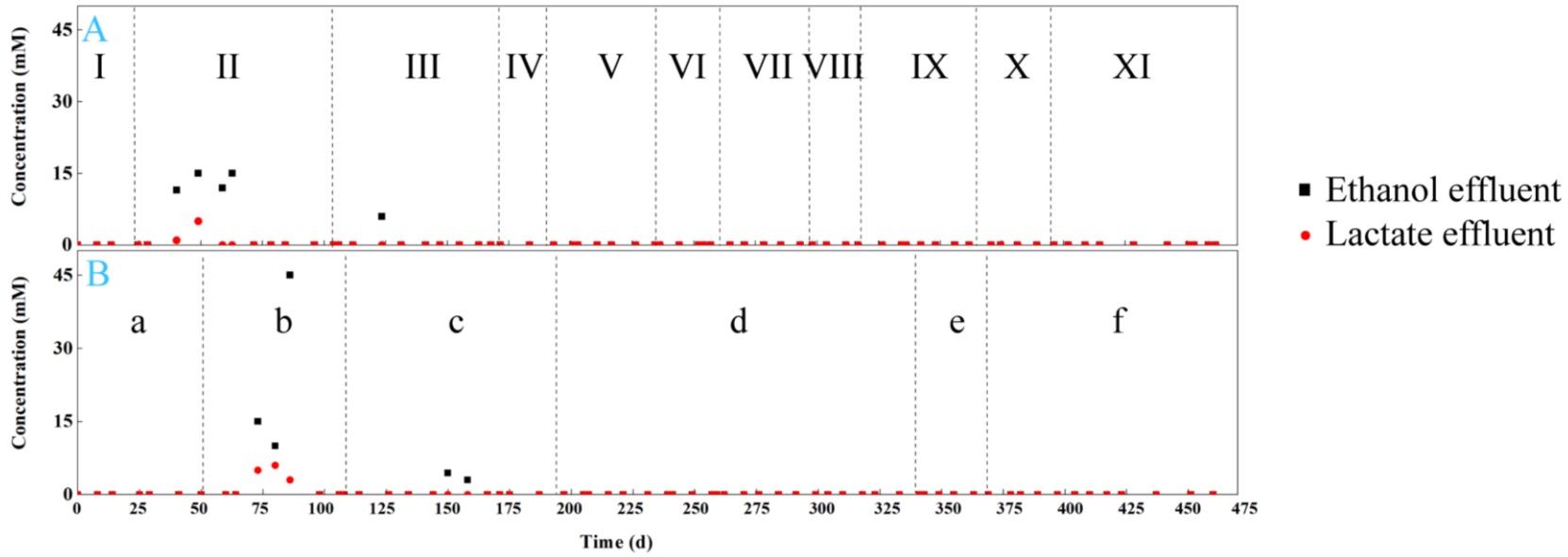

Figure S3.1. The concentration of ethanol and lactate in the effluent from test reactor (A) and control reactor (B).

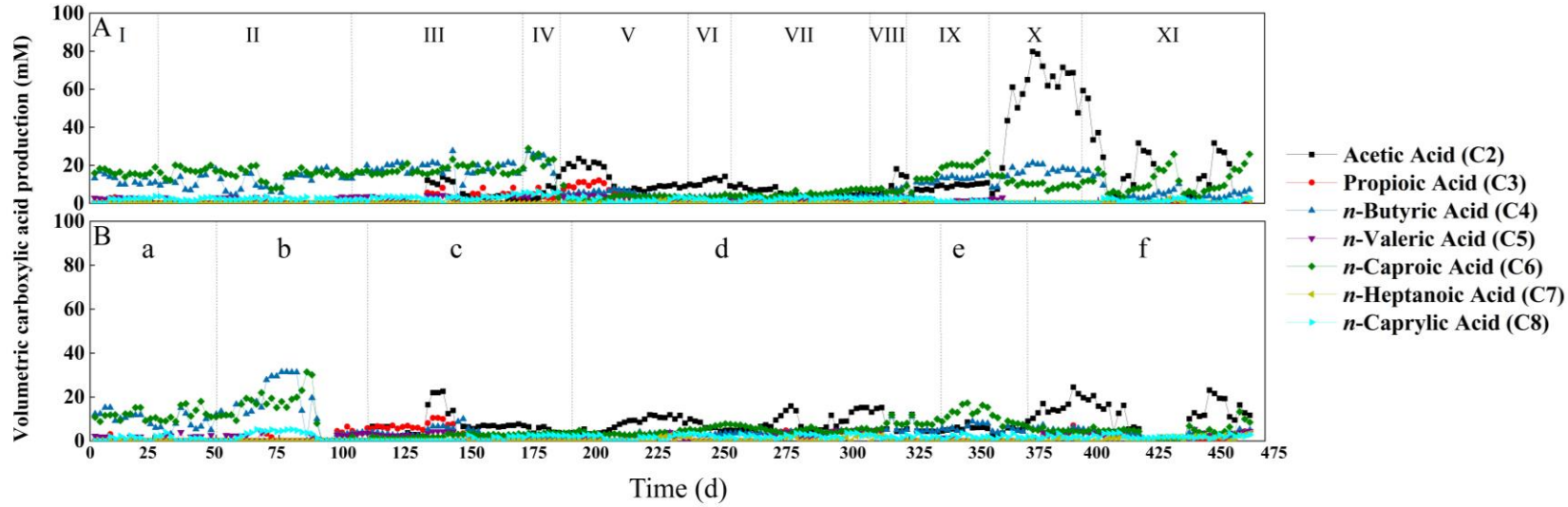

Figure S3.2. The concentration of carboxylates in the bioreactor in test reactor (A) and control reactor (B).

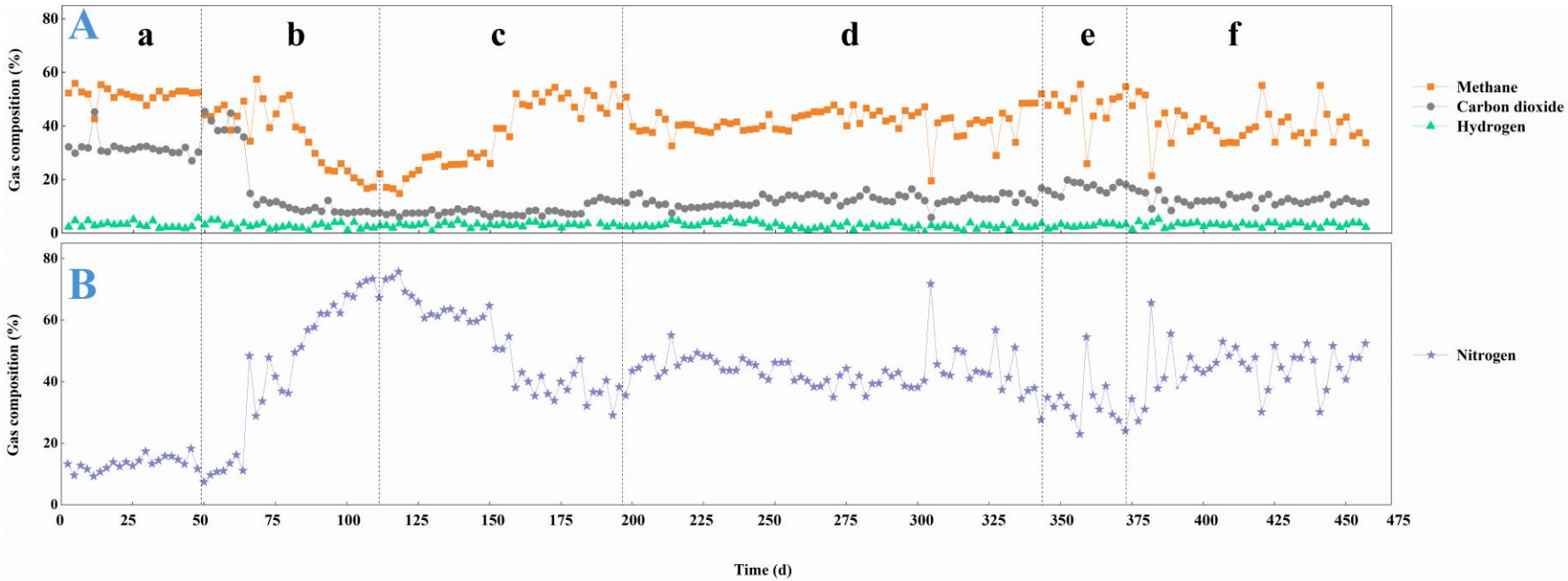

Figure S3.3. Biogas data over the operating periods in control reactor (R2): methane, carbon dioxide, and hydrogen percentages in the biogas (A); nitrogen percentages in the biogas (B).

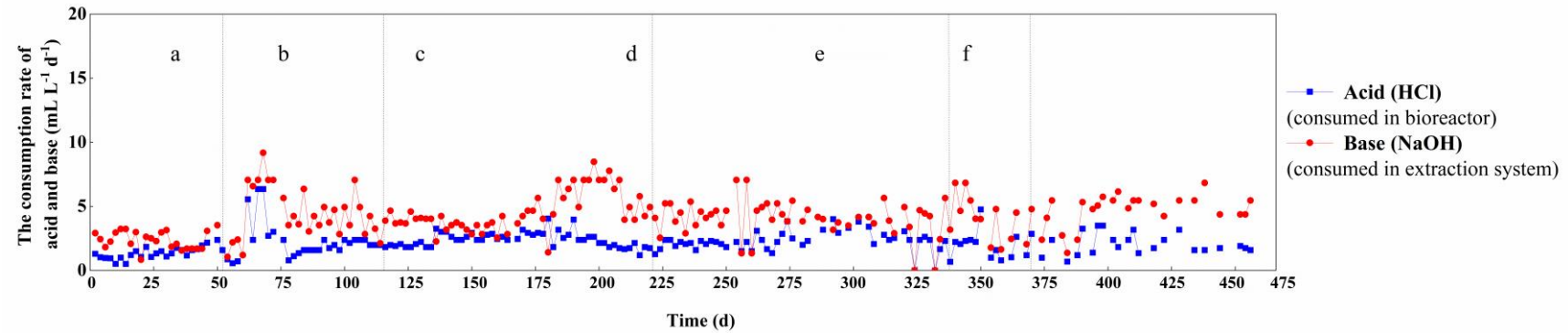

Figure S3.4 The acid consumed in bioreactor and base consumed in extraction system during operating periods **a-f** in control reactor (R2).

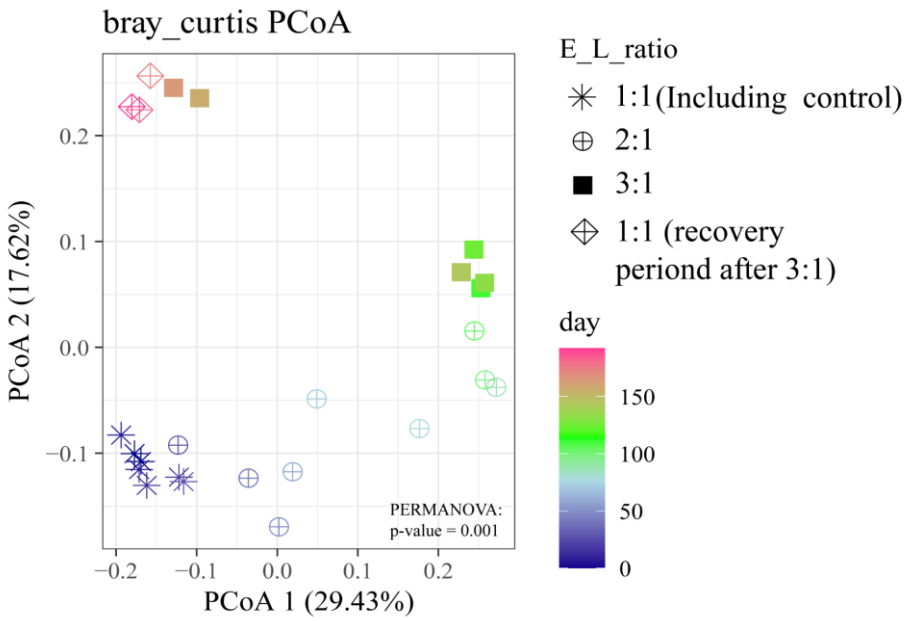

Figure S4.1. Principal coordinate analysis (PCoA) of the microbiomes with Bray-Curtis distance matrix showing microbial community among groups (E_L_ratio experiment) were significantly separated (PERMANOVA: adonis, $p < 0.001$).

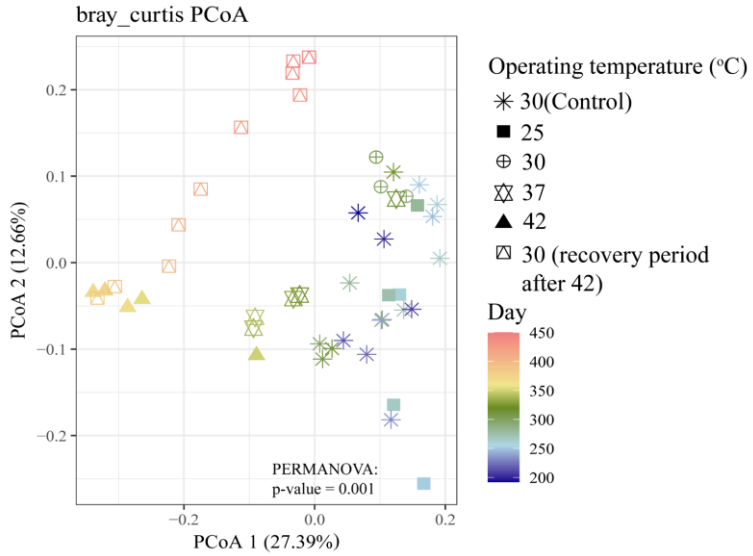

Figure S4.2. Principal coordinate analysis (PCoA) of the microbiomes with Bray-Curtis distance matrix showing microbial community among groups (operating temperature experiment) were significantly separated (PERMANOVA: adonis, $p < 0.001$).

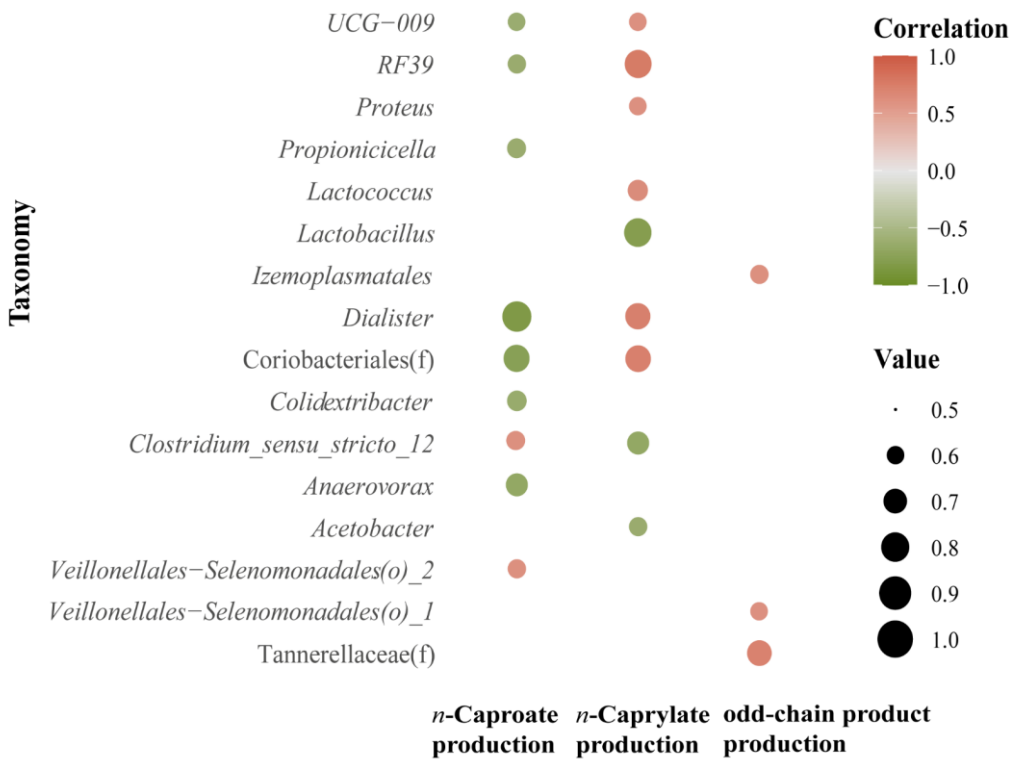

Figure S4.3. Spearman's correlation coefficient bubble chart for the content of carboxylate production relative genus (E_L_ratio experiment). The size of the bubble indicates correlation coefficients, the bigger the more correlated; The red and green color of the bubble indicates positive and negative correlations. (All genera shown in the chart are defined by a p-value < 0.05 and r >= 0.6).

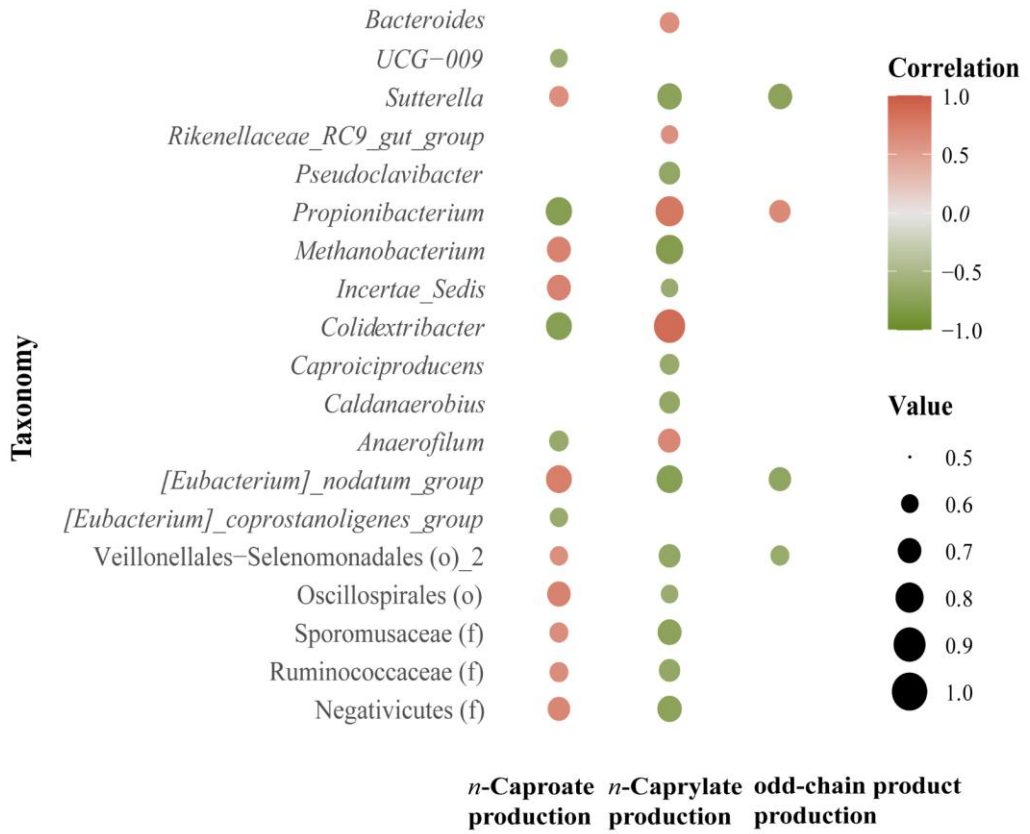

Figure S4.4. Spearman's correlation coefficient bubble chart for the content of carboxylate production relative genus (operating temperature experiment). The size of the bubble indicates correlation coefficients, the bigger the more correlated; The red and green color of the bubble indicates positive and negative correlations. (All genera shown in the chart are defined by a p-value of < 0.05 and r >= 0.6).

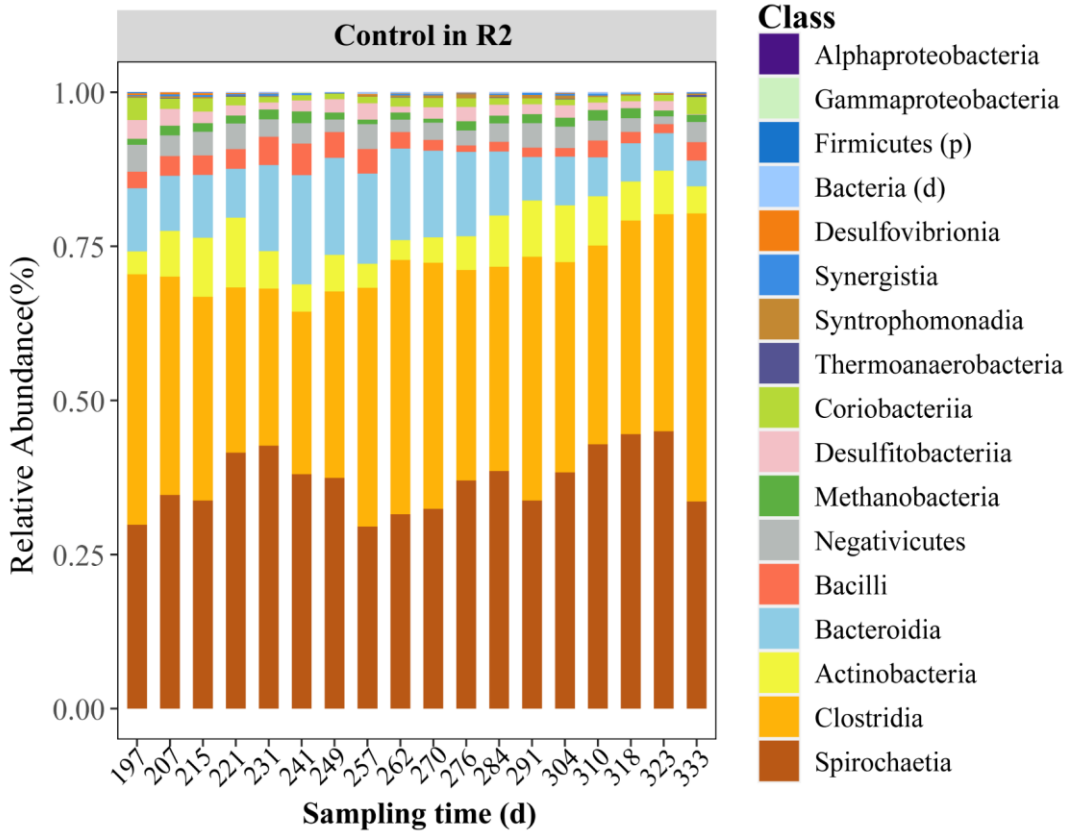

Figure S4.5. Bar graphs showing the relative abundance of reactor microbiomes during period e (control of the operating temperature experiement) in R2. OTU taxonomy is given at the Class level unless taxonomy assignment was not that specific (k: kingdom, p: phyla).

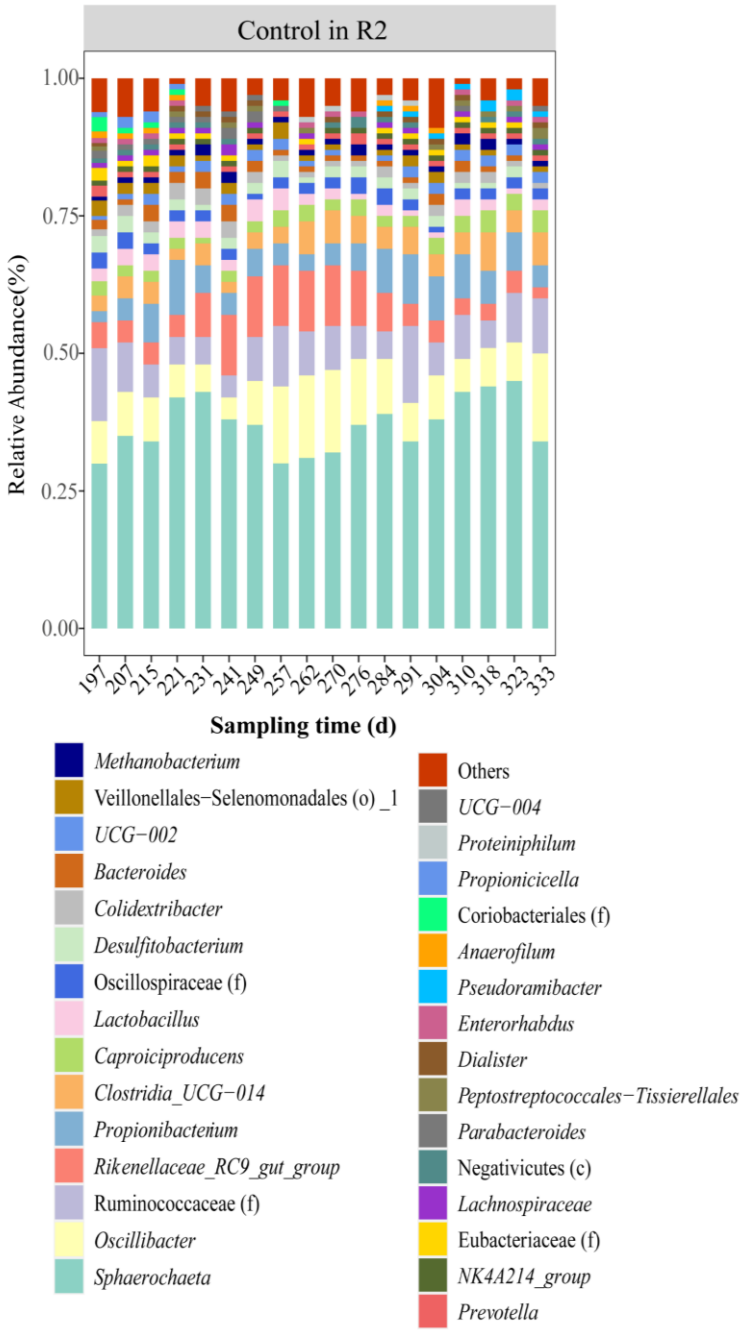

Figure S4.6. Bar graphs showing the relative abundance of the top abundant 30 genera of the reactor microbiome during period e (control of the operating temperature experiment) in R2. OTU taxonomy was given at the genus level unless taxonomy assignment was not that specific (k: kingdom, p: phyla, c: class, o: order, f: family).

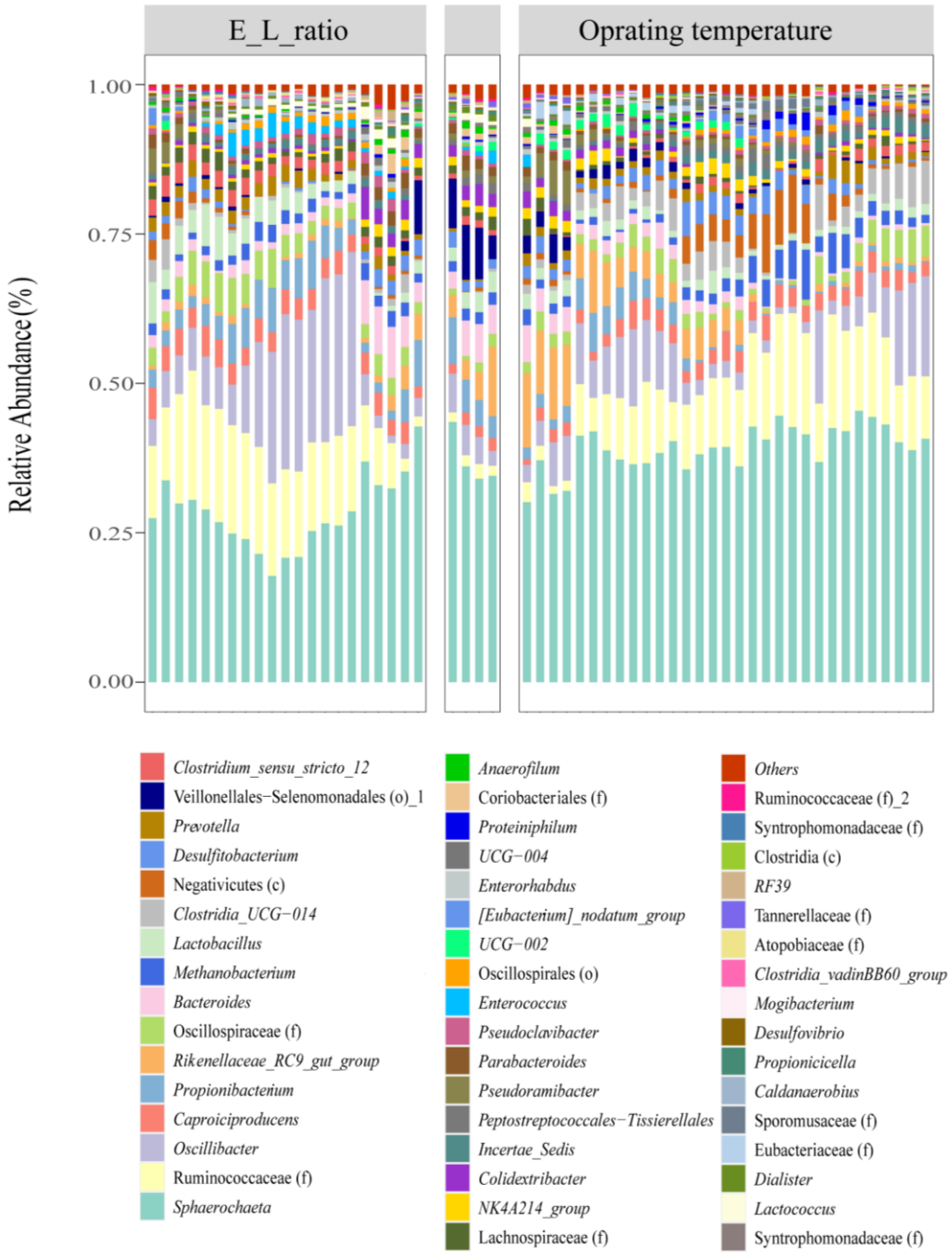

Figure S4.7. Bar graphs showing the microbial composition across the time series in R1. The legend only shows the top 50 abundant genera; "Others" includes all OTUs of low relative abundance (< 0.1%); OTUs of relative abundance below 0.01% are excluded. OTU taxonomy is given at the genus level unless taxonomy assignment was not that specific (k: kingdom, p: phyla, c: class, o: order, f: family).

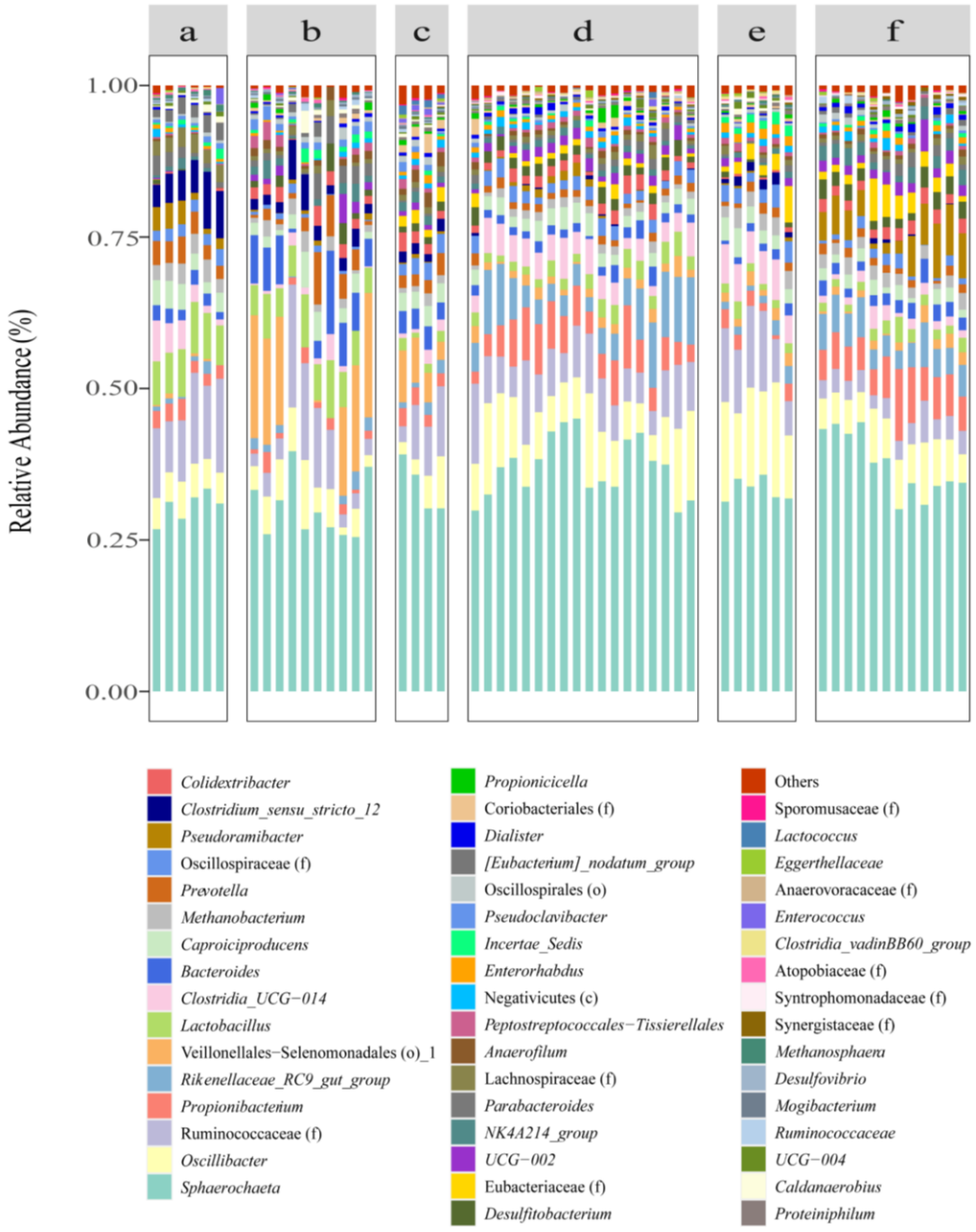

Figure S4.8. Bar graphs showing the microbial composition across the time series in R2. The legend only shows the top 50 abundant genera; "Others" includes all OTUs of low relative abundance (< 0.1%); OTUs of relative abundance below 0.01% are excluded. OTU taxonomy is given at the genus level unless taxonomy assignment was not that specific (k: kingdom, p: phyla, c: class, o: order, f: family).

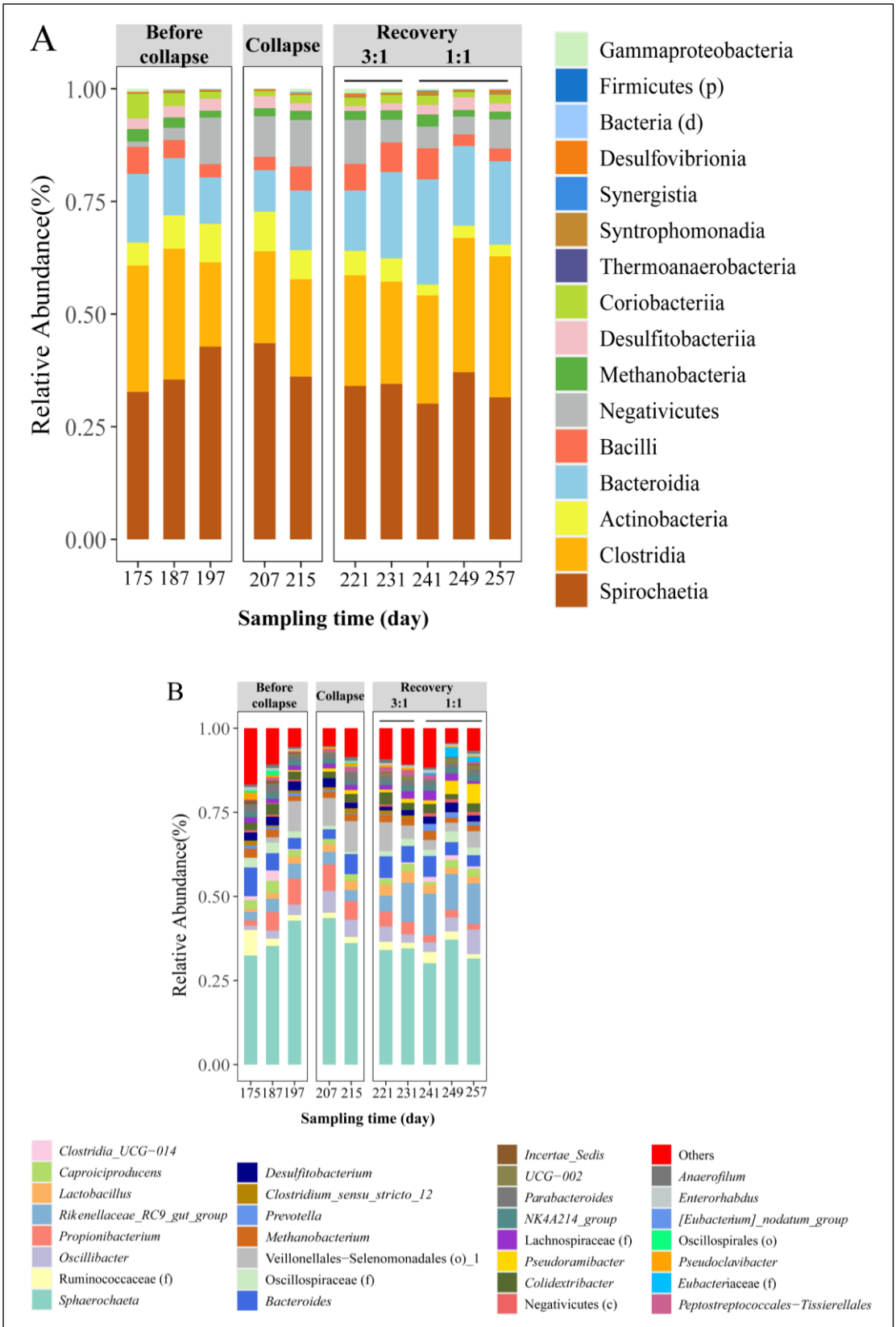

Figure S4.9. Microbial composition of the reactor microbiomes during different periods (before collapse/ during collapse/ during recovery). Bar graphs showing the relative abundance of the microbiomes at class level (A). Bar graphs showing the relative abundance of the top 30 abundant genera of the reactor microbiomes (B). OTU taxonomy was given at the genus level unless taxonomy assignment was not that specific (k: kingdom, p: phyla, c: class, o: order, f: family).

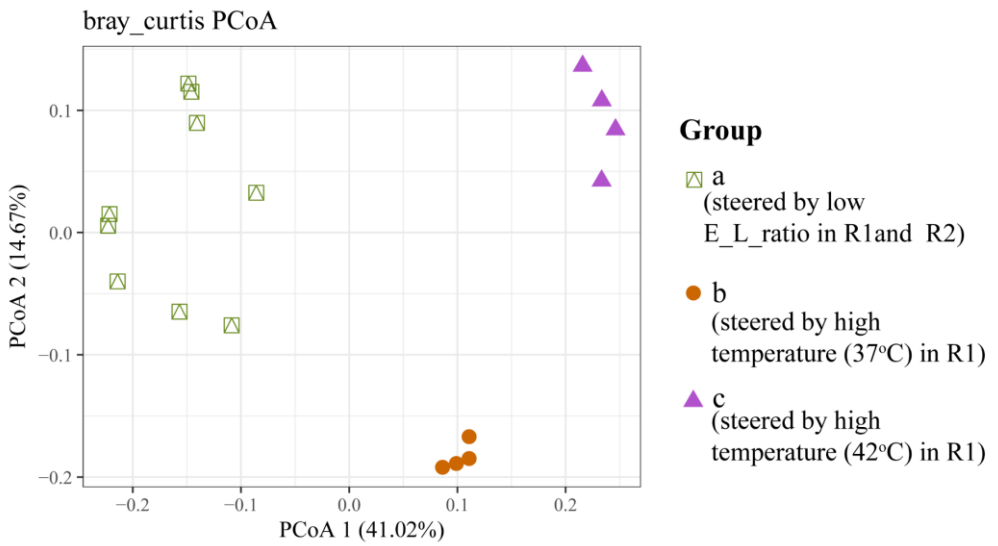

Figure S4.10. Principal coordinate analysis (PCoA) of the microbiomes shaped by different environmental factors for high *n*-caproate production with Bray-Curtis distance matrix (PERMANOVA: adonis, $p < 0.001$).

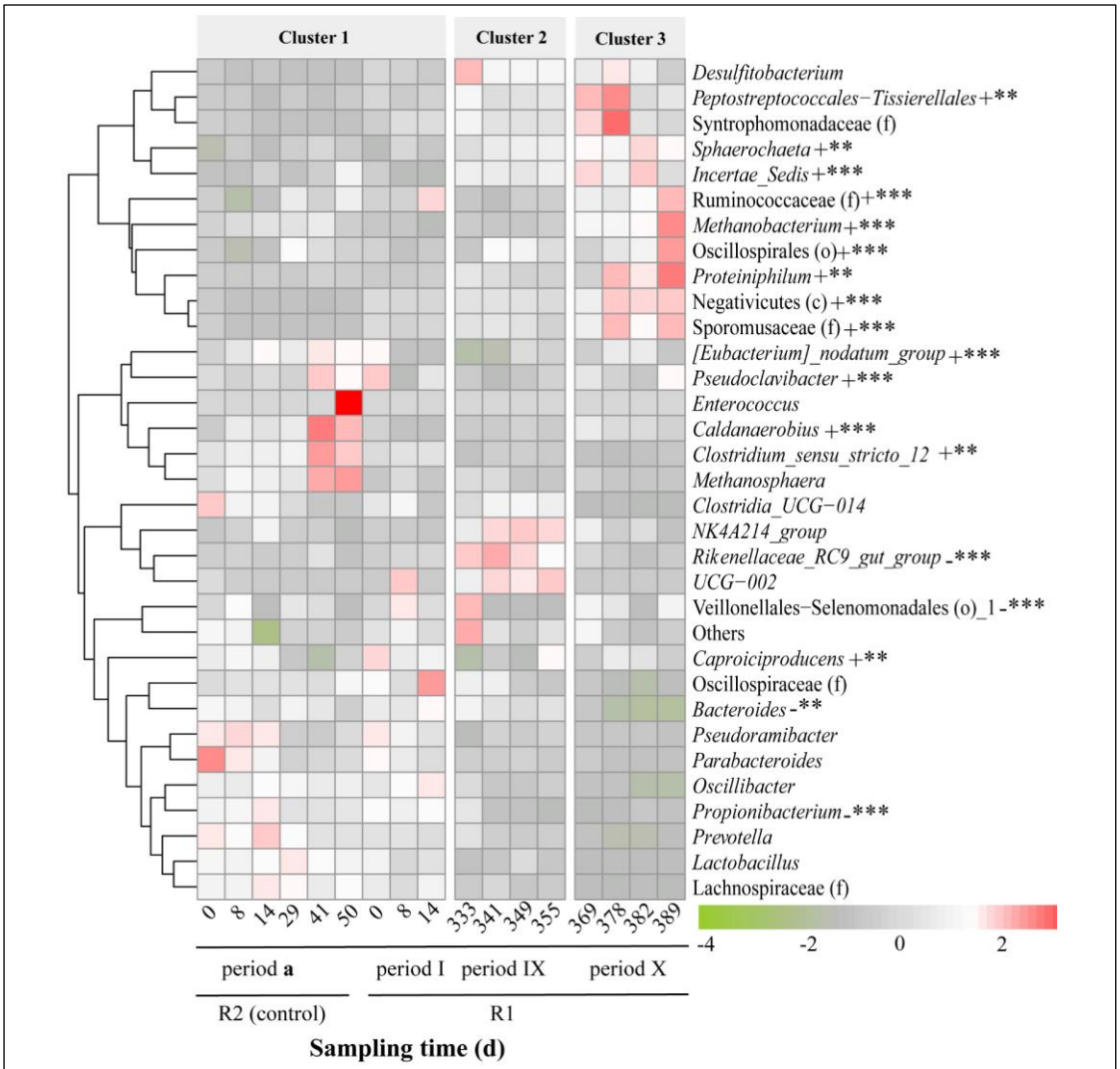

Figure S4.11. Heatmaps of the microbiomes shaped by different environmental factors for high *n*-caproate production. Relative abundance (%) is represented by the color gradient shown. OTUs that reached higher than 1% relative abundance in any one sample are represented. OTU taxonomy is given at the genus level unless taxonomy assignment was not that specific (k: Kingdom, p: Phyla, c: Class, o: order, f: family). Log-transformed relative abundance (%) is represented by the color gradient shown. The *n*-caproate production significantly correlated OTUs (the Spearman's correlation coefficient (**Figures S4.3** and **S4.4**) was marked with + or – symbols, representing whether the relative abundance of the OTUs were found to be significantly positively (+) or negatively (−) correlated with *n*-caproate production. (* indicates FDR-adjusted p-value < 0.05; ** indicates FDR-adjusted p-value < 0.01; *** indicates FDR-adjusted p-value < 0.001).

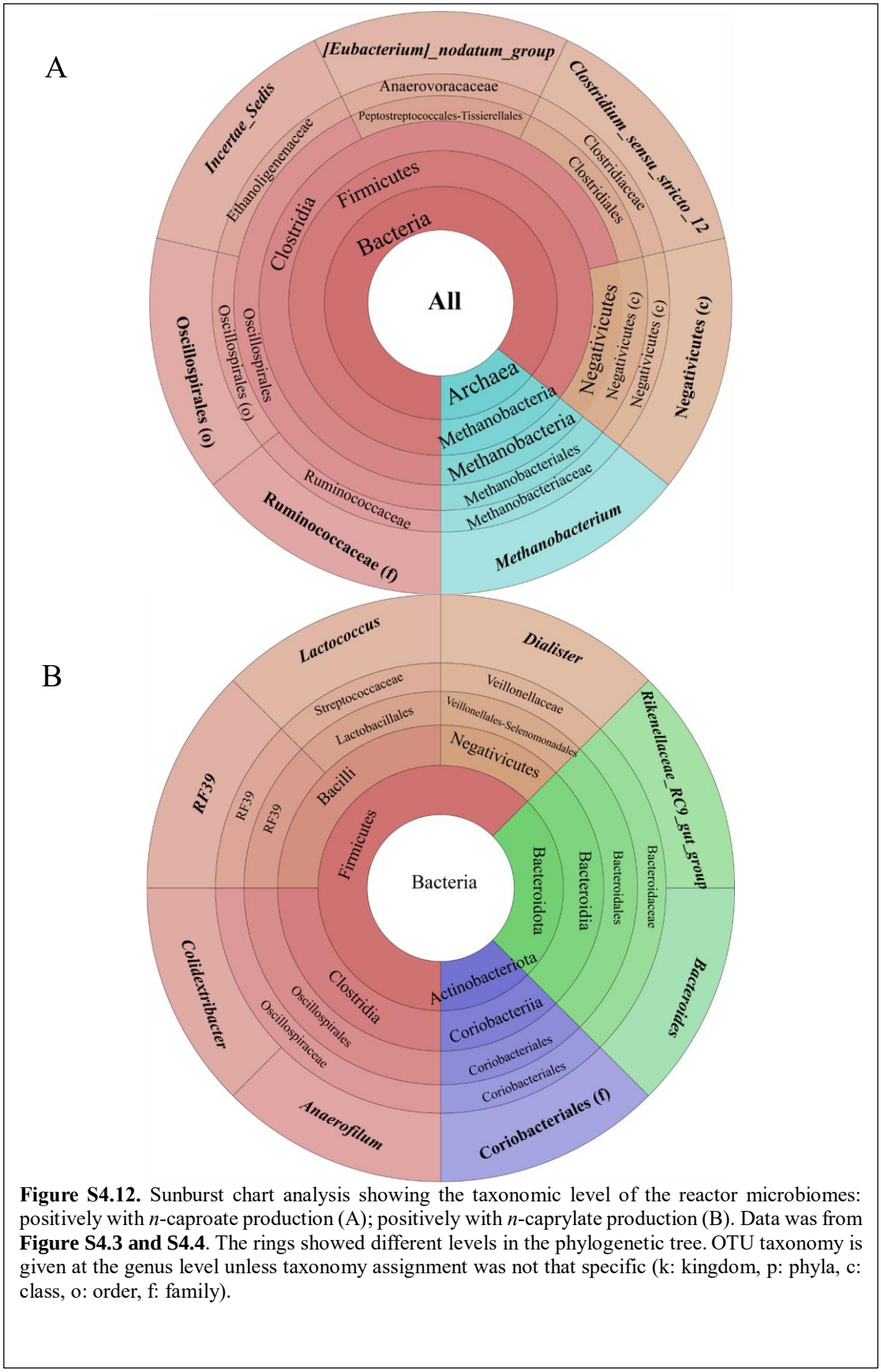

Figure S4.12. Sunburst chart analysis showing the taxonomic level of the reactor microbiomes: positively with *n*-caproate production (A); positively with *n*-caprylate production (B). Data was from **Figure S4.3 and S4.4**. The rings showed different levels in the phylogenetic tree. OTU taxonomy is given at the genus level unless taxonomy assignment was not that specific (k: kingdom, p: phyla, c: class, o: order, f: family).

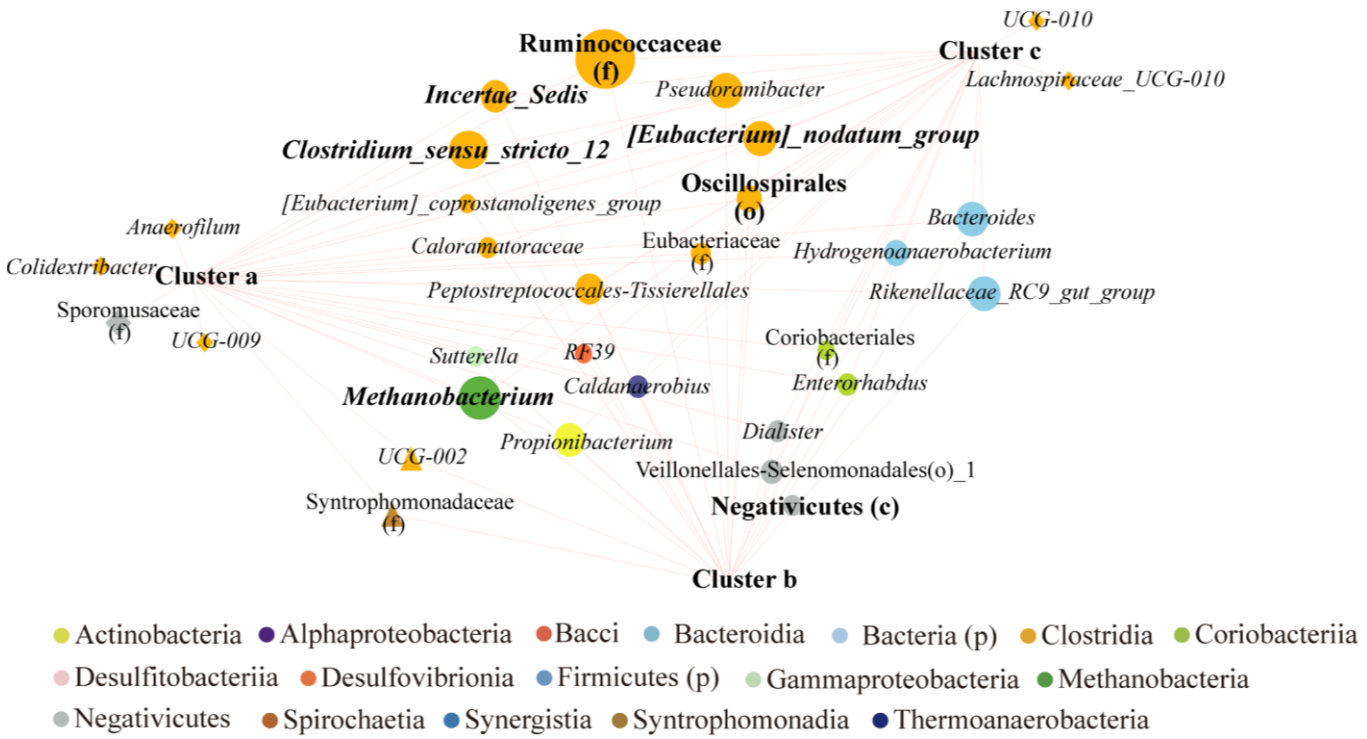

Figure S4.13. Co-occurrence network based on correlation analysis of the microbial communities from the three clusters with high production of *n*-caproate (p-value < 0.05). The edges were weighted by the strength of the correlation. The nodes were colored according to the Class to which the OTUs belonged, and were weighted by the average relatibve abundance of the OTUs in three clusters. Bold labels showing the genus was positively correlated with the production of *n*-caproate (**Figures S4.3 and S4.4**). OTU taxonomy is given at the genus level unless taxonomy assignment was not that specific (k: kingdom, p: phyla, c: class, o: order, f: family).

Table S4.1 The average alpha diversity of the microbiomes under different conditions in the biorector								
Operating condition		**Richness**	**Shannon**	**Simpson**	**Pielou**	**Chao1**	**ACE**	**goods_coverage**
R1								
E_L_ratio	1:1	53±2.65	4.14±0.15	0.87±0.02	0.72±0.03	53±2.65	53.07±2.61	1±0
	2:1	54.2±8.41	4.04±0.18	0.88±0.02	0.7±0.01	54.2±8.41	54.23±8.42	1±0
	2:1 (steady state)	42.75±8.46	3.88±0.05	0.88±0.01	0.72±0.04	42.75±8.46	46.43±5.58	1±0
	3:1	53±5.48	3.57±0.12	0.84±0.02	0.62±0.03	53±5.48	53±5.48	1±0
	3:1 (steady state)	60.5±4.95	4.16±0.17	0.86±0.02	0.7±0.04	60.5±4.95	60.5±4.95	1±0
	1:1	66.33±6.43	4.17±0.4	0.84±0.04	0.69±0.05	66.33±6.43	66.33±6.43	1±0
Collapse		59.75±5.85	3.98±0.27	0.84±0.03	0.67±0.03	59.75±5.85	59.86±5.89	1±0
Recovery		58.33±4.16	4.13±0.19	0.86±0.02	0.7±0.03	58.33±4.16	58.33±4.16	1±0
Operating temperature (°C)	25	55	4.142147	0.870989	0.716466	55	55	1
	25 (steady state)	48.25±5.38	3.68±0.08	0.82±0.01	0.66±0.02	48.25±5.38	48.25±5.38	1±0
	30	49±4.58	3.71±0.04	0.83±0.01	0.66±0.01	49±4.58	49±4.58	1±0
	37	49	3.745952	0.816104	0.667167	49	49	1
	37 (steady state)	54.25±5.12	3.84±0.13	0.83±0.01	0.67±0.01	54.25±5.12	54.25±5.12	1±0
	42	60	3.989046	0.84293	0.675321	60	60	1
	42 (steady state)	48.5±6.95	3.25±0.2	0.78±0.02	0.58±0.03	48.5±6.95	48.64±7.21	1±0
	30	46.6±5.86	3.29±0.07	0.77±0.01	0.6±0.02	46.6±5.86	46.6±5.86	1±0
	30 (steady state)	47.4±7.16	3.42±0.11	0.8±0.02	0.62±0.03	47.4±7.16	47.51±7.12	1±0
R2								
Control of the E_ L_ratio experiment		57.67±15.33	4.07±0.21	0.87±0.02	0.7±0.04	57.67±15.33	57.74±15.36	1±0
Collapse of extraction system		51.1±14.97	3.91±0.3	0.86±0.04	0.7±0.08	51.1±14.97	51.23±15.02	1±0
Recovery		68.75±6.24	4.31±0.17	0.86±0.03	0.71±0.02	68.75±6.24	68.75±6.24	1±0
Control of the operating temperature experiment		55.78±11.27	3.83±0.21	0.83±0.03	0.66±0.03	55.78±11.27	55.8±11.29	1±0
Collapse of pH sensor		53.8±7.29	3.81±0.12	0.85±0.01	0.66±0.02	53.8±7.29	53.8±7.29	1±0
Recovery		50.69±9.38	3.95±0.24	0.84±0.03	0.7±0.04	50.69±9.38	50.69±9.38	1±0

Table S4.2 The average MCCA production rate and methane composition in different experimental groups					
		Production rate (mmol C^{-1} L^{-1} d)			Mathne composition (%)
		n-Caproate	*n*-Caprylate	Odd-chain products	
Test reactor (R1)	Before collapse	13.72±3.58	50.06±10.58	26.02±16.48	40.27±5.87
	Collapse	18.31±3.34	17.66±11.31	29.93±5.71	35.95±1.73
	Recovery with an E_L_ratio of 3	16.7±0.82	35.69±3.16	25.16±2.8	43.44±0.03
	Recovery with an E_L_ratio of 1	16.58±6.91	46.94±5.42	21.57±9.13	48.35±5.82
Control reactor (R2)	Before collapse	43.87±4.08	16.69±4.63	10.63±3.14	39.88±2.5
	Period I of collapse	36.68±8.82	41.56±6.27	14.9±10.36	42.91±7.37
	Period II of collapse	17.37±1.01	23.62±2.98	42.54±2.44	24.09±6.73
	Recovery with an E_L_ratio of 1	15.86±2	8.45±2.19	40.12±6.04	24.91±4.21
	Recovery with an E_L_ratio of 3	13.12±2.66	62.44±12.81	12.6±4.7	46.73±7.6
	Recovery with an E_L_ratio of 1	10.8±2.55	51.48±18.36	13.59±5.52	39.22±1.44

Table S4.3 The average relative abundance (%) of the microbiomes at class level in each experimental group in R1

	E_L_ratio						Collapse	Recovery	Operating temperature (°C)							
	1:1	2:1	2:1 (steady state)	3:1	3:1 (steady state)	1:1 (after 3:1)			25	25 (steady state)	30	37	37 (steady state)	42	42 (steady state)	30
Spirochaetia	30.37±3.21	26.97±2.74	20.28±1.68	26.66±1.35	34.98±2.96	36.99±5.2	37.06±4.41	32.92±3.7	32.02314	39.83±2.18	37.22±1.2	40.35253	38.14±1.8	36.12061	42.66±1.64	43.15±1.66
Clostridia	44.65±1.93	46.49±1.45	54.03±1.38	54.05±3.53	34.58±1.18	25.27±5.72	22.31±1.77	28.37±3.83	32.28281	34.71±5.16	40.54±1.68	37.11048	34.99±2.23	36.74231	31.58±1.05	36.76±4.86
Actinobacteria	3.66±0.61	5.71±2.09	7.87±0.99	6.57±3.33	3.83±0.24	7.02±1.77	6.48±1.64	2.59±0.17	3.446648	5.72±1	3.68±1.62	4.270276	1.32±0.85	2.17594	1.02±0.34	1.28±0.43
Bacteroidia	7.33±0.08	5.51±1.66	4.93±0.92	4.06±0.59	12.74±1.64	12.76±2.47	13.75±4.1	19.86±3.05	18.64967	11.41±3.15	9.15±1.63	7.921519	8.98±1.49	8.63123	2.47±0.84	5.18±1.42
Bacilli	5.27±1.67	7.68±2.2	7.57±1.31	4.41±0.67	5.09±0.32	4.3±1.56	5.17±1.56	4.08±2.47	4.426346	2.76±0.47	1.82±0.69	1.783653	2.6±1.13	1.823645	1.02±0.37	1.26±0.2
Negativicutes	4.13±0.11	1.73±0.38	0.64±0.18	0.49±0.08	0.79±0.26	4.75±4.92	8.55±2.39	5.07±1.27	3.411237	2.31±0.71	2.8±0.73	3.724688	5.57±0.91	5.978655	11.11±2.12	4.2±3.4
Methanobacteria	1.89±0.73	1.88±0.6	2.78±0.72	1.68±0.57	2.36±0.8	2.18±0.64	1.96±0.15	1.96±0.64	1.794145	0.76±0.39	0.94±0.41	1.196097	2.09±0.26	2.818361	5.1±0.9	5.3±2.44
Desulfitobacteriia	1.09±0.45	1.17±0.9	0.21±0.25	0.14±0.19	2.15±1.15	2.55±0.15	1.76±0.66	2.25±0.53	1.923985	1.3±0.64	2.5±0.1	1.710209	4.37±0.9	3.357165	2.9±1.61	1.84±1.07
Coriobacteriia	0.64±0.18	1.03±0.72	0.73±0.31	0.94±0.15	2.56±1.6	3.31±1.97	1.65±0.35	1.72±0.51	1.156752	0.72±0.19	0.56±0.16	0.713461	0.45±0.32	0.331572	0.13±0.08	0.12±0.1
Thermoanaerobacteria	0.06±0.1	0.5±0.51	0.8±0.34	0.4±0.17	0.09±0.13	0.04±0.03	0±0	0.01±0.01	0	0.01±0.01	0.01±0.02	0	0.12±0.03	0.290125	0.32±0.11	0.15±0.14
Syntrophomonadia	0.38±0.22	0.69±0.32	0.12±0.14	0.26±0.08	0.29±0.19	0.27±0.03	0.37±0.19	0.71±0.24	0.377715	0.25±0.09	0.45±0.46	0.786906	0.78±0.15	0.818568	0.89±0.44	0.28±0.18
Synergistia	0.02±0.03	0±0	0.01±0.02	0±0	0±0	0±0	0.01±0.01	0.08±0.07	0	0.04±0.05	0.07±0.07	0.157381	0.31±0.07	0.569889	0.06±0.1	0.04±0.03
Desulfovibrionia	0.4±0.15	0.49±0.23	0.01±0.02	0.07±0.05	0.07±0.1	0.19±0.06	0.21±0.08	0.13±0.16	0.365911	0.14±0.11	0.19±0.1	0.272794	0.23±0.03	0.176148	0.16±0.12	0.03±0.05
Bacteria (d)	0.03±0.02	0.02±0.03	0.01±0.02	0.06±0.05	0.01±0.02	0.11±0.06	0.05±0.04	0.11±0.07	0.141643	0.01±0.02	0.07±0.02	0	0.02±0.02	0.093255	0.2±0.16	0.12±0.11
Firmicutes (p)	0±0	0.08±0.12	0±0	0.06±0.11	0±0	0±0	0.04±0.03	0±0	0	0.02±0.02	0±0	0	0±0	0	0.03±0.05	0±0
Gammaproteobacteria	0.03±0.04	0.04±0.03	0.01±0.03	0.15±0.13	0.45±0.13	0.27±0.33	0.62±0.43	0.13±0.17	0	0±0	0±0	0	0.02±0.04	0.072531	0.35±0.14	0.27±0.24
Alphaproteobacteria	0.06±0.06	0.01±0.02	0.01±0.01	0±0	0±0	0±0	0±0	0±0	0	0±0	0±0	0	0±0	0	0±0	0±0

OTU taxonomy is given at the Class level unless the taxonomy assignment was not that specific (k: kingdom, p: phyla).

Table S4.4 The average relative abundance of the microbiomes at class level in each experimental group in R2								
	Control of the E_L_ratio experiment	Collapse of extraction system		Recovery		Control of operating temperature experiment	Collapse of pH sensor	Recovery
		Period 1	Period 2	1:1	3:1			
Spirochaetia	30.46±2.44	30.69±6.04	29.46±6.6	30.24±3.81	33.84±4.24	36.95±4.9	33.66±1.93	36.99±5.17
Clostridia	43.3±2.1	40.78±8.71	23.49±4.47	24.68±2.41	34.81±6.09	34.87±5.63	47.59±2.6	34.02±4.24
Actinobacteria	3.25±0.59	2.34±0.87	3.04±1.12	4.31±2.18	3.96±1.18	6.54±2.36	2.33±1.14	6.89±2.35
Bacteroidia	7.96±2.16	11.5±11.21	14.16±3.74	11.41±0.28	8.5±1.31	10.56±4.01	4.72±1.26	10±1.29
Bacilli	8.34±1.07	8.24±2.24	5.23±0.92	5.95±1.22	3.71±0.77	2.72±1.2	2.28±1.01	2.06±0.94
Negativicutes	1.06±0.7	0.3±0.4	19.26±2.71	19.18±1.3	7.73±2.18	3.1±0.85	2.55±0.72	3.01±0.75
Methanobacteria	3.72±0.6	2.66±0.68	1.37±0.42	1.62±0.92	1.75±0.57	1.3±0.34	2.92±0.6	2.24±0.61
Desulfitobacteriia	0.17±0.29	1.17±2.28	1.82±1.44	0.98±0.94	1.24±0.24	1.76±0.71	0.34±0.38	2.23±0.84
Coriobacteriia	0.81±0.39	0.69±0.53	0.88±0.18	1.02±0.27	3.25±1.11	1.42±0.76	2.34±0.18	1.13±0.73
Thermoanaerobacteria	0.62±0.41	1.27±1.63	0.5±0.23	0.16±0.14	0.39±0.15	0.05±0.08	0.53±0.3	0.01±0.04
Syntrophomonadia	0.05±0.1	0±0	0.07±0.04	0.02±0.03	0.08±0.09	0.28±0.19	0.28±0.18	0.29±0.19
Synergistia	0±0.01	0±0	0±0	0.01±0.02	0.09±0.14	0.21±0.11	0.08±0.05	0.49±0.26
Desulfovibrionia	0.14±0.12	0.05±0.04	0.47±0.16	0.35±0.07	0.19±0.1	0.09±0.11	0.04±0.05	0.27±0.2
Bacteria (d)	0.04±0.04	0.11±0.08	0.08±0.14	0.03±0.04	0.12±0.13	0.13±0.08	0.33±0.18	0.33±0.17
Firmicutes (p)	0.01±0.01	0.02±0.04	0.13±0.05	0±0.01	0.03±0.06	0.02±0.04	0±0	0.02±0.03
Gammaproteobacteria	0.03±0.03	0.13±0.16	0±0	0.04±0.04	0.29±0.3	0.01±0.03	0.01±0.01	0±0.01
Alphaproteobacteria	0.04±0.04	0.05±0.09	0.04±0.04	0±0	0±0	0±0	0±0	0.02±0.04
OTU taxonomy is given at the Class level unless the taxonomy assignment was not that specific (k: kingdom, p: phyla).								

Table S4.5 The taxonomic level and the relative abundance of the microbiomes at genus level

Taxonomic level						Relative abundance
Domain	**Phylum**	**Class**	**Order**	**Family**	**Genus**	
Bacteria	Spirochaetota	Spirochaetia	Spirochaetales	Spirochaetaceae	*Sphaerochaeta*	0.351844
Bacteria	Firmicutes	Clostridium	Oscillospirales	Ruminococcaceae	*Ruminococcaceae (f)*	0.099021
Bacteria	Firmicutes	Clostridium	Oscillospirales	Oscillospirales	*Oscillibacter*	0.080666
Bacteria	Actinobacteriota	Actinobacteria	Propionibacteriales	Propionibacteriaceae	*Propionibacterium*	0.034097
Bacteria	Bacteroidota	Bacteroidia	Bacteroidales	Bacteroidales	*Rikenellaceae_RC9_gut_group*	0.032641
Bacteria	Firmicutes	Bacilli	Lactobacillales	Lactobacillaceae	*Lactobacillus*	0.029505
Bacteria	Firmicutes	Clostridium	Oscillospirales	Ruminococcaceae	*Caproiciproducens*	0.028328
Bacteria	Firmicutes	Clostridium	Clostridia_UCG-014	Clostridia_UCG-014	*Clostridia_UCG-014*	0.027989
Bacteria	Bacteroidota	Bacteroidia	Bacteroidales	Bacteroidaceae	*Bacteroides*	0.023899
Bacteria	Firmicutes	Clostridium	Oscillospirales	Oscillospiraceae	*Oscillospiraceae (f)*	0.022869
Bacteria	Firmicutes	Negativicutes	Veillonellales-Selenomonadales	Veillonellales-Selenomonadales (o)_1	*Veillonellales-Selenomonadales (o)_1*	0.022728
Archaea	Methanobacteria	Methanobacteria	Methanobacteriales	Methanobacteriaceae	*Methanobacterium*	0.021465
Bacteria	Bacteroidota	Bacteroidia	Bacteroidales	Prevotellaceae	*Prevotella*	0.016554
Bacteria	Firmicutes	Clostridium	Clostridiales	Clostridiaceae	*Clostridium_sensu_stricto_12*	0.015401
Bacteria	Firmicutes	Desulfitobacteriia	Desulfitobacteriales	Desulfitobacteriaceae	*Desulfitobacterium*	0.014483
Bacteria	Firmicutes	Negativicutes	Negativicutes (c)	Negativicutes (c)	*Negativicutes (c)*	0.012572
Bacteria	Firmicutes	Clostridium	Oscillospirales	Oscillospiraceae	*Colidextribacter*	0.011698
Bacteria	Firmicutes	Clostridium	Eubacteriales	Eubacteriaceae	*Pseudoramibacter*	0.011455
Bacteria	Firmicutes	Clostridium	Lachnospirales	(f) Lachnospiraceae	*Lachnospiraceae*	0.010735
Bacteria	Firmicutes	Clostridium	Oscillospirales	Oscillospiraceae	*NK4A214_group*	0.01018
Bacteria	Bacteroidota	Bacteroidia	Bacteroidales	Tannerellaceae	*Parabacteroides*	0.009543
Bacteria	Firmicutes	Clostridium	Oscillospirales	Oscillospiraceae	*UCG-002*	0.007459
Bacteria	Firmicutes	Clostridium	Oscillospirales	Ethanoligenenaceae	*Incertae_Sedis*	0.007366
Bacteria	Firmicutes	Clostridium	Peptostreptococcales-Tissierellales	Peptostreptococcales-Tissierellales	*Peptostreptococcales-Tissierellales*	0.007307

Bacteria	Firmicutes	Clostridium	Eubacteriales	Eubacteriaceae	*Eubacteriaceae (f)*	0.006637
Bacteria	Actinobacteriota	Actinobacteria	Micrococcales	Microbacteriaceae	*Pseudoclavibacter*	0.006107
Bacteria	Firmicutes	Clostridium	Oscillospirales (o)	Oscillospirales (o)	*Oscillospirales (o)*	0.005747
Bacteria	Firmicutes	Clostridium	Peptostreptococcales-Tissierellales	Anaerovoracaceae	*[Eubacterium]_nodatum_group*	0.005373
Bacteria	Actinobacteriota	Coriobacteriia	Coriobacteriales	Eggerthellaceae	*Enterorhabdus*	0.005102
Bacteria	Firmicutes	Clostridium	Oscillospirales	Ruminococcaceae	*Anaerofilum*	0.004783
Bacteria	Firmicutes	Negativicutes	Veillonellales-Selenomonadales	Veillonellaceae	*Dialister*	0.004091
Bacteria	Actinobacteriota	Coriobacteriia	Coriobacteriales	Coriobacteriales (f)	*Coriobacteriales (f)*	0.003888
Bacteria	Bacteroidota	Bacteroidia	Bacteroidales	Dysgonomonadaceae	*Proteiniphilum*	0.003697
Bacteria	Firmicutes	Bacilli	Erysipelotrichales	Erysipelatoclostridiaceae	*UCG-004*	0.00331
Bacteria	Firmicutes	Bacilli	Lactobacillales	Enterococcaceae	*Enterococcus*	0.003186
Bacteria	Actinobacteriota	Actinobacteria	Propionibacteriales	Propionibacteriaceae	*Propionicicella*	0.002689
Bacteria	Firmicutes	Thermoanaerobacteria	Thermoanaerobacterales	Thermoanaerobacteraceae	*Caldanaerobius*	0.002518
Bacteria	Firmicutes	Negativicutes	Veillonellales-Selenomonadales	Sporomusaceae	*Sporomusaceae (f)*	0.002084
Bacteria	Firmicutes	Bacilli	Lactobacillales	Streptococcaceae	*Lactococcus*	0.00198
Bacteria	Firmicutes	Clostridium	Peptostreptococcales-Tissierellales	Anaerovoracaceae	*Mogibacterium*	0.00177
Bacteria	Desulfobacterota	Desulfovibrionia	Desulfovibrionales	Desulfovibrionaceae	*Desulfovibrio*	0.001756
Bacteria	Firmicutes	Syntrophomonadia	Syntrophomonadales	Syntrophomonadaceae	*Syntrophomonadaceae (f)*	0.001663
Bacteria	Actinobacteriota	Coriobacteriia	Coriobacteriales	Atopobiaceae	*Atopobiaceae (f)*	0.001548
Bacteria	Firmicutes	Clostridium	Oscillospirales	(f) Ruminococcaceae	*Ruminococcaceae*	0.001543

Bacteria	Firmicutes	Clostridium	Clostridia_vadinBB60_group	Clostridia_vadinBB60_group	*Clostridia_vadinBB60_group*	0.001433
Archaea	Euryarchaeota	Methanobacteria	Methanobacteriales	Methanobacteriaceae	*Methanosphaera*	0.001232
Bacteria	Firmicutes	Syntrophomonadia	Syntrophomonadales	Syntrophomonadaceae (f)	*Syntrophomonadaceae (f)*	0.001189
Bacteria	Bacteria (d)	Bacteria (d)	Bacteria (d)	Bacteria (d)	*Bacteria (d)*	0.001117
Bacteria	Firmicutes	Clostridium	Peptostreptococcales-Tissierellales	Anaerovoracaceae	*Anaerovoracaceae (f)*	0.001031
Bacteria	Firmicutes	Clostridium	Clostridia (c)	Clostridia (c)	*Clostridia (c)*	0.00092
Bacteria	Firmicutes	Clostridium	Oscillospirales	[Eubacterium]_coprostanoligenes_group	*[Eubacterium]_coprostanoligenes_group*	0.000904
Bacteria	Firmicutes	Bacilli	RF39	RF39	*RF39*	0.00085
Bacteria	Actinobacteriota	Coriobacteriia	Coriobacteriales	(f) Eggerthellaceae	*Eggerthellaceae*	0.000847
Bacteria	Bacteroidota	Bacteroidia	Bacteroidales	Tannerellaceae	*Tannerellaceae (f)*	0.000814
Bacteria	Firmicutes	Clostridium	Peptostreptococcales-Tissierellales	Anaerovoracaceae	*Anaerovorax*	0.000806
Bacteria	Synergistota	Synergistia	Synergistales	Synergistaceae	*Synergistaceae (f)*	0.000786
Bacteria	Firmicutes	Clostridium	Oscillospirales	Butyricicoccaceae	*UCG-009*	0.00063
Bacteria	Firmicutes	Negativicutes	Veillonellales-Selenomonadales	Veillonellales-Selenomonadales (o)_1	*Veillonellales-Selenomonadales (o)_2*	0.000598
Bacteria	Synergistota	Synergistia	Synergistales	Synergistaceae	*Synergistaceae (f)*	0.000427
Bacteria	Firmicutes	Clostridium	Oscillospirales	Oscillospirales	*Hydrogenoanaerobacterium*	0.000399
Bacteria	Firmicutes	Clostridium	Clostridiales	(f) Caloramatoraceae	*Caloramatoraceae*	0.000396
Archaea	Euryarchaeota	Methanobacteria	Methanobacteriales	Methanobacteriaceae	*Methanobrevibacter*	0.000382
Bacteria	Proteobacteria	Gammaproteobacteria	Burkholderiales	Sutterellaceae	*Sutterella*	0.000371
Bacteria	Actinobacteriota	Coriobacteriia	Coriobacteriales	(o) Coriobacteriales	*Coriobacteriales (f)*	0.000357
Bacteria	Actinobacteriota	Actinobacteria	Propionibacteriales	Propionibacteriaceae	*Cutibacterium*	0.000344
Bacteria	Firmicutes	Bacilli	Bacillales	Planococcaceae	*Planococcaceae (f)*	0.000284
Bacteria	Actinobacteriota	Actinobacteria	Actinomycetales	Actinomycetaceae	*Actinomyces*	0.00027
Bacteria	Spirochaetota	Spirochaetia	Spirochaetales	Spirochaetaceae	*Spirochaetaceae (f)*	0.000269
Bacteria	Firmicutes	Clostridium	Oscillospirales	Oscillospiraceae	*Oscillospiraceae (f)*	0.000257
Bacteria	Firmicutes	Clostridium	Clostridia	Gracilibacteraceae	*Lutispora*	0.000256
Bacteria	Proteobacteria	Gammaproteobacteria	Enterobacterales	Morganellaceae	*Proteus*	0.000247

Bacteria	Bacteroidota	Bacteroidia	Bacteroidales	Dysgonomonadaceae	*Dysgonomonadaceae (f)*	0.000244
Bacteria	Firmicutes	Clostridium	Lachnospirales	Lachnospiraceae	*Lachnospiraceae_UCG-010*	0.000233
Bacteria	Firmicutes	Clostridium	Clostridia	Hungateiclostridiaceae	*Hungateiclostridiaceae (f)*	0.000226
Bacteria	Firmicutes	Clostridium	Oscillospirales	UCG-010	*UCG-010*	0.000223
Bacteria	Firmicutes	Clostridium	Clostridiales	Clostridiaceae	*Clostridium_sensu_stricto_14*	0.00021
Bacteria	Firmicutes	Syntrophomonadia	Syntrophomonadales	Syntrophomonadaceae	*Syntrophomonas*	0.000204
Bacteria	Firmicutes	Clostridium	Oscillospirales	Ruminococcaceae	*Incertae_Sedis*	0.000184
Bacteria	Proteobacteria	Gammaproteobacteria	Enterobacterales	Enterobacteriaceae	*Escherichia-Shigella*	0.000182
Bacteria	Firmicutes	Firmicutes (p)	Firmicutes (p)	Firmicutes (p)	*Firmicutes (p)*	0.000175
Bacteria	Firmicutes	Bacilli	Izemoplasmatales	Izemoplasmatales	*Izemoplasmatales*	0.000155
Bacteria	Proteobacteria	Alphaproteobacteria	Acetobacterales	Acetobacteraceae	*Acetobacter*	0.000129
Bacteria	Proteobacteria	Gammaproteobacteria	Pseudomonadales	Pseudomonadaceae	*Pseudomonas*	0.000116
Bacteria	Firmicutes	Clostridium	Oscillospirales	Ethanoligenenaceae	*Ethanoligenenaceae (f)*	9.52E-05
Bacteria	Firmicutes	Clostridium	Lachnospirales	Lachnospiraceae	*Tuzzerella*	7.59E-05
Bacteria	Firmicutes	Clostridium	Christensenellales	Christensenellaceae	*Christensenellaceae_R-7_group*	7.59E-05
Bacteria	Firmicutes	Bacilli	Bacillales	(o) Bacillales	*Bacillales (o)*	5.86E-05
Bacteria	Firmicutes	Clostridium	Oscillospirales	Ruminococcaceae	*CAG-352*	5.59E-05
Bacteria	Firmicutes	Clostridium	Clostridiales	Clostridiaceae	*Clostridium_sensu_stricto_1*	5.45E-05
Bacteria	Actinobacteriota	Coriobacteriia	Coriobacteriales	Atopobiaceae	*Olsenella*	5.11E-05
Bacteria	Firmicutes	Clostridium	Lachnospirales	Lachnospiraceae	*Anaerocolumna*	4.76E-05
Bacteria	Proteobacteria	Gammaproteobacteria	Xanthomonadales	Xanthomonadaceae	*Stenotrophomonas*	4.42E-05
Bacteria	Firmicutes	Clostridium	Clostridiales	Clostridiaceae	*Haloimpatiens*	4.14E-05
Bacteria	Firmicutes	Clostridium	Peptostreptococcales-Tissierellales	Peptostreptococcaceae	*Paraclostridium*	3.93E-05
Bacteria	Firmicutes	Clostridium	Clostridia	Hungateiclostridiaceae	*Ruminiclostridium*	3.52E-05
Bacteria	Bacteroidota	Bacteroidia	Bacteroidales	(o) Bacteroidales	*Bacteroidales (o)*	3.38E-05
Bacteria	Actinobacteriota	Actinobacteria	Coriobacteriales	Corynebacteriaceae	*Corynebacterium*	2.69E-05
Bacteria	Firmicutes	Bacilli	Bacillales	Planococcaceae	*Rummeliibacillus*	2.48E-05
Bacteria	Proteobacteria	Gammaproteobacteria	Enterobacterales	Erwiniaceae	*Pantoea*	2.07E-05

Bacteria	Firmicutes	Clostridium	Peptococcales	Peptococcaceae	*Peptococcaceae (f)*	1.93E-05
Bacteria	Firmicutes	Bacilli	Bacillales	Sporolactobacillaceae	*Sporolactobacillus*	1.79E-05
Bacteria	Bacteroidota	Bacteroidia	Bacteroidales	Prevotellaceae	*Prevotellaceae (f)*	1.79E-05
Bacteria	Firmicutes	Clostridium	Peptostreptococcales-Tissierellales	Peptostreptococcales-Tissierellales	*Sporanaerobacter*	1.66E-05
Bacteria	Bacteroidota	Bacteroidia	Bacteroidales	Dysgonomonadaceae	*Dysgonomonas*	1.52E-05
Bacteria	Firmicutes	Clostridium	Lachnospirales	Lachnospiraceae	*Lachnospiraceae_NK4A136_group*	1.45E-05
Bacteria	Firmicutes	Clostridium	Clostridiales	Clostridiaceae	*Clostridium_sensu_stricto_13*	1.45E-05
Bacteria	Firmicutes	Clostridium	Lachnospirales	Lachnospiraceae	*Lachnoclostridium*	1.45E-05
Bacteria	Bacteroidota	Bacteroidia	Bacteroidales	Dysgonomonadaceae	*Petrimonas*	1.17E-05
Bacteria	Firmicutes	Clostridium	Christensenellales	Christensenellaceae	*Christensenellaceae (f)*	1.17E-05
Bacteria	Bacteroidota	Bacteroidia	Bacteroidales	Muribaculaceae	*Muribaculaceae*	8.28E-06
Bacteria	Firmicutes	Negativicutes	Veillonellales-Selenomonadales	Sporomusaceae	*Acetonema*	7.59E-06
Bacteria	Firmicutes	Negativicutes	Acidaminococcales	Acidaminococcaceae	*Acidaminococcaceae (f)*	6.9E-06
Bacteria	Firmicutes	Clostridium	Christensenellales	Christensenellaceae	*Christensenellaceae (f)*	6.21E-06
Bacteria	Firmicutes	Clostridium	Peptostreptococcales-Tissierellales	Sedimentibacteraceae	*Sedimentibacter*	6.21E-06
Bacteria	Firmicutes	Bacilli	Brevibacillales (o)	Brevibacillales (o)	*Brevibacillales (o)*	6.21E-06
Bacteria	Firmicutes	Clostridium	Clostridiales	Clostridiaceae	*Clostridiaceae (f)*	5.52E-06
Bacteria	Firmicutes	Clostridium	Peptostreptococcales-Tissierellales	Peptostreptococcaceae	*Terrisporobacter*	5.52E-06
Bacteria	Firmicutes	Desulfitobacteriia	Desulfitobacteriales	Desulfitobacteriaceae	*Desulfosporosinus*	5.52E-06
Bacteria	Actinobacteriota	Actinobacteriota (p)	Actinobacteriota (p)	Actinobacteriota (p)	*Actinobacteriota (p)*	4.83E-06
Bacteria	Firmicutes	Clostridium	Eubacteriales	Eubacteriaceae	*Eubacteriaceae (f)*	4.14E-06
Bacteria	Actinobacteriota	Actinobacteria	Bifidobacteriales	Bifidobacteriaceae	*Bifidobacterium*	3.45E-06
Bacteria	Firmicutes	Clostridium	Clostridiales	Clostridiales (o)	*Clostridiales (o)*	3.45E-06
Bacteria	Actinobacteriota	Coriobacteriia	Coriobacteriales	Coriobacteriales (o)	*Coriobacteriales (o)*	2.76E-06
Bacteria	Proteobacteria	Gammaproteobacteria	Burkholderiales	Burkholderiales (o)	*Burkholderiales (o)*	2.07E-06
Bacteria	Firmicutes	Clostridium	Peptostreptococcales-Tissierellales	Peptostreptococcales-Tissierellales	*Tissierella*	1.38E-06

Bacteria	Actinobacteriota	Actinobacteria	Bifidobacteriales	Bifidobacteriaceae	*Bifidobacteriaceae (f)*	1.38E-06
Bacteria	Desulfobacterota	Desulfovibrionia	Desulfitobacteriales	Desulfovibrionaceae	*Desulfovibrionaceae (f)*	1.38E-06
Bacteria	Firmicutes	Desulfitobacteriia	Desulfitobacteriales	Desulfitobacteriaceae	*Desulfitobacteriaceae (f)*	1.38E-06
Bacteria	Firmicutes	Negativicutes	Acidaminococcales	Acidaminococcaceae	*Phascolarctobacterium*	1.38E-06
Bacteria	Actinobacteriota	Coriobacteriia	Coriobacteriales	Atopobiaceae	*Coriobacteriaceae_UCG-002*	1.38E-06

Table S4.6 The relative abundance of the genus in each experimental group in R1

	E_L_ratio						Collapse	Recovery	Operating temperature (ºC)								
	1:1	2:1	2:1 (steady state)	3:1	3:1 (steady state)	1:1 (after 3:1)			25	25 (steady state)	30	37	37 (steady state)	42	42 (steady state)	30	30 (steady state)
Sphaerochaeta	0.30368±0.03207	0.269683±0.027439	0.27±0.03	0.266161±0.013527	0.348028±0.027508	0.368128±0.053639	0.37059±0.044141	0.329101±0.03701	0.320231	0.398283±0.021793	0.371374±0.010538	0.403525	0.38094±0.017544	0.360999	0.426525±0.016439	0.435743±0.015176	0.399261±0.023066
Ruminococcaceae (f)	0.141873±0.035615	0.187615±0.01696	0.19±0.02	0.143932±0.006448	0.094372±0.001207	0.037914±0.032744	0.018835±0.003882	0.023444±0.010172	0.016879	0.084642±0.02027	0.112713±0.02063	0.065156	0.109829±0.008033	0.127966	0.165573±0.019562	0.168349±0.020246	0.113297±0.021189
Oscillibacter	0.056751±0.01061	0.080691±0.018791	0.08±0.02	0.263817±0.029483	0.036328±0.021929	0.022859±0.009356	0.046573±0.016541	0.048136±0.02276	0.075189	0.086711±0.019259	0.110302±0.016484	0.098626	0.028498±0.005708	0.02922	0.015959±0.005829	0.045619±0.018046	0.144529±0.034223
Propionibacterium	0.029687±0.00306	0.045534±0.020484	0.01±0	0.049539±0.023935	0.016701±0.000243	0.049454±0.0312	0.053578±0.018235	0.019485±0.003061	0.027266	0.054405±0.007748	0.033754±0.014362	0.037562	0.00783±0.008902	0.01046 5	0.003673±0.002852	0.007003±0.002838	0.007106±0.004439
Rikenellaceae_RC9_gut_group	0.011094±0.004271	0.011428±0.005353	0.05±0.02	0.008844±0.004349	0.009785±0.002663	0.036287±0.009629	0.058464±0.039003	0.116904±0.009646	0.102691	0.071341±0.024029	0.042322±0.003704	0.033575	0.04689±0.006725	0.04116 36	0.004869±0.005305	0.005173±0.003897	0.008532±0.002854
Lactobacillus	0.050169±0.018023	0.052099±0.017953	0.01±0	0.020245±0.003534	0.002378±0.003364	0.015522±0.006224	0.029443±0.005378	0.022306±0.00321	0.026794	0.018282±0.004864	0.014137±0.007897	0.011331	0.02156±0.011663	0.01119 1	0.008343±0.001473	0.011755±0.000521	0.015725±0.003826
Caproiciproducens	0.046125±0.005608	0.039161±0.009206	0.01±0.01	0.034202±0.004318	0.037015±0.001597	0.027116±0.008669	0.018797±0.002597	0.017607±0.007559	0.022309	0.021954±0.006404	0.039832±0.006537	0.031057	0.03028±0.012964	0.03543 7	0.035561±0.004987	0.032838±0.008128	0.026031±0.006053
Clostridia_UCG-014	0.033429±0.019	0.006504±0.003	0.02±0	0.000897±0.001	0.006376±0.000	0.015226±0.0142	0.001852±0.002	0.012298±0.004	0.00095	0.035004±0.013	0.031764±0.0157	0.00543	0.04191±0.009	0.00256	0.002786±0.002	0.0285±0.01432	0.066425±0.007

	434	144		037	005	28	371	372	61	972	76	49	501	97	188	5	954
Bacteroides	0.02251 3±0.003 574	0.01588 6±0.008 183	0.05 ±0.0 2	0.01474 4±0.000 627	0.07624 4±0.004 378	0.05663 7±0.026 447	0.05015 4±0.016 016	0.04473 6±0.015 234	0.0 413 13	0.02078 9±0.003 542	0.02831 7±0.013 623	0.0 240 27	0.01902 8±0.003 128	0.0 228 99	0.00429 2±0.004 065	0.00695 1±0.002 166	0.00638 7±0.002 157
Oscillospiraceae (f)	0.02994 ±0.0115 13	0.05895 7±0.005 84	0±0	0.02299 8±0.001 874	0.02939 6±0.009 072	0.02667 6±0.006 397	0.01356 1±0.006 467	0.02430 1±0.006 886	0.0 218 37	0.01825 2±0.004 844	0.03468 2±0.009 481	0.0 386 11	0.01756 9±0.008 94	0.0 170 97	0.00515 4±0.003 004	0.0235± 0.01314 7	0.05077 ±0.0045 09
Veillonellales-Selenomonadales (o)_3	0.00512 8±0.003 196	0.00395 2±0.002 733	0.02 ±0.0 1	0.00088 2±0.001 765	0	0.03535 8±0.048 129	0.07502 8±0.023 936	0.03471 2±0.012 137	0.0 225 45	0.01495 4±0.005 785	0.01664 6±0.003 69	0.0 160 53	0.00263 5±0.005 27	0.0 096 36	0.00472 5±0.003 214	0.00222 9±0.002 605	0.00101 7±0.001 532
Methanobacterium	0.01568 ±0.0043 56	0.01717 8±0.006 285	0.02 ±0.0 1	0.01493 9±0.005 32	0.02314 8±0.007 351	0.02146 ±0.0059 24	0.01958 5±0.001 454	0.01955 5±0.006 383	0.0 179 41	0.00764 2±0.003 887	0.00906 2±0.004 525	0.0 119 61	0.01962 9±0.002 112	0.0 281 84	0.05064 7±0.009 285	0.04537 2±0.020 191	0.02047 1±0.005 508
Prevotella	0.02218 ±0.0021 62	0.02166 9±0.003 69	0±0	0.01413 1±0.004 319	0.01648 9±0.007 017	0.00873 5±0.001 034	0.00279 3±0.002 227	0.01564 2±0.005 47	0.0 153 45	0.01268 1±0.003 504	0.01329 1±0.002 753	0.0 118 56	0.01420 9±0.005 227	0.0 105 69	0.00231 2±0.002 698	0.03384 ±0.0081 41	0.00969 3±0.002 637
Clostridium_sensu_stricto_12	0.03272 4±0.004 463	0.02630 3±0.003 051	0.03 ±0	0.01694 6±0.002 687	0.01396 5±0.001 193	0.00916 5±0.005 207	0.01131 6±0.003 06	0.00075 9±0.000 658	0.0 017 71	0	0.00531 7±0.001 312	0.0 088 13	0.01157 8±0.004 89	0.0 161 64	0.00293 4±0.002 034	0.01085 1±0.007 721	0.01680 7±0.002 989
Desulfitobacterium	0.01085 1±0.004 499	0.01169 1±0.009 041	0.01 ±0.0 1	0.00135 5±0.001 906	0.02151 5±0.011 459	0.02554 4±0.001 525	0.01754 2±0.006 649	0.02251 5±0.005 32	0.0 192 4	0.01296 ±0.0063 84	0.02500 1±0.001 036	0.0 171 02	0.04366 1±0.008 983	0.0 335 72	0.02896 1±0.016 014	0.01507 7±0.008 8	0.00314 1±0.001 934
Negativicutes (c)	0.02945 2±0.003 132	0.00912 4±0.005 502	0.04 ±0.0 1	0.00051 6±0.001 032	0.00188 5±0.002 665	0.00592 1±0.000 418	0.00189 2±0.002 956	0.01032 8±0.000 261	0.0 057 84	0.00436 7±0.003 104	0.00700 7±0.004 305	0.0 156 33	0.04316 4±0.004 311	0.0 369 91	0.08615 6±0.018 884	0.02002 ±0.0174 29	0.00564 9±0.003 377
Colidextribacter	0.00381 5±0.003 599	0.00534 6±0.001 172	0.02 ±0.0 1	0.00379 5±0.001 776	0.04027 2±0.020 145	0.02620 3±0.005 881	0.02543 3±0.007 659	0.02267 2±0.006 77	0.0 166 43	0.01299 1±0.002 63	0.00983 2±0.002 353	0.0 084 99	0.00131 7±0.002 635	0	0	0.00356 8±0.002 171	0.00397 7±0.001 599
Pseudoramibacter	0.03199 7±0.008 783	0.00178 7±0.002 753	0.01 ±0.0 1	0	0.00108 7±0.001 538	0.00184 5±0.002 308	0.01057 7±0.001 869	0.03608 3±0.023 783	0.0 567 75	0.01032 7±0.008 214	0	0	0.00909 6±0.006 422	0.0 124 34	0.00627 4±0.000 735	0.00038 4±0.000 642	0
Lachnospiraceae (f)	0.02056 6±0.005 483	0.02069 ±0.0073 75	0±0	0.01422 9±0.006 611	0.01677 ±0.0011 61	0.01429 7±0.001 537	0.01595 4±0.004 373	0.01922 6±0.010 225	0.0 060 2	0.00610 2±0.002 062	0.00632 7±0.000 779	0	0.00740 1±0.003 153	0.0 041 45	0.00083 6±0.001 155	0.00536 2±0.002 729	0.00658 9±0.005 888
NK4A214_group	0.00527 2±0.001 04	0.00684 4±0.002 048	0.06 ±0.0 1	0.00354 7±0.002 398	0.01644 7±0.005 933	0.01643 7±0.001 387	0.01332 4±0.002 53	0.01871 3±0.001 579	0.0 188 86	0.01636 1±0.009 767	0.00316 8±0.004 348	0.0 086 04	0.02254 9±0.004 936	0.0 195 83	0.00938 4±0.005 822	0.00785 9±0.002 142	0.00625 2±0.004 972
Parabacteroides	0.01656 2±0.005 939	0.00481 1±0.003 012	0±0	0.00167 ±0.0019 81	0.02028 8±0.001 01	0.02155 1±0.005 827	0.01813 3±0.004 508	0.01315 2±0.002 813	0.0 152 27	0.00677 8±0.001 025	0.00363 6±0.000 274	0.0 038 82	0.00532 4±0.000 818	0.0 066 31	0.00114 8±0.001 502	0.00124 7±0.001 706	0.00636 9±0.004 433
UCG-002	0.00477 5±0.008 27	0	0.01 ±0	0	0	0.00217 ±0.0022 61	0.00736 7±0.005 285	0.01056 2±0.009 525	0.0 155 81	0.01656 4±0.003 48	0.01274 9±0.008 786	0.0 032 53	0.01182 1±0.002 571	0.0 148 17	0	0.00004 4±0.000 087	0

Incertae_Sedis	0.002111±0.003656	0.008665±0.001886	0±0	0.010007±0.002111	0.011785±0.000468	0.007356±0.003721	0.000409±0.000817	0.001805±0.001609	0	0.003597±0.001193	0.00393±0.004029	0.009548	0.015323±0.000721	0.0974	0.018629±0.006186	0.012651±0.004411	0.021745±0.002762
Peptostreptococcales-Tissierellales	0.004619±0.001138	0.004545±0.003537	0.01±0	0.003182±0.001079	0.004101±0.001992	0.005347±0.004612	0.014085±0.003 33	0.007107±0.007331	0.010741	0.004837±0.000732	0.011066±0.005049	0.010702	0.011425±0.003159	0.012538	0.016883±0.008946	0.009698±0.000847	0.007903±0.001528
Eubacteriaceae (f)	0	0	0±0	0	0	0	0.000381±0.000762	0.015567±0.012092	0.022899	0.006995±0.006759	0.006298±0.006671	0.012381	0.004113±0.004883	0.007978	0.003104±0.004557	0	0
Pseudoclavibacter	0.006921±0.003535	0.007815±0.001864	0±0	0.010407±0.006688	0.019015±0.000024	0.010202±0.009366	0.006747±0.001673	0.002739±0.002374	0.003187	0.002049±0.002468	0.003025±0.002762	0	0.004045±0.000825	0.007357	0.006312±0.002309	0.004554±0.001281	0.008029±0.001736
Oscillospirales (o)	0.004128±0.001167	0.004355±0.003915	0.01±0	0.012539±0.002 32	0.005075±0.007177	0.006808±0.006922	0.000947±0.001473	0.000083±0.000145	0.000236	0.001695±0.001952	0	0.003882	0.006621±0.002311	0.005181	0.008001±0.003159	0.009912±0.006024	0.006695±0.001624
[Eubacterium]_no datum_group	0.014324±0.012048	0.000474±0.000045	0±0	0.000112±0.000221	0.001414±0.001999	0	0	0.000285±0.000485	0	0	0	0	0.008732±0.006856	0.020827	0.015557±0.006244	0.012727±0.006992	0
Enterorhabdus	0.004609±0.000971	0.006254±0.0044 1	0±0	0.004982±0.000713	0.0095±0.001123	0.007138±0.002787	0.004567±0.003 15	0.007095±0.001968	0.004367	0.004492±0.001988	0.003107±0.002709	0	0.002067±0.001466	0.002798	0.000487±0.000975	0.000723±0.000915	0.004477±0.003283
Anaerofilum	0.005399±0.000725	0.002561±0.001599	0±0	0.000753±0.000895	0.006934±0.004162	0.008015±0.003021	0.007344±0.004924	0.006649±0.002692	0.009207	0.005251±0.003561	0.002908±0.003783	0.005561	0.002799±0.004435	0	0	0	0.000289±0.000646
Dialister	0.000992±0.000859	0.003495±0.001214	0.01±0	0.003022±0.000911	0.005974±0.000066	0.004767±0.000507	0.008585±0.002 73	0.002541±0.002235	0.003423	0.003245±0.000209	0.003283±0.000928	0.002623	0.001232±0.001427	0.003212	0.002014±0.001141	0.001995±0.000867	0.000479±0.000518
Coriobacteriales (f)	0	0	0±0	0.000233±0.000467	0.008932±0.009453	0.022297±0.011135	0.009971±0.002564	0.010108±0.004293	0.0072	0.002727±0.000318	0	0.001574	0.002386±0.001779	0	0	0.000087±0.000174	0.000088±0.000196
Proteiniphilum	0.000293±0.000507	0.000935±0.001331	0±0	0.001067±0.000746	0.004595±0.001372	0.002002±0.003468	0.002427±0.001725	0.001821±0.001 25	0.001298	0.000879±0.001016	0.002969±0.002656	0.004931	0.003768±0.002049	0.003419	0.011836±0.006897	0.009745±0.005013	0.001521±0.001131
UCG-004	0.002406±0.002383	0.002008±0.002976	0±0	0.001479±0.000523	0.012966±0.000702	0.005287±0.001815	0.001709±0.000877	0.005001±0.001338	0.013574	0.008927±0.001398	0.003972±0.002454	0.005456	0.004039±0.002211	0.006113	0.001371±0.002742	0.001148±0.001 34	0.004491±0.001481
Enterococcus	0	0.018061±0.015766	0±0.01	0.014201±0.003817	0.007544±0.001135	0.005664±0.005 73	0.008891±0.009016	0.006755±0.011509	0	0	0	0	0	0	0	0	0
Propionicicella	0	0.000851±0.001903	0±0	0	0.002064±0.002919	0.009866±0.004513	0.003109±0.002554	0.002611±0.002359	0.004013	0.000427±0.000854	0	0.005141	0.001282±0.001481	0.0037	0.000254±0.000507	0.001967±0.002496	0.003831±0.000717
Caldanaerobius	0.000553±0.000	0.004955±0.005	0±0	0.004002±0.001	0.000898±0.001	0.000368±0.000	0	0.000081±0.0001	0	0.000071±0.000	0.000114±0.000	0	0.001239±0.000	0.0029	0.003156±0.001	0.001185±0.001	0.004458±0.003

	958	134		674	269	319		39		143	198		34	01	097	38	983
Sporomusaceae (f)	0.00501 1±0.001 329	0.00052 6±0.000 768	0±0	0.00043 9±0.000 878	0	0.00142 3±0.001 608	0.00003 1±0.000 063	0.00246 8±0.002 171	0.0 021 25	0.00053 4±0.001 068	0.00076 9±0.001 087	0.0 029 38	0.00652 8±0.001 544	0.0 087 04	0.01432 7±0.003 457	0.00392 5±0.001 881	0.00107 3±0.001 849
Lactococcus	0	0.00303 9±0.004 276	0±0	0.00563 6±0.000 85	0.01840 1±0.003 811	0.00757 9±0.007 988	0.00792 4±0.006 31	0.00456 1±0.007 899	0	0	0	0	0	0	0	0	0
Mogibacterium	0.00091 ±0.0007 88	0.00169 1±0.000 887	0.02 ±0.0 2	0.00113 2±0.001 338	0.00382 7±0.001 823	0.00380 6±0.001 612	0.00278 6±0.000 812	0.00174 ±0.0015 58	0.0 024 79	0.00158 4±0.001 082	0.00196 1±0.001 185	0	0.00145 5±0.001 128	0.0 017 61	0	0.00054 9±0.000 749	0.00189 2±0.000 478
Desulfovibrio	0.00401 5±0.001 485	0.00493 4±0.002 295	0±0	0.00066 3±0.000 459	0.00072 5±0.001 025	0.00185 ±0.0006 18	0.00210 7±0.000 757	0.00125 1±0.001 626	0.0 034 23	0.00143 1±0.001 059	0.00192 7±0.001 048	0.0 027 28	0.00234 3±0.000 251	0.0 017 61	0.00155 ±0.0012 16	0.0004± 0.00056 8	0.00102 9±0.000 99
Syntrophomonadaceae (f)	0.00314 7±0.001 198	0.00280 3±0.002 347	0±0	0.00132 3±0.000 959	0.00116 ±0.0016 4	0.00228 9±0.000 417	0.00371 9±0.001 935	0.00714 9±0.002 437	0.0 037 77	0.00214 3±0.000 466	0.00311 4±0.002 75	0.0 045 12	0.00555 5±0.001 051	0.0 065 28	0.00825 2±0.005 196	0.00184 1±0.001 783	0.00148 1±0.001 057
Atopobiaceae (f)	0.00176 8±0.000 847	0.00408 1±0.003 031	0±0	0.00415 6±0.001 714	0.00163 3±0.000 151	0.00062 7±0.001 086	0.00087 7±0.001 057	0	0	0	0	0	0	0.0 003 11	0.00084 3±0.000 375	0.00022 8±0.000 457	0.00207 4±0.001 571
Ruminococcaceae (f) _2	0.00454 2±0.001 955	0.00202 ±0.0013 39	0±0	0	0.00332 1±0.004 696	0.00116 4±0.000 329	0.00259 6±0.002 032	0.00238 3±0.001 605	0.0 003 54	0	0.00054 1±0.000 662	0	0.00087 ±0.0011 79	0	0.00094 3±0.001 246	0.00129 4±0.002 112	0.00005 4±0.000 12
Clostridia_vadinBB60_group	0.00074 1±0.000 736	0.00251 4±0.001 796	0±0	0.00290 7±0.000 54	0.00085 3±0.001 206	0.00094 6±0.000 134	0	0.00109 2±0.001 143	0.0 002 36	0.00234 4±0.001 087	0.00038 1±0.000 661	0	0.00025 5±0.000 414	0	0.00012 5±0.000 249	0.00214 ±0.0008 09	0.00303 ±0.0021 56
Methanosphaera	0.00075 2±0.001 303	0.00082 6±0.001 193	0±0	0.00188 8±0.001 411	0.00047 1±0.000 666	0.00033 8±0.000 585	0	0	0	0	0.00032 8±0.000 568	0	0.00126 9±0.001 476	0	0.00031 7±0.000 635	0	0
Syntrophomonadaceae (f)	0.00065 4±0.001 133	0.00406 3±0.001 349	0±0	0.00130 1±0.000 363	0.00178 6±0.000 242	0.00036 7±0.000 636	0	0	0	0.00040 4±0.000 809	0.00134 2±0.002 324	0.0 033 57	0.00226 5±0.000 595	0.0 016 58	0.00069 4±0.000 826	0.00074 9±0.000 501	0.00090 8±0.000 897
Bacteria (d)	0.00032 5±0.000 178	0.00017 1±0.000 302	0±0	0.00062 ±0.0005 22	0.00013 5±0.000 19	0.00110 4±0.000 643	0.00054 8±0.000 429	0.00114 7±0.000 714	0.0 014 16	0.00009 5±0.000 19	0.00071 6±0.000 232	0	0.00020 4±0.000 239	0.0 009 33	0.00201 4±0.001 598	0.00080 3±0.000 908	0.00019 7±0.000 343
Anaerovoracaceae (f)	0.00017 6±0.000 305	0.00036 7±0.000 552	0±0	0.00068 4±0.000 886	0.00047 1±0.000 666	0.00189 8±0.001 918	0	0.00171 6±0.000 659	0	0.00222 4±0.000 855	0.00195 9±0.000 923	0.0 024 13	0.00160 8±0.000 308	0.0 021 76	0.00034 5±0.000 411	0.00003 3±0.000 066	0.00046 7±0.000 297
Clostridia (c)	0.00207 5±0.002 11	0.00044 2±0.000 547	0±0	0.00017 9±0.000 217	0.00123 9±0.001 548	0.00213 2±0.001 052	0.00093 5±0.001 164	0.00053 4±0.000 504	0.0 008 26	0.00025 ±0.0002 89	0.00195 2±0.001 897	0.0 047 21	0.00158 4±0.002 187	0.0 006 22	0.00163 6±0.001 395	0.00049 3±0.000 512	0.00345 5±0.001 328
[Eubacterium]_coprostanoligenes_group	0	0	0±0	0	0.00556 5±0.007 869	0.00160 3±0.002 442	0.00011 ±0.0002 2	0.00181 5±0.001 033	0	0.00298 6±0.001 725	0.00437 5±0.001 258	0.0 031 48	0	0	0.00004 2±0.000 083	0.00294 1±0.003 396	0.00017 4±0.000 244

RF39	0	0.00010 8±0.000 243	0±0	0.00175 ±0.0018 8	0.00884 6±0.002 975	0.00846 3±0.006 876	0.00372 ±0.0026 82	0.00222 2±0.002 283	0.0 025 97	0.00039 2±0.000 463	0	0	0	0	0	0	0
Eggerthellaceae (f)	0	0	0±0	0	0.00552 ±0.0078 06	0.00299 1±0.005 181	0.00107 2±0.002 144	0	0	0	0	0.0 055 61	0	0	0	0	0
Tannerellaceae (f)	0.00066 2±0.000 378	0.00028 3±0.000 297	0±0	0.00009 2±0.000 184	0	0.00233 9±0.000 123	0.00554 6±0.004 276	0.00609 ±0.0011 95	0.0 106 23	0.00158 6±0.001 194	0.00071 ±0.0006 2	0.0 009 44	0.00057 4±0.000 732	0.0 014 51	0.00027 2±0.000 544	0	0.00014 7±0.000 217
Anaerovorax	0	0	0±0	0	0.00161 6±0.002 285	0.00429 6±0.001 035	0.00324 7±0.002 189	0.00248 1±0.002 236	0.0 070 82	0.00212 9±0.002 574	0	0	0	0	0	0	0
Synergistaceae (f)	0	0	0±0	0	0	0	0	0	0	0	0	0	0	0	0	0.00020 6±0.000 412	0.00012 4±0.000 277
UCG-009	0	0.00065 1±0.001 456	0±0	0	0.00314 ±0.0003 78	0.0031± 0.00164 1	0.00104 9±0.001 195	0.00216 9±0.002 512	0	0.00140 5±0.001 11	0.00093 5±0.000 588	0	0.00021 1±0.000 261	0	0	0	0
Veillonellales-Selenomonadales (o)_2	0.00076 6±0.000 283	0.00023 4±0.000 524	0±0	0	0	0	0	0.00066 8±0.001 157	0.0 002 36	0	0.00033 5±0.000 357	0	0.00215 2±0.000 337	0.0 012 43	0.00382 1±0.000 56	0.00060 9±0.000 936	0
Synergistaceae (f)	0.00016 4±0.000 283	0	0±0	0	0	0	0.00006 7±0.000 134	0.00081 7±0.000 708	0	0.00043 ±0.0004 99	0.00070 3±0.000 711	0.0 015 74	0.00311 8±0.000 748	0.0 056 99	0.00060 3±0.001	0.00032 2±0.000 234	0.00048 4±0.000 477
Hydrogenoanaerobacterium	0	0	0±0	0	0	0.00202 5±0.001 774	0.00086 8±0.001 02	0.00226 8±0.001 966	0.0 022 43	0.00139 6±0.000 971	0	0	0	0	0	0	0
Caloramatoraceae (f)	0	0	0±0	0.00005 5±0.000 11	0	0	0	0	0	0	0	0	0	0	0.00472 7±0.003 647	0.00296 2±0.002 498	0
Methanobrevibacter	0.00251 3±0.003 248	0.00079 7±0.001 295	0±0	0	0	0	0	0	0	0	0	0	0	0	0	0	0
Sutterella	0	0.00024 2±0.000 338	0±0	0	0.00018 1±0.000 256	0.00037 3±0.000 379	0	0	0	0	0	0	0.00019 2±0.000 384	0.0 007 25	0.00350 2±0.001 408	0.00202 6±0.002 154	0
Coriobacteriales (o)	0	0	0±0	0	0	0	0	0	0	0	0.00246 1±0.004 262	0	0	0	0	0	0.00006 6±0.000 147
Cutibacterium	0	0.00278 8±0.002 256	0±0	0.00302 7±0.002 681	0.00054 4±0.000 769	0	0	0	0	0	0	0	0	0	0	0	0
Planococcaceae (f)	0	0	0±0	0.00082 2±0.000	0	0	0	0	0	0	0.00007 9±0.000	0	0.0001± 0.0002	0	0.00013 6±0.000	0.00031 7±0.000	0

				604							137				272	634	
Actinomyces	0	0.00015 1±0.000 338	0±0	0.00272 3±0.001 572	0	0.00071 1±0.000 689	0.00133 2±0.000 861	0.00108 2±0.000 086	0	0.00029 4±0.000 343	0	0	0	0	0	0	0
Spirochaetaceae (f)	0	0	0±0	0.00045 8±0.000 915	0.00173 ±0.0020 65	0.00177 5±0.001 676	0	0.00008 3±0.000 145	0	0	0.00082 9±0.001 436	0	0.0005± 0.001	0.0 002 07	0.00004 2±0.000 083	0	0.00022 6±0.000 506
Oscillospiraceae (f)	0	0.00031 9±0.000 713	0±0	0.00005 5±0.000 11	0.00080 8±0.001 142	0	0.00050 7±0.000 593	0.00014 8±0.000 256	0.0 030 69	0	0.00022 9±0.000 396	0	0	0	0	0.00003 3±0.000 066	0.00002 2±0.000 049
Lutispora	0	0.00038 4±0.000 545	0±0	0	0	0	0	0.000111 ±0.0001 93	0	0.00016 ±0.0001 92	0.00027 8±0.000 252	0.0 011 54	0.00056 3±0.000 542	0	0.00022 1±0.000 268	0	0.00037 4±0.000 29
Proteus	0	0	0±0	0.00044 7±0.000 895	0.00257 9±0.000 161	0.00136 8±0.002 022	0.00156 1±0.001 852	0.00115 4±0.001 81	0	0	0	0	0	0	0	0	0
Dysgonomonadaceae (f)	0	0	0±0	0	0	0	0	0	0	0	0	0	0	0	0	0	0
Lachnospiraceae_ UCG-010	0.00004 2±0.000 072	0.00003 1±0.000 069	0±0	0	0	0.00023 7±0.000 411	0.00103 ±0.0002 1	0.00008 3±0.000 145	0.0 016 53	0.00032 9±0.000 38	0.00015 8±0.000 273	0.0 003 15	0.00016 7±0.000 253	0	0.00011 3±0.000 227	0	0.00001 8±0.000 04
Hungateiclostridiaceae (f)	0	0.00013 6±0.000 305	0±0	0	0.00025 4±0.000 359	0.00091 ±0.0009 3	0.00029 3±0.000 387	0	0.0 003 54	0	0	0	0.00107 6±0.001 249	0.0 040 41	0.00074 3±0.001 015	0.00020 9±0.000 272	0
UCG-010	0	0	0±0	0	0	0.00135 7±0.001 256	0.00062 9±0.000 538	0.00043 8±0.000 419	0	0.00052 8±0.000 649	0.00085 4±0.000 746	0.0 003 15	0.00005 7±0.000 115	0	0.00006 1±0.000 122	0	0
Clostridium_sensu_stricto_14	0	0.00061 3±0.001 129	0±0	0.00108 2±0.000 873	0.00105 1±0.001 487	0	0.00079 5±0.000 949	0.00076 ±0.0013 17	0	0	0	0	0	0	0	0	0
Syntrophomonas	0	0	0±0	0	0	0	0	0	0	0	0	0	0	0	0	0	0.00019 5±0.000 435
Incertae_Sedis	0	0.00023 5±0.000 479	0±0	0.00120 5±0.001 596	0	0.00155 6±0.001 595	0.00116 5±0.001 585	0	0	0	0	0	0	0	0	0	0
Escherichia-Shigella	0	0	0±0	0.00102 3±0.000 759	0	0.00038 6±0.000 669	0.00227 3±0.001 536	0	0	0	0	0	0	0	0	0	0
Firmicutes (p)	0	0.00084 2±0.001 151	0±0	0.00056 7±0.001 135	0	0	0.00044 4±0.000 307	0	0	0.00018 4±0.000 23	0	0	0	0	0.00030 3±0.000 5	0	0
Izemoplasmatales	0.00016	0	0±0	0	0	0.00038	0.00005	0	0.0	0	0	0.0	0.00027	0.0	0.00019	0	0.00030

	7±0.00029					2±0.000445	9±0.000118		01298			01049	1±0.000321	00933	3±0.000385		6±0.000322
Acetobacter	0.000566±0.000607	0.000127±0.000203	0±0	0	0	0	0	0	0	0	0	0	0	0	0	0	0
Pseudomonas	0.000251±0.000434	0	0±0	0.000073±0.000146	0.000544±0.000769	0.000498±0.000507	0.002369±0.001721	0.000139±0.000241	0	0	0	0	0	0	0	0	0
Ethanoligenenaceae (f)	0	0	0±0	0	0	0	0	0	0	0.000534±0.001068	0	0	0.00108±0.002161	0	0	0	0
Tuzzerella	0	0	0±0	0.001229±0.001604	0	0	0	0	0	0	0	0	0	0	0	0	0
Christensenellaceae_R-7_group	0	0.000102±0.000228	0±0	0	0	0	0	0	0	0	0.000568±0.000496	0	0	0	0	0	0.00006±0.000134
Bacillales (o)	0	0.00141±0.00163	0±0	0	0	0	0	0	0	0	0	0	0	0	0	0	0
CAG-352	0	0.000872±0.00195	0±0	0	0	0	0	0	0	0	0	0	0	0	0	0	0
Clostridium_sensu_stricto_1	0	0.00005±0.000113	0±0	0	0	0	0	0	0	0	0	0	0	0	0	0	0
Olsenella	0	0	0±0	0	0	0	0	0	0	0	0	0	0	0.00207	0	0.000111±0.000222	0
Anaerocolumna	0	0	0±0	0.000679±0.000812	0.000471±0.000666	0.000193±0.000334	0.000059±0.000118	0	0	0	0	0	0	0	0	0	0
Stenotrophomonas	0	0.00013±0.000291	0±0	0	0	0	0	0	0	0	0	0	0	0	0	0	0.000036±0.00008
Haloimpatiens	0	0	0±0	0	0	0	0	0	0	0	0	0	0	0	0	0	0
Paraclostridium	0	0	0±0	0.000198±0.000248	0	0	0.000207±0.000413	0.000505±0.000482	0	0	0.000229±0.000396	0	0.000033±0.000067	0	0.000034±0.000068	0	0.000036±0.00008
Ruminiclostridium	0	0	0±0	0	0.001346±0.001904	0	0	0	0	0	0	0	0	0	0	0	0
Bacteroidales (o)	0	0.00005	0±0	0	0	0	0	0.000111	0	0.00006	0.00023	0	0	0.0	0	0.00003	0

		2±0.000 117						±0.0001 92		5±0.000 13	7±0.000 41			002 07		8±0.000 076	
Corynebacterium	0	0	0±0	0	0	0	0	0	0	0	0	0	0	0.0 002 07	0	0	0
Rummeliibacillus	0	0	0±0	0	0.00079 7±0.001 128	0	0	0	0	0	0	0	0	0	0.00019 7±0.000 394	0	0
Pantoea	0	0	0±0	0	0.00117 4±0.000 391	0	0	0	0	0	0	0	0	0	0	0	0
Peptococcaceae (f)	0	0	0±0	0	0	0	0	0	0	0	0	0	0	0	0	0	0
Sporolactobacillus	0	0.00004 6±0.000 104	0±0	0	0	0.00007 9±0.000 137	0	0	0	0	0	0	0	0	0	0	0
Prevotellaceae (f)	0	0	0±0	0	0	0	0	0.00014 8±0.000 256	0	0	0	0	0	0	0	0	0
Sporanaerobacter	0	0	0±0	0	0	0	0	0	0	0	0	0	0	0	0	0	0
Dysgonomonas	0	0	0±0	0.00005 5±0.000 11	0	0	0	0	0	0	0	0	0	0	0	0	0
Lachnospiraceae_ NK4A136_group	0	0	0±0	0.00011 ±0.0002 2	0.00054 4±0.000 769	0	0	0	0	0	0	0	0	0	0	0	0
Clostridium_sensu _stricto_13	0	0	0±0	0	0	0	0	0	0	0	0	0	0	0	0	0.00006 6±0.000 132	0
Lachnoclostridium	0.00009 8±0.000 17	0	0±0	0	0	0	0.00006 7±0.000 134	0.00005 6±0.000 096	0	0	0	0	0	0	0	0	0
Petrimonas	0	0	0±0	0	0	0	0	0	0	0	0	0	0	0	0	0	0
Christensenellace ae (f)	0	0	0±0	0	0	0	0	0.00013 9±0.000 241	0	0	0	0	0.00011 2±0.000 224	0	0	0	0
Muribaculaceae	0	0	0±0	0	0	0.00009 6±0.000 167	0	0	0	0	0	0	0	0	0	0	0
Acetonema	0	0	0±0	0	0	0	0	0	0	0	0	0	0	0	0	0	0
Acidaminococcace ae (f)	0	0	0±0	0	0	0	0	0	0	0	0	0	0	0	0	0	0

Christensenellaceae (f)	0	0	0±0	0	0	0	0	0	0	0	0	0	0	0	0	0	0
Sedimentibacter	0	0	0±0	0	0	0	0	0	0	0	0.000131±0.000227	0	0	0	0	0	0
Brevibacillales (o)	0	0	0±0	0	0	0	0	0	0	0	0	0	0	0	0	0	0
Clostridiaceae (f)	0	0	0±0	0	0	0	0	0	0	0	0	0	0	0	0.000167±0.000333	0	0
Terrisporobacter	0	0	0±0	0	0	0	0	0	0	0	0	0	0	0	0	0	0
Desulfosporosinus	0	0	0±0	0	0	0	0.000045±0.00009	0	0	0	0	0	0	0	0.000042±0.000083	0	0
Actinobacteriota (p)	0	0	0±0	0	0	0	0	0	0	0	0	0	0	0	0	0	0
Eubacteriaceae (f)	0	0	0±0	0	0	0	0	0	0	0	0	0	0	0	0	0	0.000044±0.000098
Bifidobacterium	0	0	0±0	0	0	0	0	0	0	0	0	0	0	0	0	0	0
Clostridiales (o)	0	0	0±0	0	0	0.000048±0.000084	0	0	0	0	0	0	0	0	0	0.000044±0.000087	0
Coriobacteriales (o)	0	0	0±0	0	0	0	0	0	0	0	0	0	0	0	0	0	0
Burkholderiales (o)	0	0	0±0	0	0	0.000072±0.000125	0	0	0	0	0	0	0	0	0	0	0
Tissierella	0.00005±0.000087	0	0±0	0	0	0	0	0	0	0	0	0	0	0	0	0	0
Bifidobacteriaceae (f)	0	0	0±0	0.000052±0.000104	0	0	0	0	0	0	0	0	0	0	0	0	0
Desulfovibrionaceae (f)	0	0	0±0	0	0	0	0	0	0.000236	0	0	0	0	0	0	0	0
Desulfitobacteriaceae (f)	0	0	0±0	0	0	0	0	0	0	0	0	0	0.000045±0.000089	0	0	0	0
Phascolarctobacterium	0	0	0±0	0	0	0	0	0	0	0	0	0	0	0	0.000028±0.000056	0	0

Coriobacteriaceae_UCG-002	0	0	0±0	0	0	0	0	0	0	0	0	0	0	0	0	0
OTU taxonomy is given at the genus level unless the taxonomy assignment was not that specific (k: kingdom, p: phyla, c: class, o: order, f: family).																

Table S4.7 The average relative abundance of the genus in each experimental group in R2						
	Control of the E_L_ratio experiment	Collapse of extraction system	Recovery	Control of operating temperature experiment	Collapse of pH Sensor	Recovery
Sphaerochaeta	0.304604±0.024401	0.301802±0.050348	2064.740585±2518.708856	0.369454±0.048981	0.335949±0.019215	0.369732±0.051622
Ruminococcaceae (f)	0.120869±0.027425	0.075835±0.06716	457.927392±606.128654	0.077077±0.027989	0.113217±0.026214	0.038189±0.012143
Oscillibacter	0.052766±0.004843	0.05374±0.029189	273.250265±393.980274	0.090026±0.036521	0.152523±0.030962	0.069806±0.019771
Propionibacterium	0.025667±0.006401	0.01531±0.009068	152.567639±189.256784	0.057206±0.023266	0.019978±0.010202	0.063172±0.022473
Rikenellaceae_RC9_gut_group	0.007934±0.006995	0.01115±0.010564	90.230349±121.893579	0.065088±0.033334	0.014236±0.006193	0.048049±0.014505
Lactobacillus	0.073756±0.007154	0.061985±0.017864	93.567494±123.220392	0.023074±0.008755	0.016031±0.007459	0.018671±0.008056
Caproiciproducens	0.034608±0.010562	0.024498±0.017853	187.347984±225.092926	0.025079±0.007169	0.03175±0.01132	0.017976±0.008204
Clostridia_UCG-014	0.035751±0.022757	0.011176±0.012756	84.895862±123.381641	0.041289±0.013757	0.060082±0.006312	0.018766±0.011472
Bacteroides	0.020454±0.005051	0.058384±0.040451	210.135267±257.216722	0.016756±0.006928	0.01199±0.003961	0.022256±0.006583
Oscillospiraceae (f)	0.020663±0.003642	0.0068±0.004214	158.457232±190.997956	0.021273±0.005898	0.025566±0.008463	0.013717±0.009553
Veillonellales-Selenomonadales (o)_3	0.003336±0.003187	0.108641±0.09414	369.379623±501.065901	0.015543±0.007508	0.016211±0.005786	0.013496±0.008615
Methanobacterium	0.030068±0.005659	0.017304±0.00953	77.895649±105.448691	0.012663±0.003399	0.02685±0.005483	0.021632±0.005499
Prevotella	0.033568±0.009089	0.02984±0.027906	147.789653±182.926887	0.012108±0.003676	0.012831±0.005203	0.01134±0.005153
Clostridium_sensu_stricto_12	0.060043±0.021423	0.028158±0.018745	103.898519±126.175909	0.001312±0.001903	0.014592±0.004744	0.002067±0.003373
Desulfitobacterium	0.001665±0.002865	0.01307±0.015874	74.340935±88.717127	0.017561±0.007056	0.003432±0.00383	0.022273±0.008382
Negativicutes (c)	0.004226±0.004734	0.003337±0.003715	55.115706±67.803329	0.007518±0.004605	0.006858±0.003904	0.008206±0.006141
Colidextribacter	0.00152±0.002095	0.017185±0.010228	125.567302±171.853745	0.016683±0.006677	0.002998±0.001784	0.018832±0.00517
Pseudoramibacter	0.026366±0.015517	0.003507±0.004017	22.335092±30.723145	0.005648±0.006878	0.002021±0.001883	0.049313±0.02847
Lachnospiraceae (f)	0.026865±0.004227	0.009321±0.007136	59.338364±71.144771	0.007805±0.005254	0.004656±0.00595	0.007399±0.003423
NK4A214_group	0.006871±0.006114	0.012802±0.010854	86.785416±107.019639	0.008945±0.002632	0.004825±0.003785	0.01896±0.007562
Parabacteroides	0.016239±0.010653	0.019922±0.015914	31.669674±39.953545	0.007515±0.006115	0.003125±0.003261	0.011726±0.007153
UCG-002	0.000653±0.001075	0.011419±0.014725	52.783478±64.975131	0.014434±0.00546	0.00414±0.00614	0.019232±0.01066
Incertae_Sedis	0.006505±0.005355	0.008008±0.007477	16.779005±36.82931	0.00199±0.003033	0.013248±0.004438	0.005767±0.005196
Peptostreptococcales-Tissierellales	0.002214±0.001278	0.010321±0.010318	59.673114±84.884536	0.00645±0.003709	0.010135±0.002889	0.004571±0.003127
Eubacteriaceae (f)	0.000132±0.000324	0	113.452868±138.617739	0.008707±0.007012	0.019547±0.007462	0.029585±0.020363

Pseudoclavibacter	0.006804±0.00221	0.012042±0.006395	60.22769±87.965639	0.003226±0.002438	0.00194±0.00198	0.002157±0.0019
Oscillospirales (o)	0.004813±0.002701	0.0078±0.005405	55.115948±79.128133	0.003246±0.002977	0.004555±0.001379	0.004905±0.005118
[Eubacterium]_nodatum_group	0.023005±0.006419	0.00517±0.007876	1.4448±4.3332	0.001506±0.002364	0.001097±0.000734	0.004809±0.003824
Enterorhabdus	0.004706±0.002649	0.001425±0.001691	55.559914±74.853076	0.005615±0.002702	0.016115±0.001223	0.006723±0.005384
Anaerofilum	0.001445±0.001792	0.010867±0.005749	115.898304±146.068156	0.005209±0.003647	0.002449±0.001661	0.006307±0.002617
Dialister	0.002463±0.00145	0.003124±0.002144	31.336013±39.077629	0.006336±0.002863	0.00166±0.001021	0.007241±0.003831
Coriobacteriales (f)	0	0.004166±0.003302	115.675487±158.301784	0.005578±0.00635	0.002739±0.002627	0.00142±0.001918
Proteiniphilum	0.00088±0.000888	0.00328±0.002958	29.558066±38.831184	0.002996±0.002137	0.004318±0.00111	0.004746±0.002354
UCG-004	0.004209±0.001979	0.000799±0.001277	20.668631±26.365862	0.002387±0.003624	0.005951±0.004227	0.00143±0.001415
Enterococcus	0.004453±0.010908	0.000629±0.001208	44.0035±57.670647	0.000742±0.00269	0	0
Propionicicella	0	0.003676±0.00495	28.669415±41.588132	0.004801±0.006727	0.001353±0.001345	0.003578±0.003149
Caldanaerobius	0.006219±0.004146	0.007076±0.010771	24.335337±33.198499	0.000493±0.000782	0.005301±0.002991	0.0001±0.000361
Sporomusaceae (f)	0.000423±0.001036	0.000721±0.001225	12.889998±17.075683	0.001072±0.001148	0.000217±0.000485	0.000991±0.001317
Lactococcus	0	0	64.449016±87.657657	0.000708±0.002342	0	0.000161±0.000357
Mogibacterium	0.001728±0.001282	0.002557±0.001413	22.557594±30.383784	0.00201±0.000907	0.001606±0.000355	0.000814±0.000998
Desulfovibrio	0.001417±0.001236	0.002674±0.002107	11.890152±16.342501	0.000895±0.001094	0.000354±0.000485	0.002697±0.002009
Syntrophomonadaceae (f)	0.000385±0.000686	0.000165±0.000381	1.000079±2.99997	0.000081±0.000276	0.000522±0.000607	0
Atopobiaceae (f)	0.002207±0.001286	0.00234±0.002117	10.11208±16.795508	0.000818±0.000995	0.001385±0.001995	0.001134±0.001492
Ruminococcaceae (f) _2	0.002337±0.001935	0.003869±0.004088	15.890371±27.464671	0.000422±0.000816	0.000143±0.000216	0.003171±0.00455
Clostridia_vadinBB60_group	0.00103±0.000994	0.000161±0.000411	3.666959±7.77802	0.001835±0.001473	0.003785±0.000977	0.001054±0.001428
Methanosphaera	0.006401±0.002926	0.002079±0.002284	9.778516±15.270174	0.000273±0.000544	0.00235±0.001544	0.000632±0.001328
Syntrophomonadaceae (f)	0.000115±0.000282	0.000105±0.000223	3.444716±8.323201	0.002073±0.001785	0.002306±0.001666	0.002196±0.00162
Bacteria (d)	0.000352±0.000385	0.00078±0.000921	7.889525±15.019981	0.001281±0.000811	0.003334±0.001784	0.003314±0.001719
Anaerovoracaceae (f)	0.000463±0.000645	0.000306±0.000646	11.445285±14.950122	0.001972±0.001162	0.000615±0.000641	0.001095±0.001032
Clostridia (c)	0.000915±0.000683	0.000534±0.000759	5.44501±10.678055	0.000293±0.000328	0.001052±0.000995	0.000228±0.000321
[Eubacterium]_coprostanoligenes_group	0.000028±0.000069	0.000049±0.000155	19.77922±30.791724	0.00113±0.001251	0.000371±0.000828	0.000363±0.000712
RF39	0.000888±0.00102	0.000313±0.000575	6.333776±18.999834	0.000146±0.000318	0	0.00005±0.000181
Eggerthellaceae (f)	0.000769±0.001207	0.000346±0.00075	15.001067±30.756528	0.001294±0.003191	0.001956±0.002024	0.000881±0.002151

Tannerellaceae (f)	0.000346±0.000537	0.000042±0.000089	5.889354±10.203184	0.000795±0.001334	0.000225±0.000249	0.000214±0.000603
Anaerovorax	0	0.001939±0.003041	0.000059±0.000178	0.001267±0.001962	0	0.000113±0.000408
Synergistaceae (f)	0	0	2.555763±7.666589	0.001755±0.001231	0.000654±0.000616	0.004126±0.002593
UCG-009	0.00004±0.000099	0.000155±0.000374	2.778087±8.333218	0.000962±0.001122	0.000033±0.000075	0.000507±0.000689
Veillonellales-Selenomonadales (o)_2	0.000135±0.000331	0.00069±0.000919	5.556044±13.182249	0.00049±0.000836	0.000535±0.001103	0.000115±0.000413
Synergistaceae (f)	0.00004±0.000099	0.000027±0.000085	2.6669±5.385035	0.000323±0.000565	0.000181±0.000405	0.000729±0.001023
Hydrogenoanaerobacterium	0	0.00013±0.000411	1.555682±4.666619	0.000538±0.000782	0	0.000553±0.001417
Caloramatoraceae (f)	0	0	0	0	0	0.000013±0.000049
Methanobrevibacter	0.000681±0.000827	0.000205±0.000648	19.112699±30.430952	0.000103±0.000318	0	0.0001±0.000361
Sutterella	0.000194±0.000215	0.000125±0.000263	0.777904±1.715874	0	0	0
Coriobacteriales (o)	0	0.000124±0.000269	2.111354±4.371494	0.000842±0.001559	0.001091±0.001146	0.001128±0.002592
Cutibacterium	0	0	0	0	0	0
Planococcaceae (f)	0.000127±0.00031	0.002693±0.005912	0	0.000023±0.000097	0	0
Actinomyces	0.000076±0.00012	0.000341±0.000532	3.33366±6.90996	0.000016±0.000069	0	0
Spirochaetaceae (f)	0.000011±0.000027	0.000071±0.000225	5.000442±11.467128	0.000075±0.000227	0.000625±0.0006	0.000207±0.000439
Oscillospiraceae (f)	0.000167±0.000409	0.000419±0.00062	3.889231±7.720629	0.000302±0.000579	0.000115±0.000258	0.000084±0.000304
Lutispora	0	0	0	0.000258±0.000571	0	0.00128±0.000864
Proteus	0	0	9.778477±19.427534	0.000075±0.00032	0	0
Dysgonomonadaceae (f)	0	0	0	0.000242±0.000477	0.000447±0.000613	0.001623±0.001614
Lachnospiraceae_UCG-010	0	0.000507±0.000763	3.22252±9.666555	0.000344±0.000304	0.000069±0.000155	0.000183±0.000354
Hungateiclostridiaceae (f)	0.000091±0.000146	0.00001±0.000031	0.444476±1.333322	0.000081±0.000214	0.000419±0.00059	0.000127±0.00036
UCG-010	0	0.000038±0.000122	2.000136±4.092602	0.00038±0.000493	0	0.000081±0.000201
Clostridium_sensu_stricto_14	0.000153±0.000374	0	8.333911±13.619441	0	0	0
Syntrophomonas	0	0	0	0.000616±0.001092	0	0.000688±0.001353
Incertae_Sedis	0.00005±0.0001	0	8.556229±25.666414	0.000016±0.000054	0	0
Escherichia-Shigella	0.000104±0.000255	0	8.445003±19.020178	0	0	0
Firmicutes (p)	0.000061±0.000149	0.000475±0.000652	2.00013±5.999951	0.000175±0.000391	0	0.00015±0.000331
Izemoplasmatales	0	0	0	0.000062±0.000232	0.000812±0.000784	0.000336±0.00043

Acetobacter	0.000387±0.000449	0.00034±0.000625	0	0.000015±0.000048	0	0.000157±0.000386
Pseudomonas	0	0	0	0.000008±0.000036	0.000067±0.000149	0
Ethanoligenenaceae (f)	0	0	4.555851±13.666556	0	0	0.000071±0.000256
Tuzzerella	0	0	4.444738±10.3935	0	0	0
Christensenellaceae_R-7_group	0	0.000018±0.000056	0.00002±0.000059	0.00015±0.000319	0.000168±0.000258	0.000212±0.000604
Bacillales (o)	0	0	0	0.000018±0.000075	0	0
CAG-352	0.000033±0.000066	0.000088±0.000161	0.000025±0.000074	0	0	0
Clostridium_sensu_stricto_1	0.000457±0.00047	0.000071±0.000224	0	0	0	0
Olsenella	0.000434±0.000397	0.000049±0.000155	0	0	0.000078±0.000174	0
Anaerocolumna	0	0	1.000074±2.121281	0	0	0
Stenotrophomonas	0	0.000505±0.001141	0	0	0	0.00002±0.000073
Haloimpatiens	0.000274±0.000308	0	0.222237±0.666661	0	0	0
Paraclostridium	0	0	0	0.000038±0.00016	0	0
Ruminiclostridium	0	0.000085±0.000268	0.000094±0.000282	0	0	0.000017±0.000063
Bacteroidales (o)	0.000028±0.000069	0.000029±0.000091	0	0.000041±0.000111	0	0.000064±0.000176
Corynebacterium	0	0	0	0.00014±0.000273	0	0.000029±0.000103
Rummeliibacillus	0	0	0	0	0	0
Pantoea	0	0	0	0	0	0
Peptococcaceae (f)	0	0	0	0.000044±0.000186	0	0
Sporolactobacillus	0.000017±0.000042	0.000101±0.00032	0	0	0	0
Prevotellaceae (f)	0.00004±0.000099	0	0	0.000014±0.00004	0.000034±0.000076	0
Sporanaerobacter	0.000069±0.000169	0	0	0	0	0
Dysgonomonas	0.00004±0.000099	0.000036±0.000114	0	0	0	0
Lachnospiraceae_NK4A136_group	0	0	0	0	0	0
Clostridium_sensu_stricto_13	0.000066±0.000162	0	0	0	0.000083±0.000187	0
Lachnoclostridium	0.000026±0.000063	0	0	0.000007±0.00003	0	0.000036±0.000131
Petrimonas	0	0	0	0.00006±0.000255	0	0
Christensenellaceae (f)	0	0.000019±0.000061	0	0.000011±0.000048	0	0

Muribaculaceae	0.000024±0.000058	0.000036±0.000114	0	0	0	0
Acetonema	0	0	0	0	0.00005±0.000112	0.000045±0.000164
Acidaminococcaceae (f)	0	0	1.111201±3.3333	0	0	0
Christensenellaceae (f)	0	0.000031±0.000099	0.000035±0.000104	0	0	0.000019±0.000067
Sedimentibacter	0.000028±0.000069	0	0	0	0.000051±0.000114	0
Brevibacillales (o)	0	0	0	0.000021±0.000052	0	0
Clostridiaceae (f)	0	0	0	0	0	0
Terrisporobacter	0	0.000012±0.000039	0.333355±0.999992	0	0	0
Desulfosporosinus	0	0	0	0.000003±0.000011	0	0.000019±0.00007
Actinobacteriota (p)	0	0	0	0.000022±0.000091	0	0.000027±0.000097
Eubacteriaceae (f)	0	0	0	0	0	0
Bifidobacterium	0	0.000022±0.00007	0.000025±0.000074	0	0	0
Clostridiales (o)	0	0	0	0	0	0
Coriobacteriales (o)	0	0	0	0.000027±0.000113	0	0
Burkholderiales (o)	0	0	0	0	0	0
Tissierella	0	0	0	0	0	0
Bifidobacteriaceae (f)	0	0	0	0	0	0
Desulfovibrionaceae (f)	0	0	0	0	0	0
Desulfitobacteriaceae (f)	0	0	0	0	0	0
Phascolarctobacterium	0	0	0	0	0	0
Coriobacteriaceae_UCG-002	0	0.22224±0.66666	0	0	0	0
OTU taxonomy is given at the genus level unless the taxonomy assignment was not that specific (k: kingdom, p: phyla, c: class, o: order, f: family).						

Table S4.8 The average production rate and specificity (%) under different conditions			
	E_L_ratio of 1	Operating temperature of 37ºC	Operating temperature of 42ºC
Production rate (mmol C^{-1} L^{-1} d)	44.28±4.94	40.64±8.69	49.27±1.72
Specificity (%)	0.53±0.07	0.50±0.2	0.57±0.04

Table S4.9 Significance tests betwwen different microbial communities shaped by different environmental conditions for high *n*-caproate production			
	Cluster 1/Cluster 2	Cluster 1/Cluster 3	Cluster 2/Cluster 3
R^2	0.57	0.69	0.55
p-value	0.034	0.034	0.034
The permutation test (adonis) was performed on the basis of Bray–Curtis distance.			

Table S4.10 The characteristics of different microbial networks				
		Number of nodes	Number of edges	Clustering coefficient
For *n*-caprylate production		43	100	0.41
For *n*-caproate production	Network 1	41	288	0.67
	Network 2	42	135	0.61
	Network 3	46	193	0.69

Table S4.11 The average production rate and specificity under different conditions			
	E_L_ratio of 3	Operating temperatures of 25 ºC and 30ºC	A high E_L-ratio of 3 (after recovering from extraction system collapse)
Production rate (mmol C^{-1} L^{-1} d)	60.48±16.14	48.6±8.61	47.04±12.87
Specificity (%)	0.64±0.15	0.59±0.05	0.54±0.1

Table S4.12 Significance tests betwwen different microbial communities shaped by different environmental conditions for high *n*-caprylate production			
	Group a/Group b	Group a/Group c	Group b/Group c
r	0.67	0.076	-0.090
p-value	0.006	0.4545	0.767
The permutation test (anosim) was performed on the basis of Bray–Curtis distance.			

Table S4.13 The average *n*-caproate or *n*-caprylate production rate and specificity in different groups				
Groups		C6 > C8	C6 similar to C8	C8 > C6
n-caproate	Production rate (mmol C^{-1} L^{-1} d)	44.13±6.41	34.34±6.23	14.91±4.21
	Specificity (%)	0.53	/	/
n-caprylate	Production rate (mmol C^{-1} L^{-1} d)	15.28±13.13	33.19±7.52	51.15±13.14
	Specificity (%)	/	/	0.59

Table S4.14 The average production rate of odd-chain products under different conditions				
	Group 1 (period V) (with high production of odd-chain products in R1)	Group 2 (period **b**) (with high production of odd-chain products in R2)	Group 3 (period X) (with low production of odd-chain products in R1)	Group 4 (period **e**) (with low production of odd-chain products in R2)
Production rate (mmol C^{-1} L^{-1} d)	27.55±4.59	39.67±5.9	3.37±0.87	10.02±7.94

Table S4.15 Significance tests between different microbial communities shaped by different environmental factors for high or low odd-chain product production						
	Group 1/Group 2	Group 1/Group 3	Group 1/Group 4	Group 2/Group 3	Group 2/Group 4	Group 3/Group 4
R^2	0.185	0.54	0.72	8.29	0.48	0.54
p-value	0.148	0.006	0.0084	0.006	0.006	0.006
The permutation test (adonis) was performed on the basis of Bray–Curtis distance.						

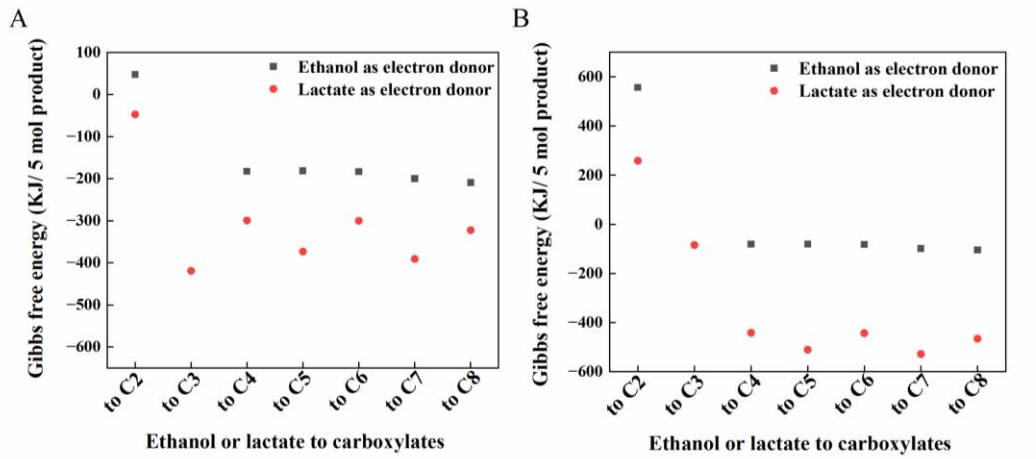

Figure S5.1 Scatter chart of the Gibbs free energy produced from ethanol (black dots) and lactate (red dots) to different carboxylate (C2/C3/C4/C5/C6/C7/C8), and the values were from **Tables S5.1 and S5.2**. The unit was KJ/5 mol products. The reaction happened with standard conditons (pH=7, 25°C) (A); pH=5.5, 30°C (B).

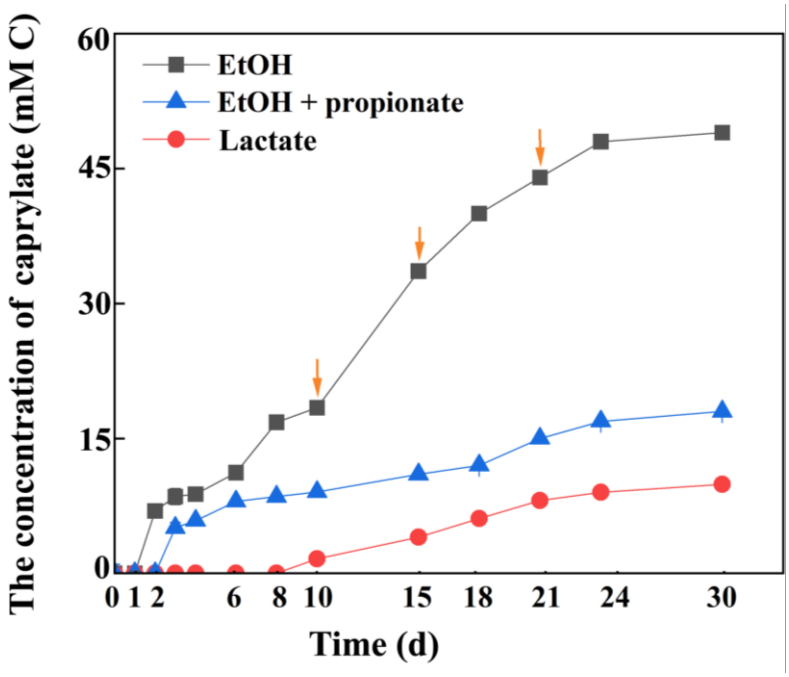

Figure S5.2 Line chart of the production of *n*-caprylate with different substrates. EtOH: with ethanol as an electron donor; EtOH + propionate: with ethanol as an electron donor and propionate as an electron acceptor; Lactate: with lactate as an electron donor. The orange arrows showing the additional addition of 100 mM electron donors into each group at different time points.

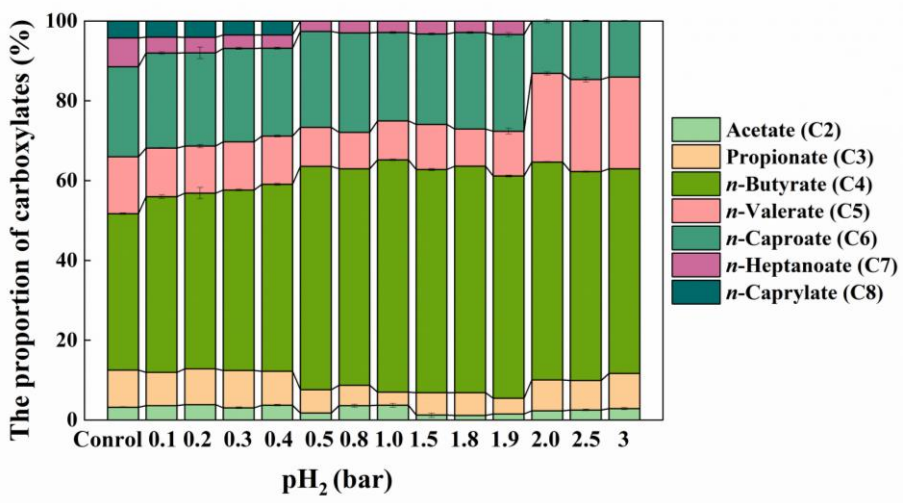

Figure S5.3 The proportion of carboxylates produced in the group with different initial pH_2.

Table S5.1 Ethanol-based chain elongation reactions [a]				
Equation	Chain Elongation Stoichiometry	$\Delta G_r°$ (kJ mol^{-1})[b]	$\Delta G_r°$ (kJ mol^{-1})[c]	Reference
Ethanol-based overall chain elongation (even-chain products)				
1	Ethanol oxidation			
	$(CH_3CH_2OH + H_2O \rightarrow CH_3COO^- + H^+ + 2H_2) \times 1$	9.89	111.40	(Spirito, Richter *et al.* 2014)
2	5× Reverse β-oxidation to C4			
	$(CH_3CH_2OH + CH_3COO^- \rightarrow CH_3(CH_2)_2COO^- + H_2O) \times 5$	-193.00	-192.9	(Spirito, Richter *et al.* 2014)
3	$6CH_3CH_2OH + 4CH_3COO^- \rightarrow 5CH_3(CH_2)_2COO^- + H^+ + 2H_2 + 4H_2O$	-182.50	-81.05	(Spirito, Richter *et al.* 2014)
4	Ethanol oxidation			
	$(CH_3CH_2OH + H_2O \rightarrow CH_3COO^- + H^+ + 2H_2) \times 1$	9.89	111.40	(Spirito, Richter *et al.* 2014)
5	5× Reverse β-oxidation to C6			
	$(CH_3CH_2OH + CH_3(CH_2)_2COO^- \rightarrow CH_3(CH_2)_4COO^- + H_2O) \times 5$	-194.00	-194.25	(Spirito, Richter *et al.* 2014)
6	$6CH_3CH_2OH + 5CH_3(CH_2)_2COO^- \rightarrow CH_3COO^- + 5CH_3(CH_2)_4COO^- + H^+ + 2H_2 + 4 H_2O$	-183.50	-82.4	(Spirito, Richter *et al.* 2014)
7	Ethanol oxidation			
	$(CH_3CH_2OH + H_2O \rightarrow CH_3COO^- + H^+ + 2H_2) \times 1$	9.89	111.40	(Spirito, Richter *et al.* 2014)

8	5× Reverse β-oxidation to C8			
	$(CH_3CH_2OH + CH_3(CH_2)_4COO^- \rightarrow CH_3(CH_2)_6COO^- + H_2O) \times 5$	-219.3	-216.5	d
9	$6CH_3CH_2OH + 5CH_3(CH_2)_2COO^- \rightarrow CH_3COO^- + 5CH_3(CH_2)_4COO^- + H^+ + 2H_2 + 4H_2O$	-209.3	-104.65	
Ethanol-based overall chain elongation (odd-chain products with additional propionate)				
10	Ethanol oxidation			
	$(CH_3CH_2OH + H_2O \rightarrow CH_3COO^- + H^+ + 2H_2) \times 1$	9.89	111.40	d
11	5× Reverse β-oxidation to C5			
	$CH_3CH_2OH + CH_3CH_2COO^- \rightarrow CH_3(CH_2)_3COO^- + H_2O \times 5$	-192	-193	d
12	$6CH_3CH_2OH + 5CH_3CH_2COO^- \rightarrow CH_3COO^- + 5CH_3(CH_2)_3COO^- + H^+ + 2H_2 + 4H_2O$	-181.5	-81.15	
13	Ethanol oxidation			
	$(CH_3CH_2OH + H_2O \rightarrow CH_3COO^- + H^+ + 2H_2) \times 1$	9.89	111.40	d
14	5× Reverse β-oxidation to C7			
	$CH_3CH_2OH + CH_3(CH_2)_2COO^- \rightarrow CH_3(CH_2)_5COO^- + H_2O \times 5$	-210.5	-210.5	d
15	$6CH_3CH_2OH + 5CH_3(CH_2)_3COO^- \rightarrow CH_3COO^- + 5CH_3(CH_2)_5COO^- + H^+ + 2H_2 + 4H_2O$	-200	-98.7	
[a]Thermodynamic information with concentrations and pressures of all components at 1 M or 1 bar; ion concentration (I) = 0; [b] pH=7 at 25°C; [c] pH=5.5 at 30°C; [d] the calculation method was based on the one mentioned in chapater 3 and data sources were from (Hanselmann 1991, Mavrovouniotis 1990).				

Table S5.2 Lactate-based chain elongation reactions[a]

Equation	Chain Elongation Stoichiometry	$\Delta G_r°$ (kJ mol^{-1})[b]	$\Delta G_r°$ (kJ mol^{-1})[c]	Reference
Lactate-based overall chain elongation (even-chain products)				
16	Lactate to C2 for ATP generation			
	$CH_3CH(OH)COO^- + H_2O \rightarrow CH_3COO^- + 2H_2 + CO_2$	-9.46	51.72	(Cavalcante, Leitão *et al*. 2017)
17	Overall Chain Elongation to C4			
	$CH_3CH(OH)COO^- + CH_3COO^- + H^+ \rightarrow CH_3(CH_2)_2COO^- + H_2O + CO_2$	-57.96	-98.73	(Cavalcante, Leitão *et al*. 2017)
18	$6CH_3CH(OH)COO^- + 5H^+ \rightarrow 5CH_3(CH_2)_2COO^- + 2H_2 + 4H_2O + 6CO_2$	-299.26	-441.93	
19	Lactate to C2 for ATP generation			
	$CH_3CH(OH)COO^- + H_2O \rightarrow CH_3COO^- + 2H_2 + CO_2$	-9.46	51.72	(Cavalcante, Leitão *et al*. 2017)
20	Overall chain elongation to C6			
	$CH_3CH(OH)COO^- + CH_3(CH_2)_2COO^- + H^+ \rightarrow CH_3(CH_2)_4COO^- + H_2O + CO_2$	-58.16	-98.96	(Cavalcante, Leitão *et al*. 2017)
21	$6CH_3CH(OH)COO^- + 5CH_3(CH_2)_2COO^- + 5H^+ \rightarrow CH_3COO^- + 5CH_3(CH_2)_4COO^- + 2H_2 + 4H_2O + 6CO_2$	-300.26	-443.08	
22	Lactic acid to C2 for ATP generation			
	$CH_3CH(OH)COO^- + H_2O \rightarrow CH_3COO^- + 2H_2 + CO_2$	-9.46	51.72	d
23	Overall chain elongation to C8			
	$CH_3CH(OH)COO^- + CH_3(CH_2)_4COO^- + H^+ \rightarrow CH_3(CH_2)_6COO^- + H_2O + CO_2$	-62.60	-103.45	d
24	$6CH_3CH(OH)COO^- + 5CH_3(CH_2)_4COO^- + 5H^+ \rightarrow CH_3COO^- + 5CH_3(CH_2)_6COO^- + 2H_2 + 4H_2O + 6CO_2$	-322.46	-465.53	d

Lactate-based overall chain elongation (odd-chain products)				
25	Lactate to C2 for ATP generation			
	$CH_3CH(OH)COO^- + H_2O \rightarrow CH_3COO^- + 2H_2 + CO_2$	-9.46	51.72	(Agler, Spirito *et al*. 2012)
26	Lactate reduction to propionate			
	(Lactate reduction to C3: as found in *Selenomonas ruminantium*) $CH_3CH(OH)COO^- + H_2O \rightarrow CH_3COO^- + CO_2 + 2H_2$ $CH_3CH(OH)COO^- + H_2 \rightarrow CH_3CH_2COO^- + H_2O \times 2$	Total = -171.87	Total = 17.84	(Agler, Spirito *et al*. 2012)
27	$CH_3CH(OH)COO^- + H_2 \rightarrow CH_3CH_2COO^- + H_2O$ (Lactate reduction to C3: as determined for *C. propionicum*)	-83.80	-16.93	(Arslan, Steinbusch *et al*. 2016)
28	Overall chain elongation to C5			
	$CH_3CH(OH)COO^- + CH_3CH_2COO^- + H^+ \rightarrow CH_3(CH_2)_3COO^- + H_2O + CO_2$	-57.96	-98.74	d
29	$10CH_3CH(OH)COO^- + 5H^+ + 5H_2 \rightarrow 5CH_3(CH_2)_3COO^- + 10H_2O + 5CO_2$	-461.67	-510.63	
30	Overall chain elongation to C7			
	$CH_3CH(OH)COO^- + CH_3(CH_2)_3COO^- + H^+ \rightarrow CH_3(CH_2)_5COO^- + H_2O + CO_2$	-61.41	-102.25	d
31	$10CH_3CH(OH)COO^- + 5H^+ + 5H_2 \rightarrow 5CH_3(CH_2)_5COO^- + 10H_2O + 5CO_2$	-390.85	-528.18	

[a]Thermodynamic information with concentrations and pressures of all components at 1 M or 1 bar, [b] pH=7 at 25°C; [c] pH=5.5 at 30°C; [d] the calculation method was based on the one mentioned in chapater 3 and data sources were from (Hanselmann 1991, Mavrovouniotis 1990).

Groups	Concentration of carboxylates consumed or produced (mM C)[a]						
	Acetate	Propionate	*n*-Butyrate	*n*-Valerate	*n*-Caproate	*n*-Heptanoate	*n*-caprylate
Without electron donors	23.70±2.33	35.06±2.80	81.67±5.41	50.73±0.98	62.32±2.14	33.48±0.08	18.67±0.38
With different electron donors							
n-Butyrate	24.05±2.33	35.80±2.80	22.00±5.41	46.60±0.98	89.22±2.14	14.72±0.084	27.20±0.38
n-valerate	37.43±1.86	50.29±3.08	27.44±1.67	-12.5±2.18	26.71±1.90	80.99±1.58	4.59±0.52
n-Caproate	16.66±0.31	30.04±4.09	136.91±11.20	30.79±1.08	40.00±3.51	1.68±0.23	4.39±0.19
n-Heptanoate	8.16±3.00	23.01±0.56	4.32±0.31	2.80±0.24	0.78±0.35	0	1.52±0.05

[a] The data represented the average of triplicate determinations after 7-day cultivation. The concentration of each product resulted from minusing the original concentration with the final concentration.

Table S5.4 The concentrations of ethanol and lactate left in the medium in each experimental group

Groups	+ 10 mM Sodium butyrate	+ 10 mM Sodium valerate	+ 10 mM Sodium caproate	+ 10 mM Sodium heptanoate
Ethanol (mM)	0	0	0	25.12±0.68
Lactate (mM)	0	0	0	12.60±0.98

Table S5.5 The concentrations of ethanol and lactate left in the medium														
Initial pH_2 (bar)	0 (Control)	0.1	0.2	0.3	0.4	0.5	0.8	1	1.5	1.8	1.9	2	2.5	3
Ethanol (mM)	0	0	0	0	0	0	0	0	13±2.80	12.5±5.41	14±3.08	26±1.67	27.5±4.09	25±11.2
Lactate (mM)	0	0	0	0	0	0	0	0	8±0.56	8±0.314	9.5±0.38	16±0.52	17.5±0.19	18±0

Appendix 4 Protocols

Protocol of Preparing 16S Ribosomal RNA Gene Amplicons for the Illumina MiSeq System

The library preparation was performed according to the *Illumina* recommendation and procedure (2022). According to this, to do the 16S rRNA gene library, we will do two PCR reactions. First, we will amplify the 16S rRNA gene from the raw samples (DNA extracted) and add the "overhang adapters", which will serve as linkers for the Illumina adaptors and the barcodes. Second, we will do a second PCR using the first PCR product as a template to add the *Illumina* primers and the barcodes.

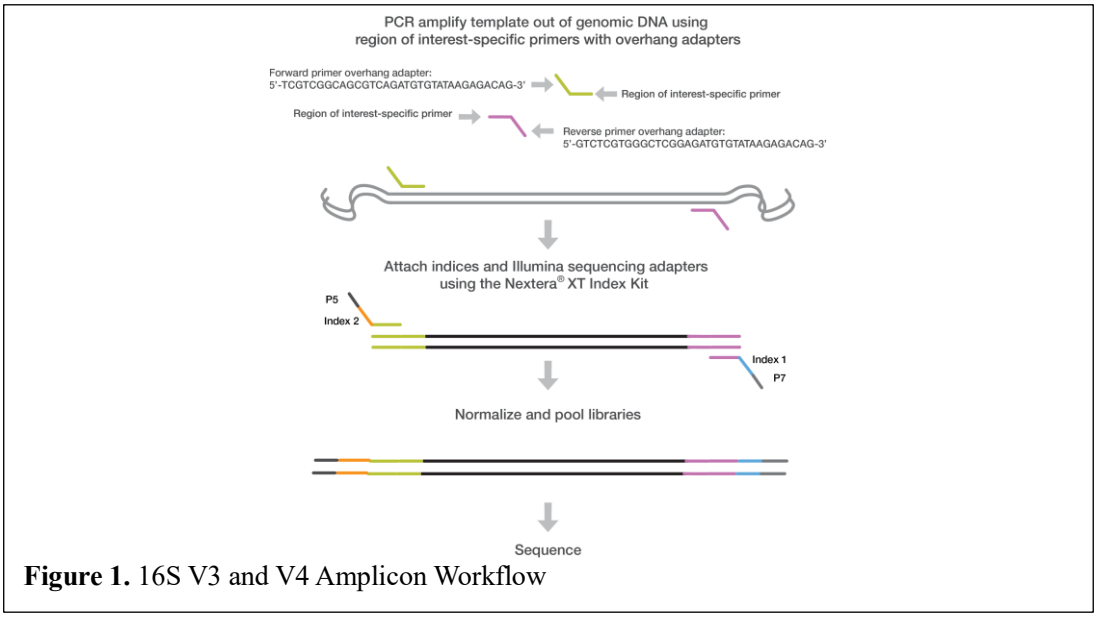

Figure 1. 16S V3 and V4 Amplicon Workflow

In the first PCR, we will use the same primers for all the samples, but, we will use a unique reverse primer for each sample in the second PCR. I will address the first PCR preparation primers, first PCR reaction, electrophoresis on 1% agarose to see PCR product, and MAG bind cleaning of the PCR product.

1. First PCR (Amplicon PCR)

1.1 Primers preparation

Forward Overhang	Forward Primer Linker	515F Forward Primer
TCGTCGGCAGCGTCAGATGTGTATAAGAGACAG	GT	GTGYCAGCMGCCGCGGTAA
Reverse Overhang	**Forward Primer Linker**	**926R Forward Primer**
GTCTCGTGGGCTCGGAGATGTGTATAAGAGACAG	GG	CCGYCAATTYMTTTRAGTTT

Figure 2. The primer for 16S V4 and V5

For the primers preparation, we will do the stock solution (100 µM), and from that, we will do the work solution (10 µM). As the primers come lyophilised, we have to reconstitute them and from that do the work solution. All the solutions **must** be done using molecular grade water.

1.2 **Stock solution preparation**

Each primer comes in a different concentration in nano moles (nmol). I will use this value to calculate the amount of water PCR grade we will use to reconstitute them and have the stock solution. As you could see, the 515F_Illu primer has a concentration of 20.2 nmol and the 9266R_Illu of 20.0 nmol.

Calculation1:

$$100\ \ \mu M_{515F\_Illu} = \frac{100\ \ \mu mol_{515F\_Illu}}{1 L_{H2O}} \rightarrow\ \ \frac{0.1\ \ nmol_{515F\_Illu}}{1 \mu L_{H2O}}$$

$$\frac{0.1\ \ nmol_{515F\_Illu}}{1 \mu L_{H2O}} \rightarrow\ \ \frac{20.2\ \ nmol_{515F\_Illu}}{\frac{0.1\ \ nmol_{515F\_Illu}}{1 \mu L_{H2O}}} = \frac{20.2\ \ nmol_{515F\_Illu}}{0.1\ \ nmol_{515F\_Illu}} = \mathbf{202 \mu L_{H2O}}$$

According to the calculations, we have to add 202 µL of PCR grade water to the 515F_Illu primer tube in order to obtain a 100 µM of stock solution. I perform the same calculations for the 926R_Illu primer with an initial concentration of 20.0 nmol. I will obtain that we have to add 200 µL of PCR-grade water to the 926R_Illu primer tube to obtain a 100 µM of stock solution. These tubes must be stored at -20°C.

1.3 **Work solution preparation**

Now, from the stock solutions (100 µM), we will prepare the work solutions (10 µM) of both primers. All the solutions **must** be done using molecular grade water. I will do it according to the calculations:

Calculation2:

$$10\ \ \mu M_{515F\_Illu} \rightarrow \frac{10\ \ \mu M_{515F\_Illu} *\ \ 500 \mu L_{H2O}}{100\ \ \mu M_{515F\_Illu}} =\ \ 50 \mu L_{515F\_Illu}$$

According to the calculations, we have to take 50 µL of 515F_Illu primer stock solution (100 µM) tube in order to obtain a work solution of 10 µM. Therefore, we have to do the same procedure for the 926R_Illu primer. Use 1.5mL Eppendorf tubes, label them and store at -20°C.

1.4 **PCR amplification**

For the first amplification of 16S rRNA gene, we will use the stock solution of the primers 515F_Illu and 926R_Illu, the Kapa HiFi master mix, molecular grade water and the DNA template (samples). For the PCR reaction, we will use a final volume of 15 µL. Therefore, the calculations for the master mix will be:

Final Volume: 15 µL (use PCR tubes) per reaction

Calculations for 1 reaction:

Kapa HiFi master mix: 7.5 µL

515F_Illu 10 µM: 0.6 µL

926R_Illu 10 µM: 0.6 µL

PCR grade water: 5.1 µL

DNA template: 1.2 µL

To make the PCR master mix for 6 samples (first we will use samples 18, 19, 20, 21, 22, 23) + the controls (C+,C-). Then the calculations for 8 reactions are in a 1.5 mL Eppendorf tube:

Kapa HiFi master mix: 60 µL

515F_Illu 10 µM: 4.8 µL

926R_Illu 10 µM: 4.8 µL

PCR grade water: 40.8 µL

The master mix should be kept on ice and well mixed. From the master mix, you should add 13.8 µL to each labelled PCR reaction tube. Then you should add 1.2 µL of each sample to the corresponding tube, mix and give them a short spin. Put the PCR tubes in the thermocycler, and make sure that the annealing temperature is 72°C.

1.5 **Gel electrophoresis – First PCR**

From the PCR products, we will perform a 1% electrophoresis gel to assess the amplification quality and possible DNA contaminants or artefacts. I will use 2 µL of the PCR product, and we will mix with other 2 µL of PCR grade water, plus 1 µL of the loading dye. The final volume of 5 µL should be mixed and spin before loading in the

electrophoresis gel. After 30-45 min, reveal the gel and assess the amplification quality, comparing it with the controls and the 1Kb DNA ladder.

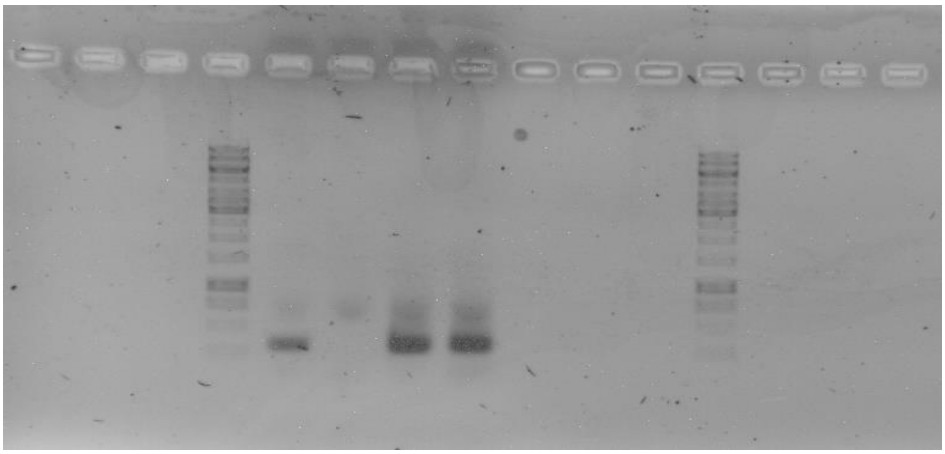

Figure 3. The electrophoresis result (Correct electrophoresis run should be similar to this one, with negative control clear, positive and samples with one dominant band and the ladder correctly separated)

1.6 **Mag-Bind PCR product cleaning**

Using the 13 µL of the PCR product, we will use the Mag-Bind total pure NGS kit. I will remove the bead solution from the fridge and let it at room temperature for 30 minutes before use. Please remember to use Eppendorf Low-bind tubes and filtered tips. Transfer the 13 µL of PCR product to a clean and sterile Low-bind Eppendorf tube and add 24 µL of the Mag-Bind beads solution. Remember to mix thoroughly to ensure the homogeneity of the solution. Do the same for all the samples PCR products, not include the controls. Mix the beads with the sample gently and let it settle for 1 minute; give it a soft spin so all the liquid will be in the bottom of the tube. Put the tubes (max. 6) on the magnetic holder and wait around 6 minutes for the beads to be attracted and gathered in the magnet. Move the tubes (without removing them from the holder) to ensure that all the beads converge to the magnet. Open the tube and remove the liquid phase (± 40 µL), and you must not disturb or touch the beads. After this, add 220 µL of analytic grade ethanol at 70% (do the solution using 99% absolute ethanol plus PCR grade water) to clean -Ethanol clean- the beads. Let it incubate for 1 minute, remove the ethanol (± 240 µL), and be careful with the tip to not touch the beads. Make sure that ethanol drops are not present inside the tube, only the beads. Repeat the ethanol cleaning steps one time and after the second time of removing the liquid and drops, let the tubes open for the ethanol to dry (± 5 minutes). After the tubes and beads are dry, add 11 µL of PCR-grade water to the beads, remove the holder's tubes, and make sure that the beads are in contact with water. Mix the beads thoroughly with the water and settle at room

temperature outside the holder for 4 minutes. After this time, put the tubes again into the holder and wait for 5 minutes. Move the tubes (without removing them from the holder) to ensure that all the beads converge to the magnet. Remove the liquid (± 10 µL) phase and put it in a sterile PCR tube. Now the PCR product is clean and ready to perform the 2nd PCR. Store the tubes with the liquid phase, correctly labelled at -20°C and prepare everything for the 2nd PCR.

1.7 **Gel electrophoresis of the cleaned PCR product**

From the PCR products cleaned, we will perform another 1% electrophoresis gel to cleaning quality. To do that, refer to the corresponding SOP in confluence in case you needed. I will use 2 µL of the PCR product, and we will mix with other 2 µL of PCR grade water, plus 1 µL of the loading dye. The final volume of 5 µL should be mixed and spin before loading in the electrophoresis gel. After 30-45 minutes, reveal the gel and assess the cleaning quality, comparing it with the controls and the 1Kb DNA ladder.

2. Second PCR (Index PCR)

I will use the index primers "Nextera XT Index kit V2 Set A" using the proposed scheme in the second PCR. I will use a unique reverse (orange) primer for each sample in the second PCR. I will address the second PCR reaction, MAG bind cleaning of the library product, electrophoresis on 1% agarose to see the library, Qubit fluorometric quantification, and DNA pooling to miseq sequencing.

2.1 **primer preparation**

Primers should be mixed within the sample similar than is presented in this figure and scheme:

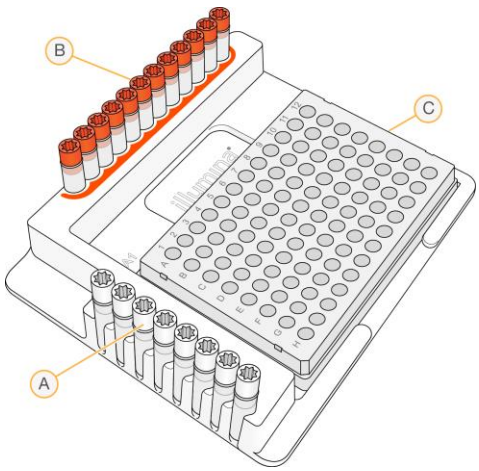

Figure 4. TruSeq Index Plate Fixture (A: index 2 primers (white caps); B: index 1 primers (orange

Table 1. The example of the primer for each sample												
Orange caps / **White caps**	**N701**	**N702**	**N703**	**N704**	**N705**	**N706**	**N707**	**N708**	**N709**	**N710**	**N711**	**N712**
S502	Sample 1	Sample 2										
S503												
S504												
S505												
S506												
S507												
S508												
S509												
S510												
S511												

For example, for sample 1, you will use the reverse primer **S502** and the forward primer **N701**, meaning that you will have a unique index combination for this sample. Next sample (number 2), you will use the same reverse primer **S502**, but now you will use the other forward primer, **N702**. This arrangement allows having 96 possible combinations for samples with different indexes for *miseq illumina*. Primers-Indexes-must be treated with special care; otherwise, they could get contaminated and lost. For using the white indexes (**S50X**), please first calculate how many samples will you prepare and then transfer that volume to a clean low bind Eppendorf tube. For example, if you will prepare libraries for 10 samples, that means that you will use the **S502** primer and the **N701** to **N710** primers. For that, you should transfer the final volume of the **S502** primer to a low-bind Eppendorf tube and dose for each sample from it. In this case, if you will prepare 10 libraries with 15µL as final volume each one, you should use 1.5µl of **S502** primer and 1.5µl of one of **N70X** primers; this means that you should transfer 15µl of the **S502** primer to a low-bind tube and dose from there to each PCR reaction tube 1.5 µL.

2.2 **PCR amplification**

For the second amplification (library prep), we will use the **S502** primer and **N70X** primers, the Kapa HiFi master mix, molecular grade water and the DNA template (First PCR product). For the PCR reaction, we will use a final volume of 15 µL. Therefore, the calculations for the master mix will be:

Final Volume: 15 µL (use PCR tubes) per reaction

Calculations for 1 reaction:

Kapa HiFi master mix: 7.5 µL

PCR grade water: 3 µL

DNA template: 1.5 µL

To make the PCR master mix for 10 PCR products (samples 18, 19, 20, 21, 22, 23 + Patrick's 4 samples). Then the calculations for 10 reactions are in a 1.5 mL Eppendorf tube of master mix:

Kapa HiFi master mix: 75 µL

PCR grade water: 30 µL

The master mix should be kept on ice and well mixed. From the master mix, you should add 10.5 µL to each labelled PCR reaction tube. Then you should add 1.5 µL of each PCR product (sample) to the corresponding tube, 1.5 µL of the **S502** primer (previously transferred in a low-bind tube), and 1.5 µL of the one of **N70X** primers**,** mix and give them a short spin. REMEMBER each sample must contain a different **N70X** primer.

Create a program in the thermocycler under the user "Andres" and name it "library nextera indexes" according to the follow parameters:

- 95°C for 3 minutes
- 8 cycles of:
  - 98°C for 20 seconds
  - 70°C for 20 seconds
  - 72°C for 45 seconds
- 72°C for 5 minutes
- Hold at 8°C.

2.3 **Mag-Bind PCR product cleaning**

Using the 15 µL of the PCR product, we will use the Mag-Bind total pure NGS kit. I will remove the bead solution from the fridge and let it at room temperature 30 minutes before use. Please remember to use Eppendorf Low-bind tubes and filtered tips.

Transfer the 15 µL of PCR product to a clean and sterile Low-bind Eppendorf tube and add 27 µL of the Mag-Bind beads solution. Remember to mix thoroughly to ensure the homogeneity of the solution. Do the same for all the second PCR products. Mix the beads with the sample gently and let it settle for 1 minute; give it a soft spin so all the liquid will be in the bottom of the tube. Put the tubes (max. 6) on the magnetic holder and wait around 6 minutes for the beads are attracted and gathered in the magnet. Move the tubes (without removing them from the holder) to ensure that all the beads converge to the magnet.

Open the tube and remove the liquid phase (± 40 µL); you must not disturb or touch the beads. After this, add 220 µL of analytic grade ethanol at 70% (do the solution using 99% absolute ethanol plus PCR grade water) to clean -Ethanol clean- the beads. Let it incubate for 1 minute, remove the ethanol (± 240 µL), and be careful with the tip to not touch the beads. Make sure that ethanol drops are not present inside the tube, only the beads. Repeat the ethanol cleaning steps one time and after the second time of removing the liquid and drops, let the tubes open for the ethanol to dry (± 5 minutes). After the tubes and beads are dry, add 13 µL of PCR-grade water to the beads, remove the holder's tubes, and make sure that the beads are in contact with water. Mix the beads thoroughly with the water and settle at room temperature outside the holder for 4 minutes. After this time, put the tubes again into the holder and wait for 5 minutes. Move the tubes (without removing them from the holder) to ensure that all the beads converge to the magnet. Remove the liquid (± 12 µL) phase and put it in a sterile PCR tube. Now the PCR product is clean and ready to be Qubit-quantified.

2.4 **Dilution 1/10 to quantifications**

From each tube of the second PCR, take 1 µL and transfer to a new PCR reaction tube, add 9 µL of PCR grade water, mixed and use it for the next steps. Store at -20°C the PCR reaction tubes for the pooling step.

2.5 **Gel electrophoresis**

From the previous dilutions, we will perform a 1% electrophoresis gel to assess the cleaning quality. To do that, refer to the corresponding SOP in confluence in case you needed. I will use 3 µL of the dilution tube, and we will mix with other 1 µL of PCR grade water, plus 1 µL of the loading dye. The final volume of 5 µL should be mixed and spin before loading in the electrophoresis gel. After 30-45 min, reveal the gel and assess the cleaning quality, comparing it with the controls and the 1Kb DNA ladder.

3. Qubit fluorometric quantification

I will use the Qubit fluorometer to measure the $_{DS}$DNA in the samples. For this we will perform a calibration (standards included). The kit is composed by quantification buffer, $_{DS}$DNA fluorescent dye, standard 1 and standard 2. Remember to use only the tubes for the qubit assay not Eppendorf tubes.

Figure 5. The product for Qubit fluorometric quantification

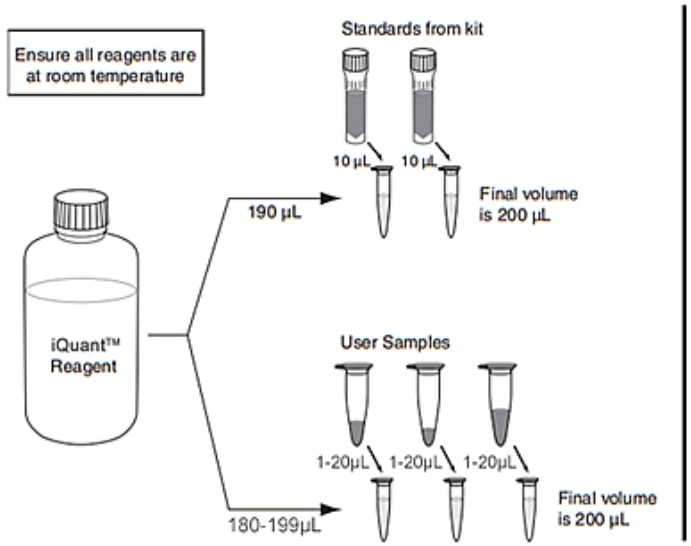

Figure 6. The workflow for Qubit fluorometric quantification

Prepare the number of necessary tubes for the quantification, in this case, 12 tubes (10 samples + 2 standards). Prepare 2 mastermix tubes (one for standards other for samples); Standards mastermix is composed of 346 µL of quantification buffer + 4 µL $_{DS}$DNA fluorescent dye (188 µL buffer + 2 µL of dye per standard). Samples master mix for the 10 samples is composed of 1960 µL of quantification buffer and 20 µL

$_{DS}$DNA fluorescent dye (196 µL buffer + 2 µL of dye per sample). Then when you have the mastermix, dose 198 µL in each one of the tubes with samples and add 2 µL of sample dilution 1/10 to each tube. For standards, dose 190 µL of mastermix in each one of the tubes (2) and then add 10 µL of standard in each tube.

Wait for 2 min at room temperature keeping the tubes in the dark place, protected from light. Then measure in the qubit fluorometer, using the $_{DS}$DNA fluorescent method. Calibrate the instrument with the standards and then begin with the samples. For samples, read the absorption and select "calculate initial concentration" select 2 µL as sample volume and the concentration in ng/µL. Register the results and finish the measurement per tube. Multiply each result by 10 and register the result. Use the formula to transform to nM, and record the results:

Equation 3 :

$$\frac{\text{Concentration in ng/ul}}{660 \text{ g/mol x average library size}} \mathbf{x}\ 10^6 = \text{concentration in mM}$$

$$\frac{15 \text{ ng/ul}}{660 \text{ g/mol x } 500 \text{ size}} \mathbf{x}\ 10^6 = 45 \text{ in mM}$$

4. DNA dilution and pooling

From DNA library stocks (stored at -20°C) make a dilution in a low bind Eppendorf tube with the final concentration of 4nM and 30 µL of the final volume; considering the concentrations measured with the qubit fluorometer. Having the solutions at 4nM, prepare the "pooling tube" (low bind tube) and make the calculations of the partition between the samples considering a final volume of 20 µL in this tube. For example, if you have 12 samples at 4nM (12 tubes), divide 20 µL by 12 = 1,67µL; take this volume from each one of the tubes and put them in the "pooling tube", achieving the 20 µL of the final volume. From this, you will have the samples pooled and ready to send to sequence in the MPI. Transport the tube on icebox and deliver in the genome centre to Dr Heike Budde.

16S rRNA gene sequence result analysis *via* qiime2

1. Create a folder to contain the following files

- BC forward
- BC reverse
- Forward Reading
- Reverse Reading

2. Create a file in QIIME 1

mkdir illumina1

cd qiime-han

3. Unified barcode in QIIME 1

extract_barcodes.py \

--input_type barcode_paired_end \

-f index1.fastq \

-r index2.fastq \

--bc1_len 6 \

--bc2_len 6 \

-o parsed_barcodes/

4. Move the file to the QIIME2 directory

##change admin permits python

chmod 755 (name of the file.extension)

##transform fastq to fastq.gz

gzip *.fastq

5. Import file

##FILES MUST HAVE THE NAME "forward" AND "reverse" AND "barcodes"

qiime tools import \

--type EMPPairedEndSequences \

--input-path seqs_unified \

--output-path seqs_unified.qza

"seqs_unified.qza" must contain the following files: "forward", "reverse" , and "barcodes"

##Check if the importation is OK

Qiime tools peek seqs_unified.qza

6. Demux the file

qiime demux emp-paired \

--i-seqs sequences_all.qza \

--m-barcodes-file Meta_barcode.tsv \

--m-barcodes-column barcode-sequence \

--p-no-golay-error-correction \

--o-per-sample-sequences illumina1-demux.qza \

--o-error-correction-details full_demux.qza

##demux without taking into account the 12nt of the golay barcode "--p-no-golay-error-correction

##Metadata must be in .tsv extension, first do it in excel, then save as text and transform to .tsv using an on-line converter

##If you want to check the metadata validity in the .tsv file, use Keemei: Validate tabular bioinformatics file formats in Google Sheets (qiime2.org)

##Pay attention in the name of the column that has the 2 barcodes (forward and reverse) concatenated, THAT name must be in the code

##Check if the artifact is OK

Qiime tools peek illumina1-demux.qza

7. Visualize the demultiplexed sequences and obtain a quality map

qiime demux summarize \

--i-data illumina1-demux.qza \

--o-visualization illumina1-dm.qzv

##Use QIIME 2 View and drag the .qzv file

8. Evaluate the mass map to define where to trim and truncate

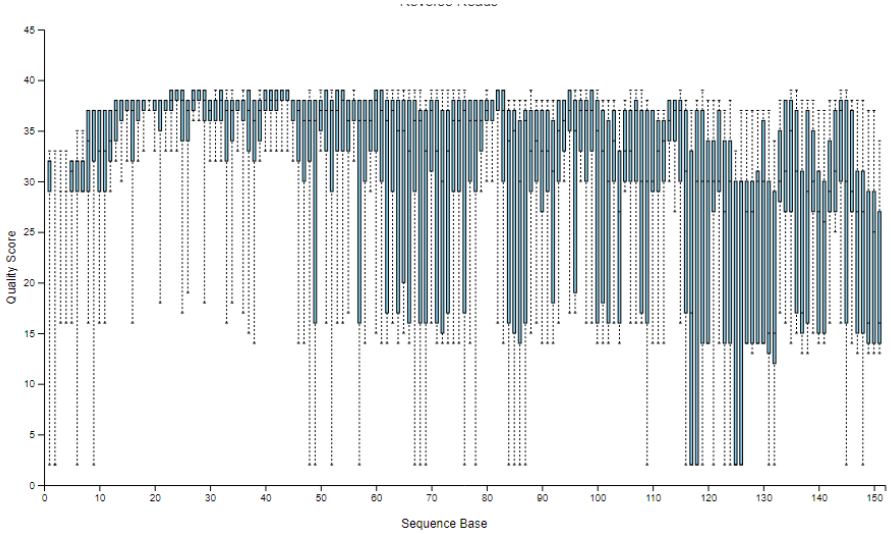

Figure 7. The mass map of sequence result

##Trim eliminates sequences on the left (initial part) including barcodes e.g. 20

##Trunc stops the pairing of the sequences where the quality is bad and omits from that part up to the end.

9. Noise Reduction Using DADA2

##qiime dada2 denoise-paired \

--i-demultiplexed-seqs illumina1-demux.qza \

--p-trim-left-f 0 \

--p-trim-left-r 0 \

--p-trunc-len-f 250 \

--p-trunc-len-r 250 \

--p-pooling-method independent \

--p-chimera-method consensus \

--p-max-ee-f 2 \

--p-max-ee-r 2 \

--p-trunc-q 1 \ ##1 because we have seqs in 120 bp with 2 of quality score and we don't wanna trunc the readings there

--p-min-overlap 70 \ ##11 because primers have 291bp and we have in total 302bp so the overlaping is only 11bp

--p-n-threads 0 \ ##use all the threads of the pc##

--o-table illumina1_table_2.qza \

--o-representative-sequences illumina1_rep-seqs_1.qza \

--o-denoising-stats illumina1_stats_3.qza

*Numero del archivo: 1: FeatureTable[Frequency] = OUT table, 2: FeatureData[Sequence] = Representative Sequences, 3: SampleData[DADA2 Stats]= Quality stats.

10. Check denoising to see how many sequences and how many OTUS results are left

##feature table-summarize

qiime feature-table summarize \

--i-table illumina1_table_2.qza \

--o-visualization illumina1_table_2.qzv \

--m-sample-metadata-file Meta_barcode.tsv

##feature table tabulate seqs

qiime feature-table tabulate-seqs \

--i-data illumina1_rep-seqs_1.qza \

--o-visualization illumina1_rep-seqs_1.qzv

##Use QIIME 2 View and drag the .qzv file

11. Making a Phylogenetic Tree of Sequences

Align sequences as it is and with masking (considering the gaps in columns)

##Work with file 1 Representative sequences

##Use MAFFT alignment (multiple alined sequence program)

qiime phylogeny align-to-tree-mafft-fasttree \

--i-sequences C_illumina2A_rep-seqs_1.qza \

--p-n-threads auto \ ##Uses all the available cores

--p-mask-max-gap-frequency 1 \ ##Retains all the sequences including the gaps

--p-mask-min-conservation 0,4 \ ##percentage of retention of a column if contains at least one character that it is present in the x% of all the sequences.

--o-alignment align-illumina2.qza \

--o-masked-alignment msk-align-illumina2.qza \

--o-tree unroo-illumina2.qza \

--o-rooted-tree roo-illumina2.qza

12. View the constructed phylogenetic tree

##Take the file .qza and uploaded in iTOL: Rooted Tree -Fasttree (embl.de)

13. Make phylogenetic tree with taller Bootstrap (10000)

##using iqtree Qiime2 feature, the plugin selects automatically the best type of phylogenetic tree, assign it and produce the tree

qiime phylogeny iqtree \

--i-alignment msk-align-illumina2.qza \

--p-n-cores auto \

--p-n-runs 10 \

--p-allnni \

--p-lbp 10000 \

--o-tree iq-illumina2.qza

14. Do taxonomic classification

a. Use first the "pre-trained" classifiers available in QIIME2 resources webpage

##GreenGenes

```
wget \
-O "gg-13-8-99-515-806-nb-classifier.qza" \
"https://data.qiime2.org/2021.8/common/gg-13-8-99-515-806-nb-classifier.qza"
##Running the classifier
qiime feature-classifier classify-sklearn \
--i-classifier gg-13-8-99-515-806-nb-classifier.qza \
--i-reads C_illumina2A_rep-seqs_1.qza \
--o-classification taxonomy.qza
##Obtaining visualizations
qiime metadata tabulate \
--m-input-file taxonomy.qza \
--o-visualization taxonomy.qzv
qiime taxa barplot \
--i-table C_illumina2A_table_2.qza \
--i-taxonomy taxonomy.qza \
--m-metadata-file Meta_barcode.tsv \
--o-visualization taxa-bar-plots.qzv
##Silva
wget \
-O "silva-138-99-515-806-nb-classifier.qza" \
"https://data.qiime2.org/2021.8/common/silva-138-99-515-806-nb-classifier.qza"
##Running the classifier
qiime feature-classifier classify-sklearn \
--i-classifier silva-138-99-515-806-nb-classifier.qza \
--i-reads C_illumina2A_rep-seqs_1.qza \
--o-classification taxonomy_Silva.qza
##Obtaining visualizations
qiime metadata tabulate \
--m-input-file taxonomy.qza \
--o-visualization taxonomy_Silva.qzv
qiime taxa barplot \
--i-table C_illumina2A_table_2.qza \
--i-taxonomy taxonomy_Silva.qza \
```

--m-metadata-file Meta_barcode.tsv \

--o-visualization taxa-bar-plots_Silva.qzv

b. Use the "pre-trained" weighted classifiers available in QIIME2 resources webpage

##**GreenGenes Weighted**

wget \

-O "gg-13-8-99-515-806-nb-weighted-classifier.qza" \

"https://data.qiime2.org/2021.8/common/gg-13-8-99-515-806-nb-weighted-classifier.qza"

qiime feature-classifier classify-sklearn \

--i-classifier gg-13-8-99-515-806-nb-weighted-classifier.qza \

--i-reads C_illumina2A_rep-seqs_1.qza \

--o-classification taxonomy_GgWeigh.qza

qiime metadata tabulate \

--m-input-file taxonomy_GgWeigh.qza \

--o-visualization taxonomy_GgWeigh.qzv

qiime taxa barplot \

--i-table C_illumina2A_table_2.qza \

--i-taxonomy taxonomy_GgWeigh.qza \

--m-metadata-file Meta_barcode.tsv \

--o-visualization taxa-bar-plots_GgWeigh.qzv

##**Silva weighted**

wget \

-O "silva-138-99-nb-weighted-classifier.qza" \

"https://data.qiime2.org/2021.8/common/silva-138-99-nb-weighted-classifier.qza"

qiime feature-classifier classify-sklearn \

--i-classifier silva-138-99-nb-weighted-classifier.qza \

--i-reads C_illumina2A_rep-seqs_1.qza \

--o-classification taxonomy_SilvWeigh.qza

qiime metadata tabulate \

--m-input-file taxonomy_SilvWeigh.qza \

--o-visualization taxonomy_SilvWeigh.qzv

qiime taxa barplot \

--i-table C_illumina2A_table_2.qza \

--i-taxonomy taxonomy_SilvWeigh.qza \

--m-metadata-file Meta_barcode.tsv \

--o-visualization taxa-bar-plots_SilvWeigh.qzv

c. Use the raw databases and train the classifier

##**GreenGenes** ##Extract trimmed

##first need to download the database with the sequences and taxonomy, use Data resources — QIIME 2 2021.8.0 documentation to download Greengenes 13_8 .tar.gz file

##Decompress the .tar.gz file, it will appear a .tar file. Decompress also that one and a folder with the sequences, trees and all the documents will appear.

##Use the sequences that are NOT aligned, QIIME2 cannot read the space "-" in the aligned sequences. Make sure that you use the Sequences (i.e., 99_otus.fasta) and the correct taxonomy file (i.e., 99_otu_taxonomy.txt).

##Mount the files in the working folder to import them

##Import Sequences:

qiime tools import \

--type FeatureData[Sequence] \

--input-path 99_otus.fasta \

--output-path 99_otus_1.qza

##Import taxonomy file:

qiime tools import \

--type FeatureData[Taxonomy] \

--input-format HeaderlessTSVTaxonomyFormat \ ##this type is cause the taxonomy doesn't have header

--input-path 99_otu_taxonomy.txt \

--output-path ref_taxonomy_2.qza

##Extract reference reads

qiime feature-classifier extract-reads \

--i-sequences 99_otus_1.qza \

--p-f-primer GTGYCAGCMGCCGCGGTAA \ ##Forward primer sequence

--p-r-primer GGACTACNVGGGTWTCTAAT \ ##Reverse primer sequence

--p-trim-right 247 \ ##Trim used in DADA2

--p-trunc-len 250 \ ##lenght of the amplified part (926-515)

--p-trim-left 0 \ ##Trim used in DADA2

--p-identity 0.80 \ ##Percentage of similarity accepted

--p-min-length 150 \

--p-max-length 310 \

--p-n-jobs 1 \ ##Number of other jobs at the same time admitted

--p-read-orientation both \

--o-reads ref-seqs-Gg-extract.qza

##Train the classifier

qiime feature-classifier fit-classifier-naive-bayes \

--i-reference-reads ref-seqs-Gg-extract.qza \

--i-reference-taxonomy ref_taxonomy_2.qza \

--o-classifier Classif_Gg_train_pink.qza

##Run the classifier as in **12a** or **12b**

##GreenGenes ##Extract trimmed(Phillip Greenspan)

##Extract reference reads

qiime feature-classifier extract-reads \

--i-sequences 99_otus_1.qza \

--p-f-primer GTGYCAGCMGCCGCGGTAA \ ##Forward primer sequence

--p-r-primer GGACTACNVGGGTWTCTAAT \ ##Reverse primer sequence

--p-trim-right 0 \ ## **NO** Trim

--p-trunc-len 291 \ ##lenght of the amplified part (806-515)

--p-trim-left 0 \ ## **NO** Trim

--p-identity 0.75 \ ##Percentage of similarity accepted

--p-min-length 150 \

--p-max-length 310 \

--p-n-jobs 1 \ ##Number of other jobs at the same time admitted

```
--p-read-orientation both \
--o-reads ref-seqs-Gg-extract.qza
##Train the classifier
qiime feature-classifier fit-classifier-naive-bayes \
--i-reference-reads ref-seqs-Gg-extract.qza \
--i-reference-taxonomy ref_taxonomy_2.qza \
--o-classifier Classif_Gg_train_green.qza
```

References

1. Abedi, E. and Hashemi, S. M. B. (2020). Lactic acid production - producing microorganisms and substrates sources-state of art. Heliyon, 6, e04974.
2. Agler, M. T., Spirito, C. M., Usack, J. G., Werner, J. J., and Angenent, L. T. (2012). Chain elongation with reactor microbiomes: upgrading dilute ethanol to medium-chain carboxylates. Energy Environ. Sci., 5, 8189-8192.
3. Agler, M. T., Spirito, C. M., Usack, J. G., Werner, J. J. and Angenent, L. T. (2014). Development of a highly specific and productive process for *n*-caproic acid production: applying lessons from methanogenic microbiomes. Water Sci. Technol., 69, 62-68.
4. Agler, M. T., Werner, J. J., Iten, L. B., Dekker, A., Cotta, M. A., Dien, B. S., and Angenent, L. T. (2012). Shaping reactor microbiomes to produce the fuel precursor *n*-butyrate from pretreated cellulosic hydrolysates. Environ. Sci. Technol., 46, 10229-10238.
5. Agler, M. T., Wrenn, B. A., Zinder, S. H., and Angenent, L. T. (2011). Waste to bioproduct conversion with undefined mixed cultures: the carboxylate platform. Trends Biotechnol., 29, 70-78.
6. Alberty, R. A. (1998). Calculation of standard transformed Gibbs energies and standard transformed enthalpies of biochemical reactants. Arch. Biochem. Biophys., 353, 116-130.
7. Alberty, R. A. (2001). Effect of temperature on standard transformed Gibbs energies of formation of reactants at specified ph and ionic strength and apparent equilibrium constants of biochemical reactions. J. Phys. Chem. B., 105, 7865-7870.
8. Alvarez, M. H., Kalscheuer, R., and Steinbuchel, A. (1997). Accumulation of storage lipids in species of *Rhodococcus* and *Nocardia* and effect of inhibitors and polyethylene glycol. Fee/Lipid, 99, 239-246.
9. Amestoy, P. R., Azzalini, A., Badics, T., Benison, G., Bowman, A., Briggs, K., et al (2022). Igraph: Network Analysis and Visualization. https://igraph.org
10. Andersen, S. J., Candry, P., Basadre, T., Khor, W. C., Roume, H., Hernandez-Sanabria, E., Coma, M. and Rabaey, K. (2015). Electrolytic extraction drives volatile fatty acid chain elongation through lactic acid and replaces chemical pH control in thin stillage fermentation. Biotechnol. Biofuels, 8, 221.
11. Andersen, S. J., Groof, V. De, Khor, W. C., Roume, H., Props, R., Coma, M., and Rabaey, K. (2017). A *Clostridium* group IV species dominates and suppresses a mixed culture fermentation by tolerance to medium chain fatty acids products. Front. Bioeng. Biotechnol., 5, 8.
12. Angenent, L. T., Richter, H., Buckel, W., Spirito, C. M., Steinbusch, K. J.J., Plugge, C. M., Strik, D. P. T. B., Grootscholten, T. I. M., Buisman, C. J. N., and Hamelers, H. V. M. (2016). Chain elongation with reactor microbiomes: open-culture biotechnology to produce biochemicals. Environ. Sci. Technol., 50, 2796-2810.
13. Angenent, L. T., Usack, J. G., Xu, J., Hafenbradl, D., Posmanik, R., and Tester, J. W. (2018). Integrating electrochemical, biological, physical, and thermochemical process units to expand the applicability of anaerobic digestion. Bioresour. Technol., 247, 1085-1094.
14. Arslan, D., Steinbusch, K. J., Diels, L., Wever, H. De, Buisman, C. J. N., and Hamelers, H. V. M. (2012). Effect of hydrogen and carbon dioxide on carboxylic acids patterns in mixed culture fermentation. Bioresour. Technol., 118, 227-234.
15. Arslan, D., Steinbusch, K. J., Diels, L., Wever, H. De, Hamelers, H. V., and Buisman, C. J. N. (2013). Selective carboxylate production by controlling hydrogen, carbon dioxide and substrate concentrations in mixed culture fermentation. Bioresour. Technol., 136, 452-460.
16. Arslan, D., Steinbusch, K. J. J., Diels, L., Hamelers, H. V., M., Strik, D. P. B. T. B., Buisman, C. J. N., and Wever, H. De (2016). Selective short-chain carboxylates production: A review of control mechanisms to direct mixed culture fermentations. Crit. Rev. Env. Sci. Tec., 46, 592-634.
17. Baleeiro, F. C. F., Ardila, M. S., Kleinsteuber, S., and Strauber, H. (2021). Effect of oxygen contamination on propionate and caproate formation in anaerobic fermentation. Front. Bioeng. Biotechnol., 9, 725443.
18. Bao, S., Wang, Q., Zhang, P., Zhang, Q., Wu, Y., Li, F., Tao, X., Wang, S., Nabi, M., and Zhou, Y. (2019). Effect of acid/ethanol ratio on medium chain carboxylate production with different vfas as the electron acceptor: Insight into carbon balance and microbial community. Energies, 12.

19. Barberan, A., Bates, S. T., Casamayor, E. O., and Fierer, N. (2012). Using network analysis to explore co-occurrence patterns in soil microbial communities. ISME J, 6, 343-351.
20. Barker, H. A. and Taha, S. M. (1942). *Clostridium kluyverii*, an organism concerned in the formation of caproic acid from ethyl alcohol. J. BACTERIOL., 43, 347-363.
21. Barker., H. A., Kamen, M. D., and Bornstein, B. T. (1945). The synthesis of butyric and caproic acids from ethanol and acetic acid by *Clostridium kluyveri*. Proc. Natl. Acad. Sci., 31, 373−381.
22. Beals, E. W. (1984). Bray-Curtis Ordination: An effective strategy for analysis of multivariate ecological data. Adv. Ecol. Res., 14, 1-55.
23. Bidzhieva, S. K., Sokolova, D. S., Grouzdev, D. S., Kostrikina, N. A., Poltaraus, A. B., Tourova, T. P., Shcherbakova,V. A., Troshina, O. Y., and Nazina, T. N. (2020). *Sphaerochaeta halotolerans* sp. nov., a novel spherical halotolerant spirochete from a Russian heavy oil reservoir, emended description of the genus *Sphaerochaeta*, reclassification of *Sphaerochaeta coccoides* to a new genus *Parasphaerochaeta* gen. nov. as *Parasphaerochaeta coccoides comb*. nov. and proposal of *Sphaerochaetaceae fam*. nov. Int. J. Syst. Evol. Microbiol., 70, 4748-4759.
24. Bidzhieva, S. K., Sokolova, D. S., Tourova, T. P., and Nazina, T. N. (2018). Bacteria of the genus *Sphaerochaeta* from low-temperature heavy oil reservoirs (Russia). Microbiology, 87, 757-765.
25. Bolyen, E., Rideout, J. R., Dillon, M. R., Bokulich, N. A., Abnet, C. C. et al., (2019). Reproducible, interactive, scalable and extensible microbiome data science using QIIME 2. Nat. Biotechnol., 37, 852-857.
26. Callahan, B. J., McMurdie, P. J., Rosen, M. J., Han, A. W. Johnson, A. J. and Holmes, S. P. (2016). DADA2: High-resolution sample inference from Illumina amplicon data. Nat. Methods, 13, 581-583.
27. Candry, P. and Ganigue, R. (2021). Chain elongators, friends, and foes.Curr. Opin. Biotechnol., 67, 99-110.
28. Candry, P., Huang, S. Carvajal-Arroyo, J. M., Rabaey, K. and Ganigue, R. (2020). Enrichment and characterisation of ethanol chain elongating communities from natural and engineered environments. Sci. Rep., 10: 3682.
29. Candry, P., Radic, L., Favere, J., Carvajal-Arroyo, J. M., Rabaey, K. and Ganigue, R. (2020). Mildly acidic pH selects for chain elongation to caproic acid over alternative pathways during lactic acid fermentation. Water Res., 186, 116396.
30. Candry, P., Ulcar, B., Petrognani, C., Rabaey, K., and Ganigue, R. (2020). Ethanol:propionate ratio drives product selectivity in odd-chain elongation with *Clostridium kluyveri* and mixed communities. Bioresour. Technol., 313, 123651.
31. Carvajal-Arroyo, J. M., Andersen, S. J., Ganigué, R., R. Rozendal, A., Angenent, L. T. and Rabaey, K. (2021). Production and extraction of medium chain carboxylic acids at a semi-pilot scale. Chem. Eng. J., 416.
32. Carvajal-Arroyo, J. M., Candry, P., Andersen, S. J., Props, R., Seviour, T., Ganigué, R. and Rabaey, K. (2019). Granular fermentation enables high rate caproic acid production from solid-free thin stillage. Green Chem., 21, 1330-1339.
33. Cavalcante, W. de. A., Leitão, R. C., Gehring, T. A., Angenent, L. T. and Santaella, S. T. (2017). Anaerobic fermentation for *n*-caproic acid production: A review. Process Biochem., 54, 106-119.
34. Chen, W. S., Huang, S., Plugge, C. M., Buisman, C. J. N., and Strik, D. P. B. T. B. (2020). Concurrent use of methanol and ethanol for chain-elongating short-chain fatty acids into caproate and isobutyrate. J. Environ. Manage., 258, 110008.
35. Chen, W. S., Strik, D. P. B. T. B., Buisman, C. J. N. and Kroeze, C. (2017). Production of caproic acid from mixed organic waste: An environmental life cycle perspective. Environ. Sci. Technol., 51, 7159-7168.
36. Cheng, S., Liu, Z., Varrone, C., Zhou, A., He, Z., Li, H., Zhang, J., Liu, W. and Yue, X. (2022). Elucidating the microbial ecological mechanisms on the electro-fermentation of caproate production from acetate *via* ethanol-driven chain elongation. Environ. Res., 203, 111875.
37. Choi, K., Jeon, B. S., Kim, Byung-Chun, Oh, Min-Kyu, Um, Youngsoon, and Sang, Byoung-In (2013). *In-situ* biphasic extractive fermentation for hexanoic acid production from sucrose by *Megasphaera elsdenii* NCIMB 702410. Appl. Biochem. Biotechnol., 171, 1094-1107.
38. Chwialkowska, J., Duber, A., Zagrodnik, R., Walkiewicz, F., Lezyk, M. and Oleskowicz-Popiel, P. (2019). Caproic acid production from acid whey *via* open culture fermentation - evaluation

of the role of electron donors and downstream processing. Bioresour. Technol., 279, 74-83.
39. Clavel, T., Lepage, P., and Charrier, C. (2014). The Family Coriobacteriaceae. The Prokaryotes, 201-238.
40. Coma, M., Vilchez-Vargas, R., Roume, H., Jauregui, R., Pieper, D. H., and Rabaey, K. (2016). Product diversity linked to substrate usage in chain elongation by mixed-culture fermentation. Environ. Sci. Technol., 50, 6467-6476.
41. Contreras-Davila, Carrion, C. A., Vonk, V. J. V. R., Buisman, C. N. J., and Strik, D. P. B. T. B. (2020). Consecutive lactate formation and chain elongation to reduce exogenous chemicals input in repeated-batch food waste fermentation. Water Res., 169, 115215.
42. Contreras-Davila, C. A., Esveld, J., Buisman, C. J. N., and Strik, D. P. B. T. B. (2021). nZVI impacts substrate conversion and microbiome composition in chain elongation from d- and l-lactate substrates. Front. Bioeng. Biotechnol., 9, 666582.
43. Contreras-Davila, C. A., Zuidema, N., Buisman, C. J. N., and Strik, D. P. B. T. B. (2021). Reactor microbiome enriches vegetable oil with *n*-caproate and *n*-caprylate for potential functionalized feed additive production *via* extractive lactate-based chain elongation. Biotechnol. Biofuels, 14, 232.
44. Counotte, G. H. M., Prins, lt, R. A., Janssen, R. H. A. M., and Debie, M. J. A. (1981). Role of *Megasphaera elsdenii* in the fermentation of d-[2-'3c] lactate in the rumen of dairy cattle. Appl. Environ. Microb, 649-655.
45. Crognale, S., Braguglia, C. M., Gallipoli, A., Gianico, A., Rossetti, S., and Montecchio, D. (2021). Direct conversion of food waste extract into caproate: Metagenomics assessment of chain elongation process. Microorganisms, 9.
46. Cronan, J. E. and Thomas, J. (2009). Chapter 17-Bacterial fatty acid synthesis and its relationships with polyketide synthetic pathways. Complex enzymes in microbial natural product biosynthesis, Part B: Polyketides, Aminocoumarins and Carbohydrates: 395-433.
47. Csardi, G., and Nepusz, T. (2005). The igraph software package for complex network research. Inter. J. Complex. Syst., 1695.
48. De Groof, V., Coma, M. Arnot, T., Leak, D. J. and Lanham, A. B. (2019). Medium-chain carboxylic acids from complex organic feedstocks by mixed culture fermentation. Molecules, 24.
49. De Leeuw, K. D., Ahrens, T. Buisman, C. J. N. and Strik, D. P. B. T. B. (2021). Open culture ethanol-based chain elongation to form medium-chain branched carboxylates and alcohols. Front. Bioeng. Biotechnol., 9, 697439.
50. De Leeuw, K. D., Buisman, C. J. N. and Strik, D. P. B. T. B. (2019). Branched medium-chain fatty acids: iso-caproate formation from iso-butyrate broadens the product spectrum for microbial chain elongation. Environ. Sci. Technol., 53, 7704-7713.
51. De Sitter, K., L. Garcia-Gonzalez, C. Matassa, L. Bertin and H. De Wever (2018). The use of membrane based reactive extraction for the recovery of carboxylic acids from thin stillage. Sep. Purif. Technol., 206, 177-185.
52. De Smit, S. M., K. D. de Leeuw, C. J. N. Buisman and D. Strik (2019). Continuous *n*-valerate formation from propionate and methanol in an anaerobic chain elongation open-culture bioreactor. Biotechnol. Biofuels, 12, 132.
53. Dewhirst, F. E., B. J. Paster, N. Tzellas, B. Coleman, J. Downes, D. A. Spratt and W. G. Wade (2001). Characterization of novel human oral isolates and cloned 16S rDNA sequences that fall in the family Coriobacteriaceae: description of *Olsenella* gen. nov., reclassification of *Lactobacillus uli* as *Olsenella uli comb*. nov. and description of *Olsenella profusa* sp. nov. Int. J. Syst. Evol. Microbiol., 51, 1797-1804.
54. Di Maio, F., P. C. Rem, K. Baldé and M. Polder (2017). Measuring resource efficiency and circular economy: A market value approach. Resour Conserv. Recy., 122, 163-171.
55. Diender, M., I. Parera Olm, M. Gelderloos, J. J. Koehorst, P. J. Schaap, A. J. M. Stams and D. Z. Sousa (2019). Metabolic shift induced by synthetic co-cultivation promotes high yield of chain elongated acids from syngas. Sci. Rep., 9, 18081.
56. Domingos, J. M. B., G. A. Martinez, A. Scoma, S. Fraraccio, F.-M. Kerckhof, N. Boon, M. A. M. Reis, F. Fava and L. Bertin (2016). Effect of operational parameters in the continuous anaerobic fermentation of cheese whey on titers, yields, productivities, and microbial community structures. Acs Sustain. Chem. Eng., 5, 1400-1407.
57. Duber, A., L. Jaroszynski, R. Zagrodnik, J. Chwialkowska, W. Juzwa, S. Ciesielski and P.

Oleskowicz-Popiel (2018). Exploiting the real wastewater potential for resource recovery – *n*-caproate production from acid whey. Green Chem., 20, 3790-3803.
58. Duber, A., R. Zagrodnik, J. Chwialkowska, W. Juzwa and P. Oleskowicz-Popiel (2020). Evaluation of the feed composition for an effective medium-chain carboxylic acid production in an open culture fermentation. Sci. Total. Environ., 728, 138814.
59. Duber, A., R. Zagrodnik, N. Gutowska, M. Łężyk and P. Oleskowicz-Popiel (2022). Lactate and ethanol chain elongation in the presence of lactose: Insight into product selectivity and microbiome composition. Acs. Sustain. Chem. Eng., 10, 3407-3416.
60. Elsden, S. R., B. E. Volcani, F. M. C. Gilchrist, and D. Lewis (1956). Properties of a fatty acid-forming organism isolated from the rumen of sheep. J. Bacteriol., 72, 681-9.
61. Engelmann, U. and N. Weiss (1985). *Megasphaera cerevisiae* sp. nov.: A new gram-negative obligately anaerobic coccus isolated from spoiled beer. Syst. Appl. Microbiol., 6, 287-290.
62. Esquivel-Elizondo, S., C. Bagci, M. Temovska, B. S. Jeon, I. Bessarab, R. B. H. Williams, D. H. Huson and L. T. Angenent (2020). The isolate *caproiciproducens* sp. 7d4c2 produces *n*-caproate at mildly acidic conditions from hexoses: Genome and rBOX comparison with related strains and chain-elongating bacteria. Front. Microbiol., 11, 594524.
63. Ezeji, J. C., D. K. Sarikonda, A. Hopperton, H. L. Erkkila, D. E. Cohen, S. P. Martinez, F. Cominelli, T. Kuwahara, A. E. K. Dichosa, C. E. Good, M. R. Jacobs, M. Khoretonenko, A. Veloo and A. Rodriguez-Palacios (2021). *Parabacteroides distasonis*: Intriguing aerotolerant gut anaerobe with emerging antimicrobial resistance and pathogenic and probiotic roles in human health. Gut Microbes, 13, 1922241.
64. Fabian Pedregosa, Gael Varoquaux, Alexandre Gramfort, Vincent Michel, and Bertrand Thirion (2011). Scikit-learn: Machine learning in python. J. Mach. Learn. Res., 12, 2825-2830.
65. Flaiz, M., T. Baur, S. Brahner, A. Poehlein, R. Daniel and F. R. Bengelsdorf (2020). *Caproicibacter fermentans* gen. nov., sp. nov., a new caproate-producing bacterium and emended description of the genus *Caproiciproducens*. Int. J. Syst. Evol. Microbiol., 70, 4269-4279.
66. Futoshi Nakazawa, Michiko Sato, Tetsuro Ikeda, Sotos Kalfas, Sergio E. Poco, Goran Sundqvist, Tsuyoshi Hashimura, and Etsuro Hoshino1 (2000). Description of *Mogibacterium pumilum* gen. nov., sp. nov. and *Mogibacterium vescum* gen. nov., sp. nov., and reclassification of *Eubacterium timidum* (holdeman et al. 1980) as *Mogibacterium timidum* gen. nov., comb. nov. Int. J. Syst. Evol. Microbiol., 50, 679-688.
67. Ge, S., J. G. Usack, C. M. Spirito, and L. T. Angenent (2015). Long-term *n*-caproic acid production from yeast-fermentation beer in an anaerobic bioreactor with continuous product extraction. Environ. Sci. Technol., 49, 8012-8021.
68. Genthner, B. R. S., C. L. Davis, and M. P. Bryant (1981). Features of rumen and sewage-sludge strains of *Eubacterium-limosum*, a methanol-utilizing and H_2-CO_2-utilizing species. Appl. Environ. Microb., 42, 12-19.
69. Gerhard Zellner, Erko Stackebrandt, Dagmar Nagel, Paul Messner, Norbert Weiss, and Josef Winter (1996). *Anaerofilum pentosovorans* gen. ~ov., sp. nov., and *Anaerofilum agile* sp. ~ov., two new, strictly anaerobic, mesophilic, acidogenic bacteria from anaerobic bioreactors. Int. J. Syst. Bacteriol., 46, 871-875.
70. Gest, H. (1995). A sereudipic legacy: Erwin Esmarch's isolation of the first photosynthetic bacterium in pure culture. Photosynth. Res., 46, 473-478.
71. Gildemyn, S., B. Molitor, J. G. Usack, M. Nguyen, K. Rabaey and L. T. Angenent (2017). Upgrading syngas fermentation effluent using *Clostridium kluyveri* in a continuous fermentation. Biotechnol. Biofuels, 10, 83.
72. Gómez, X., M. J. Cuetos, J. I. Prieto, and A. Morán (2009). Bio-hydrogen production from waste fermentation: Mixing and static conditions. Renew. Energ., 34, 970-975.
73. González-Cabaleiro, R., J. M. Lema, J. Rodríguez, and R. Kleerebezem (2013). Linking thermodynamics and kinetics to assess pathway reversibility in anaerobic bioprocesses. Energ. Environ. Sci., 6, 3780.
74. Gorvitovskaia, A., S. P. Holmes, and S. M. Huse (2016). Interpreting *Prevotella* and *Bacteroides* as biomarkers of diet and lifestyle. Microbiome, 4, 15.
75. Grootscholten, T. I., K. J. Steinbusch, H. V. Hamelers, and C. J. Buisman (2013). Chain elongation of acetate and ethanol in an upflow anaerobic filter for high rate MCFA production. Bioresour. Technol., 135, 440-445.

76. Grootscholten, T. I., K. J. Steinbusch, H. V. Hamelers, and C. J. Buisman (2013). High rate heptanoate production from propionate and ethanol using chain elongation. Bioresour. Technol., 136, 715-718.
77. Grootscholten, T. I., K. J. Steinbusch, H. V. Hamelers, and C. J. Buisman (2013). Improving medium-chain fatty acid productivity using chain elongation by reducing the hydraulic retention time in an upflow anaerobic filter. Bioresour. Technol., 136, 735-738.
78. Grootscholten, T. I. M., F. Kinsky dal Borgo, H. V. M. Hamelers, and C. J. N. Buisman (2013). Promoting chain elongation in mixed culture acidification reactors by addition of ethanol. Biomass. Bioenerg., 48, 10-16.
79. Grootscholten, T. I. M., D. P. B. T. B. Strik, K. J. J. Steinbusch, C. J. N. Buisman and H. V. M. Hamelers (2014). Two-stage medium-chain fatty acid (MCFA) production from municipal solid waste and ethanol. Appl. Energ., 116, 223-229.
80. Hamilton, N. (2022). An extension to 'ggplot2', for the creation of ternary diagrams.
81. Han, W., P. He, L. Shao, and F. Lu (2018). Metabolic interactions of a chain elongation microbiome. Appl. Environ. Microbiol., 84, e01614-18.
82. Han, W., P. He, L. Shao, and F. Lu (2019). Road to full bioconversion of biowaste to biochemicals centering on chain elongation: A mini-review. J. Environ. Sci. (China), 86, 50-64.
83. Hanselmann, K. W. (1991). Microbial energetics applied to waste repositories. Experientia, 47.
84. Hashsham, S. A., A. S. Fernandez, S. L. Dollhopf, F. B. Dazzo, R. F. Hickey, J. M. Tiedje, and C. S. Criddle (2000). Parallel processing of substrate correlates with greater functional stability in methanogenic bioreactor communities perturbed by glucose. Appl. Environ. Microbiol., 66, 4050-4057.
85. He, P., W. Han, L. Shao, and F. Lu (2018). One-step production of C6-C8 carboxylates by mixed culture solely grown on CO. Biotechnol. Biofuels., 11, 4.
86. Henning Seedorf, W. F. F., H. B. Birgit Veith, A. S. Heiko Liesegang, Marcus Miethke, , J. H. Wolfgang Buckel, Fuli Li, and R. K. T. Christoph Hagemeier, and Gerhard Gottschalk (2008). The genome of *Clostridium kluyveri*, a strict anaerobe with unique metabolic features. P. Natl. Acad. Sci. 105, 2128–2133.
87. Hernandez, P. A., M. Zhou, I. Vassilev, S. Freguia, Y. Zhang, J. Keller, P. Ledezma, and B. Virdis (2021). Selective extraction of medium-chain carboxylic acids by electrodialysis and phase separation. ACS Omega, 6, 7841-7850.
88. Hetzel, M., M. Brock, T. Selmer, A. J. Pierik, B. T. Golding, and W. Buckel (2003). Acryloyl-CoA reductase from *Clostridium propionicum*: An enzyme complex of propionyl-CoA dehydrogenase and electron-transferring flavoprotein. Eur. J. Biochem., 270, 902-910.
89. Hollister, E. B., A. K. Forrest, H. H. Wilkinson, D. J. Ebbole, S. A. Malfatti, S. G. Tringe, M. T. Holtzapple, and T. J. Gentry (2010). Structure and dynamics of the microbial communities underlying the carboxylate platform for biofuel production. Appl. Microbiol. Biotechnol., 88, 389-399.
90. Holtzapple, M. T. and C. B. Granda (2009). Carboxylate platform: the MixAlco process part 1: comparison of three biomass conversion platforms. Appl. Biochem. Biotechnol., 156, 95-106.
91. Huang, C. B., Y. Alimova, T. M. Myers, and J. L. Ebersole (2011). Short- and medium-chain fatty acids exhibit antimicrobial activity for oral microorganisms. Arch. Oral. Biol., 56, 650-654.
92. Iino, T., K. Mori, K. Tanaka, K. I. Suzuki, and S. Harayama (2007). *Oscillibacter valericigenes* gen. nov., sp. nov., a valerate-producing anaerobic bacterium isolated from the alimentary canal of a Japanese corbicula clam. Int. J. Syst. Evol. Microbiol., 57, 1840-1845.
93. Illumina company.16s-metagenomic-library-prep-guide-15044223-b.
94. J Gregory Caporaso, Justin Kuczynski, Jesse Stombaugh, Kyle Bittinger, Frederic d Bushman, Elizabeth K Costello, Noah Fierer, Antonio Gonzalez peña, Julia K Goodrich, Jeffrey I Gordon, Gavin A Huttley, Scott T Kelley, Dan Knights, Jeremy E Koenig, Ruth E Ley, Catherine A Lozupone, Daniel Mcdonald, Brian D Muegge, Meg Pirrung, Jens Reeder, Joel R Sevinsky, Peter J Turnbaugh, William A Walters, Jeremy Widmann, Tanya Yatsunenko, Jesse Zaneveld and Rob Knight (2010). QIIME allows the analysis of high-throughput community sequencing data. Nat. Methods, 7, 335.
95. Jeon, B. S., O. Choi, Y. Um and B. I. Sang (2016). Production of medium-chain carboxylic acids by *Megasphaera* sp. MH with supplemental electron acceptors. Biotechnol. Biofuels, 9,

129.
96. Jeon, B. S., B.-C. Kim, Y. Um, and B.-I. Sang (2010). Production of hexanoic acid from D-galactitol by a newly isolated *Clostridium* sp. BS-1. Appl. Microbiol. Biotechnol., 88, 1161-1167.
97. Jeon, B. S., S. Kim, and B.-I. Sang (2017). *Megasphaera hexanoica* sp. nov., a medium-chain carboxylic acid-producing bacterium isolated from a cow rumen. Int. J. Syst. Evol. Micr., 67, 2114-2120.
98. Jiang, Y., N. Chu, D. K. Qian and R. Jianxiong Zeng (2020). Microbial electrochemical stimulation of caproate production from ethanol and carbon dioxide. Bioresour. Technol., 295, 122266.
99. Joshi, S., A. Robles, S. Aguiar and A. G. Delgado (2021). The occurrence and ecology of microbial chain elongation of carboxylates in soils. ISME J, 15, 1907-1918.
100. Jumas-Bilak, E., H. Jean-Pierre, J. P. Carlier, C. Teyssier, K. Bernard, B. Gay, J. Campos, F. Morio and H. Marchandin (2005). *Dialister micraerophilus* sp. nov. and *Dialister propionicifaciens* sp. nov., isolated from human clinical samples. Int. J. Syst. Evol. Microbiol., 55, 2471-2478.
101. Karri, S., R. Sierra-Alvarez, and J. A. Field (2006). Toxicity of copper to acetoclastic and hydrogenotrophic activities of methanogens and sulfate reducers in anaerobic sludge. Chemosphere, 62, 121-127.
102. Kennedy, S. R., S. Prost, I. Overcast, A. J. Rominger, R. G. Gillespie, and H. Krehenwinkel (2020). High-throughput sequencing for community analysis: the promise of DNA barcoding to uncover diversity, relatedness, abundances and interactions in spider communities. Dev Genes. Evol., 230, 185-201.
103. Khor, W. C., S. Andersen, H. Vervaeren, and K. Rabaey (2017). Electricity-assisted production of caproic acid from grass. Biotechnol. Biofuels, 10, 180.
104. Kim, H., S. Kang and B. I. Sang (2022). Metabolic cascade of complex organic wastes to medium-chain carboxylic acids: A review on the state-of-the-art multi-omics analysis for anaerobic chain elongation pathways. Bioresour. Technol., 344, 126211.
105. Kleerebezem, R., B. Joosse, R. Rozendal and M. C. M. Van Loosdrecht (2015). Anaerobic digestion without biogas? Rev. Environ. Sci. Bio., 14, 787-801.
106. Kleerebezem, R. and M. C. van Loosdrecht (2007). Mixed culture biotechnology for bioenergy production. Curr. Opin. Biotechnol., 18, 207-212.
107. Kleerebezem, R. and Van Loosdrecht, M. C. M. (2010). A generalized method for thermodynamic state analysis of environmental systems. Crit. Rev. Env. Sci. Tec., 40, 1-54.
108. Koch, C., S. Muller, H. Harms and F. Harnisch (2014). Microbiomes in bioenergy production: from analysis to management. Curr. Opin. Biotechnol., 27, 65-72.
109. Kolde, R. (2019). Implementation of heatmaps that offers more control over dimensions and appearance. URL: https://CRAN.R-project.org/package=pheatmap.
110. Koster, I. W. and Koomen, E. (1988). Ammonia inhibition of the maximum growth rate of hydrogenotrophic methanogens at various pH-levels and temperatures. Appl. Microbiol. Biotechnol., 28, 500-505.
111. Krause, T., J. T. Wassan, P. Mc Kevitt, H. Wang, H. Zheng, and M. Hemmje (2021). Analyzing large microbiome datasets using machine learning and big data. BioMedInformatics, 1(3), 138-165.
112. Kucek, L. A., M. Nguyen, and L. T. Angenent (2016). Conversion of L-lactate into *n*-caproate by a continuously fed reactor microbiome. Water Res., 93, 163-171.
113. Kucek, L. A., C. M. Spirito, and L. T. Angenent (2016). High *n*-caprylate productivities and specificities from dilute ethanol and acetate: chain elongation with microbiomes to upgrade products from syngas fermentation. Energ. Environ. Sci., 9, 3482-3494.
114. Kucek, L. A., J. Xu, M. Nguyen, and L. T. Angenent (2016). Waste conversion into *n*-caprylate and *n*-caproate: resource recovery from wine lees using anaerobic reactor microbiomes and in-line extraction. Front. Microbiol., 7, 1892.
115. Kuroda, T. H. A. S. (1993). Presence of lactate dehydrogenase and lactate racemase in *Megasphaera elsdenii* grown on glucose or lactate. Appl. Environ. Microb., 59, 255-259.
116. Lambrecht, J., N. Cichocki, F. Schattenberg, S. Kleinsteuber, H. Harms, S. Muller and H. Strauber (2019). Key sub-community dynamics of medium-chain carboxylate production. Microb. Cell. Fact., 18, 92.

117. Langille, M. G., J. Zaneveld, J. G. Caporaso, D. McDonald, D. Knights, J. A. Reyes, J. C. Clemente, D. E. Burkepile, R. L. Vega Thurber, R. Knight, R. G. Beiko and C. Huttenhower (2013). Predictive functional profiling of microbial communities using 16S rRNA marker gene sequences. Nat. Biotechnol., 31, 814-821.
118. Lanjekar, V. B., N. P. Marathe, V. V. Ramana, Y. S. Shouche and D. R. Ranade (2014). *Megasphaera indica* sp. nov., an obligate anaerobic bacteria isolated from human faeces. Int. J. Syst. Evol. Micr., 64, 2250-2256.
119. Lawson, C. E., W. R. Harcombe, R. Hatzenpichler, S. R. Lindemann, F. E. Loffler, M. A. O'Malley, H. Garcia Martin, B. F. Pfleger, L. Raskin, O. S. Venturelli, D. G. Weissbrodt, D. R. Noguera and K. D. McMahon (2019). Common principles and best practices for engineering microbiomes. Nat. Rev. Microbiol., 17, 725-741.
120. Lee, G. H., M. S. Rhee, D. H. Chang, J. Lee, S. Kim, M. H. Yoon and B. C. Kim (2013). *Oscillibacter ruminantium* sp. nov., isolated from the rumen of Korean native cattle. Int J Syst Evol Microbiol, 63, 1942-1946.
121. Lee, N. R., C. H. Lee, D. Y. Lee and J. B. Park (2020). Genome-scale metabolic network reconstruction and in silico analysis of hexanoic acid producing *Megasphaera elsdenii*. Microorganisms, 8, 539.
122. Legendre, P. A. A., M. J. (1999). Distance-based redundancy analysis: Testing multispecies responses in multifactorial ecological experiments. Ecol. Monogr., 69, 1-24.
123. Kucek, Leo A., Xu, J. J., Nguyen, M., and Angenent, L. T. (2016). Waste conversion into *n*-caprylate and *n*-caproate: resource recovery from wine lees using anaerobic reactor microbiomes and in-line extraction. Front. Microbiol., 7, 1892.
124. Li, F., J. Hinderberger, H. Seedorf, J. Zhang, W. Buckel and R. K. Thauer (2008). Coupled ferredoxin and crotonyl coenzyme A (CoA) reduction with NADH catalyzed by the butyryl-CoA dehydrogenase/Etf complex from *Clostridium kluyveri*. J. Bacteriol., 190, 843-850.
125. Li, W., M. Ren, L. Duo, J. Li, S. Wang, Y. Sun, M. Li, W. Ren, Q. Hou, J. Yu, Z. Sun and T. Sun (2020). Fermentation characteristics of *Lactococcus lactis* subsp. lactis isolated from naturally fermented dairy products and screening of potential starter isolates. Front. Microbiol., 11, 1794.
126. Li, Z., Y. Lou, J. Ding, B. F. Liu, G. J. Xie, N. Q. Ren and D. Xing (2020). Metabolic regulation of ethanol-type fermentation of anaerobic acidogenesis at different pH based on transcriptome analysis of *Ethanoligenens harbinense*. Biotechnol. Biofuels, 13, 101.
127. Lindley, B. N. D., P. Loubiere, S. Pacaud, C. Mariotto and G. Goma (1987). Novel products of the acidogenic fermentation of methanol during growth of E*eubacterium limosum* in the presence of high concentrations of organic acids. J. Gen. Appl. Microbiol., 133, 3557-3563.
128. Liou, J. S., D. L. Balkwill, G. R. Drake, and R. S. Tanner (2005). *Clostridium carboxidivorans* sp. nov., a solvent-producing clostridium isolated from an agricultural settling lagoon, and reclassification of the acetogen *Clostridium scatologenes* strain SL1 as *Clostridium drakei* sp. nov. Int. J. Syst. Evol. Microbiol., 55, 2085-2091.
129. Liu, B., S. Kleinsteuber, F. Centler, H. Harms and H. Strauber (2020). Competition between butyrate fermenters and chain-elongating bacteria limits the efficiency of medium-chain carboxylate production. Front. Microbiol., 11, 336.
130. Liu, B., D. Popp, N. Muller, H. Strauber, H. Harms and S. Kleinsteuber (2020). Three novel Clostridia isolates produce *n*-caproate and iso-butyrate from lactate: comparative genomics of chain-elongating bacteria. Microorganisms, 8, 1970.
131. Lozupone, C., M. E. Lladser, D. Knights, J. Stombaugh, and R. Knight (2011). UniFrac: an effective distance metric for microbial community comparison. ISME J, 5, 169-172.
132. Catherine Lozupone and Rob Knight (2005). UniFrac: a new phylogenetic method for comparing microbial communities. Appl. Environ. Microbiol., 71, 8228-8235.
133. Marounek, Katerina Fliegrova and S. Bartos (1989). Metabolism and some characteristics of ruminal strains of *Megasphaera elsdnii*. AMB Express, 55, 1570-1573.
134. Marounek, M., K. Fliegrova and S. and bartos (1989). Metabolism and some characteristics of ruminal strains of *Megasphaera elsdenii*. Appl. and Environ. Microbiol., 55, 1570-1573.
135. Marshall, C. W., E. V. LaBelle, and H. D. May (2013). Production of fuels and chemicals from waste by microbiomes. Curr. Opin. Biotechnol., 24, 391-397.
136. Mavrovouniotis, M. L. (1990). Group contributions for estimating standard Gibbs energies of formation of biochemical compounds in aqueous solution. Biotechnol. Bioeng., 36, 1070-1082

137. Mavrovouniotis, M. L. (1991). Estimation of standard Gibbs energy changes of biotransformations. J. Biol. Chem., 266, 14440-14445.
138. Mazzucotelli, Cintia Anabela, Ponce, Alejandra Graciela, Kotlar, Catalina Elena, and Moreira, María del Rosario (2013). Isolation and characterization of bacterial strains with a hydrolytic profile with potential use in bioconversion of agroindustial by-products and waste. Food. Sci. Tech., 33, 295-303.
139. Miyazaki, M., S. Sakai, K. M. Ritalahti, Y. Saito, Y. Yamanaka, Y. Saito, A. Tame, K. Uematsu, F. E. Loffler, K. Takai, and H. Imachi (2014). *Sphaerochaeta multiformis* sp. nov., an anaerobic, psychrophilic bacterium isolated from subseafloor sediment, and emended description of the genus *Sphaerochaeta*. Int. J. Syst. Evol. Microbiol., 64, 4147-4154.
140. Munoz-Tamayo, R., B. Laroche, E. Walter, J. Dore, S. H. Duncan, H. J. Flint, and M. Leclerc (2011). Kinetic modeling of lactate utilization and butyrate production by key human colonic bacterial species. FEMS Microbiol. Ecol., 76, 615-624.
141. Nzeteu, C. O., A. C. Trego, F. Abram and V. O'Flaherty (2018). Reproducible, high-yielding, biological caproate production from food waste using a single-phase anaerobic reactor system. Biotechnol. Biofuels, 11, 108.
142. Oksanen, J., Simpson, G. L., Blanchet, F. G., Kindt, R., Legendre, P., Minchin, P. R., et al. (2022). vegan: Community Ecology Package 2.6-2.
143. Otto, K. (1983). Carbohydrate metabolism in lactic acid bacteria. An tonie van Leeuwenhoek, 49, 209-224.
144. Park, S., M. Yasin, J. Jeong, M. Cha, H. Kang, N. Jang, I. G. Choi and I. S. Chang (2017). Acetate-assisted increase of butyrate production by *Eubacterium limosum* KIST612 during carbon monoxide fermentation. Bioresour. Technol., 245, 560-566.
145. Phillip Greenspan, Eugene P. Mayer, And Stanley D. Fowler (1985). Nile Red: A selective fluorescent stain for intracellular lipid droplets. J. Cell. Biol., 100.
146. Phillips, J. R., H. K. Atiyeh, R. S. Tanner, J. R. Torres, J. Saxena, M. R. Wilkins and R. L. Huhnke (2015). Butanol and hexanol production in *Clostridium carboxidivorans* syngas fermentation: Medium development and culture techniques. Bioresour. Technol., 190, 114-121.
147. Piwowarek, K., E. Lipinska, E. Hac-Szymanczuk, M. Kieliszek and I. Scibisz (2018). *Propionibacterium* spp.-source of propionic acid, vitamin B12, and other metabolites important for the industry. Appl. Microbiol. Biotechnol., 102, 515-538.
148. Stephen R. Harper and Frederick G. Pohland (1986). Recent developments in hydrogen management during anaerobic biological. Biotechnol. Bioeng. XXVIII: 585-602.
149. Prabhu, R., E. Altman and M. A. Eiteman (2012). Lactate and acrylate metabolism by *Megasphaera elsdenii* under batch and steady-state conditions. Appl. Environ. Microbiol, 78, 8564-8570.
150. Quast, C., E. Pruesse, P. Yilmaz, J. Gerken, T. Schweer, P. Yarza, J. Peplies, and F. O. Glockner (2013). The SILVA ribosomal RNA gene database project: improved data processing and web-based tools. Nucleic. Acids. Res. 41(Database issue): D590-596.
151. Quince, C., A. W. Walker, J. T. Simpson, N. J. Loman. and N. Segata (2017). Shotgun metagenomics, from sampling to analysis. Nat. Biotechnol., 35, 833-844.
152. Raunkjær, K., Hvitved-Jacobsen, T., and Nielsen, P.H., (1994). Measurement of pools of protein, carbohydrate and lipid in domestic wastewater. Wat. Pea., 28, 251-262.
153. Revelle, W. (2022). psych: Procedures for Psychological, Psychometric, and Personality Research.
154. Richter, H., B. Molitor, M. Diender, D. Z. Sousa, and L. T. Angenent (2016). A narrow pH range supports butanol, hexanol, and octanol production from syngas in a continuous co-culture of *Clostridium ljungdahlii* and *Clostridium kluyveri* with in-line product extraction. Front. Microbiol., 7, 1773.
155. Ricotta, C. and J. Podani (2017). On some properties of the Bray-Curtis dissimilarity and their ecological meaning. Ecol. Complex., 31, 201-205.
156. Rios-Covian, D., S. Arboleya, A. M. Hernandez-Barranco, J. R. Alvarez-Buylla, P. Ruas-Madiedo, M. Gueimonde and C. G. de los Reyes-Gavilan (2013). Interactions between *Bifidobacterium* and *Bacteroides* species in co-fermentations are affected by carbon sources, including exopolysaccharides produced by *bifidobacteria*. Appl. Environ. Microbiol., 79, 7518-7524.
157. Rios-Covian, D., B. Sanchez, N. Salazar, N. Martinez, B. Redruello, M. Gueimonde and C. G.

de Los Reyes-Gavilan (2015). Different metabolic features of *Bacteroides fragilis* growing in the presence of glucose and exopolysaccharides of *bifidobacteria*. Front. Microbiol., 6,825.
158. Ritalahti, K. M., S. D. Justicia-Leon, K. D. Cusick, N. Ramos-Hernandez, M. Rubin, J. Dornbush and F. E. Loffler (2012). *Sphaerochaeta globosa* gen. nov., sp. nov. and *Sphaerochaeta pleomorpha* sp. nov., free-living, spherical *spirochaetes*. Int. J. Syst. Evol. Microbiol., 62, 210-216.
159. Rodriguez, J., R. Kleerebezem, J. M. Lema and M. C. van Loosdrecht (2006). Modeling product formation in anaerobic mixed culture fermentations. Biotechnol. Bioeng., 93, 592-606.
160. Roghair, M., T. Hoogstad, D. Strik, C. M. Plugge, P. H. A. Timmers, R. A. Weusthuis, M. E. Bruins and C. J. N. Buisman (2018). Controlling ethanol use in chain elongation by CO_2 loading rate. Environ. Sci. Technol., 52, 1496-1505.
161. Roghair, M., Y. Liu, J. C. Adiatma, R. A. Weusthuis, M. E. Bruins, C. J. N. Buisman and D. Strik (2018). Effect of *n*-caproate concentration on chain elongation and competing processes. ACS Sustain. Chem. Eng., 6, 7499-7506.
162. Roghair, M., Y. Liu, D. Strik, R. A. Weusthuis, M. E. Bruins and C. J. N. Buisman (2018). Development of an effective chain elongation process from acidified food waste and ethanol into *n*-caproate. Front. Bioeng. Biotechnol., 6, 50.
163. Rossi, R., G. Pastorelli, S. Cannata and C. Corino (2010). Recent advances in the use of fatty acids as supplements in pig diets: A review. Anim. Feed. Sci. Tech., 162, 1-11.
164. Saha, S., B. Basak, J. H. Hwang, E. S. Salama, P. K. Chatterjee and B. H. Jeon (2020). Microbial symbiosis: A network towards biomethanation. Trends Microbiol., 28, 968-984.
165. Scarborough M. J., Lawson, C. E., Hamilton, J. J., Donohue, T. J., Noguera D. R. (2018). Metatranscriptomic and Thermodynamic Insights into Medium-Chain Fatty Acid Production Using an Anaerobic Microbiome. MSystems, 3, e00221-00218.
166. Scarborough, M. J., G. Lynch, M. Dickson, M. McGee, T. J. Donohue, and D. R. Noguera (2018). Increasing the economic value of lignocellulosic stillage through medium-chain fatty acid production. Biotechnol. Biofuels, 11, 200.
167. Scarborough, M. J., K. S. Myers, T. J. Donohue, and D. R. Noguera (2020). Medium-chain fatty acid synthesis by "*candidatus weimeria bifida*" gen. nov., sp. nov., and "*candidatus pseudoramibacter fermentans*" sp. nov." Appl. Environ. Microbiol., 86, e02242-19.
168. Seedorf, H., W. F. Fricke, B. Veith, H. Bruggemann, H. Liesegang, A. Strittmatter, M. Miethke, Buckel, W., Julia Hinderberger, Fuli Li, Christoph Hagemeier, Rudolf K. Thauer, and Gerhard Gottschalk (2008). The genome of *Clostridium kluyveri*, a strict anaerobe with unique metabolic features. Proc. Natl. Acad. Sci., 105, 2128–2133
169. Shannon, C. E. (1948). A mathematical theory of communication. Mob. Comput. Commun. Re., 5.
170. Shannon, P., A. Markiel, O. Ozier, N. S. Baliga, J. T. Wang, D. Ramage, N. Amin, B. Schwikowski and T. Ideker (2003). Cytoscape: a software environment for integrated models of biomolecular interaction networks. Genome Res., 13, 2498-2504.
171. Wasewar, K. L. and Shende, D. Z. (2010). Extraction of caproic acid using tri-n-butyl phosphate in benzene and toluene at 301k. J. Chem. Eng. Data, 55, 4121–4125.
172. Siggins, A., A. M. Enright, and V. O'Flaherty (2011). Methanogenic community development in anaerobic granular bioreactors treating trichloroethylene (TCE)-contaminated wastewater at 37ºC and 15ºC. Water Res., 45, 2452-2462.
173. Sikora, A., M. Baszczyk, M. Jurkowski, and U. Zielenkiewicz (2013). Lactic acid bacteria in hydrogen-producing consortia: on purpose or by coincidence? licensee InTech. This is an open access chapter distributed under the terms of the Creative Commons Attribution License (http://creativecommons.org/licenses/by/3.0)
174. Siriwongrungson, V., R. J. Zeng, and I. Angelidaki (2007). Homoacetogenesis as the alternative pathway for H_2 sink during thermophilic anaerobic degradation of butyrate under suppressed methanogenesis. Water Res., 41, 4204-4210.
175. Smith, E. A. and Macfarlane, G. T. (1998). Enumeration of amino acid fermenting bacteria in the human large intestine: effects of pH and starch on peptide metabolism and dissimilation of amino acids. FEMS Microbiol. Ecol., 25, 355-368.
176. Song, Y., J. Shin, Y. Jeong, S. Jin, J. K. Lee, D. R. Kim, S. C. Kim, S. Cho and B. K. Cho (2017). Determination of the genome and primary transcriptome of syngas fermenting *Eubacterium limosum* ATCC 8486. Sci. Rep., 7, 13694.

177. Spirito, C. M., A. M. Marzilli, and L. T. Angenent (2018). Higher Substrate ratios of ethanol to acetate steered chain elongation toward *n*-caprylate in a bioreactor with product extraction. Environ. Sci. Technol., 52, 13438-13447.
178. Spirito, C. M., H. Richter, K. Rabaey, A. J. Stams, and L. T. Angenent (2014). Chain elongation in anaerobic reactor microbiomes to recover resources from waste. Curr. Opin. Biotechnol., 27, 115-122.
179. Steinbusch, K. J., H. V. Hamelers, and C. J. N. Buisman (2008). Alcohol production through volatile fatty acids reduction with hydrogen as electron donor by mixed cultures. Water Res., 42, 4059-4066.
180. Steinbusch, K. J. J., H. V. M. Hamelers, C. M. Plugge and C. J. N. Buisman (2011). Biological formation of caproate and caprylate from acetate: fuel and chemical production from low grade biomass. Energy Environ. Sci., 4, 216-224.
181. Straathof, A. J., S. Sie, T. T. Franco, and L. A. van der Wielen (2005). Feasibility of acrylic acid production by fermentation. Appl. Microbiol. Biotechnol., 67, 727-734.
182. Sträuber, H., F. Bühligen, S. Kleinsteuber and M. Dittrich-Zechendorf (2018). Carboxylic acid production from ensiled crops in anaerobic solid-state fermentation - trace elements as pH controlling agents support microbial chain elongation with lactic acid. Eng. Life Sci., 18, 447-458.
183. Sträuber, H., R. Lucas and S. Kleinsteuber (2016). Metabolic and microbial community dynamics during the anaerobic digestion of maize silage in a two-phase process. Appl. Microbiol. Biotechnol., 4, 479-491.
184. Suzanne Read, Massimo Marzorati, Beatriz C. M. Guimarães, and Nico Boon (2011). Microbial resource management revisited: successful parameters and new concepts. Appl. Microbiol. Biotechnol., 90, 861–871.
185. Tang, J., X. C. Wang, Y. Hu, Y. Zhang and Y. Li (2017). Effect of pH on lactic acid production from acidogenic fermentation of food waste with different types of inocula. Bioresour. Technol., 224, 544-552.
186. Tao, Y., X. Zhu, H. Wang, Y. Wang, X. Li, H. Jin and J. Rui (2017). The complete genome sequence of *Ruminococcaceae* bacterium CPB6: A newly isolated culture for efficient *n*-caproic acid production from lactate. J. Biotechnol., 259, 91-94.
187. Tarasov, A. L., Borzenkov, I. A., and Belyayev, S. S. (2011). Investigation of the trophic relations between anaerobic microorganisms from an underground gas repository during methanol utilization. Microbiology, 80, 180-187.
188. Tholozan, J. L., J. P. Touzel, E. Samain, J. P. Grivet, G. Prensier and G. and Albagnac (1992). *Clostridium neopropionicum* sp. nov., a strict anaerobic bacterium fermenting ethanol to propionate through acrylate pathway. Arch. Microbiol., 157, 249-257.
189. The R Project for Statistical Computing. http://www.R-project.org/. Accessed on November 9, 2021.
190. Tinh Van Nguyen, T. V., Jonah Mortier, Bin Liu, Ilse Smets, Kristel Bernaerts, Karoline Faust, Rob Lavigne, Laurent Poughon, Claude-Gilles Dussap, and Dirk Springael (2023). Isolation and characterization of a thermophilic chain elongating bacterium that produces the high commodity chemical *n*-caproate from polymeric carbohydrates. Bioresour. Technol., 367, 128170.
191. Tomlinson, N. and H. A. Barker (1954). Carbon dioxide and acetate utilization by *Clostridium Kluyveri*. J. Biol. Chem., 209, 585-595.
192. Urban, C., J. Xu, H. Sträuber, T. R. dos Santos Dantas, J. Mühlenberg, C. Härtig, L. T. Angenent and F. Harnisch (2017). Production of drop-in fuels from biomass at high selectivity by combined microbial and electrochemical conversion. Energy Environ. Sci., 10, 2231-2244.
193. Usack, J. G. and L. T. Angenent (2015). Comparing the inhibitory thresholds of dairy manure co-digesters after prolonged acclimation periods: Part 1-performance and operating limits. Water Res., 87, 446-457.
194. Van Immerseel, F., J. De Buck, F. Boyen, L. Bohez, F. Pasmans, J. Volf, M. Sevcik, I. Rychlik, F. Haesebrouck and R. Ducatelle (2004). Medium-chain fatty acids decrease colonization and invasion through *hil*A suppression shortly after infection of chickens with *Salmonella enterica* serovar Enteritidis. Appl. Environ. Microbiol., 70, 3582-3587.
195. Vasudevan, D., H. Richter and L. T. Angenent (2014). Upgrading dilute ethanol from syngas fermentation to *n*-caproate with reactor microbiomes. Bioresour. Technol., 151, 378-382.

196. Wallace, R. J., L. C. Chaudhary, E. Miyagawa, N. McKain and N. D. Walker (2004). Metabolic properties of *Eubacterium pyruvativorans*, a ruminal 'hyper-ammonia-producing' anaerobe with metabolic properties analogous to those of *Clostridium kluyveri*. Microbiology, 150, 2921-2930.
197. Wallace, R. J., N. McKain, N. R., McEwan, E., Miyagawa, L. C., Chaudhary, T. P., King, N. D., Walker, J. H. A. Apajalahti, and C. J. Newbold (2003). *Eubacterium pyruvativorans* sp. nov., a novel non-saccharolytic anaerobe from the rumen that ferments pyruvate and amino acids, forms caproate and utilizes acetate and propionate. Int. J. Syst. Evol. Microbiol., 53, 965-970.
198. Wang, H., X. Li, Y. Wang, Y. Tao, S. Lu, X. Zhu and D. Li (2018). Improvement of *n*-caproic acid production with *Ruminococcaceae* bacterium CPB6: selection of electron acceptors and carbon sources and optimization of the culture medium. Microb. Cell. Fact., 17, 99.
199. Wang, Q., G. M. Garrity, J. M. Tiedje and J. R. Cole (2007). Naive Bayesian classifier for rapid assignment of rRNA sequences into the new bacterial taxonomy. Appl. Environ. Microbiol., 73, 5261-5267.
200. Wang, Q., C. D. Wang, C. H. Li, J. G. Li, Q. Chen and Y. Z. Li (2015). *Clostridium luticellarii* sp. nov., isolated from a mud cellar used for producing strong aromatic liquors. Int. J. Syst. Evol. Microbiol., 65, 4730-4733.
201. Wang, Y., J. Wu, M. Lv, Z. Shao, M. Hungwe, J. Wang, X. Bai, J. Xie, Y. Wang and W. Geng (2021). Metabolism characteristics of lactic acid bacteria and the expanding applications in food industry. Front. Bioeng. Biotechnol., 9, 612285.
202. Kenealy, W. R. and Waselefsky, D. M. (1985). Studies on the substrate range of *Clostridium kluyveri*: the use of propanol and succinate. Arch. Microbiol., 141,184-197.
203. Wei, Y., B. Ren, S. Zheng, X. Feng, Y. He, X. Zhu, L. Zhou and D. Li (2021). Effect of high concentration of ammonium on the production of *n*-caproate: Recovery of a high-value biochemical from food waste via lactate-driven chain elongation. Waste Manag., 128, 25-35.
204. Weimer, P. J. and R. A. Kohn (2016). Impacts of ruminal microorganisms on the production of fuels: how can we intercede from the outside? Appl. Microbiol. Biotechnol., 100, 3389-3398.
205. Weimer, P. J. and G. N. Moen (2013). Quantitative analysis of growth and volatile fatty acid production by the anaerobic ruminal bacterium *Megasphaera elsdenii* T81. Appl. Microbiol. Biotechnol., 97, 4075-4081.
206. Weimer, P. J., M. Nerdahl and D. J. Brandl (2015). Production of medium-chain volatile fatty acids by mixed ruminal microorganisms is enhanced by ethanol in co-culture with *Clostridium kluyveri*. Bioresour. Technol., 175, 97-101.
207. Weimer, P. J. and D. M. Stevenson (2012). Isolation, characterization, and quantification of *Clostridium kluyveri* from the bovine rumen. Appl. Microbiol. Biotechnol., 94, 461-466.
208. Werner, J. J., D. Knights, M. L. Garcia, N. B. Scalfone, S. Smith, K. Yarasheski, T. A. Cummings, A. R. Beers, R. Knight and L. T. Angenent (2011). Bacterial community structures are unique and resilient in full-scale bioenergy systems. Proc. Natl. Acad. Sci., 108, 4158-4163.
209. Wickham, H. (2016). ggplot2: Elegant Graphics for Data Analysis. Springer-Verlag New York. ISBN: 978-3-319-24277-4.
210. Wilbanks, B. and Trinh, C. T. (2017). Comprehensive characterization of toxicity of fermentative metabolites on microbial growth. Biotechnol. Biofuels, 10, 262.
211. Willems, A. A. C. and Matthew D. (1996). Phylogenetic relationships of the genera *Acetobacterium* and *Eubacterium sensu strict0* and reclassification of *Eubacterium alactolyticum* as *Pseudoramibacter alactolyticus gen*. nov., comb. nov. INT. J. SYST. EVOL. MICR., 46, 1083-1087.
212. Wittebolle, L., M. Marzorati, L. Clement, A. Balloi, D. Daffonchio, K. Heylen, P. De Vos, W. Verstraete and N. Boon (2009). Initial community evenness favours functionality under selective stress. Nature, 458, 623-626.
213. Wu, Q., X. Bao, W. Guo, B. Wang, Y. Li, H. Luo, H. Wang and N. Ren (2019). Medium-chain carboxylic acids production from waste biomass: Current advances and perspectives. Biotechnol. Adv., 37, 599-615.
214. Wu, Q., X. Feng, Y. Chen, M. Liu and X. Bao (2020). Continuous medium chain carboxylic acids production from excess sludge by granular chain-elongation process. J. Hazard. Mater., 402, 123471.
215. Wu, Q., X. Feng, W. Guo, X. Bao and N. Ren (2020). Long-term medium-chain carboxylic

acids production from liquor-making wastewater: Parameters optimization and toxicity mitigation. Chem. Eng. J., 388.
216. Wu, Q., W. Guo, X. Bao, X. Meng, R. Yin, J. Du, H. Zheng, X. Feng, H. Luo and N. Ren (2018). Upgrading liquor-making wastewater into medium chain fatty acid: Insights into co-electron donors, key microflora, and energy harvest. Water Res., 145, 650-659.
217. Wu, Q., W. Guo, S. You, X. Bao, H. Luo, H. Wang and N. Ren (2019). Concentrating lactate-carbon flow on medium chain carboxylic acids production by hydrogen supply. Bioresour. Technol., 291, 121573.
218. Wu, Q., W. Ren, W. Guo and N. Ren (2022). Effect of substrate structure on medium chain fatty acids production and reactor microbiome. Environ. Res., 204, 111947.
219. Wu, S. L., J. Sun, X. Chen, W. Wei, L. Song, X. Dai and B. J. Ni (2020). Unveiling the mechanisms of medium-chain fatty acid production from waste activated sludge alkaline fermentation liquor through physiological, thermodynamic and metagenomic investigations. Water Res., 169, 115218.
220. Xie, S., J. Ma, L. Li, Q. He, P. Xu, S. Ke and Z. Shi (2021). Anaerobic caproate production on carbon chain elongation: Effect of lactate/butyrate ratio, concentration and operation mode. Bioresour. Technol., 329, 124893.
221. Xu, J., B. Bian, L. T. Angenent and P. E. Saikaly (2021). Long-term continuous extraction of medium-chain carboxylates by pertraction with submerged hollow-fiber membranes. Front Bioeng Biotechnol, 9, 726946.
222. Xu, J., J. J. Guzman, S. J. Andersen, K. Rabaey and L. T. Angenent (2015). In-line and selective phase separation of medium-chain carboxylic acids using membrane electrolysis. Chem. Commun., 51, 6847-6850.
223. Xu, J., J. Hao, J. J. L. Guzman, C. M. Spirito, L. A. Harroff and L. T. Angenent (2017). Temperature-phased conversion of acid whey waste into medium-chain carboxylic acids *via* lactic acid: No external e-donor. Joule, 2, 1-16.
224. Yang, Peixian, Leng, Ling, Tan, Giin-Yu Amy, Dong, Chengyu, Leu, Shao-Yuan, Chen, Wen-Hsing, Lee, Po-Heng (2018). Upgrading lignocellulosic ethanol for caproate production *via* chain elongation fermentation. Int. Biodeter. Biodegr., 135, 103-109.
225. Yesil, H., H. Taner, F. Ugur Nigiz, N. Hilmioglu and A. E. Tugtas (2018). Pervaporative separation of mixed volatile fatty acids: A study towards integrated vfa production and separation. Waste Biomass. Valori., 11, 1737-1753.
226. Yin, Y., Y. Zhang, D. B. Karakashev, J. Wang and I. Angelidaki (2017). Biological caproate production by *Clostridium kluyveri* from ethanol and acetate as carbon sources. Bioresour. Technol., 241, 638-644.
227. Yu, J., Z. Huang, P. Wu, M. Zhao, H. Miao, C. Liu and W. Ruan (2019). Performance and microbial characterization of two-stage caproate fermentation from fruit and vegetable waste *via* anaerobic microbial consortia. Bioresour. Technol., 284, 398-405.
228. Yu, J., J. Liao, Z. Huang, P. Wu, M. Zhao, C. Liu and W. Ruan (2019). Enhanced anaerobic mixed culture fermentation with anion-exchange resin for caproate production. Processes, 7, 404.
229. Yundong Wang, Y. L., Yi Li, Jingyi Wang, Zhenyu Li, and Youyuan Dai (2001). Extraction Equilibria of Monocarboxylic Acids with Trialkylphosphine Oxide. J. Chem. Eng. 46, 831-837.
230. Zagrodnik, R., A. Duber, M. Lezyk and P. Oleskowicz-Popiel (2020). Enrichment versus bioaugmentation-microbiological production of caproate from mixed carbon sources by mixed bacterial culture and *Clostridium kluyveri*. Environ. Sci. Technol., 54, 5864-5873.
231. Zhang, W., S. Wang, F. Yin, Q. Cao, T. Lian, H. Zhang, Z. Zhu and H. Dong (2022). Medium-chain carboxylates production from co-fermentation of swine manure and corn stalk silage *via* lactic acid: Without external electron donors. Chem. Eng. J., 439.
232. Zhang, Y., X. Pan, J. Zuo and J. Hu (2022). Production of *n*-caproate using food waste through thermophilic fermentation without the addition of external electron donors. Bioresour. Technol., 343, 126144.
233. Zhu, X., X. Feng, C. Liang, J. Li, J. Jia, L. Feng, Y. Tao and Y. Chen (2021). Microbial ecological mechanism for long-term production of high concentrations of *n*-caproate *via* lactate-driven chain elongation. Appl. Environ. Microbiol., 87, e03075-20.
234. Zhu, X., Y. Tao, C. Liang, X. Li, N. Wei, W. Zhang, Y. Zhou, Y. Yang and T. Bo (2015). The synthesis of *n*-caproate from lactate: A new efficient process for medium-chain carboxylates

production. Sci. Rep., 5, 14360.
235. Zhu, X., Y. Zhou, Y. Wang, T. Wu, X. Li, D. Li and Y. Tao (2017). Production of high-concentration *n*-caproic acid from lactate through fermentation using a newly isolated *Ruminococcaceae* bacterium CPB6. Biotechnol. Biofuels, 10, 102.
236. Zinder, S. H., Anguish, T., and Cardwell, S. C. (1984). Selective Inhibition by 2-bromoethanesulfonate of methanogenesis from acetate in a thermophilic anaerobic digestor. Appl. Environ. Microb., 47, 1343-1345.
237. Zorz, J. K., Sharp, C., Kleiner, M., Gordon, P. M. K., Pon, R. T., Dong, X. and Strous, M. (2019). A shared core microbiome in soda lakes separated by large distances. Nat. Commun., 10, 4230.